GEOCHEMICAL AND PETROLOGICAL STUDIES OF PERMO-CARBONIFEROUS TALCHIR FORMATION AROUND CHIRIMIRI, DISTRICT KORIYA, INDIA

THESIS

SUBMITTED FOR THE AWARD OF THE DEGREE OF

Doctor of Philosophy

IN

GEOLOGY

BY

KHANSA ZAIDI

DEPARTMENT OF GEOLOGY
ALIGARH MUSLIM UNIVERSITY
ALIGARH-202002 (INDIA)

2015

Dr. Sarwar Rais
Associate Professor

DEPARTMENT OF GEOLOGY
ALIGARH MUSLIM UNIVERSITY
ALIGARH -202002, INDIA
Phones : Off. : 091 (571) 2700615
Fax : 0571-2700528
E-mail : raissarwar@yahoo.co.in

Dated : 15.1.2015

Certificate

This is to certify that the work presented in the Ph.D. thesis entiled ""**Geochemical and Petrological studies of Permo-Carboniferous, Talchir Formation, around Chirimiri, district Koriya, India**"." submitted by **Miss. Khansa Zaidi** has been carried out and completed under my supervision. The work is original contribution to the existing knowledge of the subject and has not been submitted before for any other degree at this or any other university.

She is allowed to submit this thesis for the award of the degree of **Doctor of Philosophy** in **Geology** of the Aligarh Muslim University, Aligarh, India.

Sarwar Rais

Dr. Sarwar Rais 15/1/2015
Supervisor

DEPARTMENT OF GEOLOGY
ALIGARH MUSLIM UNIVERSITY, ALIGARH-202002 INDIA

CANDIDATE'S DECLARATION

I, **Khansa Zaidi** Department of **Geology** certify that the work embodied in this thesis is my own bonafied work carried out by me under the supervision of Dr. Sarwar Rais, Associate Professor at Aligarh Muslim University, Aligarh. The matter embodied in this Ph.D. thesis has not been submitted for the award of any other degree.

I declare that I have faithfully acknowledge, given credit to and referred to the research workers whenever their works have been cited in the text and the body of the thesis. I further certify that I have not willfully lifted up some other's work, para, text, data, result, etc. reported in the journals, book magazines, reports, dissertations thesis, etc., or available at web-sites and included them in this Ph.D. thesis and cited as my own work.

Date: 15/11/2015 Khansa Zaidi
(Khansa Zaidi)

.....

CERTIFICATE FROM THE SUPERVISOR

This is to certify that the above statement made by the candidate is correct to the best of my knowledge.

Sarwar Rais 15/11/2015
Dr. Sarwar Rais
Associate Professor
(Supervisor)
Department of Geology

(Signature of the Chairman of the Department with seal)

CHAIRMAN
Department of Geology
A. M. U., ALIGARH

DEPARTMENT OF GEOLOGY,
ALIGARH MUSLIM UNIVERSITY, ALIGARH-202002, INDIA

COURSE WORK EXAMINATION AND PRE-SUBMISSION SEMINAR COMPLETION CERTIFICATE

This is to certify that Miss. Khansa Zaidi, Department of Geology has satisfactorily completed the course work examination and pre-submission seminar requirement which is part of her Ph.D. programme.

Date: 16.1.15

(Signature of the Chairman of the Department)

Department of Geology
A. M. U., ALIGARH

Tribute to,

My school teachers

Dr. Singhasan Rao, Mr. Rajendra Singh

and

My strength; *My family*

CONTENT

Acknowledgement

First and foremost, I offer my sincere gratitude to the Almighty, for making things and situations possible for me what seems impossible. Without whose countless blessings the work would not have been completed.

At this moment of accomplishment of my work I would like to express gratitude to my supervisor Dr. Sarwar Rais, for providing me an excellent atmosphere to carry out the research work, signing stipends without delay so I do not have to face any financial problem regarding my research work.

Beside my supervisor, I am also thankful to the Chairmen, who held this post in the tenure of my research work, Prof. Dr. Mahshar Raza, Prof. Dr. Liyaqat Ali Khan Rao for co-operating, providing full support and necessary facilities in the department. Moreover, I want to give my gratitude to Prof. Dr. A.H.M Ahmad, Incharge of sedimentology laboratory, for providing the facility and valuable suggestions related with field geology for samples collection and Dr. Mohammad Shamim Khan for evaluating and carefully incorporating corrections in my thesis, making my work valuable. I also want to give my profound thanks to Prof. Dr. M. E. A. Mondal, for his encouragement and motivations whenever i felt low during my research.

I am also sincerely thankful to authors who send me their manuscripts through emails that were not accessible to me.

I also acknowledge the altruistic support of N.K Tripathi, General Manager of Chirimiri Coalfield Chhattisgarh India and Dr. Thamban Meloth scientist at National Centre of Antarctic and Ocean Research, Goa

The assistance provided by Dr. Abhay Mudholkar and Dr. V. Purnachandra Rao scientists at National Institute of Oceanography, to generate geochemical data for my thesis is duly acknowledged. I would also like to thank University Sophisticated Instrumentation Facility, Centre A.M.U, Aligarh for taking SEM photographs.

The Financial assistance received from the University Grants Commission as Maulana Azad National Fellowship is immensely acknowledged.

I am also thankful to R. L Gulla owner of Bhavani Lodge, who guide me about the geographical locations and the driver who took me to every corner of the town.

I extend my sincere word of thanks to Mr. Tavheed Khan, for his sincere, selfless help that he extended to me throughout my research work.

I am indebted to my seniors Ms. Sheeba Rehman, Mr. Dheeraj Raghuvanshi, Ms. Sayema Jamal, Ms. Sana Iftekhar, my best friend Ms. Sana Naqvi, Ms. Sameena Parween, and Ms. Talat Jawed, for constantly encouraging, motivating and helping in my chores. Incalculable support and aid provided by Dr. Javed Ganai, Dr. Anis, Mr. Javed Raoof, Mr. Aejaz Ahmad Siddiqui, Mr. Noman

Ashraf and Ms. Naseem-us-saba are worthy to be appreciated. I also owe my success to Mr. Zahoor-ul-Islam for his valuable edifications.

I am also thankful to my fellow mates Mr. Ranjeet. K. Das, Ms. Nazrana Mohammadi, Ms. Afreen Noori, and Ms. Sarah Khatoon, for directly or indirectly assisting me.

Finally, I would like to acknowledge those people, around whom my life revolves, my parents, sisters, brother, brother –in- law, nephew and niece. I further extend my love, gratitude, respect to beloved mother and my inspiration my father who always stands by me during my tough times.

Ms. Khansa Zaidi

List of Figures.....

Figure 4.2.2: Al_2O_3 versus TiO_2 bivariate plot for sandstones and shales of Talchir Formation, Chirimiri, district Koriya, Chhattisgarh India (McLennan et. al, 1979).

Figure 4.2.3: Discriminant function diagram for provenance signatures of Talchir sandstones and shales, Chirimiri, Koriya district, using major oxide ratios (after Roser and Korsch, 1988), where DF1 = $30.638TiO_2/Al_2O_3 - 12.541Fe_2O_3^t/Al_2O_3 + 7.329MgO/Al_2O_3 + 12.031Na_2O/Al_2O_3 + 35.402K_2O/Al_2O_3 - 6.382$, DF2 = $56.500TiO_2/Al_2O_3 - 10.879Fe_2O_3(t)/Al_2O_3 + 30.875MgO/Al_2O_3 - 5.404Na_2O/Al_2O_3 + 11.112K_2O/Al_2O_3 - 3.89$.

Figure 4.2.4: TiO_2 vs Zr plot for sandstones and shales of Talchir Formation, Chirimiri, district Koriya, Chhattisgarh India (Hayashi et. al., 1997).

Figure 4.2.5: Th/Co vs. La/Sc plot showing silicic composition of sandstones and shales of Talchir Formation in Chirimiri, district Koriya, Chhattisgarh India (Cullers, 2002).

Figure 4.2.6: Bivariate plot La/Th versus Hf for bulk discrimination of different arc composition and sources for sandstones and shales of Talchir Formation, Chirimiri, district Koriya, Chhattisgarh India (Floyd and Leveridge, 1987).

Figure 4.2.7: La/Th vs. Th/Yb bivariate plot for sandstones and shales of Talchir Formation, Chirimiri, district Koriya, Chhattisgarh, India (McLennan et al., 1980).

Figure 4.2.8: Bivariate plot of Cr/V vs. Y/Ni (Floyd and Leveridge, 1987) for the Talchir sandstones and shales, Chirimiri, district Koriya, Chhattisgarh, India.

Figure 4.2.9: Plot of Eu/Eu* versus (Gd/Yb) n for sandstone and shales of the studied samples of Talchir Formation Chirimiri area, district Koriya, Chhattisgarh India (McLennan and Taylor, 1991).

Figure 4.3.1: Th/Sc versus Zr/Sc provenance and recycling discrimination diagram for sandstones and shales of Talchir Formation, Chirimiri, district Koriya, Chhattisgarh, India (after McLennan et al., 1993).

Figure 4.4.1: The (K_2O/Na_2O) versus SiO_2 discrimination diagram to decipher tectonic setting of sandstones and shales of Talchir Formation, Chirimiri district Koriya, Chhattisgarh, India (Roser and Korsch, 1986).

Figure 4.2.2: Discriminant function diagram for tectonics settings of Talchir sandstones and shales, Chirimiri, district Koriya, Chhattisgarh India, using major oxide ratios (Bhatia, 1983), where DF1 = $-0.0447SiO_2-0.972TiO_2+0.008Al_2O_3-0.267Fe_2O_3^t+0.208FeO-3.082MnO+0.140MgO+0.195CaO+0.719Na_2O-0.032K_2O+7.510P_2O_5+0.303$, DF2=$-0.421SiO_2+1.988TiO_2-0.526Al_2O_3-0.551Fe_2O_3-1.610FeO+2.720MnO+0.881MgO-0.907CaO-0.177Na_2O-1.840K_2O+7.244P_2O_5+43.57$.

Figure 4.4.3: Major element composition of Talchir sandstones and shales, Chirimiri area, Son-Mahanadi basin district Koriya, Chhattisgarh India for discrimination of tectonic setting plotted against $Fe_2O_3^{(t)}$ +MgO wt % (where Fe_2O_3 represents total iron). Dotted lines represent major fields of tectonic setting. Fields are A – Oceanic island arc; B – Continental Island arc; C – Active continental margin; D – Passive margin (Bhatia, 1983).

Figure 4.4.4: La-Th-Sc ternary diagram for sandstones and shales of Talchir Formation with associated rocks biotite granite, granite, ultramafic, gabbro, and diorite rock exposed in pathalgaon, Son-Mahanadi basin Chhattisgarh.

Figure 4.4.5: Th-Co-Zr/10 and Th-Sc-Zr/10 ternary diagram for sandstones and shales of Talchir Formation, Chirimiri, Koriya district, Chhattisgarh to decipher tectonic setting of the sediments using trace elements (Bhatia and Crook, 1986). **Figure 4.4.5:** (b) A – Oceanic Island arc, B – Continental Island arc, C – Active Continental Margin, D – Passive Margin fields after (Bhatia and Crook, 1986).

Figure 4.4.6: Rare earth chondrite normalised plot for sandstones and associated shales of Talchir Formation and associated rocks (Biotite granite, Granite, Ultramafic, Gabbro and Diorite) exposed in the Son-Mahanadi basin, Chhattisgarh, India.

Figure 5.2.1: A-CN-K ternary diagram showing weathering trend of sediments of Talchir Formation, Koriya district, Chhattisgarh, India (Nesbitt and Young 1984).

Figure 5.2.2: K_2O versus Al_2O_3 bivariate diagram showing distribution of sandstones and shales of Talchir Formation, Chirimiri, Koriya district, Chhattisgarh, India (Cox et al., 1995).

Figure 5.2.3: Th/U versus Th bivariate plot for the sandstones and shales of Talchir Formation Chirimiri, district Koriya, Chhattisgarh, India (McLennan et al. 1993).

Figure 5.4.1: Bivariate plots between SiO_2 vs $Al_2O_3+K_2O+Na_2O$ for sandstones and shales of Talchir Formation, Chirimiri, district Koriya, Chhattisgarh, India (Suttner and Dutta, 1986).

Figure 5.4.2: XRD graphs of sandstones and shales of Talchir Formation.

List of Tables.....

List of Plates.....

Plate 2.3.7: (M) Thin section Microphotograph of ferruginous cement and (N) Arrows indicating pore filling clay around the grains boundaries, found in sandstones of Talchir Formation, Chirimiri, district Koriya, Chhattisgarh, India.

Plate 2.3.8: (O) Thin section Microphotograph showing undifferentiated matrix. (P) Arrow indicates post depositional iron cement in sandstones of Talchir Formation, Chirimiri, district Koriya, Chhattisgarh, India.

Plate 5.4.1: Scanning electron microphotograph showing (A) Chlorite and (B) Illite clay minerals in samples of Talchir Formation, Chirimiri, district Koriya, Chhattisgarh, India.

Plate 5.4.2: Scanning electron microphotograph showing (C) Kaolinite and (D) Smectite clay minerals in samples of Talchir Formation, Chirimiri, district Koriya, Chhattisgarh, India.

CHAPTER – 1

INTRODUCTION

INTRODUCTION

1.1 General Statement

The term 'Gondwana' was first introduced by H.B. Medlicott (1872), after the ancient Kingdom of the Gond (an aboriginal tribe) who still inhabits in many parts of central India. These continental deposits of enormous thickness found in many parts of peninsular India have been designated as the Gondwana 'System' or the Gondwana Supergroup. Occurrence of deposits having similar characters was one of the major facts that led to the inference of the existence of a vast continent in the Southern Hemisphere the "Gondwanaland" (Suess, 1885), which assembled at around 550 Ma (Meert & Van der Voo 1997). The Gondwana Supercontinent comprised of India, Antarctica, Australia, Madagascar, South Africa and South America. Many parts of Gondwana Supercontinent were covered by ice sheet during Permo-Carboniferous time. The Gondwana glaciation is modelled as a single, massive, ice sheet centered over the paleo-south pole located in Antarctica and extending outward into the mid-latitudes (Scotese, 1997; Ziegler et al., 1997; Hyde et al., 1999), which continuously waxed and waned across it for about 100 million years (Veevers and Powell, 1987; Frake and Francis, 1998; Frakes et al., 1992; Ziegler et al., 1997; Hyde et al., 1999; Blakey, 2008; Buggisch et al, 2011). Conversely, recent researches show numerous evidences of small local ice centres that advanced and retreated several times in the Gondwanaland (Crowell and Frakes, 1970; Caputo and Crowell, 1985; Lopez-Gamundi, 1997; Isabell et al., 2003, 2011; Fielding et al., 2008a, 2008b, 2008d, Gulbranson et al., 2010). The Gondwana stratigraphy of Peninsular India is considered from Late Carboniferous to Early Cretaceous. These rocks were deposited after a long hiatus since Proterozoic (Robinson, 1967, Pascoe, 1968; Veevers and Tewari, 1995, Mukhopadhyay, et al., 2010). The Gondwana strata in peninsular India are represented by nearly 4000 meters pile of tillites, conglomerates, sandstones, shales along with thick seams of coal (Vaidhanadham and Ramakrishna, 2008). The Gondwana basins are largely distributed in the form of linear belts aligned along present day peninsular rivers. The major basins are Koel-Damodar, Son-Mahanadi, Pranhita-Godavari and Satpura (Figure 1.1). Beside these some Gondwana occurrences are reported along the Himalayas and east coast of India. The most Gondwana basins of Peninsular India represent half grabens bounded by high angle

(- 60°) normal faults (Tewari, 1999). The Gondwana litho-fills make nonconformity with Archean and Proterozoic Formations. In spite of the differences in the geological and tectonic settings there are close similarities in the litho-fills of all the rift basins of peninsular India (Casshayap, 1979). The advent of Gondwana formation was marked by the prevalence of an ice sheet which covered large portion of the Indian Peninsula. Subsequent melting of the ice sheet led to deposition of moraines and silt in periglacial lakes and glaciated valleys. The Talchir Formation, the lowermost member of Indian Gondwanas, thus came into existence and marks the end of glacial period. It extends into all the regions of the Gondwana basins in India (Veevers and Tewari, 1995).

The Gondwana Supergroup forms one of the most important rock systems in Indian geology because of the fact that almost all important coal occurrences in the country are located within the rocks of this system (Radhakrishan, 1991). Two schemes of stratigraphic classification of Gondwana strata of India have been followed. Medlicott and Blandford (1879) first proposed a two-fold classification and divided Gondwana 'Formation' into 'Lower' and 'Upper'. The Lower Gondwana is characterised by the 'Glossopteris' flora and the 'Upper' by 'Ptilophyllum' flora. This two-fold classification was favoured by Fox (1931, 1934), Krishnan (1949, 1982), Ghosh and Basu (1969), Kutty (1969), Mitra (1972) and many more. On the basis of depositional environment, prevailing climate and occurrence of 'Discroidium' flora, Fiestmentel (1881) adopted a tripartite scheme of classification and divided these rocks as Lower, Middle and Upper Gondwana. This three-fold classification was supported by Vredenburg (1914), Wadia (1926), Roychowdhury et al (1973) and others. However two-fold classification of Gondwana sediments is more popular as it has also been adopted by Geological Survey of India (Table 1.1.1)

Initially stratigraphers (Hughes, 1885) classified Indian Gondwanas into 'System', 'Series', 'Stage', Sub-stage', the hierarchy evolved through convention and usage. However, following the publication of the 'Code of Stratigraphical Nomenclature of India' (1971), many workers have adopted litho- stratigraphic classification for these sediments and gave status of 'Supergroup' to Gondwana Strata of India (Qidwai, 1972; Khan, 1978; Tewari, 1980; Kumar, 1984; Rais, 1985 etc.).

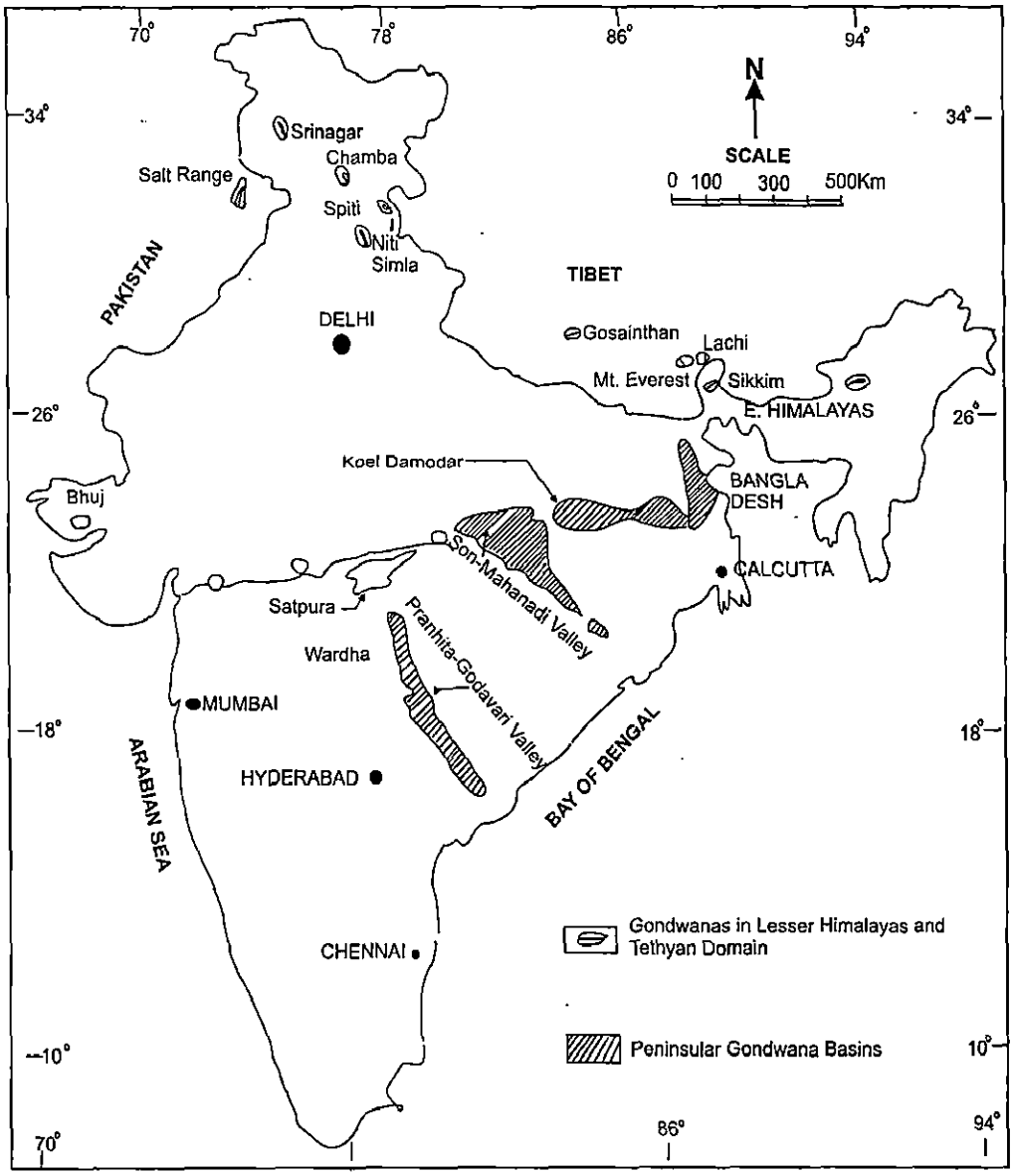

Figure 1.1.1 Map of India showing Gondwana basins of Peninsular India during Permian times (Jha N., 2005).

Table 1.1.1 General Gondwana succession of Son-Mahanadi Graben (after Pandey and Dave, 1998)

Age	Supergroup	Formation Rock unit	Lithology	Thickness
Palaeocene to upper Cretaceous	Deccan Trap	Deccan Trap Basalt/intrusive and extrusive	Fine grained basalts and dolerites	
----------Unconformity----------				
Upper Cretaceous		Lametas	Hard cherty limestone and calcareous conglomerates	40m
----------Unconformity----------				
Lower Cretaceous	Upper Gondwana	Bansa-Chandiya	White clays, silty sandstone, clayey silt, and Quartzone sandstone towards the top	125m
Rhaetic to Norian		Parsora Formation	Purplish white, Kaolinitic sandstone, Pebble beds, Maroon to crimson clays	400 to 600m
Lower Norian to Carnian		Tikki Formation	Laminations of white fine grained sandstone, Occasional siltstone	200m approx.
Upper Permian to Lower Triassic		Pali Formation/ Kamthi Upper Member	Brownish to buff sandstone and some pebble beds, dark brown to brick red clays and carbonaceous clays and hard ferruginous sandstone in Kamthi Formation	200m to 300 m
----------Contact gradational to unconformable----------				
Upper Permian	Lower Gondwana	Raniganj/Kamthi Formation (Lower member)	Flaggy sandstone with thin laminated alternations of carbonaceous shale, siltstone in Raniganj Fm. Medium grained, brown, ferruginous sandstone and micaceous carbonaceous shales in Kamthi formation	400m
Middle Permian		Barren Measures	Moderately hard, ferruginous, greyish sandstone, Occasional grey shales, laminated siltstone, red mottled clays. Some haematitic bands	125m to 300m
Lower Permian		Barakar Formation	Sandstones with alternations of shale/siltstone and thick coal seam and carbonaceous shale	200m to 1150m
		Karharbari Formation	Mottled ferruginous, hard sandstone, carbonaceous shales with occasional coal seams	100m
		Talchir Formation	Basal boulder beds in clay/silty matrix followed by alternations of shales, siltstones and sandstone. Shales are olive green to buff splintery.	50m to 450m
----------Unconformity----------				
Precambrian to Archean		Unclassified/ Dharwar/Bijawar/ Cuddapah	Gneisses, Schist, quartzites, phyllites, pegmatites, granites and cherty limestone	

The sedimentation in Gondwana basins of India evolved through a complex interplay of faulting, changes in sea level and climate. There are two different views regarding the aerial extent of the Gondwana sediments. According to one view the sedimentation was confined to the river valley grabens and it was contemporaneous with faulting. The other view holds that the Gondwana basins were originally wider and the rocks have been preserved only in the down-faulted grabens (Veevers and Tewari, 1995). Basement lineaments have played a vital role in the development of major sedimentary basins of the world (Mial, 1984). Peninsular India, like other parts of the world, is also marked by an array of lineaments, which have controlled the origin and evolution of various sedimentary basins through space and time (Tewari and Maejima, 2010).

The name "Talchir Group" was given by Blandford et al.,(1856) for a sequence of basal boulder bed, greenish shales, sandstones and rhythmic sandstone and shales. The interbedded sequence of sandstone, siltstone and or shale (rhythmite) is characterized by occasional sole structures, dropstones, ripple marks and flaser bedding. The varying facies assemblages of Talchir sequence in different basins do not favour uniform regional depositional model except basal tillite of glacial origin. The Talchir sediments generally favour mixed facies of glacio-fluvial, glacio-lacustrine and/or shallow marine to tidal flat environment (Tewari and Casshayap, 1982). The Talchir Formation has been assigned late Carboniferous to early Permian age on the basis of marine fossils of Asselian-Sakamarine period (around 290 ± 4 Ma) found in these sediments at few isolated locations (Ghosh, 1954; Ghosh and Mittra, 1975; Bangert et al., 1999). The mean palaeo-current was west-north westerly and north during the deposition of Talchir sediments in parts of Son-Mahanadi valley basin (Rais, 1985) and shifted towards North-West and North in the overlying Karharbari and Barakar times (Tewari and Casshyap, 1982). The retreat of Talchir glaciers from eastern peninsular India in late Palaeozoic gave way to streams which flowed dominantly from East-South east to West-North West (Tewari and Casshayap, 1982). Because of rich deposits of bituminous coal, the Gondwana strata of India in general and Lower Gondwana in particular, has been a subject of keen geological interest. But most of the work in Gondwana basins was aimed exclusively towards the discovery of economically potent new coal bearing sediments and very little attention was paid to understand the sedimentary characters of the associated barren sediments.

However, in the last few decades, a good number of geologists have investigated these rocks giving emphasis on their sedimentary characters with more sophisticated modern scientific approach. Some of the notable geoscientists are Sengupta (1966, 1970); Srivastava and Israili (1968); Casshyap (1970a, b, 1973, 1980); Casshyap et al., (1971,1978a, b, 1981b, 1982c, 1983a, b, d); Qidwai (1972); Rizvi(1972); Khan(1978); Tewari(1980); Kumar(1984); and others. But except few geoscientist (Ganju and Srivastava, 1958, Ahmad, 1975a, b, Das and Sen, 1980, Rais, 1997, Dasgupta and Sahoo, 2007, Chakraborty and Ghosh, 2008, Bhattacharya, 2006, 2010, 2012), very little work has been done on the different aspects of Talchir rocks.

1.2 Location of Study Area

The study area is located around Chirimiri, a small town, situated in the southern part of erstwhile Korea state (earlier part of Sarguja). The area of investigation spreads over an area of about 125sq.km and falls within latitude $23^0$8' & $23^0$15' and longitude $82^0$17' & $82^0$25' in the Survey of India Toposheet no 64I/8. Rocks of Talchir Formation are exposed along stream channels flowing in the vicinity of Chirimiri town (Figure1.2.1). Matrix supported conglomerate is found exposed near Dhanuhar stream pink granite boulder and some other clasts are two faceted and exhibits faint striations(Plate1.6.1). In Plate1.6.2 alternate sequence of Tillite and sandstone is found along side Kudra stream. Olive green, thinly laminated Shales (Plate1.6.7) and medium grained sandstones (Plate1.6.3,4 and 5) succeeded by lemon yellow alternate beds of shale and sandstones (Plate1.6.6) are found exposed in these stream channels. A Vertical section of alternate beds of thinly laminated mudstones and sandstones of variable thickness found exposed along Kudra stream section (Plate1.6.8). The dips are usually less than 5^0 and at places the beds are even horizontal. However, nowhere in the study area complete sequence of the Talchir Formation is found exposed. Raja Rao (1983) surveyed Chirimiri area and proposed stratigraphic succession (Table1.2.1).

The area of present investigation is a part of Hasdo-Arand basin, which occupies the central portion of the Son-Mahanadi master basin, the largest intracratonic rift basin of peninsular India. The Mahakoshal supracrustals lie in the north of Son-Mahanadi Gondwana basin. Rocks of Sausar mobile belt and Betul supracrustals are exposed in the south, whereas the eastern and south eastern fringes of the Son-Mahanadi basin are constituted by granite-gneissic complex of

Chotanagpur terrain and Precambrian rocks of Singhbhum and Bastar cratons, respectively. To the west of the Son-Mahanadi basin unclassified Precambrian migmatites and geneisses are exposed (Roy et al., 2000). Tectonically, the basin has been divided into three blocks i.e., Son, Hasdo-Arand and Mahanadi, separated from each other by ENE-WSW trending prominent basement ridges. Spatial distribution of rock units, variation in the thickness of sediments, different disposition of structural elements and contrasting lineament-trends of these three blocks suggest that each underwent a different sedimentation and tectonic history independent of other (Dotiwala and Pangtey, 1997).

Table 1.2.1 Stratigraphic succession of Chirimiri, Koriya district, Chhattisgarh India (Raja Rao, 1983)

Age	Formation	Lithology
Upper cretaceous to Lower Eocene(?)	Deccan Traps	Basic flows, dykes and Sills
Lower Permian to Early Permian	Barakar	Essentially sandstone with subordinate Shales and coal seams (230m to 435m)
Upper Carboniferous	Talchir	Predominantly olive green shales and Medium to fine grained sandstone
	Unconformity	
Precambrian		Granite, Gniesses and Quratzite

1.3 Scope of the Present Work

The present study aims to study the petrological and geochemical aspects of Talchir Formation found around Chirimiri. The area is located in Hasdo-Arand block situated in the, central part of Son-Mahanadi basin. During the field work 50 rock samples were collected out of which 29 representative sandstone samples were chosen for petrographic studies and 30 samples were selected for geochemical analysis. Thin sections of sandstones were prepared and studied using petrological microscope, to determine the modal composition. In the 30 rock a sample, 26 belongs to sandstone and remaining 4 are shale samples. In geochemical testing 42 elements were analysed. Major Oxides were determined by XRF (X-ray fluorescence), Trace elements and REE's by ICP-MS (Inductive coupled plasma mass spectrometer). Clay minerals are also analysed and identified by XRD (X-ray diffractometer) instrument. Photographs of clay minerals found in sandstones and shales of Talchir Formation were taken from SEM (Scanning Electron Microscope).

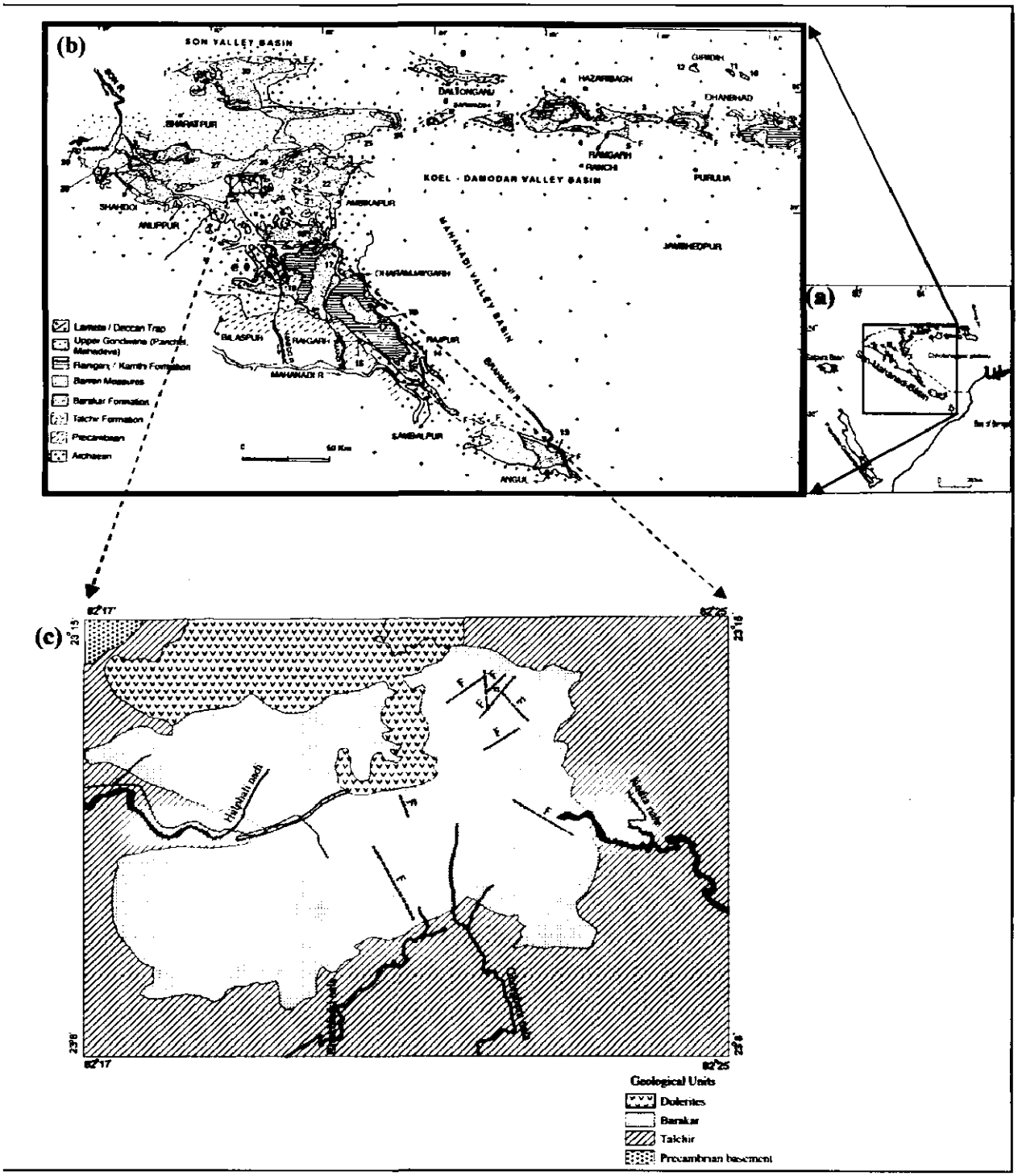

Figure 1.2.1: (a) Outline map of showing eastern coast with palaeoflow direction modified by Tewari and Veevers, 1993, (b) Map showing distribution of Gondwana rocks in Son-Mahanadi basin and Koel Damodar valley basin by Casshyap and Srivastava, 1987, (c) Geological map of Chirimiri, district Koriya, Chhattisgarh, India (Raja Rao, 1983).

The Petrological investigation is utilised to classify and constrain nature of provenance. By synthesising all the information's gathered through petrographic, geochemical and XRD analyses, the ultimate goal was achieved with regards to classification and source area identification of these sandstones. The available evidences were also used to understand the tectonic setting of the depositional basin and paleoclimate prevailing during Permo-carboniferous time in this part of Peninsular India.

1.4 Geography of the Study Area

The study area Chirimiri is located in district Koriya of Chhattisgarh state of India. Unlike other peninsular Gondwana basins, this region is marked by high hills with steep scarps and deep gorges along the course of the streams. The general elevation ranges from 630m to 650 m above MSL. Bartunga (875.1 m.) and Angau (863. 4m) hills are prominent landmarks. The northern part of the coalfield is marked by prominent escarpment formed by Barakar rocks, which are capped by basaltic lava flows. On the east, Bijaur-Jharia and the Ghorgheda are the major streams flowing to the east and south direction, respectively. On the western side the most important stream is the Halphali nala, which originates from the highlands near Chirimiri and flows westward across the Barakars and the Talchir sediments to join the Hasdo river. This stream flows through deep gorges reavealing excellent sections of Barakar and Talchir formations. The area experiences moderate climate. In the winter months minimum temprature goes down to 10 degrees. Rainfall is quite high, the average being 150 cm per year.

1.5 Previous Work

In view of vast resource of Coal, the Gondwana sediments of India in general and Lower Gondwanas in particular have been a subject of keen geological interest. However, most of the work in Gondwana basins was aimed exclusively towards the discovery of potent coal-bearing strata, and very little attention was paid to understand the sedimentology of associated barren sediments. Rocks of Talchir Group are much neglected litho units of the Gondwana Supergroup, although these sediments preserve some peculiar rock types that reflect their history of deposition and paleoclimate prevailing at the close of Carboniferous and beginning of Permian periods. Blandford et al (1856) first studied the Gondwana succession of Talchir basin, Odisha and classified it as the lowermost units in the entire Gondwana

sequence. Blandford et al., (op.cit) favoured origin of Talchir sediments with glaciers. Later on advance investigations in the fields of sedimentology, stratigraphy and paleogeography led many pioneer researchers like Casshyap and Qidwai (1974), Das and Sen (1980), Tewari and Casshayap (1982), Mukhopadhyay and Bhattacharya (1994), Rais (1985, 1997), Veevers and Tewari (1995), Tewari (1999), Bhattacharya et al (2004, 2005, 2006) and Bhattacharya and Bhattacharya (2010, 2012) also supported the conclusion that Talchir Formation is of glacial, glacio-fluvial, glacio-lacustrine and/or glacio-marine origin.

However, very limited data is available on the textural and geochemical characters of these rocks as not much attention has been paid on these aspects of the rocks. Suttner and Dutta (1986), and Tewari (1998), concluded that Talchir sandstones are immature to sub-mature lithic arkosic to arkosic wacke to sometimes arenite. Major, Trace elements, rare earth elements and stable isotopic analyses of the Gondwana rocks, found in different basin of India have been carried out by Suttner and Dutta (1986), Rao et al (1994), Bhattacharya et al. (2002), Ghosh and Sarkar (2010), Rajan et al. (2012).

1.6 Purpose of Investigation

Lowermost member of Gondwana Supergroup, the Talchir Formation, almost with all probability is believed to have direct or indirect relation with Permocarboniferous glaciation in Southern Hemisphere. Talchir Formation extends in all the regions of the Gondwana basins of India.

There appear a reasonable number of isolated outliers, where Talchir rocks are exposed at present but knowledge about their origin is far from satisfactory. The study area, around Chirimiri town, district Koriya, Chhattisgarh, where Talchir rocks stand almost virgin as regard to the origin and the study of processes involved during their sedimentation, whatever, we know is generalised account given by earlier workers, who were more interested in locating new coal bearing horizons.

The present task is aimed at to understand and study the petrological and geochemical characters of these sediments. The data thus generated is employed to constrain the nature and tectonic setting of provenance, characterisation of depositional basin, paleoweathering and paleoclimatic conditions prevailing at the time of deposition of Talchir rocks of the study area.

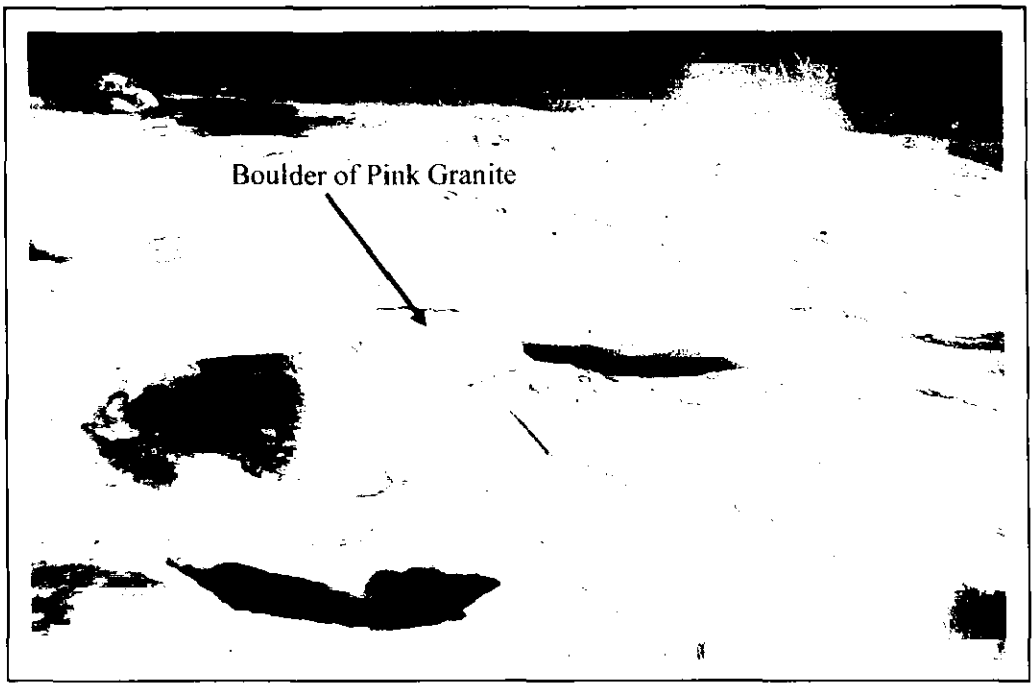

Plate 1.6.1: Matrix supported conglomerate/ tillite near Dhanuhar stream in Chirimiri coalfield, district Koriya, Chhattisgarh India.

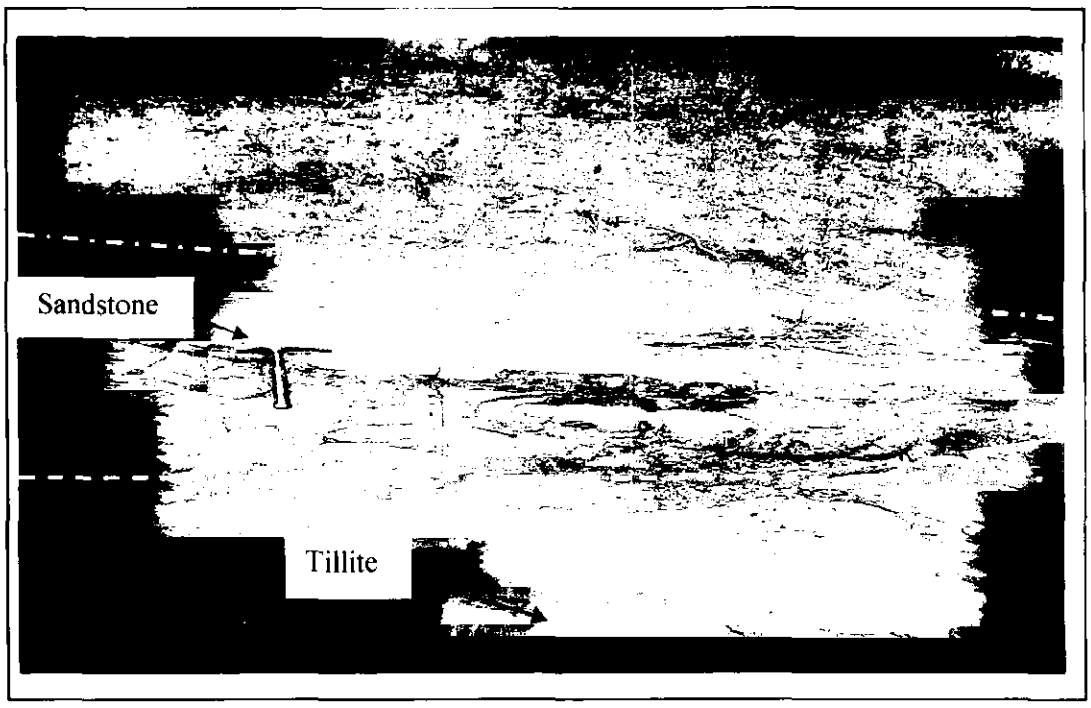

Plate 1.6.2: Tillite, Sandstone bed along side Kudra nala, Chirimiri Coalfield, Koriya district, Chhattisgarh India

Plate 1.6.3: Sandstone with occurrence of few pebbles of quartzite (encircled) found near Kudra stream section in Chirimiri, district Koriya, Chhattisgarh, India.

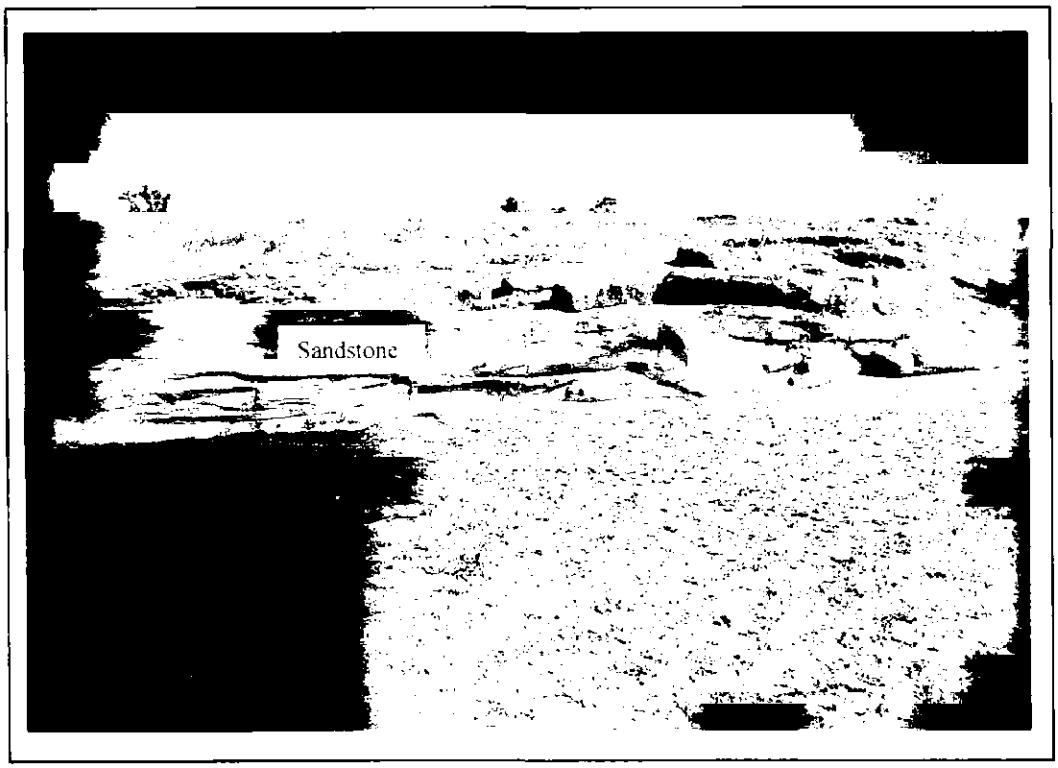

Plate 1.6.4: Sandstone along Ghorghera stream section in Chirimiri, district Koriya, Chhattisgarh, India.

Plate 1.6.5: Olive green sandstone along Halphali stream near Nagpur Village Road, Chirimiri, district Koriya, Chhattisgarh, India.

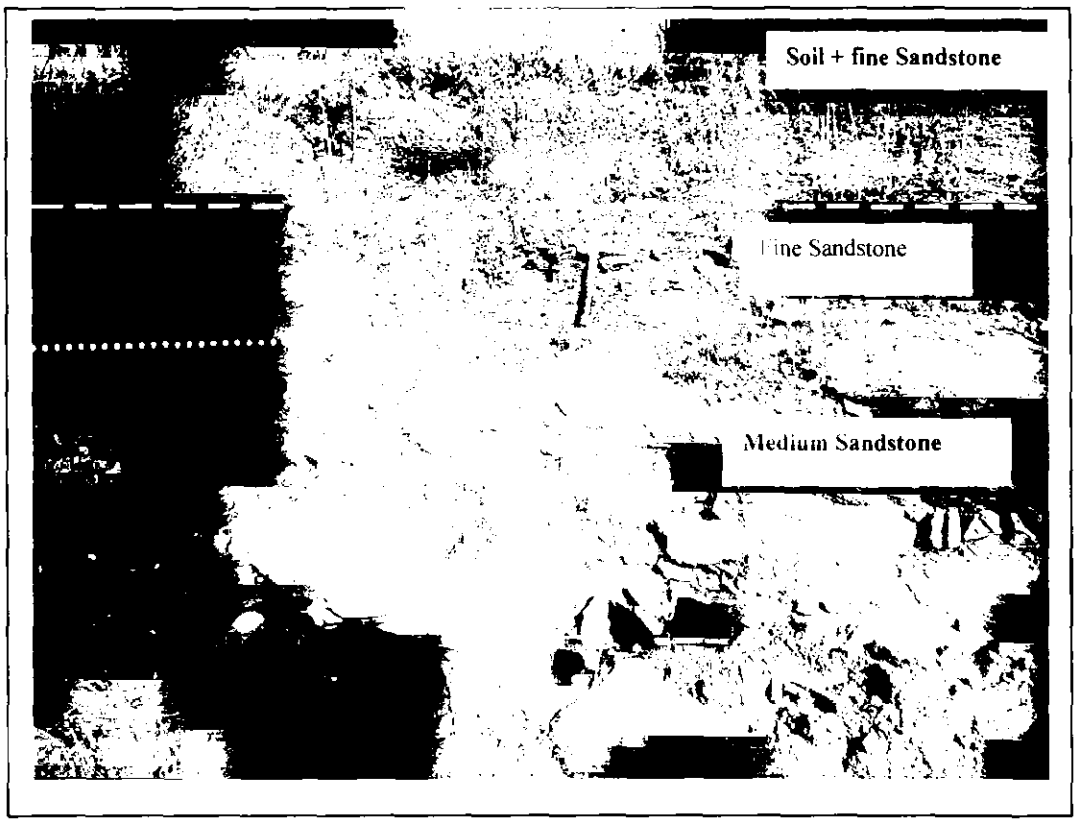

Plate 1.6.6: Lemon Yellow colour sandstone with fining upward sequence, along Nagpur Village Road, Chirimiri, district Koriya, Chhattisgarh India.

Plate 1.6.7: Olive green thinly laminated shale along stream near Bhukbhuki Village, Chirimiri, Koriya district, Chhattisgarh, India.

Plate 1.6.8: Alternate beds of thinly laminated mudstones and sandstones of variable thickness, along Kudra stream section, Baikunthpur road Chirimiri, district Koriya, Chhattisgarh, India.

CHAPTER – 2

PETROGRAPHY

PETROGRAPHY

2.1 General statement

Sediments and sedimentary rocks occupy the largest surface area of the earth. Among these rocks sandstone is the most extensively studied rock both petrographically and geochemically. Sandstone is a terrigenous rock formed due to induration of particles with diameters ranging from 2mm to 1/16 (0.0625) mm. Sandstones constitute between 10 percent and 20 percent of sedimentary cover of the Earth. Like other clastic sedimentary rocks the composition of sandstone is the ultimate result of a number of factors like relief, composition of source rock and climate (Johnsson 1993; Suttner & Dutta, 1986; Dickenson et al., 1983). The intent of study of sedimentary rocks is to reconstruct and interpret the history from the initial erosion of the parent rocks to the final burial and diagenesis of the sediments.

The composition of sandstones can be ascertained by two fundamental procedures: Petrography (mineral composition and texture) and/or geochemical analysis (von Eynatten et al., 2003). Classical technique of modal analysis of detrital frame work grains is a reliable method to determine the composition of sandstones. Modal analysis involves determining the volume fraction of constituent minerals in a rock by studying the thin section under petrological microscope. This method provides an accurate data of distribution and volume of the mineral percent present within the thin section. It is well established to quantitative detrital modes, calculated from point counting in thin section to infer provenance of sandstones (Dickinson and Suczeck, 1979).

Petrological data helps to differentiate between grains of detrital origin to those of insitu grains, grain size, and textural characters. Pattern of distribution of grains reveals mode of transportation and the condition of the current prevailing at the time of deposition of the sediments. Tectonic setting of the provenance apparently exerts primary control on composition of sandstones (Dickinson et al., 1983). Petrographic studies of Gondwana sediments of India are very sketchy. At present there is paucity of detailed petrographic data on these sediments. Some notable contributions on the modal analysis has been made by Khan, (1978) Tewari, (1980), Rais, (1985) Ramanamurthy, (1985), etc. However, no information about detailed petrographic investigation, on Talchir sediments of Chirimiri area is available in the published literature.

2.2 Sampling and Methodology

Talchir Formation, the lowermost unit of Gondwana Supergroup, is overlain by Barakar Formation in the study area. 50 samples were collected out of which 29 samples were selected for detailed petrography. Fresh samples of sandstones and shales belonging to Talchir Formation were collected along stream and road cuttings covering the entire area both in space and time. The rocks samples collected in the vicinity of Chirimiri town have been christened as Chirimiri sandstones and those from Chirimiri-Baikunthpur road cuttings have been named as Baikunthpur sandstones. Thin sections were prepared following standard procedure. Petrography is carried out using Gazzi-Dickenson's method (Dott, 1964; Basu et al., 1976; Dickinson and Suczeck 1979; Ingersoll et al, 1984; Dickinson et al., 1983; and Suttner & Dutta 1986) Compositional percentages of samples were based on 350 point counts per thin section for modal analysis. Parameters like QFR, QtFL, QmFLt, QpLvLs, QmPK and Qt/F+Rx vs. Qp/F+Rx have been employed for classification of sandstones and identification of nature of provenance, paleoclimate, and tectonic regime of the depositional basin and also for classification of sandstones. Clay, iron cement, and carbonate cement and matrix were not taken into consideration for this method albeit types of cement and matrix were analysed in petrography. Mineral grains showing slight alteration were treated as fresh and counted. Data thus generated was recalculated and presented in tables respectively and plotted in different triangular diagrams (Dickinson, 1985).

2.3 Modal Analysis

2.3.1Talchir Sandstone

The Talchir sandstone samples collected from around Chirimiri and Baikunthpur road, Koriya district, Chhattisgarh, are characterised by abundance of quartz, feldspar and lithic fragments with small fraction of heavy minerals. A detailed petrographic investigation of the Talchir sandstones of the study area is as follows:

(a) Quartz: The percentage of quartz ranges from 44.06 to 72.22 percent in the thin sections of sandstones of Chirimiri area and 36.00 to 57.59 percent in sandstones of Baikunthpur road section. Quartz is represented by both monocrystalline and polycrystalline quartz. Monocrystalline quartz grains are more abundant than polycrystalline variety in these thin sections. A few monocrystalline quartz grains show straight to undulatory extinction and first order yellow to grey interference

colours. Grains with grey interference colour show intense deformation, Boehm lamella (strain lamella) has also been noted in some of these grains. Quartz grains are usually anhedral, sub rounded to round and oblate in shape. Few quartz grains also exhibit inclusions of some heavy minerals (Plate 2.3.1 (A) and (B)).

(b) Feldspar: In order of abundance, detrital feldspar comes next to quartz. Different varieties of feldspar range from 10.08 to 32.26 percent in Chirimiri sandstone and 16.66 to 55.55 percent in Baikunthpur sandstones by volume. K-feldspar dominates over plagioclase and orthoclase is more abundant than microcline and plagioclase. Majority of microcline and plagioclase grains are fresh, however, some of them show alteration along cleavage planes. Few orthoclase grains also exhibit alteration. Grains of perthite are also found in some of the studied samples (Plate 2.3.2 (C, D) and 2.3.3 (E, F)

(c) Lithic Fragments: Rock fragments range from 0.87 to 12.18 in Chirimiri sandstones and 1.88 to 12.5 percent in Baikunthpur sandstones by volume. Sedimentary rock fragments such as shale, chert and siltstone are most dominant followed by fragments of gneiss, phyllite and schist (Plate 2.3.4, G, H) with few fragments of granite. Flakes and laths of muscovite and biotite have also been identified in these thin sections. The mica ranges from 0.21 to 16.66 in Chirimiri sandstones and 0.46 to 6.24 in Baikunthpur sandstones (Plate 2.3.4, K, L).

(d) Heavy Minerals: Talchir sandstones of the study area are characterised by abundance of several varieties of heavy minerals. Some of the common heavy minerals identified in these sandstones are zircon, garnet and opaque. Rutile, epidote, tourmaline have also been noted in small number in these thin sections of sandstones (Plate 2.3.5 (J)).

(e) Matrix: The entire framework of these sandstones is bounded by very fine clayey matrix. The clay matrix ranges from 2 to 31.25 percent in Chirimiri sandstone and 0.02 to 20.85 percent in Baikunthpur sandstones. Iron cement around the edges of grains constituents has also been noted in most of the samples. The Iron cement ranges from 0.01 to 3.8 in Chirimiri sandstone and 0.04 to 9.25 percent in Baikunthpur sandstones. In some Chirimiri sandstones samples calcite cement has also been observed and it ranges from 0 to 3.57 percent (Plate 2.3.7 and 2.3.8), whereas it is absent in Baikunthpur sandstones.

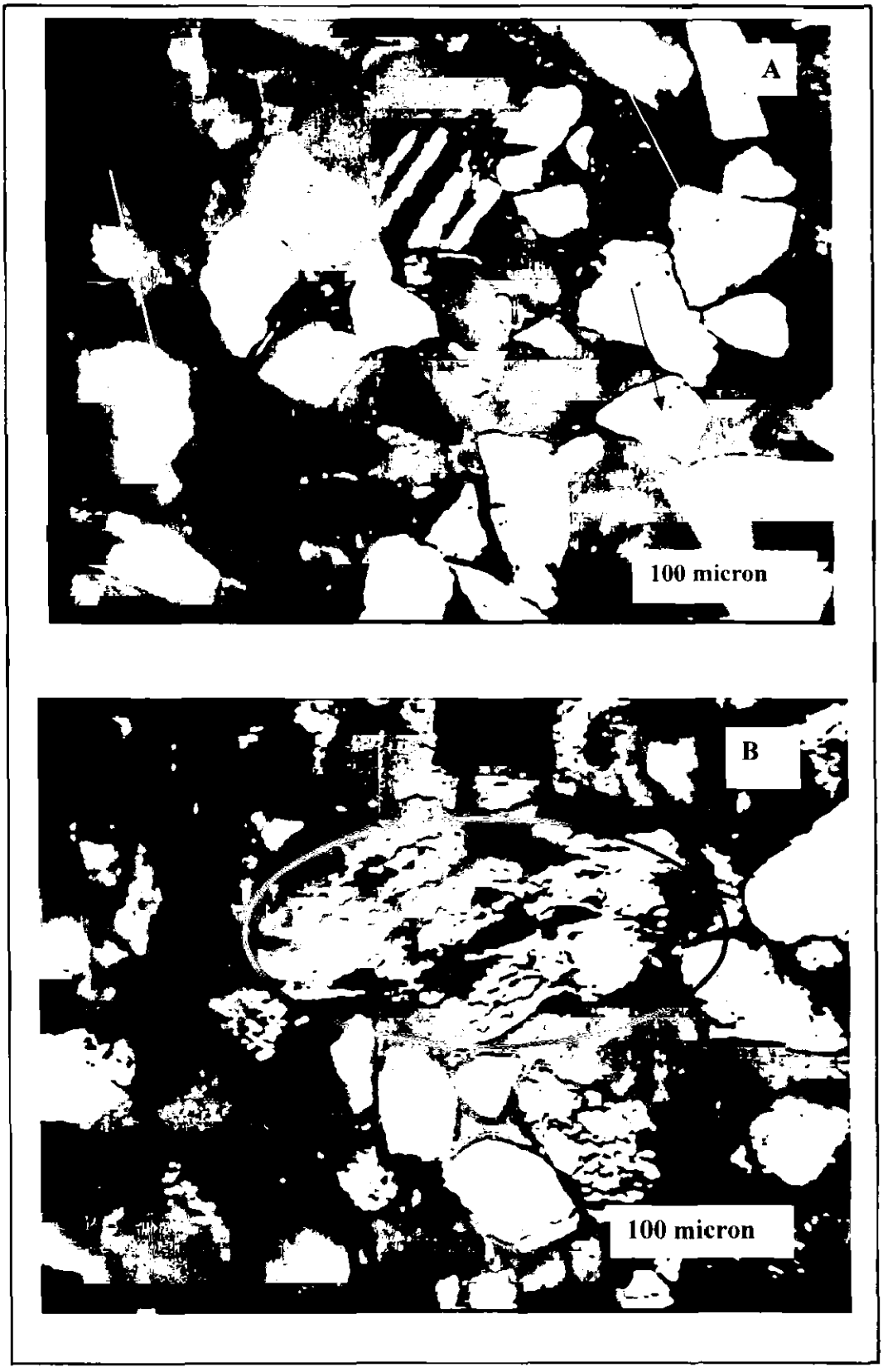

Plate 2.3.1: (A) Thin section microphotograph of Monocrystalline quartz and (B) Polycrystalline quartz present in sandstones of Talchir Formation, Chirimiri, district Koriya, Chhattisgarh, India

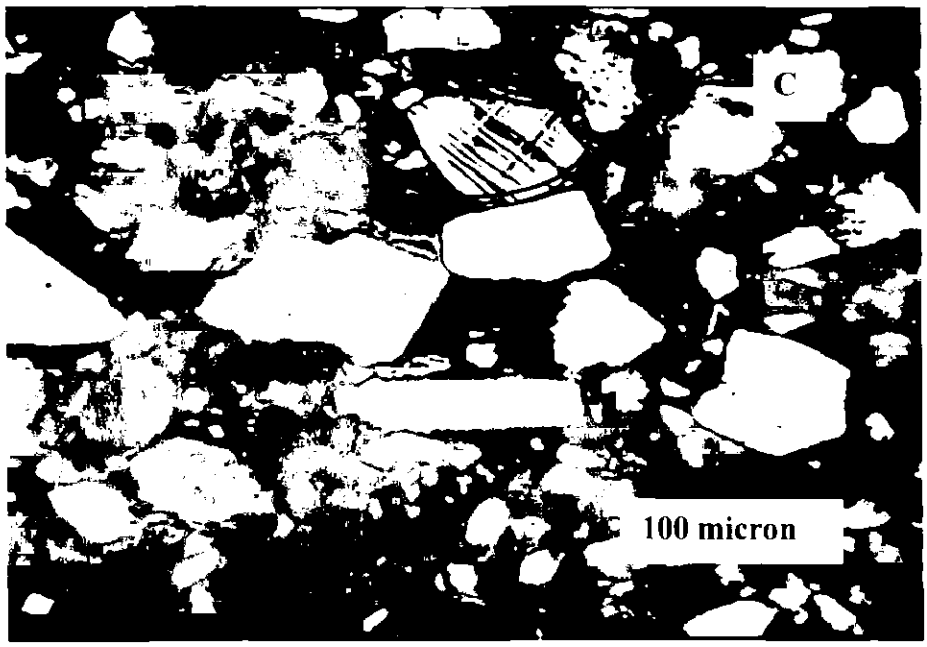

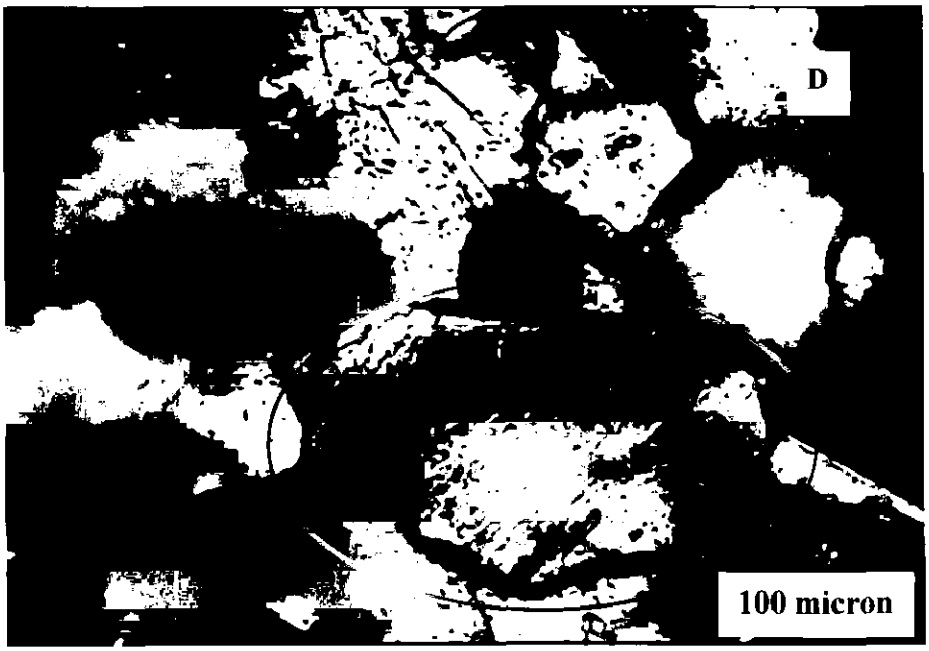

Plate 2.3.2: (C) Thin section microphotograph of Microcline grain (D) Orthoclase grain found in sandstones of Talchir formation, Chirimiri, district Koriya, Chhattisgarh, India

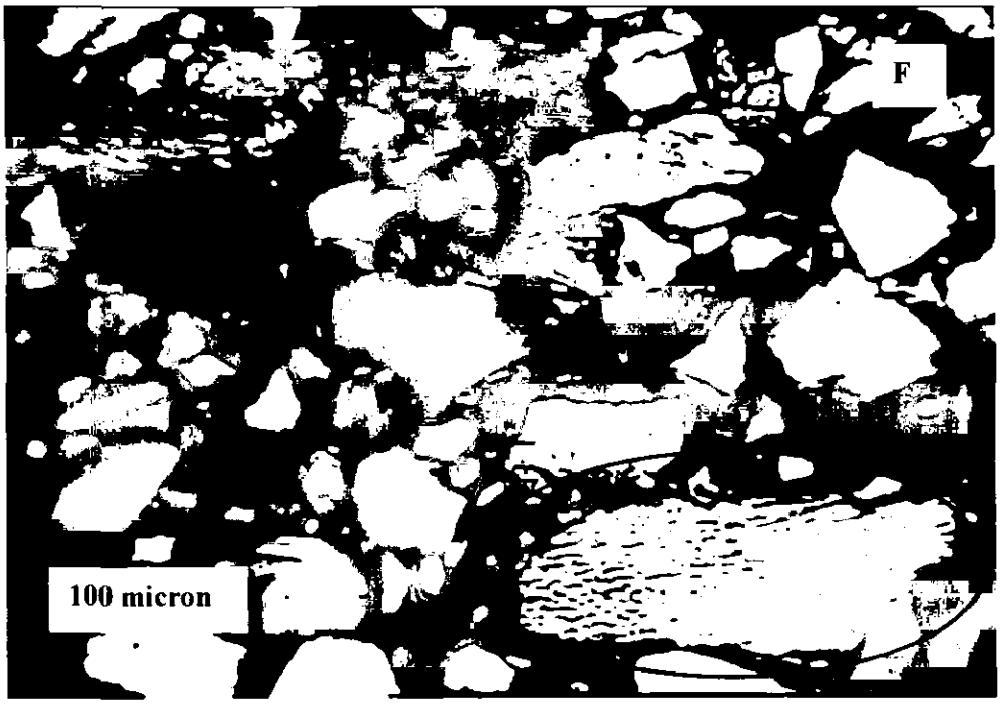

Plate 2.3.3: (E) Thin section microphotograph of Plagioclase grain with quartz inclusion (F) perthite grain found in sandstones of Talchir Formation, Chirimiri, district Koriya, Chhattisgarh, India.

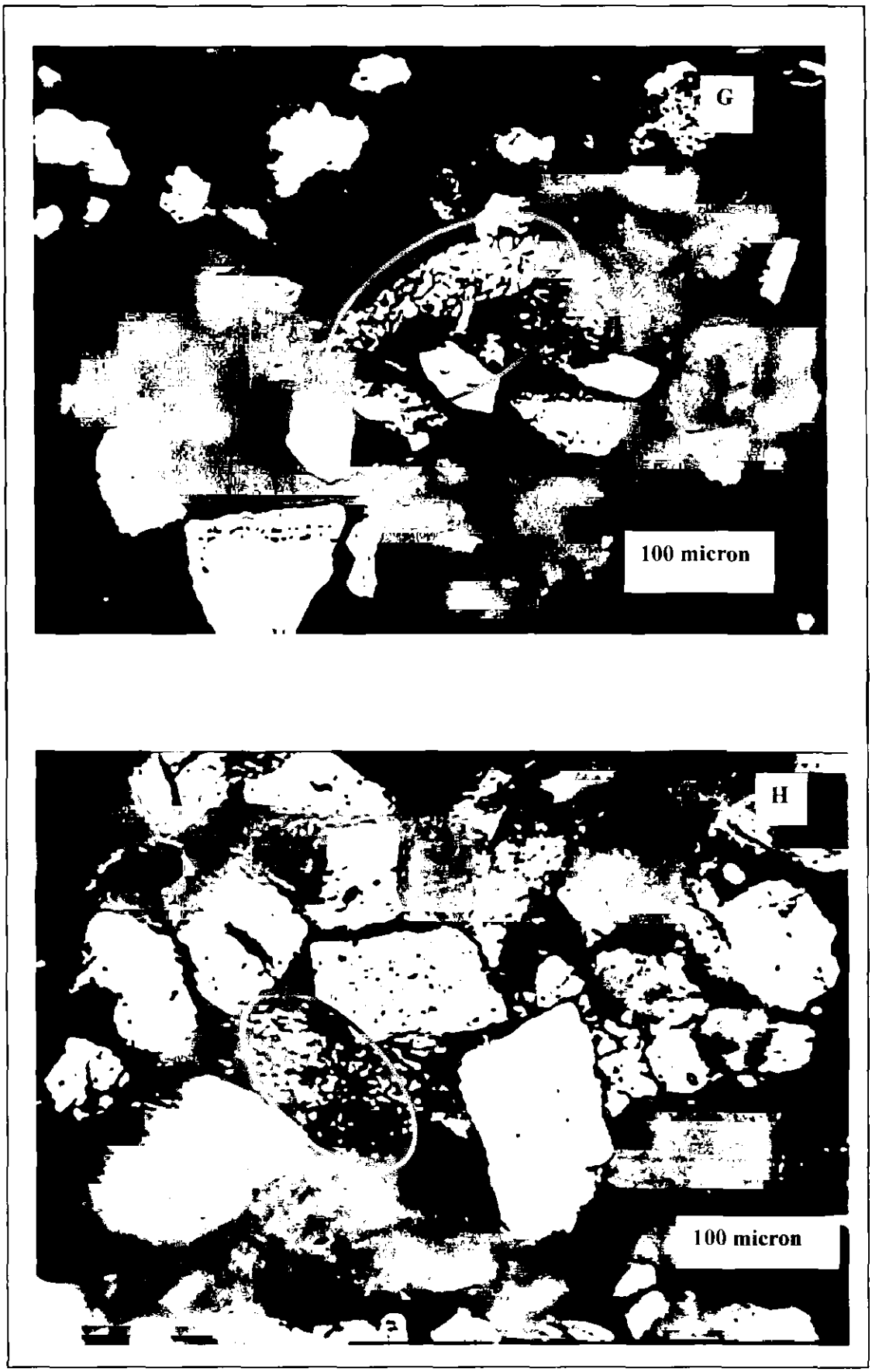

Plate 2.3.4: (G) Thin section microphotograph of schist rock fragment and (H) Phyllite rock fragment found in sandstones of Talchir Formation, Chirimiri, district Koriya, Chhattisgarh, India.

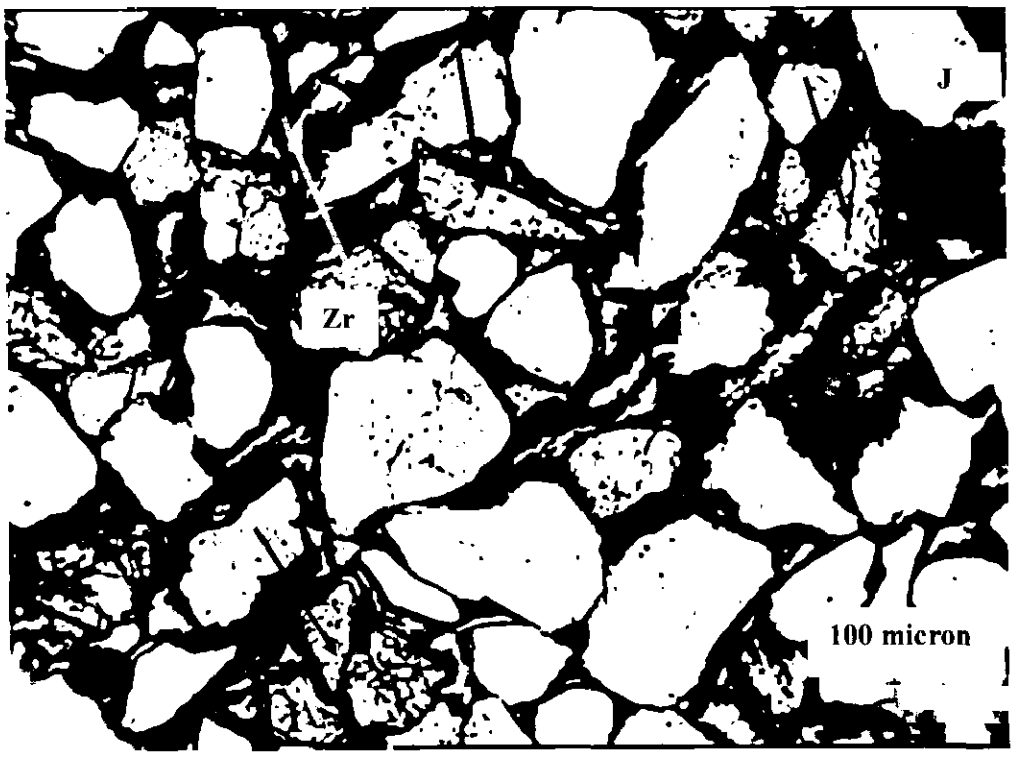

Plate 2.3.5: (I) Thin section microphotograph of granite detrital grain with inclusion of heavy mineral and (J) heavy minerals found in the sandstones of Talchir Formation, Chirimiri, district Koriya, Chhattisgarh, India

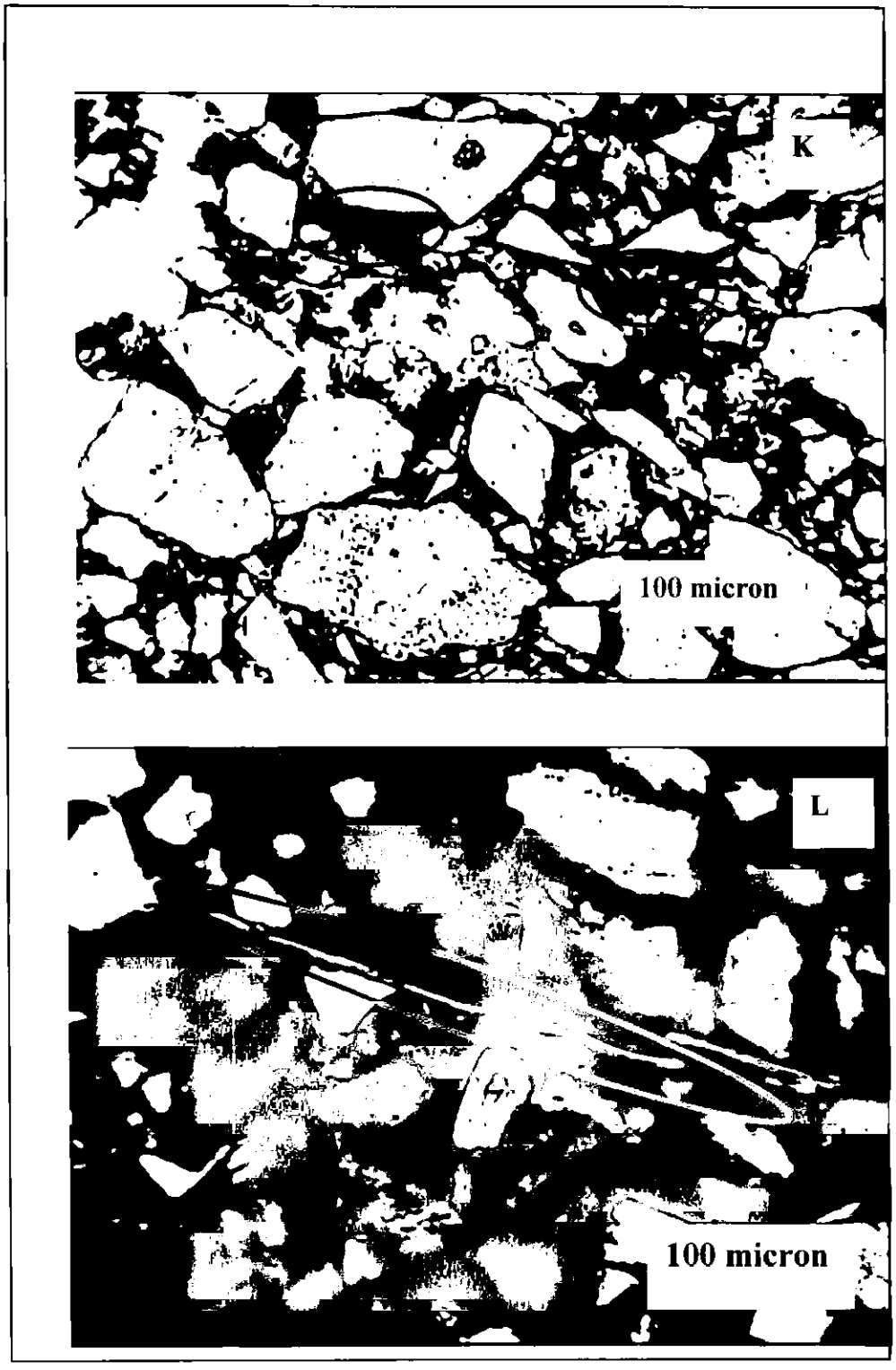

Plate 2.3.6: (K) Thin section Microphotograph of Biotite mineral and (L) a small ribbon of muscovite flake found in sandstones of Talchir Formation, Chirimiri, district Koriya, Chhattisgarh, India

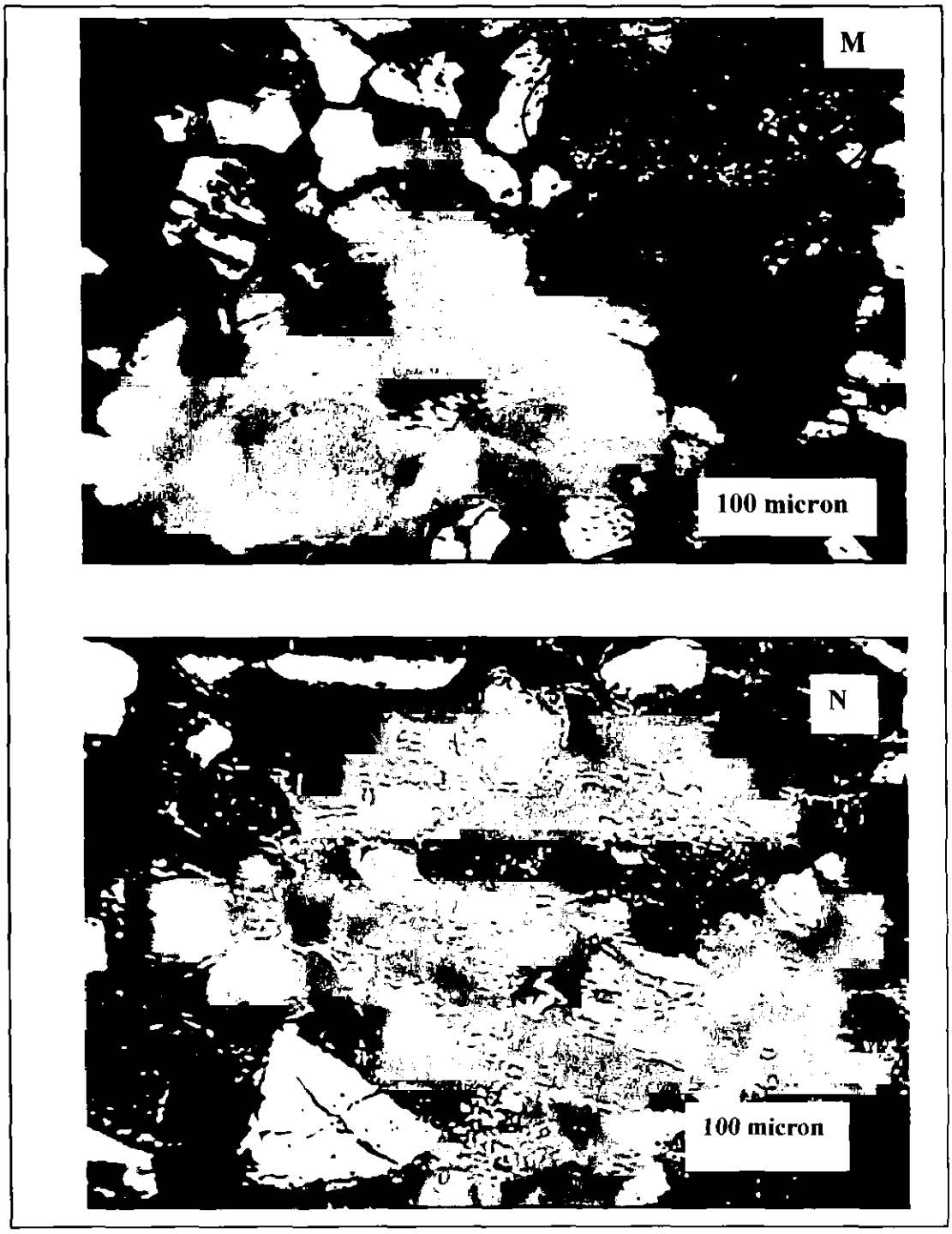

Plate 2.3.7: (M) Thin section Microphotograph of ferruginous cement and (N) Arrows indicating pore filling clay around the grains boundaries, found in sandstones of Talchir Formation, Chirimiri, district Koriya, Chhattisgarh, India.

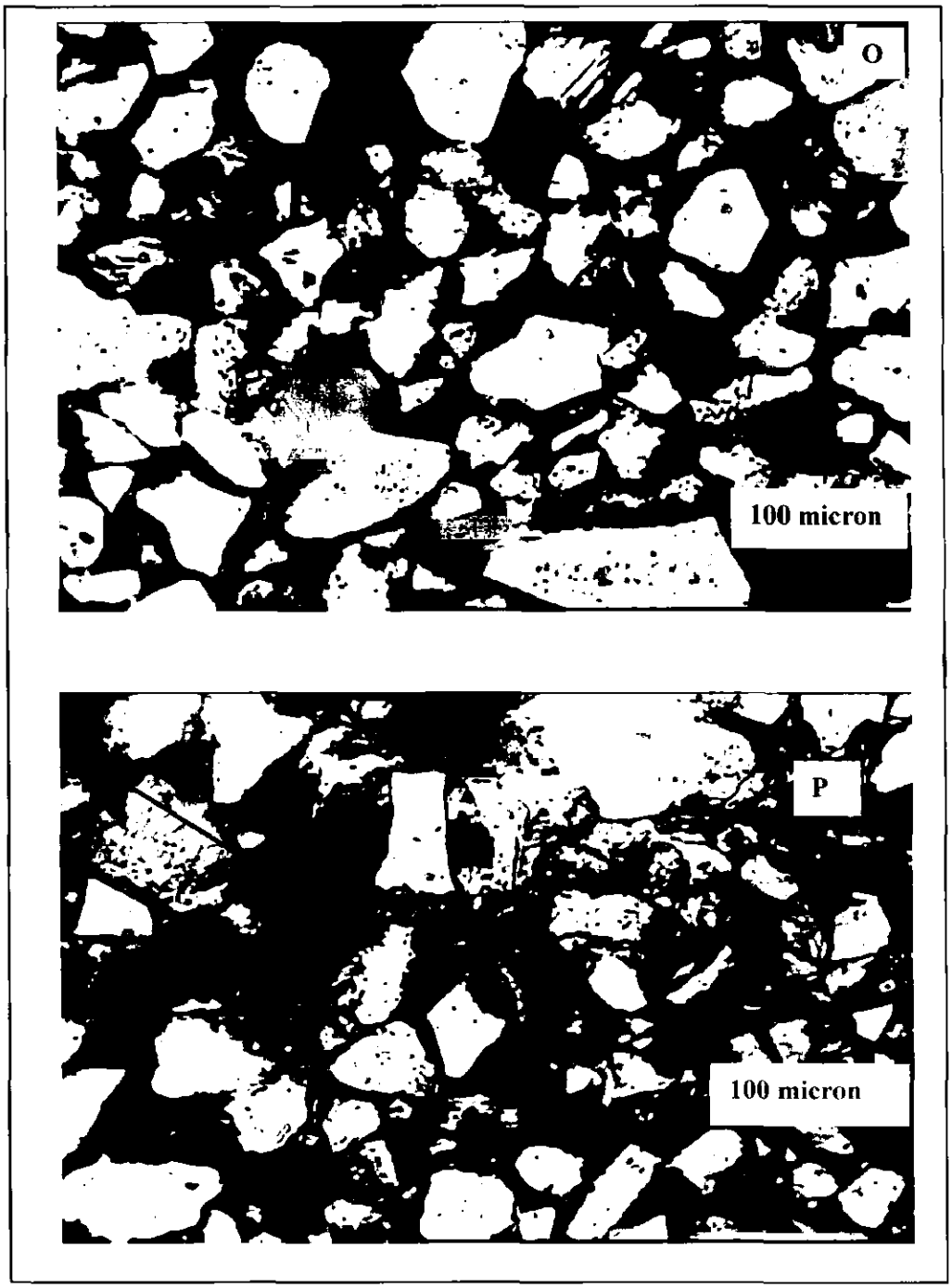

Plate 2.3.8: (O) Thin section Microphotograph showing undifferentiated matrix. (P) Arrow indicates post depositional iron cement in sandstones of Talchir Formation, Chirimiri, district Koriya, Chhattisgarh, India

Table 2.3.1: Recalculated modal abundances of sandstones of Talchir Formation in Chirimiri area, district Koriya, Son-Mahanadi basin Chhattisgarh India.

		Quartz			Feldspar			Mica			Rock Fragment					Cement/Matrix			
		Monocrystalline	Polycrystalline																
	S.No	Common	recrystallized	stretched	Orthoclase	Microcline	Plagioclase	Muscovite	Biotite	Chert	Shale	Siltstone	Phyllite	Schist	Granite/Gneiss	Iron	Clay	Calcite	Total
Chirimiri Sandstone	NT1	44.06	0	0	22.03	5.93	0	5.93	0	0.84	0	0	0.03	0	0	0	21.18	0	10
	NT2	45.2	0	0	31.05	1.36	8.21	3	0	0	1	0	0	0	0	0.18	10	0	10
	NT3	48.24	0	0	13.15	8.77	13.15	2.63	0	0.87	2.63	0	1.5	0	0	3.8	5.26	0	10
	NT5	46.96	0	0	15.15	1.51	7.57	12.12	0	0	3.03	0	0.03	0	0	0	13.63	0	10
	NT7	36.66	0	0	10	0	13.33	16.66	0	0	13.33	0	0	0	0	0.02	10	0	10
	RB8	70.93	0.98	0	16.25	0.98	4.43	0	0	0	0.49	0	0	1.97	0.03	0	3.94	0	10
	RB9	60.71	0	0	18.45	4.76	2.38	0	0	0	3.57	0	0	3.57	0.02	0	6.54	0	10
	RB10	67.74	0	0	11.29	0	11.29	0	0	0	0	0	0	0	0	0.01	9.67	0	10
	RB12	47.07	1.96	0	23.52	1.96	5.88	0	0	0	0	0	0	3.92	0	0	15.68	0.01	10
	RB13	72.22	0	0	8.88	4.44	1.11	0	0	0	0	0		0	0	0.02	13.33	0	10
	RB14	50	0	0	19.64	3.75	8.92	0	0.21	0.89	0.89	0.63	2.53	0	2.69	0.93	8.92	0	10
	GN1	50.22	11.76	0	15.83	7.69	3.61	0.54	0.25	2	3	0	0.11	0.02	2	0	2	0.97	10
	GN2	62.26	4.05	0.45	15.76	2.25	2.25	1	0	6	0	0	0.13	0	0	0	5.85	0	10
	GN3	47.91	0	0	12.5	2.08	2.08	0	0	4.16	0	0	0.02	0	0	0	31.25	0	10
	GN4	52.97	1.19	0	18.45	4.76	2.38	3.57	0	7	0	0	0.7	0	0	0	8	0.98	10
	GN5	68.04	0	0	10.3	0	7.21	0	0	2.06	0	0	0	0.02	0	0	12.37	0	10
	GN6	60	1.42	2.85	12.85	2.85	0	0	0	1.42	4.28	2.85	0	0	0.06	0.42	11	0	10
	GN7	57.79	5.5	0	13.3	3.21	7.79	0.45	0	1.37	0	0	0	1	1.83	0.2	7.33	0.23	10
	GN8	52.86	11.47	0	12.29	2.04	0.81	2.45	0	0.81	0.4	0	0.24	2	2.25	3.45	8.28	0.65	10
	GN9	48.21	5.35	0	20.98	1.78	2.23	0	0	3.57	3.12	1.99	2	1.5	0	0.35	5.35	3.57	10
	GN10	63.18	1.36	0.45	19.09	2.72	2.27	0	0	1.81	0.45	0	0.22	0	0.45	0	8	0	10
	GN11	73.1	6.72	0	5.88	3.36	0.84	0	0	1.68	0	0	0	0	0	0	8.4	0.02	10
Sandstone	BBK1	41.07	0	0	27.67	2.67	0	3.57	2.67	1.78	3.57	0	0.05	2.67	0.89	0	13.39	0	10
	BBK3	34.25	1.85	0	29.62	0	0	4.62	0	0	0	0	0.05	1.85	0	9.25	18.51	0	10
	BBK4	37.93	0	0	44.82	5.17	3.44	2.58	0	2.58	0.86	0	0	0.86	1.72	0.04	0	0	10
	BBK5	38.88	0	0	55.55	0	0	0	0	0	5.55	0	0	0	0	0	0.02	0	10
	BBK6	49.3	8.29	0	19.81	2.76	8.29	0.46	0	0.46	0	0	1.42	0	0	0	9.21	0	10
	BBK7	33.33	16.66	0	2.08	6.25	8.33	0	0	0	0	0	0	12.5	0	0	20.85	0	10
	BBK8	45.39	2.12	0	39	0	0	2.12	0	0	0	0	0	2.12	0	0.74	8.51	0	10

Table 2.3.2: Keys for Petrographic and other parameters used in this study (after Dickinson 1985)

QFR		
	Q	Total Quartz grains (Qm+Qp)
	Qm	monocrystalline quartz
	Qp	polycrystalline quartz
	F	Total Feldspar (P+K)
	P	Plagioclase
	K	alkali feldspar
	R	Total rock fragments including chert
QtFL		
	Qt	Total quartz grains (Qm+Qp)
	Qm	monocrystalline quartz
	Qp	polycrystalline quartz
	F	Total Feldspar (P+K)
	P	Plagioclase
	K	alkali feldspar
	L	Total lithic fragments
QmFLt		
	Qm	monocrystalline quartz
	F	Total Feldspar (P+K)
	P	Plagioclase
	K	alkali feldspar
	Lt	Total rock fragments including polycrystalline quartz
QpLvLs		
	Qp	polycrystalline quartz
	Lv	Total volcanic and Meta-volcanic rock fragments
	Ls	Total sedimentary rock fragments
LmLvLs		
	Lm	Total metamorphic rock fragments
	Lv	Total volcanic rock fragments
	Ls	Total sedimentary rock fragments
Qp/F+RF vs. Qt/F+RF		
	Qt	Total quartz grains (Qm+Qp)
	Qm	monocrystalline quartz
	Qp	polycrystalline quartz
	F	Total Feldspar (P+K)
	RF	Total rock fragments

Table 2.3.3: Recalculated data of Talchir Formation Sandstones in parts of Chirimiri, district Koriya, Chhattisgarh, India (after Dickinson, 1985).

		QFR			QtFL			QmFLt			QmPK			QpLvLs				
	S.No	Q	F	R	Qt	F	L	Qm	F	Lt	Qm	P	K	Qp	Lv	Ls	Qp/F+R	Qt/F+R
Sandstone	NT1	73.36	17.86	8.78	77.38	17.86	4.76	63.59	17.86	18.55	66.66	4.44	28.9	70	0	30	0.11	1.52
	NT2	68.86	21.15	9.99	72.12	21.15	6.73	64.46	21.15	14.00	76	3	21	45.5	0	54.5	0.12	1.37
	NT3	64.95	24.24	10.81	69.70	24.24	6.06	60.00	24.24	15.76	74.2	3.22	22.58	0	0	100	0.25	1.1
	NT5	59.34	29.25	11.41	61.90	29.25	8.84	60.00	29.25	10.75	67.42	3.02	29.56	13.33	0	86.67	0.21	1.23
	NT7	71.72	21.00	7.28	77.00	21.00	2.00	70.00	21.00	9.00	79.53	8.43	12.04	0	0	100	0.13	1.18
	RB8	71.38	17.35	11.27	74.20	17.35	8.45	70.00	17.35	12.65	79.24	0	20.76	33.33	0	66.67	0.03	1.38
	RB9	67.00	27.60	5.40	68.75	27.60	3.65	65.00	27.60	7.40	69.38	9.82	20.8	66.67	16.66	16.67	0.17	1.55
	RB10	76.33	18.41	5.26	78.61	18.41	2.99	65.26	18.41	16.33	77.84	1.2	20.96	80.02	11.41	8.57	0.12	1.55
	RB12	60.23	29.47	10.30	63.16	29.47	7.37	60.00	29.47	10.53	65.85	3.04	31.11	44.44	0	55.56	0.06	1.56
	RB13	67.20	26.23	6.57	70.78	26.23	2.99	65.00	26.23	8.77	72.39	2.6	25.01	40	10	50	0.11	1.56
	RB14	75.00	11.00	14.00	87.27	11.00	1.82	73.00	11.00	16.00	87.27	2	10.73	80	0	20	0.26	1.64
	GN1	58.00	38.37	3.63	60.46	38.37	1.17	57.00	38.37	4.63	60.47	0	39.55	0	0	100	0.28	2.05
	GN2	48.00	40.35	11.65	57.89	40.35	1.76	47.00	40.35	12.65	56.90	0	43.1	0	0	100	0.16	1.54
	GN3	46.00	43.26	10.74	52.40	43.26	4.34	44.00	43.26	12.74	55	15	30	0	0	100	0.23	1.68
	GN4	50.00	39.48	10.52	55.26	39.48	5.26	49.75	39.48	10.77	58.33	5.55	36.12	0	0	100	0.03	1.62
	GN5	60.50	29.17	10.33	68.83	29.17	2	60.00	29.17	10.83	65	0	35	0	0	100	0.2	0.91
	GN6	65.00	28.43	6.57	68.94	28.43	2.63	62.00	28.43	9.57	70.49	4.26	25.25	66.66	0	33.34	0.17	2
	GN7	64.00	24.58	11.42	68.57	24.58	6.85	60.00	24.58	15.42	73.61	2.47	23.92	0	0	100	0.21	1.05
	GN8	73.36	23.64	3.00	76.31	23.64	0.05	70.00	23.64	6.36	76.36	1.81	21.83	0	0	0	0.7	1.95
	GN9	52.00	34	14.00	65	34	1	51.00	34	15.00	60	7.5	32.5	0	0	0	0.	1.69
	GN10	78.00	16.46	5.54	82	16.46	1.54	70.00	16.46	13.54	85.71	1.3	12.99	0	0	0	0.06	1.46
	GN11	58.00	35.96	6.04	62.92	35.96	1.12	55.00	35.96	9.04	63.64	0	36.36	33.33	0	66.67	0.15	1.92
	Average	**64.01**	**27.15**	**8.84**	**69.07**	**27.15**	**3.79**	**61.00**	**27.15**	**11.83**	**70.06**	**3.58**	**26.37**	**26.06**	**1.73**	**58.58**	**0.18**	**1.52**
	BBK1	49	42	9	50.00	42	8.00	42.00	42	16.00	51	0	49	0	14.29	85.71	0.11	0.83
	BBK3	53	44	3	55.00	44	1.00	50.00	44	6.00	53.62	0	46.38	100	0	0	0.05	1.14
	BBK4	70	24	6	72.00	24	4.00	60.00	24	16.00	42.3	3.84	53.86	100	0	0	0.05	1.43
	BBK5	41	49	10	50.00	49	1.00	40.00	49	11.00	45.5	0	54.5	0	33.33	66.67	0.17	1.17
	BBK6	38.89	55	6.11	44.00	55	1.00	35.00	55	10.00	63.69	10.71	25.6	100	0	0	0.35	0.63
	BBK7	68	22	10	76.77	22	1.23	60.00	22	18.00	66.66	16.66	16.68	90	0	10	0.26	1.72
	BBK8	56.62	40	3.38	59.00	40	1.00	51.00	40	9.00	57.37	0	42.63	75	0	25	0.03	1.3
	Average	**53.79**	**39.43**	**6.78**	**58.11**	**39.43**	**2.46**	**48.29**	**39.43**	**12.29**	**54.31**	**4.46**	**41.24**	**66.43**	**6.80**	**26.77**	**0.15**	**1.17**

2.4 Petrological Classification

Folk (1980) scheme of sandstone classification is adopted in the present work. Talchir sandstone samples of Chirimiri area, district Koriya has been plotted in ternary diagram (Figure 2.4.1). The figure shows that these sandstones can be classified as arkose, sub-arkose, and lithic-arkose types. The data obtained from petrography was recalculated in percentage as Quartz (Qt), Feldspar (F) and Rock fragments (L) and plotted in ternary as QtFL and QmFLt to constrain the provenance and tectonic setting of the source rock of the studied Talchir sandstones (Dickinson and Suczeck, 1979; Dickinson, 1985).

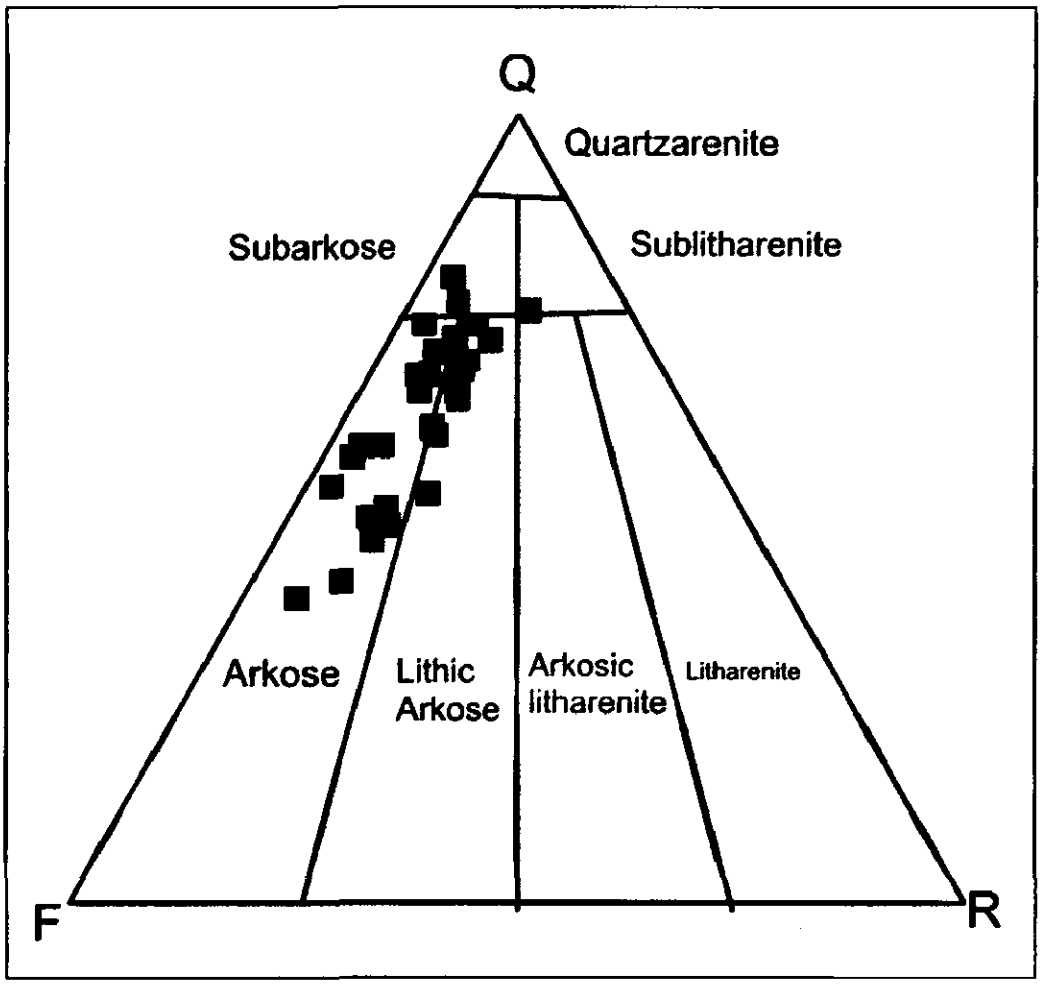

Figure 2.4.1: QFR ternary diagram for classification of Sandstones of Talchir Formation, Chirimiri, district Koriya, Chhattisgarh, India (after Folk, 1980)

2.5 Tectonic Setting of Provenance

In QtFL and QmFLt (Figure 2.5.1 and 2.5.2) ternary plots of Talchir sandstones fall in continental block, which is further classified into three regions such as craton interior, transitional continental region, and basement uplift. Basement uplift is the areas located along incipient rift belts and transform rupture zone within continental blocks. These tectonic zones shed arkosic sands mainly into adjacent linear troughs or local pull-a-part basins (Dickinson, 1985). The majority of these sediments fall in transitional region followed by basement uplift and recycled orogeny. The rock fragment based QpLvLs (Figure 2.5.4) diagrams show that some of these sediments have also been derived from collision suture and fold thrust belt areas.

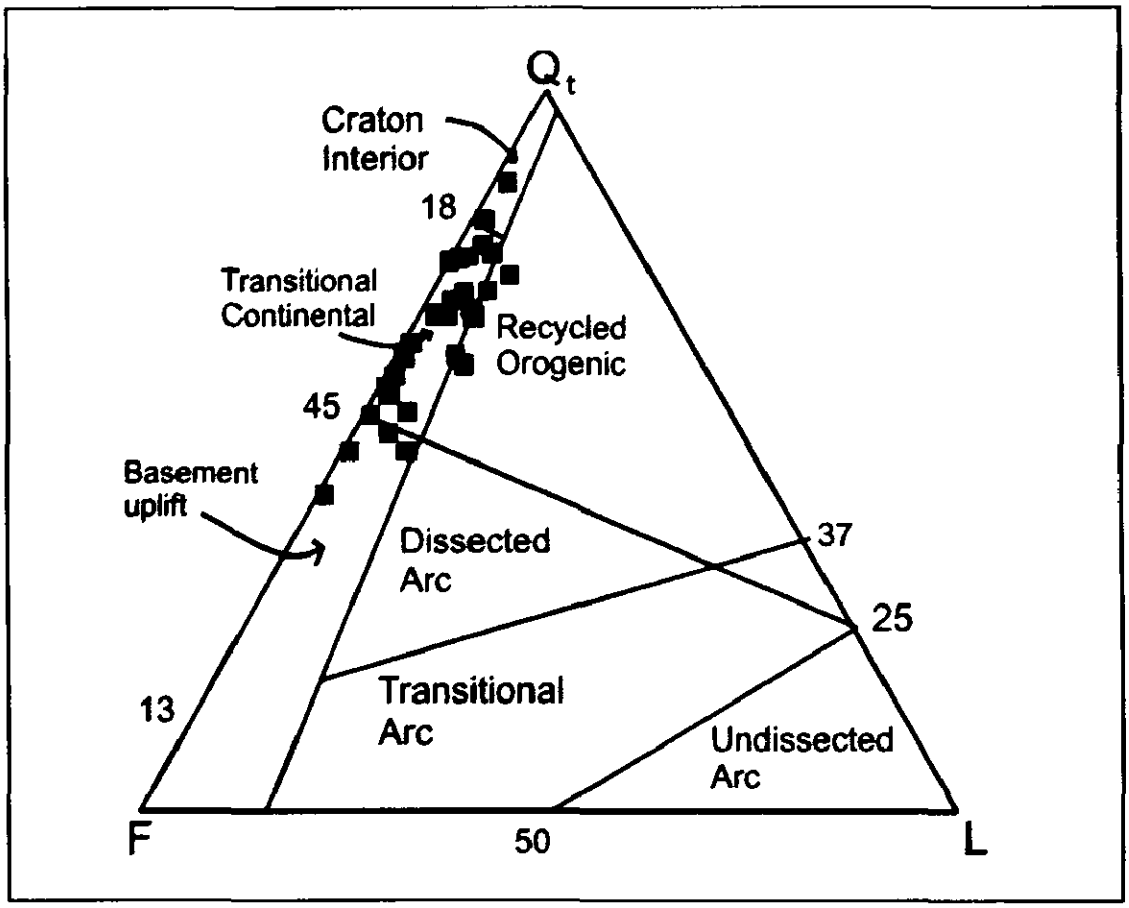

Figure 2.5.1: QtFL ternary diagram for sandstones of Talchir Formation, Chirimiri, district Koriya, Chhattisgarh, India (Dickinson, 1985).

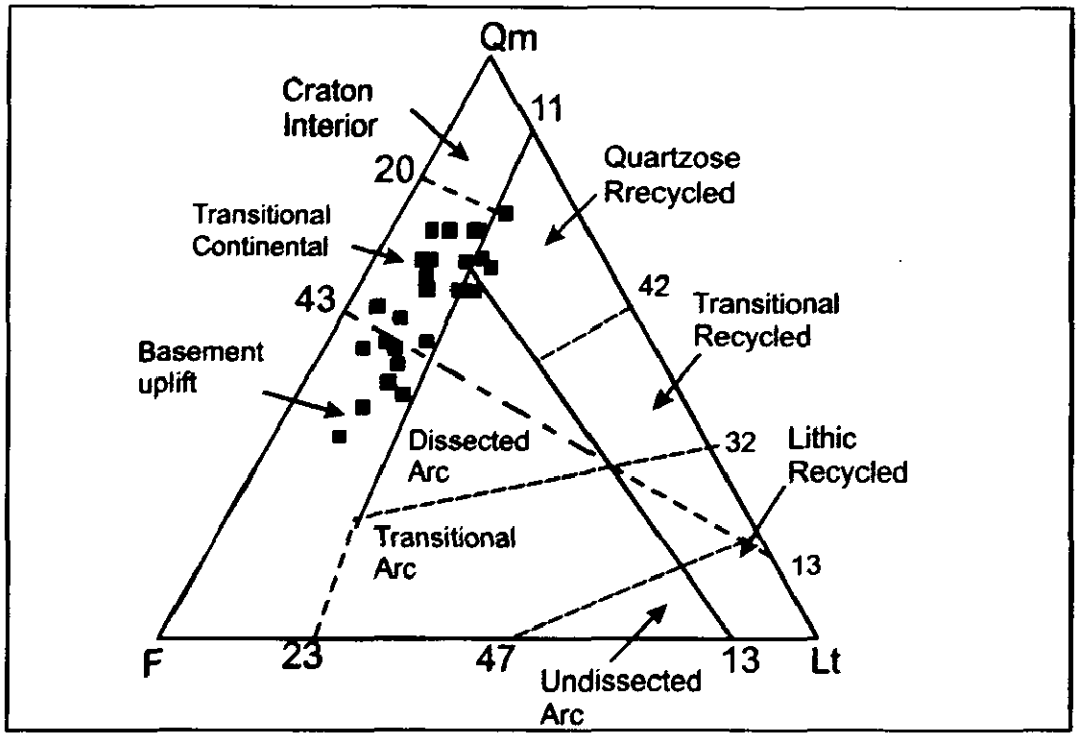

Figure 2.5.2: QmFLt ternary diagram for sandstones of Talchir Formation, Chirimiri, district Koriya, Chhattisgarh, India (Dickinson, 1985)

■ Baikunthpur Sandstone ■ Chirimiri Sandstone

In the QmPK (Figure 2.5.3) ternary diagram these sediments fall in between Qm-K line, this suggests that these sediments have been derived from continental block, which provides compositionally immature to sub mature sediments to the basin.

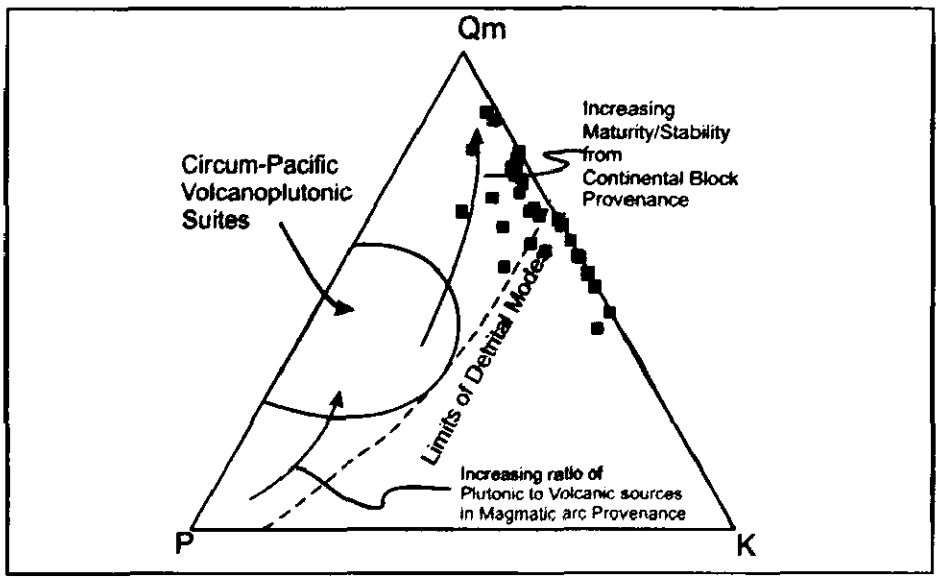

Figure 2.5.3: QmPK ternary diagram for sandstones of Talchir Formation in Chirimiri, district Koriya, Chhattisgarh, India (Dickinson, 1985).

■ Baikunthpur Sandstone ■ Chirimiri Sandstone

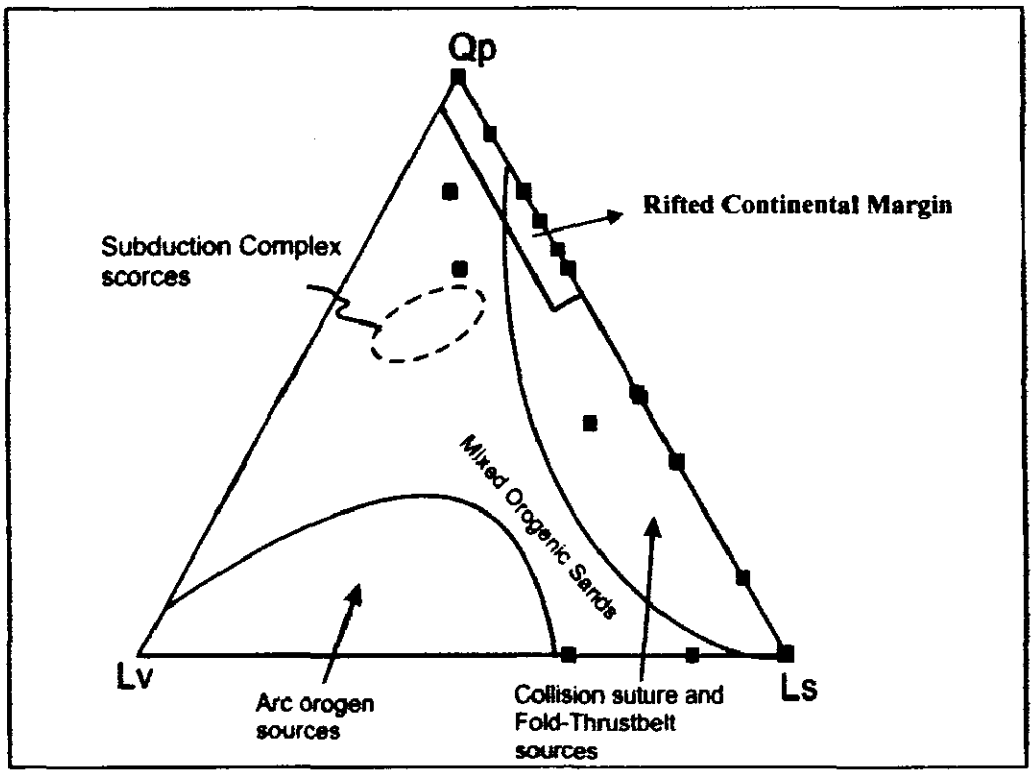

Figure 2.5.4: QpLvLs ternary diagram for sandstones of Talchir Formation in Chirimiri, district Koriya, Chhattisgarh, India (Dickinson, 1985).

■ Baikunthpur Sandstone ■ Chirimiri Sandstone

Bivariate plot of Qp/F+R versus Qt/F+R (Suttner and Dutta 1986) demonstrate that at the time of deposition of Talchir sandstones during Late Carboniferous to Early Permian the climate was semi-arid to semi-humid in this part of peninsular India.

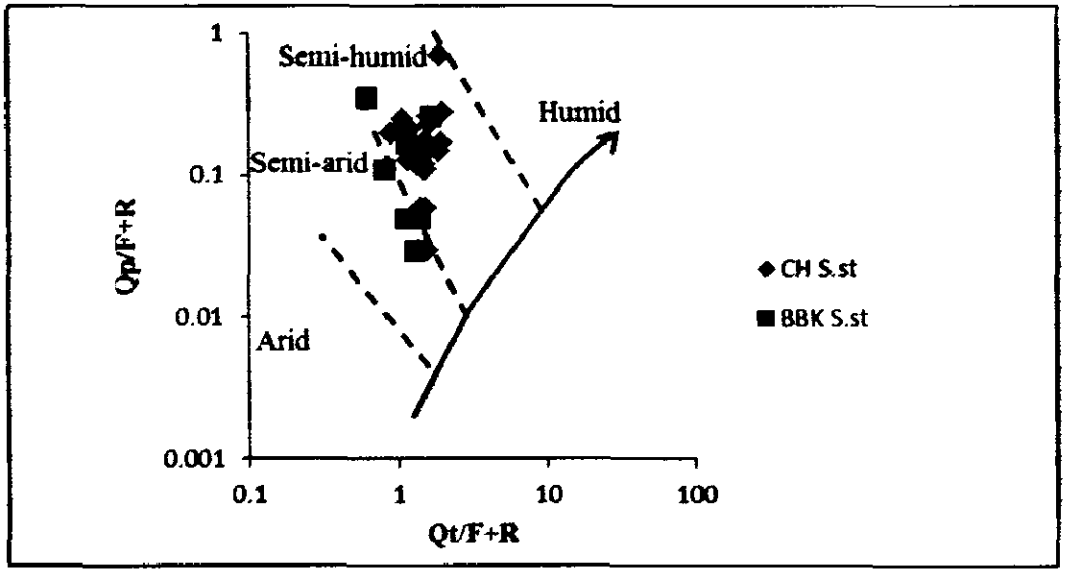

Figure 2.5.5: Binary diagram of Qt/F+R versus Qp/F+R (after Suttner and Dutta, 1986) for sandstones of Talchir Formation, Chirimiri, district Koriya, Chhattisgarh, India

Afore discussed petrological data reveals that the component particle of these Talchir sandstones of Chirimiri area, Koriya district have been derived from transitional margin of a continental block. Transitional regions are rifted portion of continent and most of the Gondwana sediments in India occur only in rifted graben (Mukhopadhyay et al., 2010). Continental block and recycled orogen have variety of rocks, ranging from felsic-intermediate-mafic igneous, metamorphic and sedimentary to volcano-sedimentary assemblages. Craton interior provides more quartz and feldspar rich sand as compared to transitional block, whereas basement uplift mostly supplies feldspathic sand to the depositional basin. Recycled orogen sediments are sedimentary and subordinate volcanic rocks, which are metamorphosed and exposed to the surface of erosion by uplift of fold belts. The sediments that were derived from transitional continental block; have their source within complex thrust sheets and recycled orogen. The studied samples show that during late Palaeozoic Era the climate changed gradually from Cold frigid arid glacial to Semi arid and humid due to drifting of Indian sub continent towards the equator (Suttner and Dutta, 1986). The presence of iron oxide cement in these studied thin section also an indicator of humid climate, which might have formed post-depositionally in hot, arid or semiarid climate (Basu, 1976; Walker, 1967; Folk, 1968).

These sandstones comprise variety of mono crystalline quartz ranging from angular to subrounded grains. In some of these grains strain lamellae also been observed. Angularity of grains signify that the sediments belong to from first cycle of erosion and have been transported from short distance whereas subrounded to rounded grains indicate second cycle of erosion or longer distance of transportation. The abundance of non-undulatory monocrystalline quartz over undulatory quartz suggests a plutonic source. Automorphic inclusion of heavy mineral like zircon and tourmaline are found in monocrystalline quartz fragments and grains of perthite are direct evidences of granitic source of these sandstones (Plate 2.3.3 (E and F) and 2.3.5 (J)). Some of the monocrystalline quartz are free from any inclusion of heavy minerals and show slight undulose extinction signifying that older gneissic or schistose rocks might have been the source of such grains (Pettijohn, 1975).

CHAPTER – 3

GEOCHEMISTRY

GEOCHEMISTRY

3.1 General Statement

The term "geochemistry" was first used by the German-Swiss chemist Christian Friedrich Schönbein in 1838 to study chemical signatures of the rocks. Geochemistry has flourished in the quantitative approach that grew to dominate earth science in the second half of the twentieth century. The contributions of geochemistry to this advance stage have been simply enormous. The lithochemical signatures are since then being used to solve the geological problems. Geochemical analysis of rocks has helped to understand many aspects of earth science which not hitherto known (White, 2013).

The geochemistry of sedimentary rocks reveals much important information about the evolution of the earth crust through geological times (McLennan and Taylor, 1980; McLennan and Taylor, 1991). It also complements the petrographic data generated by the study of thin sections of coarse clastic rocks. The composition of clastic sediments is affected by source area lithologies, weathering processes, transport and sorting, redox environment and diagenesis (Johnsson, 1993). These geological processes leave characteristics geochemical signatures, making sedimentary rocks as the most important repository of geochemical data available for the reconstruction of ancient earth surface environment (Sageman and Lyons; 2004).

3.2 Mobility Assessment

The chemical composition of sedimentary rocks can provide information for provenance, source area weathering and tectonics until it is not affected by the post depositional processes (Bhatia, 1993). The predominant factor that controls the mobility of major elements is the mineralogy of parent rocks (Harris and Adams, 1966). The mobile elements are derived from unstable minerals like feldspar and micas whereas, immobile are concentrated in resistant phase. The mobility and redistribution of elements is also influenced by tectonic processes, climatic and environmental conditions. The elements are dived into two groups as immobile and mobile. The immobile elements are Zr, Hf, Fe, Al, Th, Nb, Sc and REE while mobile elements include Ca, Na, P. K, Sr, Rb, Ba, Mg and Si (Middelburg et al., 1988). This classification regarding the mobile or immobile nature of elements is based on their geochemical behaviour during weathering conditions. Na and Ca are most mobile during chemical weathering than K because Na and Ca reside in plagioclase mineral

whose alteration rate is faster than K-feldspar. In the category of immobile elements particularly Al, Ti and Zr are helpful for estimation of nature of source rocks (Taylor and McLennan, 1985). At times some immobile minerals become mobile when their environmental conditions change for example U, Fe, Ce, and Eu.

In order to assess the mobility of major and trace elements in the sandstones and shales samples of Talchir Formation, binary diagrams are plotted wherein immobile elements Al_2O_3 and Zr are taken on abscissa and all other elements on ordinate. It is evident from these diagrams that most of the elements show magmatic relationship with Al_2O_3 and Zr (Figure 3.2.1).These relationships in Talchir Formation sandstones and shales indicate that their primary abundances have not been affected by post depositional processes (Figure 3.2.2).

Furthermore, binary diagrams involving mobile elements, K_2O versus Rb and Rb versus Sr and Ba also display positive linear relationship observed in primary igneous rocks. It further affirms primary geochemical abundance of even suspected mobile elements.

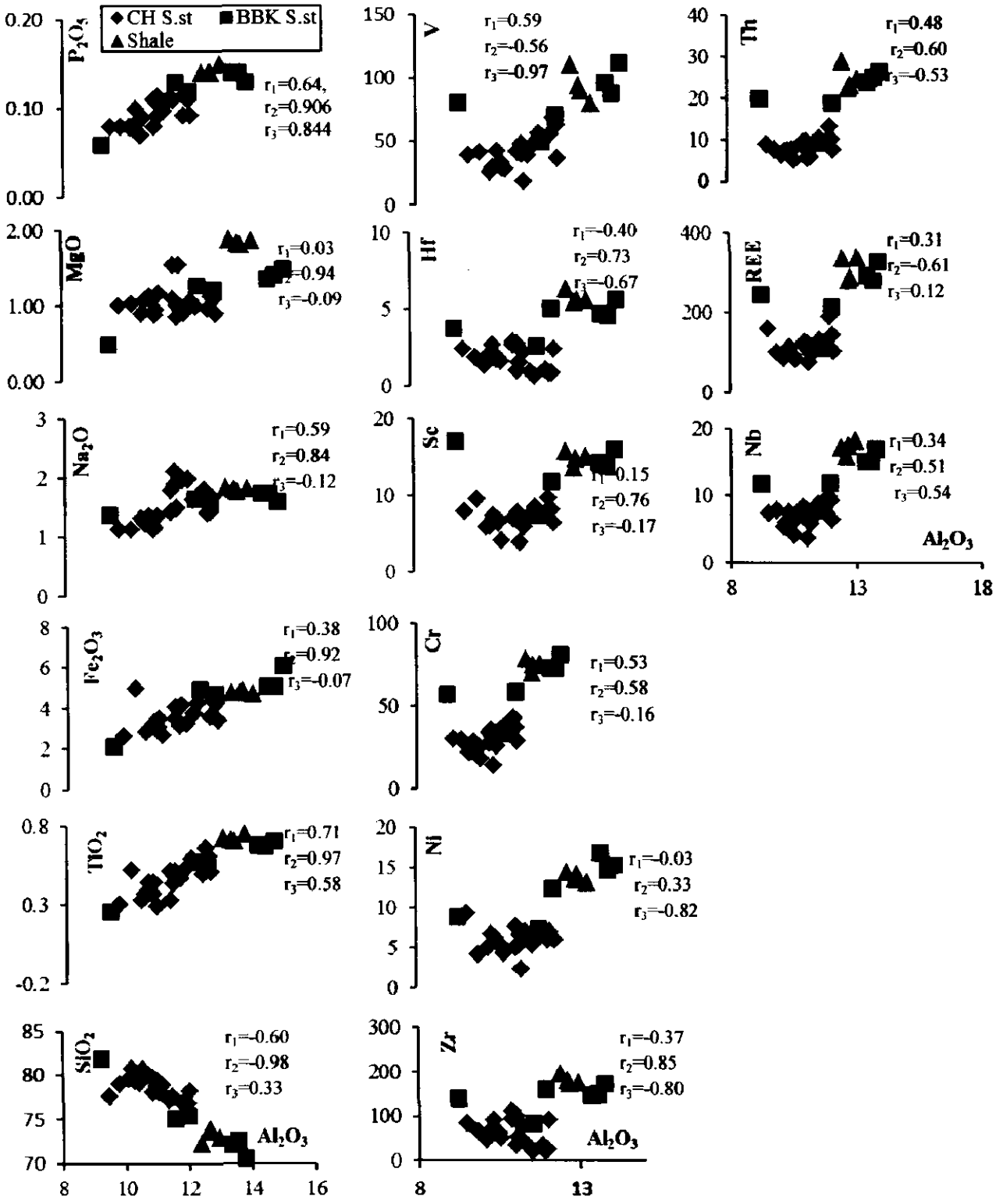

Figure 3.2.1: Al_2O_3 versus major oxides and trace element co-variation diagram of the Sandstones of Chirimiri, Baikunthpur and associated Shales of Chirimiri, district Koriya, Chhattisgarh, India. Index r_1=Chirimiri sandstone, r_2=Baikunthpur sandstone, r_3=Shales

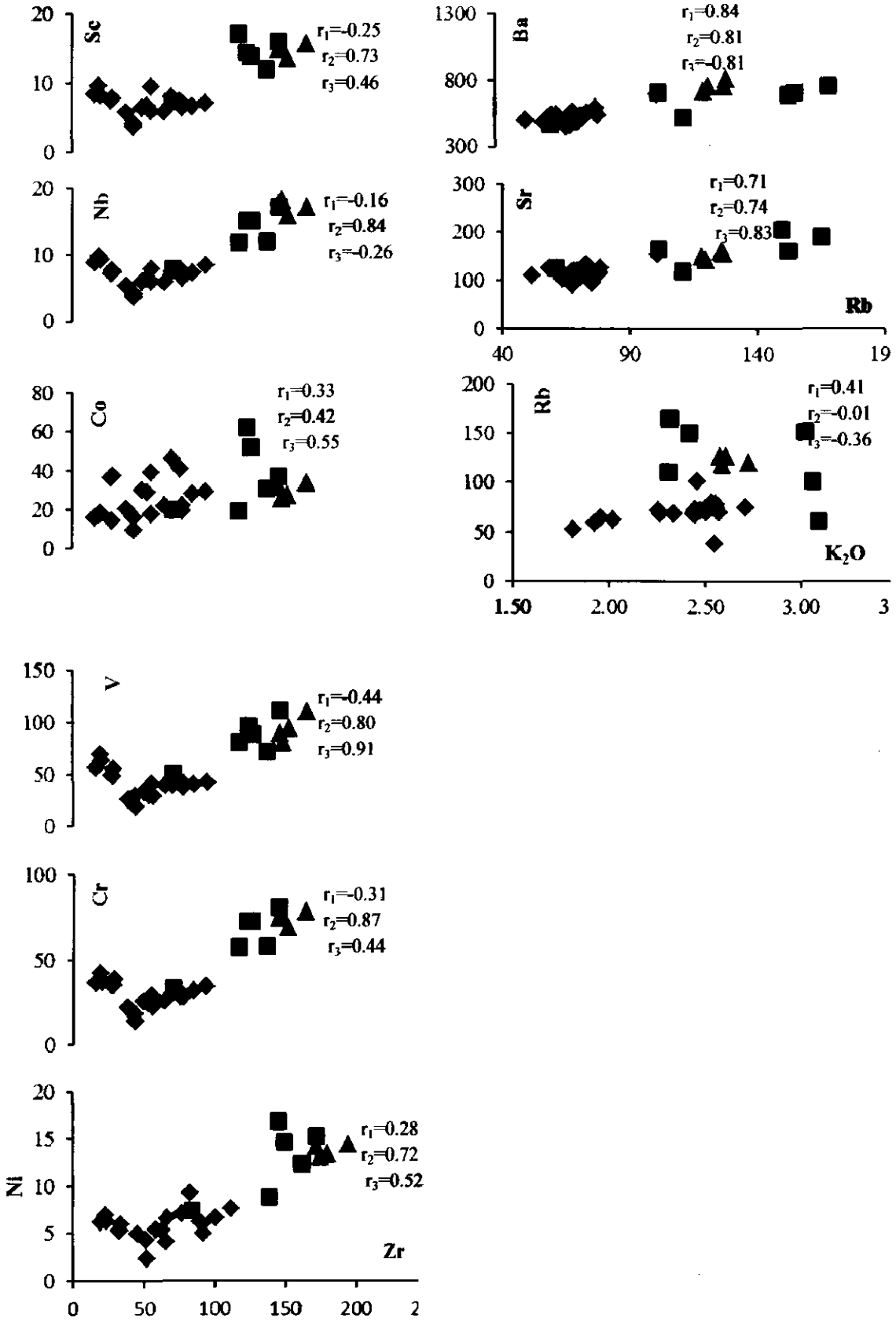

Figure 3.2.2 Zr, K_2O and Rb versus other trace elements, co-variation diagram of the Sandstones of Chirimiri, Baikunthpur and associated Shales of Chirimiri district Koriya, Chhattisgarh, India. Index r_1=Chirimiri sandstone, r_2=Baikunthpur sandstone, r_3=Shales

3.3 Analytical Technique

Geochemical analysis requires careful handling of both the rock samples and equipment in order to avoid any contamination during analysis. The samples were powdered upto -200 mesh sizes in a pulveriser. Each time bowl and the balls were cleaned by the acetone. Fresh tissue papers were used for soaking the moisture. The powdered samples were stored carefully in air tight plastic containers. The Major Oxides were analysed by XRF-technique and trace elements by ICP-MS following the procedure as described below. International rock standards were analysed along with the samples QLO-1(Quartz Latite) in case of major oxides with ± 10% accuracy and for trace elements SCO-1(Cody shale) and JR-1 (Japanese rhyolite) were used to check the validity of analysis. Accuracy of the measurements was confirmed by measurements of blanks and repeated measurements of the international standards digested along with the sediment samples. The relative standard deviation estimates based on repeat analyse of standards for all elements analysed are better than ± 5%.

3.3.1 Beads Preparation

Uniform glass beads were made through high temperature re-melting, therefore, the accuracy of analysis can be notably improved. Out of 1 to 1.2g of powdered rock samples (final requirement) 0.5500g was taken. To remove the moisture the sample powders were heated overnight in an oven at a temperature of about 105° to 110° C. The samples were left to cool down at room temperature. Samples were weighed along with the crucible to note loss of moisture. Weighed the flux Spectromelt A1000* of MERCK® 5.5000gm keeping the ratio of samples and flux 1:10 (*Composition of A1000 flux – di-Lithium tetra-borate with Lithium bromide – 0.0.7%). Rock sample and Spectromelt A1000 flux were mixed in the platinum crucible and the mixture was placed in the bead making Minifuse-2 machine of panalytical. A pre-programmed method was run and the sample was fused/ melted with flux in the crucible using the furnace. Later on composite red hot melt was poured in casting dish and allowed to cool to form a glass bead for XRF analyses. The XRF analysis of these Talchir sandstone and shale samples of Chirimiri area was carried out at NIO (National Institute of Oceanography Dona-Paula, Goa.

3.3.2 Open Acid-Digestion Method

Trace element analysis was carried out in the wet chemistry laboratory of NCAOR (National Centre of Antarctic and Ocean Research) Vasco-Da-Gama Goa, following Open Acid-digestion method. Homogenized samples were kept in oven at 60^0 C for half an hour to remove the moisture content. 50 mg of the every rock sample was taken on a butter paper and transferred carefully in a clean Teflon beaker. 6ml of nitric acid (HNO_3), 3-4ml of Hydrofluoric acid (HF) (depending on the silica content of the sample) and 1-2ml of Perchloric acid ($HClO_4$) were added. All the samples were placed on Q-block an automatic operating system to digest the samples. The sample solutions were heated to dryness taking care till a clear single drop of the solution left in the beaker. Later the solution drop was removed from the beaker and diluted with 5-10 ml of 2% HNO_3. The beaker content was transferred into volumetric flask quantitatively using 2% HNO_3. 1ppb of Rh (Rhodium) was added as internal standard to the same volumetric flask and finally made the volume up to the mark. Ready solution are put in HDPE bottles and analysed in ICP-MS (Thermo Elemental X7-series with collision cell technology).

3.4 Geochemical Characteristics of Sandstones of Talchir Formation

3.4.1 Major Oxides:-

Major oxides constitutes the whole rock chemistry, expressed in weight percent and are usually >1%. Major elements chemistry has been used to know the distinctive composition of source rocks, to discriminate the tectonic setting, to calculate the petrographic characteristic, intensity of weathering, or to classify the rocks. The enrichment of silica in sedimentary rocks is a degree of sandstone maturity which reflects duration, weathering intensity and destruction of minerals during transport. The distinctive petrographic characteristics displayed by Chirimiri and Baikunthpur sandstones of Talchir Formation are also envisaged in their geochemical abundance. The SiO_2 of the Chirimiri sandstone ranges from 77.23 to 80.61 with average value of 78.60, in Baikunthpur sandstone it ranges from 72.11 to 81.89 with average of 74.64. These values are higher than Post-Archean Australian shale (PAAS, SiO_2 = 62.8%, Taylor and McLennan, 1985) and that of average Upper Continental Crust (UCC, SiO_2 = 66.6%, Rudnick and Gao, 2003). The concentration of Al_2O_3 in the analysed Chirimiri sandstones ranges from 9.50- 12.03 with average of 10.91, Baikunthpur sandstone it is 9.23 to 13.79 with average of 12.24. The SiO_2/Al_2O_3 ratio

in Chirimiri sandstones varies from 6.44 to 8.16 (average 7.24) while in Baikunthpur sandstone it varies from 5.35 to 8.87 with (average of 6.28). This suggests that the sandstones of Talchir Formation are compositionally immature.

The presence of higher amount of K_2O and Na_2O is attributed to higher content of K-feldspar and plagioclase respectively. The K_2O concentration in Chirimiri sandstones ranges from 1.93 to 2.71 (average 2.37), Baikunthpur sandstone it ranges from 2.31 to 3.09 (average 2.70) whereas Na_2O in Chirimiri sandstone is 1.24 to 1.91 (average 1.53) and in Baikunthpur sandstone from 1.38 to 1.79 (average 1.62). Sandstone samples of Talchir Formation possess higher concentration of K_2O than Na_2O which indicates that these sandstones are enriched in K-feldspar. This interpretation is in concurrence to the modal abundance of sandstone where K-feldspar significantly dominates over plagioclase.

The K_2O/Al_2O_3 ratio of sediments is used as an indicator of the original composition of ancient sediments. The K_2O/Al_2O_3 ratios vary significantly in different potassium and alumina bearing minerals. For example in alkali feldspar K_2O/Al_2O_3 ratio is ~0.41, illite ~0.3 and in clay minerals ~0.0 (Cox et al., 1995). The K_2O/Al_2O_3 ratio of chirimiri sandstones ranges from 0.17 to 0.26 with (average 0.21) and in Baikunthpur sandstone 0.19 to 0.26 (average 0.22). This suggests that illite is one of the important constituent of clay mineral assemblage present in finer sediment fraction of these sandstones.

3.4.2 Trace Elements

3.4.2.1 Large Ion Lithophile Elements (LILE):- Rb, Sr, Th, U, Ba, Cs

LILE are also referred as alkaline earth elements. The concentration of LILE in the Chirimiri sandstones ranges 37 to 101ppm for Rb (average 69), 0 to 4ppm for Cs (average 2), 51 to 152 ppm for Sr (average 112), 5 to 13 ppm for Th (average 8), 0.8 to1.3 ppm for U (average 1) and 245 to 693ppm for Ba (average 509). On the other hand Baikunthpur sandstones are significantly enriched in LILE than Chirimiri sandstones (Table 5.1). Rb ranges from 61 to 165 (average 123), Cs 2 to 4 ppm (average 3), Sr 124 to 205 ppm (average 160), Th 9 to 26 ppm (average 20), U 1 to 3ppm (average 2) and Ba 466 to 759 ppm (average 641) in Baikunthpur sandstone. In the potassium rich minerals, such as K-feldspar, and biotite, Rb generally coexists with potassium while Sr tends to enrich in Ca-bearing minerals (Dasch, 1969).

Relatively high values of Rb in Talchir Formation sandstones indicate dominance of K-feldspar bearing rocks in the source terrain.

3.4.2.2 High Field Strength Elements (HFSE):- Zr, Hf, Nb, Ta, and Y

Small size and highly charged cations are referred to as HFSE. The elements Hf^{+4} and Zr^{+4}, Nb^{+5} and Ta^{+5} have similar size and cationic charge therefore poses similar geochemical behaviour. Due to their immobile behaviour HFSE can be used to evaluate the composition of the provenance (Taylor and McLennan, 1985). The HFSE concentration in the Chirimiri sandstones ranges 9 to 31ppm Y (average 16), 23 to 112 ppm Zr (average 61), 1 to 3 ppm Hf (average 2), 1 to 3 ppm for Ta (average 2), 5 to 10ppm Nb (average 7). The Baikunthpur sandstones possess 19 to 36 ppm Y (average 28), 84 to 172 ppm Zr (average 142), 3 to 6 Hf (average 4), 8 to 17 Nb (average 13) and 2 to 3 ppm Ta (average 3). The concentration of HFSE in Baikunthpur sandstones is relatively higher than Chirimiri sandstones.

3.4.2.3 Transition Elements:- Sc, V, Cr, Co, Cu, Zn

The elements that have partially filled outermost d-orbital are grouped as d-block elements in periodic table. This group of elements include Sc, V, Cr, Co, Ni, Cu, and Zn. This clan of elements is more concentrated in mafic than in felsic igneous rocks, therefore their concentration are useful to know source rock composition. Cr is also used in identifying accessory detrital components, like chromite, which is normally derived from mafic to ultramafic source (Zimmermann and Bahlburg, 2003). The concentration of Sc in Chirimiri sandstones ranges from 4 to 10ppm (average 7), V ranges from 18.45 to 68.67ppm (average 41), Cr ranges from 14 to 42ppm (average 29), Ni ranges from 2 to 9ppm (average 6) and Co ranges from 9.36 to 46.17ppm (average 25). The Baikunthpur sandstones are characterised by the concentration of Sc ranging from 7 to 17ppm (average 13), V from 50 to 111.74ppm (average 83), Cr from 33 to 81 ppm (average 62), Ni from 7 to 17 ppm (average 13) and Co from 36.9 to 62.15 ppm (average 37). Like LILE and HFSE the Baikunthpur sandstones are also enriched in TTE compared to Chirimiri sandstones.

3.4.2.4 Rare Earth Elements (REE):-

REEs are the most useful of all trace elements. The rare earth series comprises elements from La to Lu in the periodic table. All REEs have very similar geochemical and physical properties. This arises from the fact that they all poses stable 3^+ valance states. While a small number of REE also exists in oxidation state possessing valency other than 3^+ such as Ce^{4+} and Eu^{2+}. This property of these elements has geological

importance. The REE are regarded as amongst the least soluble trace elements and immobile during low grade metamorphism, weathering and hydrothermal alteration. The concentrations of REE present in sediments are chiefly transported as particulate matter and reflect the chemistry of their source. The effects of weathering and diagenesis are minor but sometimes REE are mobilized during weathering, and reprecipitated at the site of weathering (Nesbitt, 1979; Nesbitt et al., 1990; Milodowski and Zalasiewicz, 1991).

The REE distribution pattern in the sandstones samples of Talchir Formation show enrichment in LREE, and display almost flat HREE pattern (Figure 3.4.2.4) when Chondrite normalised REE. Pattern of Chirimiri sandstones are characterised by enriched LREE (La/Sm_N 4.25 to 5.69, average 4.93) and nearly flat HREE (Gd_N/Yb_N 1 to 2.37, average 1.77) with no or positive Eu anomaly (Eu/Eu* 0.97 to 1.54, average 1.18) (Figure 3.4.2.4 (a)). Similarly, Baikunthpur sandstones also show LREE enrichment (La/Sm_N 4.41 to 5.62, average 4.78), flat HREE (Gd_N/Yb_N 1.57 to 2.32, average 2.13) and moderate sink at Eu (Eu/Eu* 0.78 to 1, average 0.84) (Figure 3.4.2.4 (b)). Like major and other trace elements, Baikunthpur sandstone posses' higher content of REE too, but the shape of chondrite normalized REE profiles are nearly identical. It is clearly evident from distinctive modal mineralogy and geochemical characteristics of Chirimiri and Baikunthpur sandstones that their detritus was supplied by two different types of rocks.

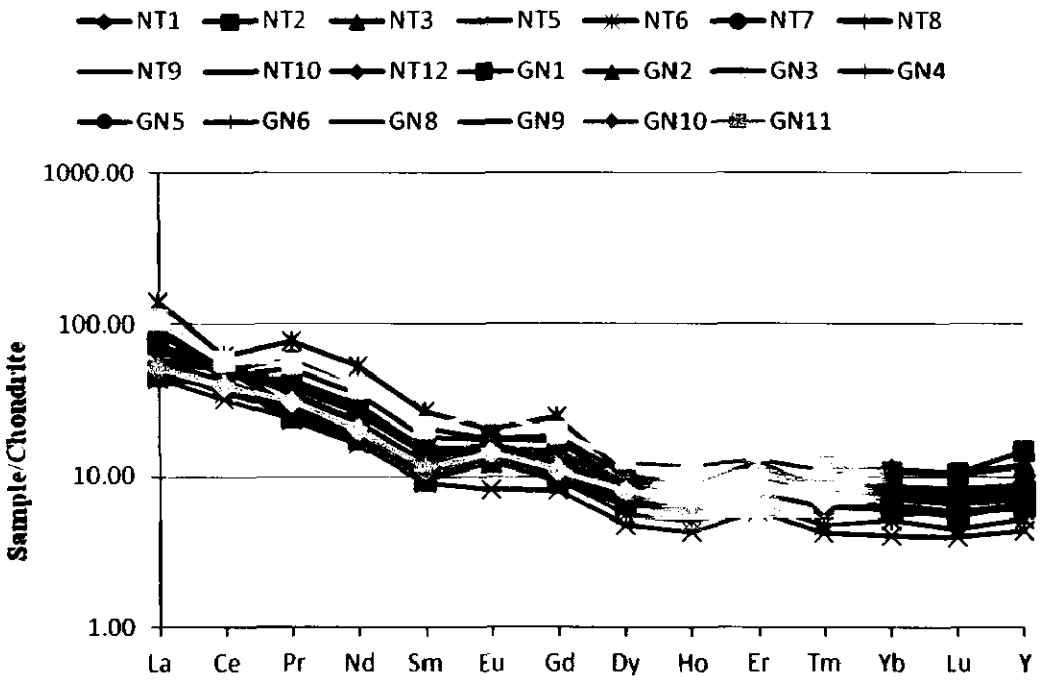

Figure 3.4.2.4: (a) Rare earth element chondrite normalise trend of Chirimiri sandstones, Chirimiri, district Koriya, Chhattisgarh, India

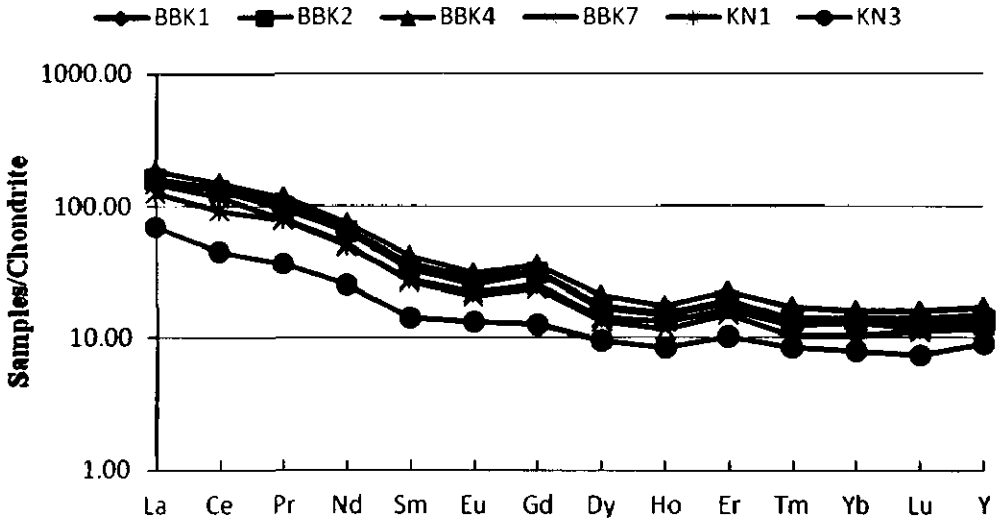

Figure 3.4.2.4: (b) Rare earth element chondrite normalise trend of Baikunthpur sandstones, Chirimiri, district Koriya, Chhattisgarh, India

3.5 Geochemical Characters of Shales of Talchir Formation

It is very difficult in the field to constrain stratigraphic position of shales because of their isolated exposures in streams cuttings. Their geochemical attributes makes them close associates of Baikunthpur sandstones, i.e. have received sediments from same source terrain. The SiO_2 concentration in the shales varies from 72.23 to 73.88 (average 73.19), Al_2O_3 is 12.37 to 12.97 (average 12.67). The SiO_2/Al_2O_3 ratio in shales ranges from 5.62 to 5.84 (average 5.78). The K_2O concentrations ranges from 2.59 to 2.73, (average 2.63) and Na_2O from 1.78 to 1.84 (average 1.82). The K_2O/Al_2O_3 for shales is 0.21. The concentration of Rb ranges from 118 to 127 ppm (average 123), Cs from 2.35 to 2.73ppm (average 3), Sr from 141 to 160 ppm (average 151), Th from 23ppm to 29ppm (average, 25), U from 3 to 4ppm (average, 3) and Ba from 718ppm to 812ppm (average, 760). The concentration Zr in shales ranges from173 to 195ppm (average, 181), Hf from 5 to 6ppm (average, 6), Nb from 16 to 18 ppm (average, 17), Y from 31 to 38ppm (average, 34), the value of Ta in all shale samples is 3. The concentration of TTE such as Sc are 14 to 16ppm (average, 15), V ranges from 80.5 to 110.24 ppm (average, 94), Cr from 69.22 to 77.97 ppm (average, 74), Co from 25.42 to 33.55 ppm (average, 29), Cu from17.16 to 28.34 ppm (average, 21), Zn from 83.48 to 110.96 ppm (averages, 95) and Ni from 13.07 to 14.18 (average, 14). The shales are also characterised by LREE enrichment $\{(La/Sm)_N$ 4.30 to 4.77, average 4.58$\}$and flat HREE $\{(Gd/Yb)_N$ 1.97 to 2.94, average, 2.34$\}$ with minor negative Eu anomaly (Eu/Eu* 0.75 to 0.83, average, 0.80).

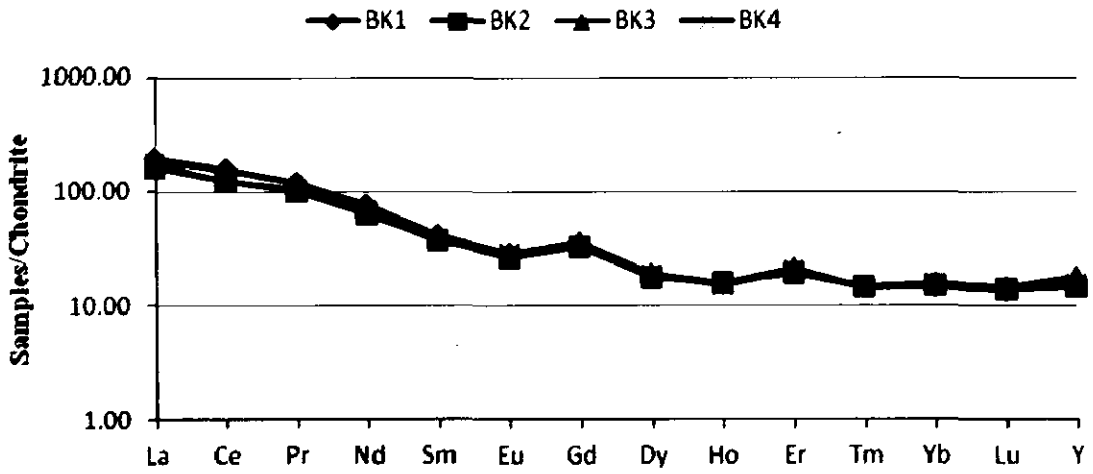

Figure 3.5.1 Rare earth element chondrite normalised pattern for shales of Talchir Formation, Chirimiri, district Koriya, Chhattisgarh, India

3.6 Comparison of Talchir Sandstones and Shales with UCC and PAAS

Normalised multi-element diagrams are an extension of the more familiar chondrite-normalised REE diagram in which other trace elements and major oxides are added. These diagrams are particularly useful in depicting basalt chemistry albeit their use has been extended to all igneous and some sedimentary rocks. The processes controlling the trace element of sedimentary composition may be investigated using normalization diagrams similar to those for spider diagrams. The most commonly used normalising values are average post-Archean shale, and the North-American shale (NASC) representing average crustal material, sometimes average upper continental crust is also used. Multi-elements diagram contains heterogeneous mix of trace elements, therefore show greater number of peaks and troughs reflecting different behaviour of different group of elements (Rollinson, 1993). Such an approach is also used in this study where samples of Talchir Formation are normalised with average upper continental crust and post Archean shale (Figure 3.6.1). It is evident from this figure that the shapes of the UCC and PAAS normalised patterns of Chirimiri sandstones, Baikunthpur sandstones and shales mimic each other in almost all the elements. The Chirimiri sandstones are slightly enriched only in SiO_2 but variably depleted in all other elements compared to UCC and PAAS (Figure 3.6.1 and 2).

The Baikunthpur sandstones and shales shows more or less similar pattern in both UCC and PAAS normalised spider diagram and nearly super impose each other.

The Baikunthpur sandstones and shales are enriched in major oxides like SiO_2, TiO_2, TTE (Co, Cr, Sc, and Zn), LILE (Rb, Ba, and Th) only shales are enriched in U, and HFSE (Nb) and all REEs are enriched in both Baikunthpur sandstones and shales (Figure 3.6.1). In PAAS normalised pattern Baikunthpur sandstones and shales completely superimpose each other and minor enrichment in SiO_2, Na_2O, Co, Zn, Ba, Th, Nb and all REEs.

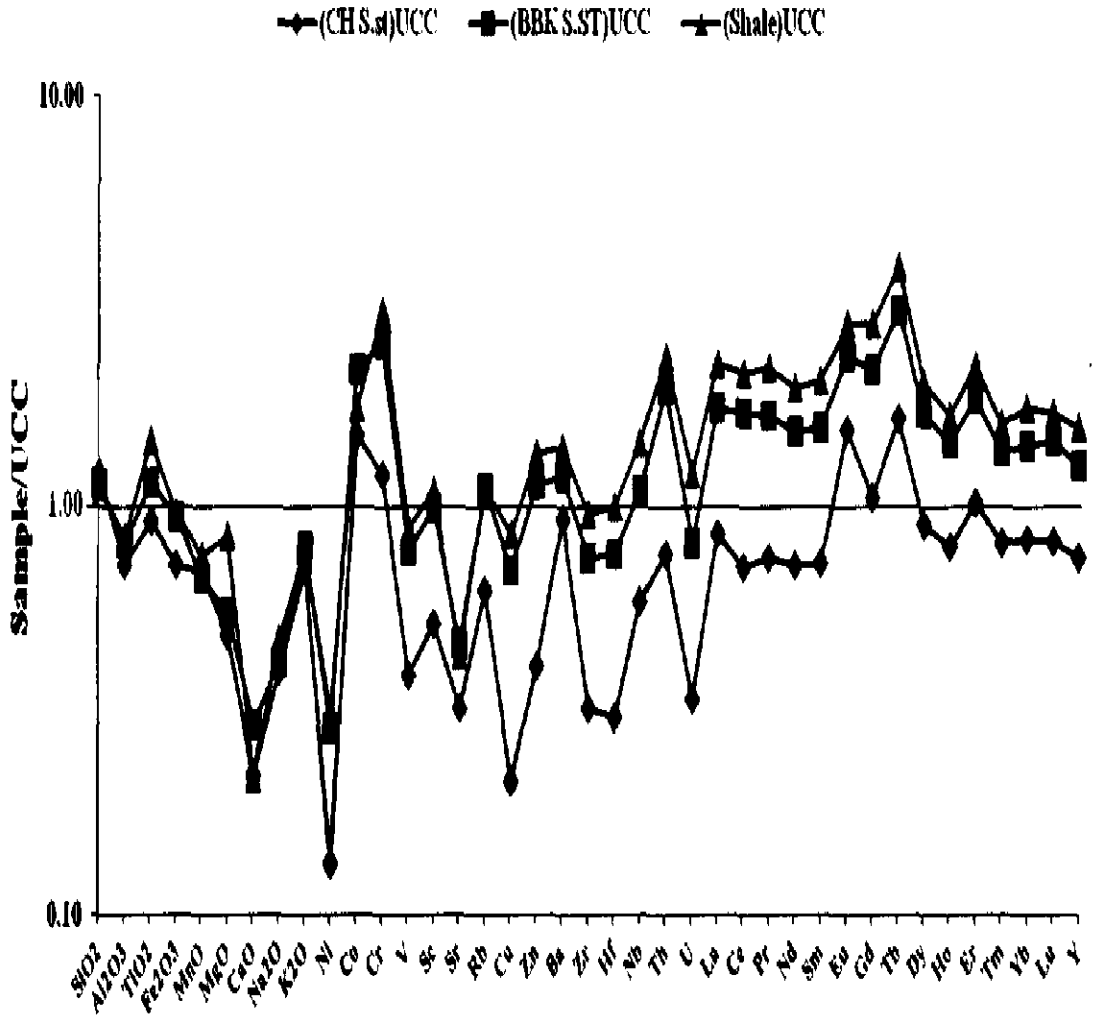

ure 3.6.1: UCC normalised spider diagram of major oxides, trace and rare earth elements for sandstones and shales of Talchir Formation, rimiri, district Koriya, Chhattisgarh, India (Taylor and McLennan, 1985).

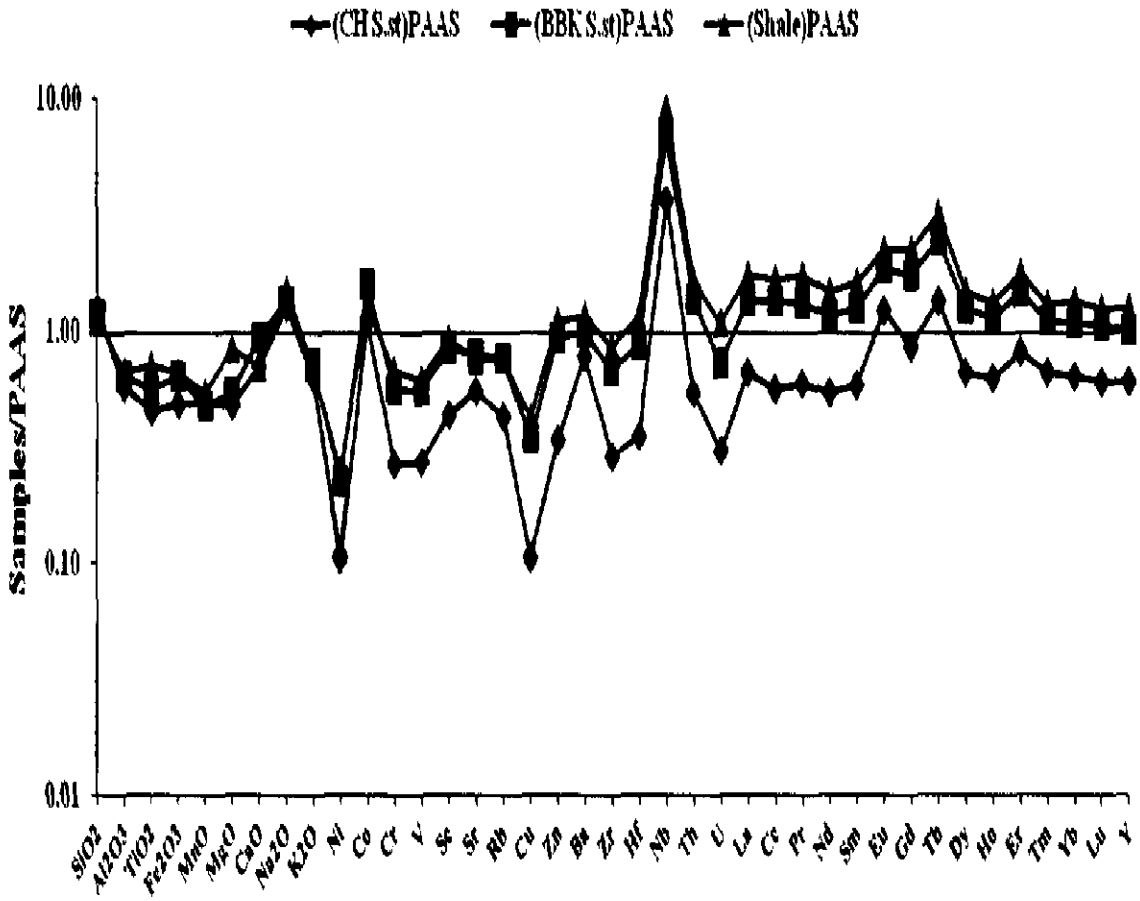

Figure 3.6.2: PAAS normalised spider diagram of major oxides, trace and rare earth elements for sandstones and shales of Talchir Formation, Chirimiri, district Koriya, Chhattisgarh, India (Taylor and McLennan, 1985).

Table 3.6.1: Upper continental crust and Post-Archean Australian shale normalised values of clastics of Talchir Formation, exposed in Chirimiri, district Koriya, Chhattisgarh, India

	UCC Normalised			PAAS Normalised		
Element	CH S.st	BBK S.st	Shale	CH S.st	BBK S.st	Shales
SiO_2	1.19	1.13	1.11	1.25	1.19	1.17
Al_2O_3	0.72	0.81	0.83	0.58	0.65	0.67
TiO_2	0.92	1.14	1.44	0.46	0.57	0.72
Fe_2O_3	0.71	0.94	0.96	0.49	0.65	0.66
MnO	0.69	0.67	0.75	0.50	0.48	0.55
MgO	0.48	0.55	0.84	0.48	0.55	0.84
CaO	0.22	0.29	0.22	0.71	0.94	0.70
Na_2O	0.39	0.42	0.47	1.28	1.35	1.52
K2O	0.70	0.80	0.77	0.64	0.73	0.71
Ni	0.13	0.29	0.31	0.11	0.23	0.25
Co	1.49	2.16	1.73	1.10	1.60	1.28
Cr	1.18	2.50	2.97	0.27	0.57	0.67
V	0.39	0.78	0.87	0.28	0.55	0.62
Sc	0.51	0.99	1.09	0.44	0.84	0.92
Sr	0.32	0.46	0.43	0.56	0.80	0.75
Rb	0.62	1.10	1.10	0.43	0.77	0.77
Cu	0.21	0.69	0.85	0.11	0.35	0.42
Zn	0.41	1.12	1.34	0.34	0.94	1.12
Ba	0.92	1.17	1.38	0.78	0.99	1.17
Zr	0.32	0.75	0.95	0.29	0.68	0.86
Hf	0.30	0.76	0.99	0.35	0.88	1.15
Nb	0.58	1.09	1.43	3.67	6.90	9.04
Th	0.76	1.91	2.31	0.55	1.37	1.66
U	0.34	0.81	1.20	0.30	0.73	1.09
La	0.85	1.73	2.21	0.67	1.36	1.73
Ce	0.71	1.67	2.11	0.57	1.34	1.69
Pr	0.74	1.66	2.17	0.60	1.34	1.74
Nd	0.72	1.51	1.95	0.55	1.16	1.49
Sm	0.72	1.54	2.02	0.59	1.25	1.64
Eu	1.53	2.30	2.78	1.24	1.88	2.27
Gd	1.05	2.15	2.78	0.86	1.75	2.27
Tb	1.62	2.98	3.82	1.35	2.48	3.17
Dy	0.90	1.67	2.00	0.67	1.25	1.49
Ho	0.79	1.43	1.66	0.64	1.15	1.34
Er	1.01	1.82	2.20	0.82	1.47	1.78
Tm	0.81	1.35	1.58	0.67	1.11	1.30
Yb	0.83	1.39	1.73	0.64	1.09	1.35
Lu	0.82	1.44	1.68	0.61	1.07	1.25
Y	0.75	1.25	1.54	0.61	1.02	1.26

Table 3.6.2: Range of variation and average geochemical composition of the clastics rocks of Talchir Formation and UCC, PAAS, Felsic and Basic rocks

Element	Chirimiri Sandstone			Baikunthpur Sandstone			Shales			Bt-Granite	Granite	Ultramafic	Gabbro	Diorite	UCC	PAAS
	Min	Max	Avrg	Min	Max	Avrg	Min	Max	Avrg	Average	Average	Average	Average	Average		
SiO_2	76.63	80.81	78.60	70.60	81.89	74.64	73.19	72.23	73.19	73.01	64.52	50.54	47.95	58.15	66.00	62.80
Al_2O_3	9.50	12.03	10.91	9.23	13.79	12.24	12.67	12.39	12.67	0.04	0.28	0.44	0.84	0.65	15.20	18.90
TiO_2	0.29	0.66	0.46	0.26	0.70	0.57	0.72	0.70	0.72	14.15	15.91	4.02	12.20	12.92	0.50	1.00
Fe_2O_3	2.64	5.00	3.56	2.13	6.10	4.69	4.79	4.74	4.79	2.19	3.33	12.29	12.31	8.52	5.00	7.22
MnO	0.03	0.10	0.06	0.04	0.07	0.05	0.06	0.06	0.06	0.04	0.06	0.21	0.19	0.15	0.08	0.11
MgO	0.86	1.54	1.06	0.50	1.49	1.21	1.85	1.81	1.85	0.24	1.09	19.05	10.42	4.90	2.20	2.20
CaO	0.59	2.98	0.92	0.78	1.97	1.22	0.91	0.83	0.91	0.70	3.19	7.26	9.98	6.94	4.20	1.30
Na_2O	1.13	2.12	1.53	1.38	1.75	1.62	1.82	1.78	1.82	3.55	3.81	0.33	1.15	1.89	3.90	1.20
K_2O	1.82	2.71	2.37	2.31	3.09	2.70	2.63	2.58	2.63	5.53	3.14	0.06	0.36	0.22	3.40	3.70
P_2O_5	0.07	0.12	0.09	0.06	0.14	0.12	0.14	0.14	0.14	0.04	0.13	0.08	0.19	0.18	-	0.16
CIA	47.37	70.59	61.58	50.00	65.00	61.02	66.65	66.65	66.65	-	-	-	-	-	57.61	-
PIA	48.34	72.97	66.57	52.97	70.77	65.11	67.77	66.92	67.77	-	-	-	-	-	-	-
ICV	0.12	0.16	0.13	0.12	0.17	0.15	0.17	0.16	0.17	-	-	-	-	-	-	-
CIW	32.18	76.68	70.37	61.13	76.23	71.04	73.07	72.32	73.07	-	-	-	-	-	-	-
Na_2O/K_2O	0.46	1.03	0.66	0.53	0.72	0.61	0.69	0.67	0.69	0.64	1.21	5.66	3.16	8.51	1.15	0.32
SiO_2/Al_2O_3	6.42	8.16	7.24	5.28	8.87	6.28	5.78	5.62	5.78	1825.13	232.07	115.24	57.06	89.80	4.34	3.32
K_2O/Na_2O	0.97	2.17	1.62	1.39	1.88	1.67	1.45	1.39	1.45	1.56	0.82	0.18	0.32	0.12	0.87	3.08
K_2O/Al_2O_3	0.16	0.26	0.22	0.19	0.26	0.22	0.21	0.21	0.21	88.63	13.71	0.76	1.37	2.92	0.26	0.06
Fe_2O_3+MgO	3.66	6.28	4.64	2.63	7.59	5.91	6.65	6.60	6.65	2.42	4.42	31.34	22.73	13.42	7.20	9.42
Al_2O_3/SiO_2	0.12	0.16	0.14	0.11	0.19	0.17	0.17	0.18	0.17	0.00	0.00	0.01	0.02	0.01	0.23	0.30
$Al_2O_3/(CaO+Na_2O)$	0.01	0.04	0.02	0.10	0.24	0.14	0.09	0.11	0.10	3.60	3.90	0.39	1.23	1.99	7.52	15.74
Al_2O_3/TiO_2	18.16	36.38	24.79	19.65	35.50	22.92	17.60	17.21	17.60	0.00	0.02	0.11	0.07	0.05	30.40	18.90
Ni	2.41	9.24	5.85	7.39	16.84	12.56	13.07	14.40	13.78	3.00	0.00	340.43	72.50	18.75	44.00	55.00
Co	9.39	46.17	25.35	19.08	62.15	36.72	25.42	33.55	29.46	89.50	0.00	70.43	54.50	69.75	17.00	23.00
Cr	14.24	42.42	29.46	33.06	80.56	62.42	69.22	77.97	74.23	8.00	11.60	1364.00	207.63	25.25	25.00	110.00
V	18.47	68.67	41.40	49.88	111.74	82.99	80.50	110.24	93.52	-	-	-	-	-	107.00	150.00
Se	3.77	9.59	7.00	7.39	17.11	13.43	13.54	15.72	14.77	2.45	7.78	58.00	55.50	34.50	13.60	16.00
Sr	51.35	152.07	111.71	117.51	205.24	160.29	140.87	159.85	150.90	54.50	191.00	41.29	267.13	349.50	350.00	200.00
Rb	36.91	101.05	69.06	61.08	164.94	123.35	118.23	126.76	122.80	80.00	113.40	2.57	10.75	4.75	112.00	160.00
Cu	1.92	7.79	5.32	7.87	26.62	17.30	17.16	28.34	21.24	-	-	-	-	-	25.00	50.00
Zn	14.68	42.87	28.78	29.88	117.88	79.50	83.48	110.96	94.89	16.00	0.00	95.43	83.00	74.75	71.00	85.00
Ba	245.45	693.13	508.51	466.45	758.56	641.32	718.04	811.83	759.93	880.00	606.00	252.57	306.00	287.00	550.00	650.00
Zr	19.50	111.85	61.00	84.24	172.33	142.12	172.59	195.18	180.81	40.50	112.60	40.14	54.38	71.25	190.00	210.00
Hf	0.67	2.91	1.76	2.60	5.69	4.41	5.45	6.37	5.76	1.25	2.36	0.49	1.52	4.56	5.80	5.00
Nb	3.66	9.77	6.96	7.80	17.06	13.11	15.85	18.19	17.18	15.50	9.40	5.43	4.25	6.25	12.00	1.90
Th	4.93	13.08	8.13	9.15	26.27	20.48	22.22	28.88	24.69	8.50	9.00	1.26	0.98	1.91	10.70	14.90
U	0.59	1.27	0.94	1.12	2.99	2.26	3.09	3.65	3.37	-	-	-	-	-	2.80	3.10
Y	9.17	31.21	16.39	19.09	35.90	27.55	30.87	38.00	33.96	10.50	16.60	12.00	20.63	16.75	22.00	2.00
Th/Co	0.18	0.74	0.37	0.38	1.03	0.62	0.73	0.96	0.84	0.09	-	0.02	0.02	0.03	0.63	0.65
Th/Cr	0.22	0.39	0.28	0.28	0.35	0.32	0.31	0.37	0.33	1.06	0.78	0.00	0.00	0.08	0.43	0.14

Contd...

Zr/Th	1.77	13.46	8.10	5.97	9.21	7.25	6.76	8.11	7.37	4.76	12.51	31.97	55.48	37.40	17.76	14.09
Th/U	6.37	10.81	8.69	8.17	9.61	9.00	6.87	7.91	7.32	-	-	-	-	-	3.82	4.81
Cr/V	0.59	0.84	0.73	0.66	0.82	0.75	0.71	0.94	0.80	-	-	-	-	-	0.23	0.73
U/Th	0.09	0.16	0.12	0.10	0.12	0.11	0.13	0.15	0.14	-	-	-	-	-	0.26	0.21
V/Cr	1.19	1.69	1.39	1.22	1.51	1.34	1.07	1.41	1.26	-	-	-	-	-	4.28	1.36
Y/Ni	1.84	5.99	2.89	1.86	2.73	2.27	2.29	2.64	2.46	3.50	0.00	0.04	0.28	0.89	0.50	0.04
Rb/Sr	0.47	0.79	0.63	0.49	0.95	0.77	0.79	0.85	0.81	1.47	0.59	0.06	0.04	0.01	0.32	0.80
Zr/Hf	28.29	38.44	34.05	30.29	36.73	32.49	30.64	33.07	31.45	32.40	47.71	82.40	35.80	15.62	32.76	42.00
La/Th	2.33	4.56	3.11	2.34	2.78	2.57	2.40	2.92	2.70	3.46	3.06	2.40	10.32	8.18	2.80	2.56
Zr/Sc	2.32	15.82	9.29	0.16	0.26	0.22	11.63	13.31	12.27	16.53	14.48	0.69	0.98	2.07	13.97	13.13
Th/Sc	0.79	1.48	1.17	0.27	0.46	0.37	1.57	1.84	1.67	3.47	1.16	0.02	0.02	0.06	0.79	0.93
Cr/Ni	3.24	7.05	5.16	0.16	0.26	0.22	5.14	5.77	5.39	2.67	0.00	4.01	2.86	1.35	0.57	2.00
Cu/Zn	0.13	0.26	0.18	0.27	0.46	0.37	0.19	0.26	0.22	-	-	-	-	-	0.35	0.59
Ni/Co	0.15	0.39	0.25	0.27	0.46	0.37	0.43	0.51	0.47	0.03	0.00	4.83	1.33	0.27	2.59	2.39
La	16.42	51.31	25.42	25.40	68.14	51.99	59.83	71.54	66.23	29.40	27.58	3.01	10.11	15.58	30.00	38.20
Ce	31.13	60.51	45.45	43.19	143.97	107.05	118.19	151.36	134.83	69.50	49.21	6.90	22.66	26.75	64.00	79.60
Pr	3.25	10.67	5.27	5.05	16.05	11.80	13.78	16.76	15.38	-	-	-	-	-	7.10	8.83
Nd	11.62	37.99	18.62	17.91	53.24	39.37	45.18	55.45	50.67	12.10	16.84	4.14	11.58	12.22	26.00	33.90
Sm	2.08	6.28	3.26	3.25	9.63	6.94	8.48	9.69	9.09	2.50	3.44	2.27	2.76	2.88	4.50	5.55
Eu	0.72	2.29	1.34	1.15	2.69	2.03	2.31	2.52	2.45	0.55	1.75	0.41	0.92	1.15	0.88	1.08
Gd	2.45	7.54	3.99	3.81	10.94	8.15	9.99	11.31	10.58	-	-	-	-	-	3.80	4.66
Tb	0.58	2.59	1.04	0.98	2.61	1.91	2.34	2.55	2.44	0.32	1.14	0.21	0.46	0.68	0.64	0.77
Dy	1.83	4.97	3.15	3.65	8.00	5.86	6.69	7.26	6.99	-	-	-	-	-	3.50	4.68
Ho	0.37	1.07	0.63	0.73	1.49	1.14	1.30	1.34	1.33	-	-	-	-	-	0.80	0.99
Er	1.45	3.69	2.32	2.56	5.55	4.19	4.84	5.39	5.06	-	-	-	-	-	2.30	2.85
Tm	0.15	0.41	0.27	0.30	0.60	0.45	0.51	0.53	0.52	-	-	-	-	-	0.33	0.40
Yb	1.00	2.73	1.82	1.97	3.92	3.07	3.68	3.98	3.81	0.72	2.36	7.93	1.74	2.09	2.20	2.82
Lu	0.15	0.40	0.26	0.28	0.60	0.46	1.63	1.75	1.68	0.09	0.29	0.12	0.26	0.29	0.32	0.43
ΣREE	73.20	188.11	112.86	110.23	327.43	244.39	280.64	339.69	311.06	115.18	102.61	24.99	50.49	61.62	146.37	184.76
ΣLREE	65.22	169.05	99.37	95.95	293.72	201.57	249.48	307.28	278.65	114.05	98.82	16.73	48.03	58.57	132.48	171.82
ΣHREE	7.98	20.62	13.49	14.28	33.71	25.22	31.16	34.08	32.41	1.13	3.79	8.26	2.46	3.06	13.89	17.60
LREE/HREE	4.87	8.74	7.43	6.72	10.19	8.56	8.00	9.48	8.59	100.92	26.07	2.02	19.54	19.17	9.54	9.76
La/Sc	2.04	5.35	3.63	3.19	4.25	3.85	4.36	4.75	4.48	12	3.55	0.05	0.18	0.45	2.21	2.39
La/Co	0.49	2.88	1.17	0.95	2.86	1.60	2.03	2.81	2.28	0.33	0.00	0.04	0.19	0.22	1.76	1.66

Contd...

La	44.74	139.81	69.27	69.21	185.67	141.67	163.02	194.93	180.46	80.11	75.15	8.21	27.55	42.44	81.74	104.09
Ce	32.53	63.23	47.49	45.13	150.44	111.86	123.50	158.16	140.89	72.62	51.42	7.21	23.68	27.95	66.88	83.18
Pr	23.72	77.88	38.49	36.86	117.15	86.11	100.58	122.34	112.26	72.62	51.42	7.21	23.68	27.95	51.82	64.45
Nd	16.34	53.43	26.19	25.19	74.88	55.37	63.54	77.99	71.27	17.02	23.68	5.83	16.28	17.18	36.57	47.68
Sm	9.00	27.19	14.10	14.07	41.69	30.04	36.71	41.95	39.35	10.82	14.89	9.81	11.93	12.45	19.48	24.03
Eu	8.28	26.32	15.44	13.22	30.92	23.28	26.55	28.97	28.16	6.26	20.16	4.66	10.60	13.22	10.11	12.41
Gd	8.01	24.64	13.05	12.45	35.75	26.64	32.65	36.96	34.58	6.26	20.16	4.66	10.60	13.22	12.42	15.23
Tb	10.00	44.66	17.92	16.90	45.00	32.90	40.34	43.97	42.11	5.52	19.69	3.67	7.97	11.72	11.03	13.28
Dy	4.80	13.04	8.28	9.58	21.00	15.37	17.56	19.06	18.35	5.52	19.69	3.67	7.97	11.72	9.19	12.28
Ho	4.35	12.57	7.42	8.58	17.51	13.40	15.28	15.75	15.57	5.52	19.69	3.67	7.97	11.72	9.40	11.63
Er	5.82	14.82	9.33	10.28	22.29	16.83	19.44	21.65	20.32	5.52	19.69	3.67	7.97	11.72	9.24	11.45
Tm	4.21	11.52	7.51	8.43	16.85	12.50	14.33	14.89	14.61	5.52	19.69	3.67	7.97	11.72	9.27	11.24
Yb	4.03	11.01	7.33	7.94	15.81	12.37	14.84	16.05	15.35	2.90	9.50	31.97	7.00	8.43	8.87	11.37
Lu	3.94	10.50	6.85	7.35	15.75	12.07	810.24	997.38	891.21	2.36	7.66	3.15	6.82	7.48	8.40	11.29
Y	4.37	14.86	7.81	9.09	17.10	13.12	810.24	997.38	891.21	-	-	-	-	-	-	-
Eu/Eu*	0.81	1.54	1.18	0.78	1.00	0.84	0.74	0.82	0.76	-	-	-	-	-	-	-
(Gdn/Ybn)	1.00	2.94	1.80	1.57	2.30	2.11	2.15	2.37	2.25	-	-	-	-	-	-	-
La/SmN	4.25	5.69	4.93	4.41	5.62	4.78	4.30	4.77	4.58	7.40	5.05	0.84	2.31	3.41	4.20	4.33
La/Ybn	4.80	16.67	9.56	8.71	14.52	11.36	10.75	13.14	11.76	27.59	7.91	0.26	3.94	5.04	9.21	9.15

Table 3.6.3: Geochemical composition of Chirimiri sandstones of Talchir Formation, Chirimiri, district Koriya, Chhattisgarh, India. Major oxides in wt%, trace elements in ppm; Eu/Eu* = $\{Eu_N/(Sm_N*Gd_N)^{1/2}\}$. Normalising values are after Taylor and McLennan, (1985).

	Chirimiri sandstone																					
Element	NT1	NT2	NT3	NT5	NT6	NT7	RB 8	RB9	RB10	RB12	GN1	GN2	GN3	GN4	GN5	GN6	GN8	GN9	GN10	GN11	Min	Max	Avrg
SiO2	76.79	77.23	78.19	77.58	76.63	76.92	78.79	79.68	78.97	79.39	79.58	79.06	78.2	80.68	78.06	79.16	79.44	79.25	80.81	77.61	76.63	80.81	78.60
Al2O3	11.82	11.38	12.03	11.51	11.90	11.98	11.00	10.90	11.19	11.02	10.11	9.83	11.1	10.55	10.9	10.46	10.32	10.44	10.21	9.5	9.50	12.03	10.91
TiO2	0.49	0.54	0.51	0.59	0.66	0.60	0.44	0.33	0.47	0.48	0.33	0.52	0.51	0.29	0.51	0.44	0.44	0.37	0.37	0.3	0.29	0.66	0.46
Fe2O3	3.63	3.77	3.42	4.25	4.38	4.24	3.15	3.51	3.28	3.27	2.86	5	4.17	2.7	4.05	3.5	3.29	3.11	3.04	2.64	2.64	5.00	3.56
MnO	0.04	0.05	0.03	0.03	0.04	0.04	0.05	0.05	0.05	0.05	0.07	0.1	0.06	0.07	0.07	0.06	0.08	0.06	0.05	0.07	0.03	0.10	0.06
MgO	0.97	1.08	0.90	0.99	1.13	1.09	0.86	1.10	0.91	1.00	0.9	1.027	1.54	1.17	1.54	0.95	1.13	0.88	1.08	1.01	0.86	1.54	1.06
CaO	0.77	0.84	0.71	0.72	0.72	0.70	0.61	0.59	0.65	0.65	1.15	0.76	0.75	0.65	0.74	1.11	0.85	1.3	1.14	2.98	0.59	2.98	0.92
Na2O	1.82	1.99	1.68	1.64	1.41	1.44	1.91	1.8	1.98	2.12	1.32	1.14	1.51	1.37	1.44	1.17	1.36	1.13	1.24	1.14	1.13	2.12	1.53
K2O	2.02	1.93	2.26	1.82	1.96	2.27	2.58	2.54	2.53	2.44	2.56	2.34	2.55	2.71	2.51	2.45	2.56	2.45	2.48	2.46	1.82	2.71	2.37
P2O5	0.09	0.11	0.09	0.11	0.12	0.11	0.09	0.08	0.10	0.11	0.08	0.08	0.11	0.09	0.11	0.07	0.1	0.07	0.08	0.08	0.07	0.12	0.09
CIA	60	60	60	70.59	70.59	70.59	61.11	61.11	61.11	61.11	58.82	66.67	64.71	62.50	58.82	58.82	58.82	58.82	60.01	47.37	47.37	70.59	61.58
PIA	68.65	65.88	70.32	70.43	72.97	72.32	65.9	66.91	65.57	64.24	63.26	68.97	68.3	68.83	68.68	66.37	66.51	64.78	64.14	48.34	48.34	72.97	66.57
ICV	0.13	0.13	0.13	0.12	0.13	0.13	0.12	0.12	0.13	0.12	0.16	0.13	0.12	0.13	0.13	0.14	0.12	0.14	0.14	0.12	0.12	0.16	0.13
CIW	72.88	70.28	74.83	74.18	76.67	76.68	72.13	73.00	71.61	70.26	70.34	74.96	74.15	75.37	74.50	72.57	73.08	71.16	32.18	56.53	32.18	76.68	70.37
Na2O/K2O	0.90	1.03	0.74	0.91	0.72	0.63	0.74	0.71	0.78	0.87	0.52	0.49	0.59	0.51	0.57	0.48	0.53	0.46	0.50	0.46	0.46	1.03	0.66
SiO2/Al2O3	6.49	6.79	6.50	6.74	6.44	6.42	7.16	7.31	7.06	7.20	7.90	8.04	7.07	7.65	7.16	7.57	7.70	7.59	7.91	8.16	6.42	8.16	7.24
K2O/Na2O	1.11	0.97	1.35	1.10	1.39	1.58	1.35	1.41	1.28	1.15	1.94	2.04	1.69	1.98	1.74	2.09	1.88	2.17	2.00	2.16	0.97	2.17	1.62
Al2O3/SiO2	0.15	0.15	0.15	0.15	0.16	0.16	0.14	0.14	0.14	0.14	0.13	0.12	0.14	0.13	0.14	0.13	0.13	0.13	0.13	0.12	0.12	0.16	0.14
K2O/Al2O3	0.17	0.17	0.19	0.16	0.16	0.19	0.23	0.23	0.23	0.22	0.25	0.24	0.23	0.26	0.23	0.23	0.25	0.23	0.24	0.26	0.16	0.26	0.22
Fe2O3+MgO	4.60	4.85	4.32	5.24	5.51	5.33	4.00	4.60	4.18	4.28	3.76	6.28	5.72	3.88	5.59	4.46	4.43	4.01	4.13	3.66	3.66	6.28	4.64
Al2O3/TiO2	24.12	21.07	23.69	19.50	18.16	19.84	25.29	33.23	24.02	23.11	30.64	18.90	21.69	36.38	21.37	23.77	23.45	28.22	27.59	31.67	18.16	36.38	24.79

Contd...

Al2O3/SiO2	0.15	0.15	0.15	0.15	0.16	0.16	0.14	0.14	0.14	0.14	0.13	0.12	0.14	0.13	0.14	0.13	0.13	0.13	0.13	0.12	0.12	0.16	0.14
Al2O3/(CaO+Na2O)	0.02	0.02	0.02	0.02	0.02	0.02	0.02	0.02	0.02	0.02	0.02	0.01	0.04	0.03	0.02	0.02	0.02	0.02	0.02	0.02	0.01	0.04	0.02
Ni	5.99	5.36	5.95	6.17	6.95	6.26	5.33	7.58	7.03	6.64	5.04	4.16	2.41	4.35	5	5.32	6.2	5.44	6.66	9.24	2.41	9.24	5.85
Co	37.42	36.38	22.06	15.95	17.79	18.16	14.33	29	21.87	27.53	20.02	17.53	9.39	16.11	19.05	28.78	40.42	29.78	39.27	46.17	9.39	46.17	25.35
Cr	38.21	35.61	29.19	36.94	42.42	37.19	35.5	34	25.64	31.53	21.88	29.33	14.2	18.45	27.9	24.38	28.4	25.85	22.68	29.91	14.24	42.42	29.46
V	55.3	49.21	36.78	56.35	68.67	62.77	47.86	42.14	39.36	39.74	26.08	41.43	18.5	28.65	41.44	29.59	42.28	33.42	29.15	39.23	18.47	68.67	41.40
Sc	7.81	7.45	6.45	8.4	9.59	8.2	7.77	7.07	5.86	6.66	5.92	9.5	3.77	4.17	6.95	6.8	7.3	6.43	6.01	7.91	3.77	9.59	7.00
Sr	124.5	123.92	111.6	109.26	103.3	105.2	117.37	124.5	115.2	117	130.9	90.07	51.4	94.42	97.6	115	113.35	128.7	108.8	152.07	51.35	152.07	111.71
Rb	61	58.68	71.66	51.89	63.54	68.22	69.64	78.62	77.45	68.46	73.34	67.71	36.9	75.03	68.94	67.03	78.08	72.29	71.17	101.05	36.91	101.05	69.06
Cu	7.79	7.55	4.94	7.19	7.52	6.56	7.19	5.64	5.07	4.94	4.14	4.59	1.92	3.36	4.92	3.05	4.72	3.3	5.73	6.36	1.92	7.79	5.32
Zn	31	32.77	27.23	42.87	36.02	34.02	28	30.13	29.58	28.78	24.05	31.36	14.7	25.98	28.77	22.3	28.61	22.6	22.74	33.64	14.68	42.87	28.78
Ba	536	481.65	485.3	498.02	531.7	534.7	557.67	531.9	557.9	471.8	524.2	458.4	245	552.9	459.8	452.3	591.97	528.6	477.3	693.13	245.45	693.13	508.51
Zr	34.65	32.7	91.75	19.5	23.2	24.21	33.66	111.9	77.14	100.9	45.86	66.1	52.1	51.6	92.41	63.12	90.04	59.13	66.76	83.22	19.50	111.85	61.00
Hf	1.04	0.92	2.42	0.67	0.82	0.82	0.96	2.91	2.19	2.78	1.32	1.85	1.5	1.58	2.66	1.85	2.68	1.76	2	2.38	0.67	2.91	1.76
Nb	7.38	7.19	6.48	8.71	9.77	9.19	7.74	8.33	5.78	7.2	5.36	7.88	3.66	4.1	7.4	6.36	7.51	5.92	5.98	7.35	3.66	9.77	6.96
Th	9.65	8.68	7.58	10.29	13.08	10.07	9.47	9.16	5.73	7.8	6.22	7.46	5.57	4.93	9.18	7.44	7.34	7.22	6.93	8.75	4.93	13.08	8.13
U	1.09	0.95	1.08	1.15	1.21	1.02	1.09	1.27	0.9	1.13	0.64	0.8	0.59	0.66	1.09	0.89	1.01	0.71	0.75	0.83	0.59	1.27	0.94
Y	13.24	16.41	13.15	15.5	18.3	18.37	13.07	17.07	12.92	16.63	13.87	24.92	9.17	11.1	17.94	16.46	18.35	15.08	15.06	31.21	9.17	31.21	16.39
Th/Co	0.26	0.24	0.34	0.65	0.74	0.55	0.66	0.32	0.26	0.28	0.31	0.43	0.59	0.31	0.48	0.26	0.18	0.24	0.18	0.19	0.18	0.74	0.37
Th/Cr	0.25	0.24	0.26	0.28	0.31	0.27	0.27	0.27	0.22	0.25	0.28	0.25	0.39	0.27	0.33	0.31	0.26	0.28	0.31	0.29	0.22	0.39	0.28
Zr/Th	3.59	3.77	12.10	1.90	1.77	2.40	3.55	12.21	13.46	12.94	7.37	8.86	9.36	10.47	10.07	8.48	12.27	8.19	9.63	9.51	1.77	13.46	8.10
Th/Cr	0.25	0.24	0.26	0.28	0.31	0.27	0.27	0.27	0.22	0.25	0.28	0.25	0.39	0.27	0.33	0.31	0.26	0.28	0.31	0.29	0.22	0.39	0.28
Zr/Th	3.59	3.77	12.10	1.90	1.77	2.40	3.55	12.21	13.46	12.94	7.37	8.86	9.36	10.47	10.07	8.48	12.27	8.19	9.63	9.51	1.77	13.46	8.10
Th/U	8.85	9.14	7.02	8.95	10.81	9.87	8.69	7.21	6.37	6.90	9.72	9.33	9.44	7.47	8.42	8.36	7.27	10.17	9.24	10.54	6.37	10.81	8.69
Cr/V	0.69	0.72	0.79	0.66	0.62	0.59	0.74	0.81	0.65	0.79	0.84	0.71	0.77	0.64	0.67	0.82	0.67	0.77	0.78	0.76	0.59	0.84	0.73
U/Th	0.11	0.11	0.14	0.11	0.09	0.10	0.12	0.14	0.16	0.14	0.10	0.11	0.11	0.13	0.12	0.12	0.14	0.10	0.11	0.09	0.09	0.16	0.12

Contd...

V/Cr	1.45	1.38	1.26	1.53	1.62	1.69	1.35	1.24	1.54	1.26	1.19	1.41	1.30	1.55	1.49	1.21	1.49	1.29	1.29	1.31	1.19	1.69	1.39
Y/Ni	2.21	3.06	2.21	2.51	2.63	2.93	2.45	2.25	1.84	2.50	2.75	5.99	3.80	2.55	3.59	3.09	2.96	2.77	2.26	3.38	1.84	5.99	2.89
Rb/Sr	0.49	0.47	0.64	0.47	0.62	0.65	0.59	0.63	0.67	0.59	0.56	0.75	0.72	0.79	0.71	0.58	0.69	0.56	0.65	0.66	0.47	0.79	0.63
Zr/Hf	33.32	35.54	37.91	29.10	28.29	29.52	35.06	38.44	35.22	36.30	34.74	35.73	34.74	32.66	34.74	34.12	33.60	33.60	33.38	34.97	28.29	38.44	34.05
La/Th	2.60	3.16	2.67	3.19	3.92	3.46	2.93	2.33	3.54	3.44	2.75	2.60	2.95	3.82	2.93	2.66	3.30	2.58	2.80	4.56	2.33	4.56	3.11
Zr/Sc	4.44	4.39	14.22	2.32	2.42	2.95	4.33	15.82	13.16	15.15	7.75	6.96	13.82	12.37	13.30	9.28	12.33	9.20	11.11	10.52	2.32	15.82	9.29
Th/Sc	1.24	1.17	1.18	1.23	1.36	1.23	1.22	1.30	0.98	1.17	1.05	0.79	1.48	1.18	1.32	1.09	1.01	1.12	1.15	1.11	0.79	1.48	1.17
Cr/Ni	6.38	6.64	4.91	5.99	6.10	5.94	6.66	4.49	3.65	4.75	4.34	7.05	5.91	4.24	5.58	4.58	4.58	4.75	3.41	3.24	3.24	7.05	5.16
Cu/Zn	0.25	0.23	0.18	0.17	0.21	0.19	0.26	0.19	0.17	0.17	0.17	0.15	0.13	0.13	0.17	0.14	0.16	0.15	0.25	0.19	0.13	0.26	0.18
Ni/Co	0.16	0.15	0.27	0.39	0.39	0.34	0.37	0.26	0.32	0.24	0.25	0.24	0.26	0.27	0.26	0.18	0.15	0.18	0.17	0.20	0.15	0.39	0.25
La	25.10	27.43	20.25	32.81	51.31	34.89	27.78	21.31	20.27	26.81	17.08	19.38	16.42	18.84	26.88	19.77	24.22	18.65	19.38	39.89	16.42	51.31	25.42
Ce	48.89	44.64	50.49	44.31	60.51	48.98	49.30	55.60	41.52	51.06	37.39	40.21	31.13	33.85	52.45	38.50	48.02	38.56	38.59	55.03	31.13	60.51	45.45
Pr	5.39	5.98	3.99	6.98	10.67	8.06	5.41	4.73	4.07	5.63	3.39	4.00	3.25	3.78	5.53	3.88	4.91	3.85	4.33	7.64	3.25	10.67	5.27
Nd	18.92	21.31	13.80	24.65	37.99	27.33	19.89	16.20	14.40	20.10	12.55	14.41	11.62	12.90	20.73	13.53	16.60	13.39	14.69	27.44	11.62	37.99	18.62
Sm	3.31	3.62	2.24	4.28	6.28	4.93	3.34	2.94	2.61	3.48	2.17	2.87	2.08	2.29	3.59	2.44	2.91	2.23	2.63	4.89	2.08	6.28	3.26
Eu	1.22	1.34	1.10	1.52	1.82	1.56	1.27	1.26	1.32	1.42	1.18	1.19	0.72	1.29	1.37	1.11	1.46	1.17	1.25	2.29	0.72	2.29	1.34
Gd	4.00	4.29	2.90	5.32	7.54	5.75	3.91	3.45	3.21	4.15	2.80	3.38	2.45	2.88	4.53	3.15	3.69	3.05	3.41	5.98	2.45	7.54	3.99
Tb	0.87	1.02	0.71	1.19	1.59	1.31	2.59	0.84	0.79	0.96	0.69	1.04	0.58	0.65	1.09	0.83	0.95	0.78	0.86	1.45	0.58	2.59	1.04
Dy	2.71	3.35	2.52	3.34	3.93	3.83	2.59	2.92	2.51	3.11	2.48	4.70	1.83	2.15	3.51	3.23	3.50	2.84	3.04	4.97	1.83	4.97	3.15
Ho	0.52	0.65	0.51	0.63	0.74	0.73	0.51	0.60	0.50	0.61	0.54	1.01	0.37	0.43	0.70	0.62	0.73	0.57	0.59	1.07	0.37	1.07	0.63
Er	2.09	2.38	1.90	2.52	3.05	2.81	1.93	2.26	1.84	2.29	1.95	3.19	1.45	1.59	2.59	2.26	2.50	2.03	2.15	3.69	1.45	3.69	2.32
Tm	0.22	0.27	0.22	0.26	0.29	0.30	0.22	0.25	0.34	0.25	0.23	0.39	0.15	0.17	0.30	0.27	0.32	0.25	0.24	0.41	0.15	0.41	0.27
Yb	1.56	1.88	1.53	1.86	2.08	2.17	1.51	1.80	1.41	1.79	1.53	2.73	1.00	1.27	2.05	1.88	2.10	1.78	1.77	2.65	1.00	2.73	1.82
Lu	0.22	0.27	0.22	0.26	0.31	0.29	0.22	0.25	0.22	0.26	0.21	0.40	0.15	0.17	0.30	0.26	0.31	0.25	0.25	0.40	0.15	0.40	0.26
ΣREE	115.02	118.43	102.38	129.93	188.11	142.94	120.47	114.41	95.01	121.92	84.19	98.90	73.20	82.26	125.62	91.73	112.22	89.40	93.18	157.80	73.20	188.11	112.86
ΣLREE	102.83	104.32	91.87	114.55	168.58	125.75	106.99	102.04	84.19	108.50	73.76	82.06	65.22	72.95	110.55	79.23	98.12	77.85	80.87	137.18	65.22	169.05	99.37

Contd...

ΣHREE	12.19	14.11	10.51	15.38	19.53	17.19	13.48	12.37	10.82	13.42	10.43	16.84	7.98	9.31	15.07	12.50	14.10	11.55	12.31	20.62	7.98	20.62	13.49
LREE/HREE	8.44	7.39	8.74	7.45	8.63	7.32	7.94	8.25	7.78	8.08	7.07	4.87	8.17	7.84	7.34	6.34	6.96	6.74	6.57	6.65	4.87	8.74	7.43
La/Sc	3.21	3.68	3.14	3.91	5.35	4.25	3.58	3.01	3.46	4.03	2.89	2.04	4.36	4.52	3.87	2.91	3.32	2.90	3.22	5.04	2.04	5.35	3.63
La/Co	0.67	0.75	0.92	2.06	2.88	1.92	1.94	0.73	0.93	0.97	0.85	1.11	1.75	1.17	1.41	0.69	0.60	0.63	0.49	0.86	0.49	2.88	1.17
	Normalised																						
La	68.39	74.74	55.18	89.40	139.81	95.07	75.69	58.07	55.23	73.05	46.54	52.81	44.74	51.34	73.24	53.87	65.99	50.82	52.81	108.69	44.74	139.81	69.27
Ce	51.09	46.65	52.76	46.30	63.23	51.18	51.52	58.10	43.39	53.35	39.07	42.02	32.53	35.37	54.81	40.23	50.18	40.29	40.32	57.50	32.53	63.23	47.49
Pr	39.34	43.65	29.12	50.95	77.88	58.83	39.49	34.53	29.71	41.09	24.74	29.20	23.72	27.59	40.36	28.32	35.84	28.10	31.61	55.77	23.72	77.88	38.49
Nd	26.61	29.97	19.41	34.67	53.43	38.44	27.97	22.78	20.25	28.27	17.65	20.27	16.34	18.14	29.16	19.03	23.35	18.83	20.66	38.59	16.34	53.43	26.19
Sm	14.33	15.67	9.70	18.53	27.19	21.34	14.46	12.73	11.30	15.06	9.39	12.42	9.00	9.91	15.54	10.56	12.60	9.65	11.39	21.17	9.00	27.19	14.10
Eu	14.02	15.40	12.64	17.47	20.92	17.93	14.60	14.48	15.17	16.32	13.56	13.68	8.28	14.83	15.75	12.76	16.78	13.45	14.37	26.32	8.28	26.32	15.44
Gd	13.07	14.02	9.48	17.39	24.64	18.79	12.78	11.27	10.49	13.56	9.15	11.05	8.01	9.41	14.80	10.29	12.06	9.97	11.14	19.54	8.01	24.64	13.05
Tb	15.00	17.59	12.24	20.52	27.41	22.59	44.66	14.48	13.62	16.55	11.90	17.93	10.00	11.21	18.79	14.31	16.38	13.45	14.83	25.00	10.00	44.66	17.92
Dy	7.11	8.79	6.61	8.77	10.31	10.05	6.80	7.66	6.59	8.16	6.51	12.34	4.80	5.64	9.21	8.48	9.19	7.45	7.98	13.04	4.80	13.04	8.28
Ho	6.11	7.64	5.99	7.40	8.70	8.58	5.99	7.05	5.88	7.17	6.35	11.87	4.35	5.05	8.23	7.29	8.58	6.70	6.93	12.57	4.35	12.57	7.42
Er	8.39	9.56	7.63	10.12	12.25	11.29	7.75	9.08	7.39	9.20	7.83	12.81	5.82	6.39	10.40	9.08	10.04	8.15	8.63	14.82	5.82	14.82	9.33
Tm	6.18	7.58	6.18	7.30	8.15	8.43	6.18	7.02	9.55	7.02	6.46	10.96	4.21	4.78	8.43	7.58	8.99	7.02	6.74	11.52	4.21	11.52	7.51
Yb	6.29	7.58	6.17	7.50	8.39	8.75	6.09	7.26	5.69	7.22	6.17	11.01	4.03	5.12	8.27	7.58	8.47	7.18	7.14	10.69	4.03	11.01	7.33
Lu	5.77	7.09	5.77	6.82	8.14	7.61	5.77	6.56	5.77	6.82	5.51	10.50	3.94	4.46	7.87	6.82	8.14	6.56	6.56	10.50	3.94	10.50	6.85
Y	6.30	7.81	6.26	7.38	8.71	8.75	6.22	8.13	6.15	7.92	6.60	11.87	4.37	5.29	8.54	7.84	8.74	7.18	7.17	14.86	4.37	14.86	7.81
Eu/Eu*	1.02	1.04	1.32	0.97	0.81	0.90	1.07	1.21	1.39	1.14	1.46	1.17	0.97	1.54	1.04	1.22	1.36	1.37	1.28	1.29	0.81	1.54	1.18
(Gdn/Ybn)	2.08	1.85	1.54	2.32	2.94	2.15	2.10	1.55	1.85	1.88	1.48	1.00	1.99	1.84	1.79	1.36	1.42	1.39	1.56	1.83	1.00	2.94	1.80
La/SmN	4.77	4.77	5.69	4.83	5.14	4.45	5.24	4.56	4.89	4.85	4.95	4.25	4.97	5.18	4.71	5.10	5.24	5.26	4.64	5.13	4.25	5.69	4.93
La/Ybn	10.87	9.86	8.94	11.92	16.67	10.86	12.43	8.00	9.71	10.12	7.54	4.80	11.10	10.02	8.86	7.11	7.79	7.08	7.40	10.17	4.80	16.67	9.56

Table 3.6.4: Geochemical composition of shales of Talchir Formation, Chirimiri, district Koriya, Chhattisgarh, India. Major oxides in wt%, trace elements in ppm; Eu/Eu* = $\{Eu_N/(Sm_N*Gd_N)^{1/2}\}$. Normalising values are after Taylor and McLennan (1985).

	Shales						
Element	BK1	BK2	BK3	BK4	Min	Max	Average
SiO2	72.94	73.71	72.23	73.88	73.19	72.23	73.19
Al2O3	12.97	12.62	12.39	12.69	12.67	12.39	12.67
TiO2	0.75	0.71	0.72	0.7	0.72	0.70	0.72
Fe2O3	4.74	4.76	4.76	4.88	4.79	4.74	4.79
MnO	0.06	0.06	0.06	0.06	0.06	0.06	0.06
MgO	1.87	1.83	1.88	1.81	1.85	1.81	1.85
CaO	0.97	0.92	0.92	0.83	0.91	0.83	0.91
Na2O	1.84	1.81	1.85	1.78	1.82	1.78	1.82
K2O	2.73	2.59	2.58	2.61	2.63	2.58	2.63
P2O5	0.15	0.14	0.14	0.14	0.14	0.14	0.14
CIA	66.66	66.65	66.65	66.65	66.65	66.65	66.65
PIA	67.56	67.74	66.92	68.86	67.77	66.92	67.77
ICV	0.16	0.17	0.17	0.17	0.17	0.16	0.17
CIW	72.97	72.99	72.32	74.01	73.07	72.32	73.07
Na2O/K2O	0.67	0.70	0.72	0.68	0.69	0.67	0.69
SiO2/Al2O3	5.62	5.84	5.83	5.82	5.78	5.62	5.78
K2O/Na2O	1.49	1.43	1.39	1.47	1.45	1.39	1.45
K2O/Al2O3	0.21	0.21	0.21	0.21	0.21	0.21	0.21
Fe2O3+MgO	6.62	6.60	6.66	6.70	6.65	6.60	6.65
Al2O3/TiO2	17.29	17.77	17.21	18.13	17.60	17.21	17.60
Al2O3/SiO2	0.18	0.17	0.17	0.17	0.17	0.18	0.17
Al2o3/(CaO+Na2O)	0.10	0.11	0.09	0.10	0.09	0.11	0.10
Ni	13.07	13.48	14.4	14.18	13.07	14.40	13.78
Co	25.42	27.16	33.55	31.71	25.42	33.55	29.46
Cr	75.41	69.22	77.97	74.33	69.22	77.97	74.23
V	80.5	93.81	110.24	89.54	80.50	110.24	93.52
Sc	15.07	13.54	15.72	14.74	13.54	15.72	14.77
Sr	140.87	147.46	159.85	155.43	140.87	159.85	150.90
Rb	120.13	118.23	126.07	126.76	118.23	126.76	122.80
Cu	19.61	17.16	19.83	28.34	17.16	28.34	21.24
Zn	83.48	89.2	95.93	110.96	83.48	110.96	94.89
Ba	753.17	718.04	756.68	811.83	718.04	811.83	759.93
Zr	175.23	180.22	195.18	172.59	172.59	195.18	180.81
Hf	5.62	5.45	6.37	5.58	5.45	6.37	5.76
Nb	18.19	15.85	17.16	17.5	15.85	18.19	17.18
Th	24.51	22.22	28.88	23.14	22.22	28.88	24.69
U	3.35	3.09	3.65	3.37	3.09	3.65	3.37

contd...

Y	34.48	30.87	38	32.47	30.87	38.00	33.96
Th/Co	0.96	0.82	0.86	0.73	0.73	0.96	0.84
Th/Cr	0.33	0.32	0.37	0.31	0.31	0.37	0.33
Zr/Th	7.15	8.11	6.76	7.46	6.76	8.11	7.37
Th/U	7.32	7.19	7.91	6.87	6.87	7.91	7.32
Cr/V	0.94	0.74	0.71	0.83	0.71	0.94	0.80
U/Th	0.14	0.14	0.13	0.15	0.13	0.15	0.14
V/Cr	1.07	1.36	1.41	1.20	1.07	1.41	1.26
Y/Ni	2.64	2.29	2.64	2.29	2.29	2.64	2.46
Rb/Sr	0.85	0.80	0.79	0.82	0.79	0.85	0.81
Zr/Hf	31.18	33.07	30.64	30.93	30.64	33.07	31.45
La/Th	2.92	2.69	2.40	2.78	2.40	2.92	2.70
Zr/Sc	11.63	13.31	12.42	11.71	11.63	13.31	12.27
Th/Sc	1.63	1.64	1.84	1.57	1.57	1.84	1.67
Cr/Ni	5.77	5.14	5.41	5.24	5.14	5.77	5.39
Cu/Zn	0.23	0.19	0.21	0.26	0.19	0.26	0.22
Ni/Co	0.51	0.50	0.43	0.45	0.43	0.51	0.47
La	71.54	59.83	69.3	64.24	59.83	71.54	66.23
Ce	151.36	119.62	150.16	118.19	118.19	151.36	134.83
Pr	16.76	13.78	16.44	14.54	13.78	16.76	15.38
Nd	55.45	45.18	53.97	48.08	45.18	55.45	50.67
Sm	9.69	8.76	9.43	8.48	8.48	9.69	9.09
Eu	2.48	2.31	2.52	2.49	2.31	2.52	2.45
Gd	10.78	9.99	11.31	10.25	9.99	11.31	10.58
Tb	2.55	2.36	2.52	2.34	2.34	2.55	2.44
Dy	6.94	6.69	7.26	7.08	6.69	7.26	6.99
Ho	1.32	1.34	1.34	1.3	1.30	1.34	1.33
Er	5	4.84	5.39	5.01	4.84	5.39	5.06
Tm	0.51	0.52	0.53	0.52	0.51	0.53	0.52
Yb	3.68	3.76	3.98	3.81	3.68	3.98	3.81
Lu	1.63	1.66	1.75	1.69	1.63	1.75	1.68
ΣREE	339.69	280.64	335.9	288.02	280.64	339.69	311.06
ΣLREE	307.28	249.48	301.82	256.02	249.48	307.3	278.65
ΣHREE	32.41	31.16	34.08	32.00	31.16	34.08	32.41
LREE/HREE	9.48	8.01	8.86	8.00	8.00	9.48	8.59
La/Sc	4.75	4.42	4.41	4.36	4.36	4.75	4.48
La/Co	2.81	2.20	2.07	2.03	2.03	2.81	2.28
Chondrite Normalised							
La	195	163	189	175	163.02	194.93	180.46
Ce	158	125	157	124	123.50	158.16	140.89
Pr	122	101	120	106	100.58	122.34	112.26
Nd	78	64	76	68	63.54	77.99	71.27

contd...

Sm	42	38	41	37	36.71	41.95	39.35
Eu	29	27	29	29	26.55	28.97	28.16
Gd	35	33	37	33	32.65	36.96	34.58
Tb	44	41	43	40	40.34	43.97	42.11
Dy	18	18	19	19	17.56	19.06	18.35
Ho	16	16	16	15	15.28	15.75	15.57
Er	20	19	22	20	19.44	21.65	20.32
Tm	14	15	15	15	14.33	14.89	14.61
Yb	15	15	16	15	14.84	16.05	15.35
Lu	905	810	997	852	810.24	997.38	891.21
Y	905	810	997	852	810.24	997.38	891.21
Eu/Eu*	0.74	0.75	0.75	0.82	0.74	0.82	0.76
Gd/YbN	2.37	2.15	2.30	2.18	2.15	2.37	2.25
La/SmN	4.65	4.30	4.63	4.77	4.30	4.77	4.58
La/Ybn	13.14	10.75	11.77	11.39	10.75	13.14	11.76

Table 3.6.5: Geochemical composition of Baikunthpur sandstone of Talchir Formation Chirimiri area, district Koriya, Major elements in Oxide wt%, trace elements in ppm, normalising values after Taylor and McLennan (1985)

	Baikunthpur sandstone								
Element	BBK1	BBK2	BBK4	BBK5	BBK6	BBK7	Min	Max	Average
SiO2	75.44	75.15	72.11	72.65	70.6	81.89	70.60	81.89	74.64
Al2O3	11.97	11.55	13.36	13.56	13.79	9.23	9.23	13.79	12.24
TiO2	0.54	0.57	0.68	0.67	0.7	0.26	0.26	0.70	0.57
Fe2O3	4.74	4.94	5.1	5.11	6.1	2.13	2.13	6.10	4.69
MnO	0.05	0.05	0.05	0.06	0.07	0.04	0.04	0.07	0.05
MgO	1.22	1.27	1.36	1.41	1.49	0.495	0.50	1.49	1.21
CaO	1.57	1.27	0.78	0.9	0.83	1.97	0.78	1.97	1.22
Na2O	1.57	1.66	1.75	1.75	1.61	1.38	1.38	1.75	1.62
K2O	2.32	2.31	3.06	3.09	3.02	2.42	2.31	3.09	2.70
P2O5	0.12	0.13	0.14	0.14	0.13	0.06	0.06	0.14	0.12
CIA	60	61.11	65	65	65	50	50.00	65.00	61.02
PIA	63.43	64.15	69.96	69.36	70.77	52.97	52.97	70.77	65.11
ICV	0.15	0.15	0.12	0.17	0.16	0.16	0.12	0.17	0.15
CIW	68.70	69.57	75.61	75.02	76.23	61.13	61.13	76.23	71.04
Na2O/K2O	0.68	0.72	0.57	0.57	0.53	0.57	0.53	0.72	0.61
SiO2/Al2O3	6.3	6.5	5.4	5.35	5.28	8.87	5.28	8.87	6.28
K2O/Na2O	1.48	1.39	1.75	1.76	1.88	1.75	1.39	1.88	1.67
K2O/Al2O3	0.19	0.20	0.23	0.23	0.22	0.26	0.19	0.26	0.22
Fe2O3+MgO	5.97	6.23	6.47	6.54	7.59	2.63	2.63	7.59	5.91
Al2O3/TiO2	22.17	20.26	19.65	20.24	19.70	35.50	19.65	35.50	22.92
Al2O3/SiO2	0.16	0.15	0.19	0.19	0.19	0.11	0.11	0.19	0.17
Al2o3/(CaO+Na2O)	0.10	0.10	0.11	0.10	0.16	0.24	0.10	0.24	0.14
Ni	16.84	14.60	15.35	8.86	12.31	7.39	7.39	16.84	12.56
Co	62.15	52.07	36.9	19.08	30.49	19.62	19.08	62.15	36.72
Cr	73	73	81	57	58	33	33.06	80.56	62.42
V	96.17	88.29	111.74	80.55	71.32	49.88	49.88	111.74	82.99
Sc	14	14	16	17	12	7	7.39	17.11	13.43
Sr	161	205	190	118	164	124	117.51	205.24	160.29
Rb	152	150	165	111	101	61	61.08	164.94	123.35
Cu	21.68	22.98	26.62	13.65	11.01	7.87	7.87	26.62	17.30
Zn	110.59	96.42	117.88	53.06	69.14	29.88	29.88	117.88	79.50
Ba	704	692	759	519	708	466	466.45	758.56	641.32
Zr	146	150	172	139	162	84	84.24	172.33	142.12
Hf	5	5	6	4	5	3	2.60	5.69	4.41
Nb	15	15	17	12	12	8	7.80	17.06	13.11
Th	24	25	26	20	19	9	9.15	26.27	20.48
U	3	3	3	2	2	1	1.12	2.99	2.26
Y	31	28	36	24	27	19	19.09	35.90	27.55
Th/Co	0.38	0.48	0.71	1.03	0.62	0.47	0.38	1.03	0.62

Th/Cr	0.33	0.35	0.33	0.34	0.32	0.28	0.28	0.35	0.32
Zr/Th	6.11	5.97	6.56	7.04	8.59	9.21	5.97	9.21	7.25
Zr/Sc	10.21	10.76	10.74	8.11	13.64	11.40	8.11	13.64	10.81
Th/U	8.90	9.46	8.79	9.61	9.06	8.17	8.17	9.61	9.00
Cr/V	0.76	0.82	0.72	0.71	0.82	0.66	0.66	0.82	0.75
U/Th	0.11	0.11	0.11	0.10	0.11	0.12	0.10	0.12	0.11
V/Cr	1.32	1.22	1.39	1.41	1.22	1.51	1.22	1.51	1.34
Y/Ni	1.86	1.93	2.34	2.73	2.17	2.58	1.86	2.73	2.27
Rb/Sr	0.95	0.73	0.87	0.94	0.62	0.49	0.49	0.95	0.77
Zr/Hf	30.82	32.75	30.29	36.73	31.92	32.40	30.29	36.73	32.49
La/Th	2.48	2.34	2.59	2.77	2.44	2.78	2.34	2.78	2.57
Th/Sc	0.20	0.24	0.23	0.26	0.16	0.26	0.16	0.26	0.22
Cr/Ni	0.27	0.28	0.42	0.46	0.40	0.38	0.27	0.46	0.37
Cu/Zn	0.20	0.24	0.23	0.26	0.16	0.26	0.16	0.26	0.22
Ni/Co	0.27	0.28	0.42	0.46	0.40	0.38	0.27	0.46	0.37
La	59.24	58.73	68.14	54.57	45.88	25.4	25.40	68.14	51.99
Ce	130	124.01	143.97	112.28	88.84	43.19	43.19	143.97	107.05
Pr	14.33	13.39	16.05	11.12	10.84	5.05	5.05	16.05	11.80
Nd	48.05	45.62	53.24	36.63	34.77	17.91	17.91	53.24	39.37
Sm	8.45	7.73	9.63	6.11	6.47	3.25	3.25	9.63	6.94
Eu	2.44	2.18	2.69	1.77	1.92	1.15	1.15	2.69	2.03
Gd	9.79	9.44	10.94	7.22	7.71	3.81	3.81	10.94	8.15
Tb	2.2	2.16	2.61	1.66	1.84	0.98	0.98	2.61	1.91
Dy	6.68	6.37	8	5	5.43	3.65	3.65	8.00	5.86
Ho	1.28	1.26	1.49	0.97	1.11	0.73	0.73	1.49	1.14
Er	4.79	4.55	5.55	3.66	4.04	2.56	2.56	5.55	4.19
Tm	0.49	0.48	0.6	0.36	0.44	0.3	0.30	0.60	0.45
Yb	3.46	3.34	3.92	2.54	3.177	1.97	1.97	3.92	3.07
Lu	0.53	0.47	0.6	0.43	0.45	0.28	0.28	0.60	0.46
ΣREE	291.73	279.73	327.43	244.32	212.92	110.23	110.23	327.43	244.39
ΣLREE	262.51	251.66	293.72	222.48	188.72	95.95	95.95	293.72	219.17
ΣHREE	29.22	28.07	33.71	21.84	24.20	14.28	14.28	33.71	25.22
LREE/HREE	8.98	8.97	8.71	10.19	7.80	6.72	6.72	10.19	8.56
La/Sc	4.15	4.22	4.25	3.19	3.87	3.44	3.19	4.25	3.85
La/Co	0.95	1.13	1.85	2.86	1.50	1.29	0.95	2.86	1.60
	Chondrite Normalised								
La	161.42	160.03	185.67	148.69	125.01	69.21	69.21	185.67	141.67
Ce	135.84	129.58	150.44	117.32	92.83	45.13	45.13	150.44	111.86
Pr	104.60	97.74	117.15	81.17	79.12	36.86	36.86	117.15	86.11
Nd	67.58	64.16	74.88	51.52	48.90	25.19	25.19	74.88	55.37
Sm	36.58	33.46	41.69	26.45	28.01	14.07	14.07	41.69	30.04
Eu	28.05	25.06	30.92	20.34	22.07	13.22	13.22	30.92	23.28
Gd	31.99	30.85	35.75	23.59	25.20	12.45	12.45	35.75	26.64
Tb	37.93	37.24	45.00	28.62	31.72	16.90	16.90	45.00	32.90

Contd...

Dy	17.53	16.72	21.00	13.12	14.25	9.58	9.58	21.00	15.37
Ho	15.04	14.81	17.51	11.40	13.04	8.58	8.58	17.51	13.40
Er	19.24	18.27	22.29	14.70	16.22	10.28	10.28	22.29	16.83
Tm	13.76	13.48	16.85	10.11	12.36	8.43	8.43	16.85	12.50
Yb	13.95	13.47	15.81	10.24	12.81	7.94	7.94	15.81	12.37
Lu	13.91	12.34	15.75	11.29	11.81	7.35	7.35	15.75	12.07
Y	14.88	13.42	17.10	11.53	12.71	9.09	9.09	17.10	13.12
Eu/Eu*	0.82	0.78	0.80	0.81	0.83	1.00	0.78	1.00	0.84
(Gdn/Ybn)	2.29	2.29	2.26	2.30	1.97	1.57	1.57	2.30	2.11
La/SmN	4.41	4.78	4.45	5.62	4.46	4.92	4.41	5.62	4.78
La/Ybn	11.57	11.88	11.75	14.52	9.76	8.71	8.71	14.52	11.36

CHAPTER – 4

PROVENANCE COMPOSITION & TECTONIC SETTING

PROVENANCE COMPOSITION AND TECTONIC SETTING

4.1 General Statement

Provenance studies aim to decipher the composition, its geological evolution and constrain the tectonic setting of the depositional basin of sedimentary rocks. A meaningful provenance analysis necessarily concentrates on the evaluation of indicators that have been inherited from the original source areas (Zimmermann and Bahlburg, 2003). The geochemical analysis of sedimentary rocks is a valuable tool for provenance studies of sedimentary rocks provided that the bulk composition is not severely affected by diagenesis, metamorphism or other alteration processes (McLennan et al., 1993). The relations of major elements of sedimentary rocks to upper crustal composition are considerably less established than REE, Sc, Th and HFSE due to their mobility during weathering, sedimentation, diagenesis and metamorphism (McLennan and Taylor 1991; McLennan et al., 1990; Condie et al., 1992; Cullers, 1995; Madhavaraju and Ramasamy, 2002; Armstrong-Altrin et al., 2004). Thus, it has been emphasised to constrain provenance on the basis of immobile elements. Since the concentration of major oxides of both Chirimiri and Baikunthpur sandstones are primary, it has been used to get basic idea about the source rocks. Nevertheless more emphasis is placed on immobile trace elements for the interpretation of source lithologies of the clastic rocks of Talchir Formation.

4.2 Provenance Composition

Provenance analysis of sediments is aimed to reconstruct the parent-rock assemblages of sediments and the climatic and physiographic conditions under which sediments were formed (Weltje and Eynatten von, 2004). The petrographic interpretations of Talchir sandstones of Chirimiri, Koriya district, Chhattisgarh suggests transitional margin and basement uplift of Continental block provenance as the source lithologies for these sediments. This petrographic interpretation is in consonant with the geochemical data of Talchir sandstone and shale samples as they appear closely similar in composition to Upper Continental Crust and Post Archean Australian Shale. Numerous geochemical techniques have been developed to identify the provenance composition, tectonic setting, and environmental conditions with the help of major elements, trace elements, rare earth elements. An idea about the nature

f provenance composition can be obtained by major element mobility assessment iagram (Figure 3.2.1).

The magmatic relationship between various elements as envisaged from these iagrams, suggests that the detritus was predominantly derived from an igneous errain. Moreover the positive correlation of Al_2O_3 with K_2O, Na_2O and TiO_2 is an ndication of their detrital phase. It is observed that Al_2O_3 is positively correlated vith Na_2O (r = 0.59), TiO_2 (r = 0.71) and negative with K_2O (r = -0.58) in sandstones f Chirimiri. A similar strong positive high correlation is seen in Baikunthpur andstones K_2O (r = 0.78), TiO_2 (r = 0.98), Na_2O (r = 0.84) and in associated shales $_2O$ (r = 0.92) and TiO_2 (r = 0.59) with Al_2O_3. The magnitude of positive correlation s strong in Baikunthpur and shales than Chirimiri sandstones which suggests that Baikunthpur sandstones and shales have dissimilar source than Chirimiri sandstones. l_2O_3 versus TiO_2 binary diagram (Figure 4.2.2) is used to discriminate igneous rock pectrum of the source terrain in the diagram of an igneous terrain (McLennan et. al, 979). In this diagram Chirimiri sandstone samples occupy granite and granodiorite egions, Baikunthpur sandstone fall in granodiorite region whereas associated shales e in the region of granite and basalts. This indicates that the provenance composition f the clastic rocks of Talchir Formation is granitic to granodioritic.

The values of K_2O/Na_2O ratio greater than 1 indicate abundance of K-feldspar ver plagioclase. This ratio can be used to know the composition of source rocks and veathering intensity (Lindsey, 1999). The K_2O/Na_2O ratio increases with progressive ncrease in weathering. The K_2O/Na_2O ratio ranges from 0.97 to 2.16 (average, 1.62) n Chirimiri sandstones, in Baikunthpur sandstones from 1.39 to 1.88 (average, 1.67) nd in shales from 1.39 to1.48 (average, 1.49) indicating predominance of granitic ocks in the source terrain. The Fe_2O_3 and MgO are mainly found in mafic minerals nd their low abundances signify depletion of mafic minerals in the source rocks. The e_2O_3 in the Chirimiri sandstones ranges from 2.64 to 5 (average, 3.56), in aikunthpur sandstone 2.13 to 6.1 (average, 4.69) and in shales ranges from 4.74-4.78 verage, 4.79). Similarly MgO ranges from 0.86 to 1.54 (average, 1.06) in Chirimiri andstones, in Baikunthpur sandstone 0.49 to 1.27 (average 1.21) and in shales 6.60 to .65 (average, 6.70). Low values of these ferromagnesian elements indicate depleted nafic components in the mafic provenance. The index of chemical alteration can also e used as a guide to know the composition of source rocks because sediments that

derived from basement rocks particularly in glacial climate closely reflects the composition of its provenance due to absence of chemical weathering (Kalsbeek, 1971 and 1974). The CIA values of sandstones and shales of Talchir Formation are greater than UCC but less than PAAS (UCC CIA= 50.47, PAAS = 75 Taylor and McLennan, 1985). The average CIA value of Chirimiri sandstone is 61.58, in Baikunthpur sandstone average is 61.02 and in shales average is 66.66 which are closer to Upper Continental Crust. It suggests Upper Continental Crust like source for the clastic rocks of Talchir Formation.

Le Maitre used CaO-Na_2O-K_2O diagram to discriminate felsic igneous rocks of the provenance. In this ternary diagram samples of Talchir clastics fall in granite and granodiorite region (Figure 4.2.1) which complements the interpretation of Al-Ti diagram (Figure 4.2.2). The Al_2O_3/TiO_2 ratio is also used as an indicator of source composition. The Al_2O_3/TiO_2 ratio values assigned for various igneous rocks are which 3 to 8 in mafic rock, 8 to 21 in intermediate rock and 21 to 70 in felsic rock (Hayashi et al., 1997). This ratio in Chirimiri sandstone ranges from 18.16 to 36.38 (average 24.78), Baikunthpur sandstone 19.64 to 35.50 (average, 22.91) and in associated shales 17.20 to 18.12 (average, 17.60). This also indicates that the source terrain was composed of intermediate to felsic rocks. The major elements discriminant function diagram is also used to infer provenance signatures (Roser and Korsch, 1988).

This diagram suggests a predominantly siliceous source composition, possessing intermediate to felsic components for the clastics of Talchir Formation (Figure 4.2.3). Immobile elements based binary diagram (TiO_2 versus Zr) firmly endorses the inferences of major element data. This diagram also indicates minor contribution from basic igneous rocks (Figure 4.2.4). The Rb/Sr ratio in Chirimiri sandstones ranges from 0.47 to 0.79 (average 0.62), in Baikunthpur sandstone from 0.49 to 0.95 (average, 0.82) and 0.79 - 0.85 (average 0.81) in shales. These values of Rb/Sr are greater than Upper Continental Crust (Rb/Sr = 0.32) but close to Post Archean Australian Shale (Rb/Sr = 0.80) indicating a source similar to UCC or PAAS.

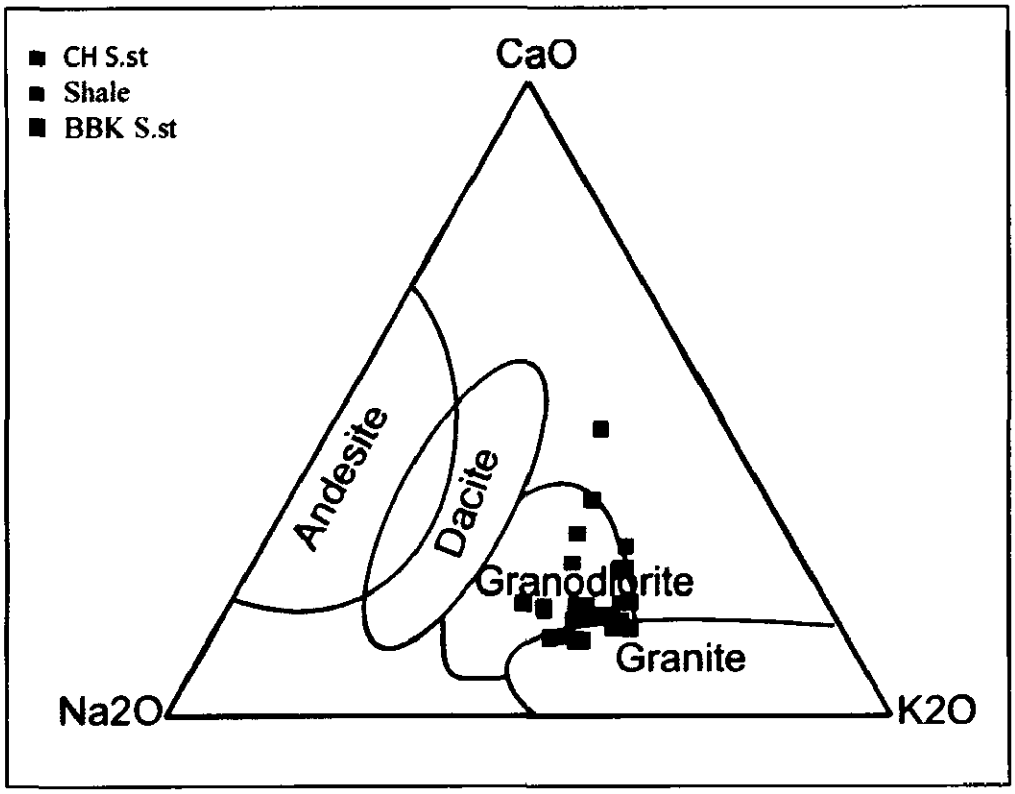

Figure 4.2.1 CaO-Na_2O-K_2O ternary plot for sandstones and shales of Talchir Formation, Chirimiri, district Koriya, Chhattisgarh, India (Le Maitre, 1976).

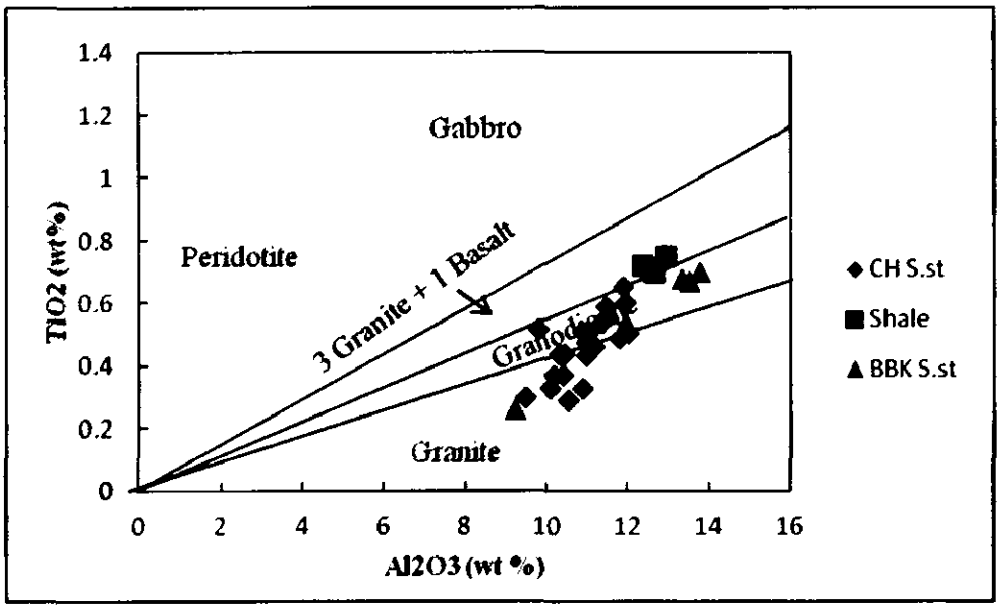

Figure 4.2.2: Al_2O_3 versus TiO_2 bivariate plot for sandstones and shales of Talchir Formation, Chirimiri, district Koriya, Chhattisgarh, India (McLennan et. al, 1979)

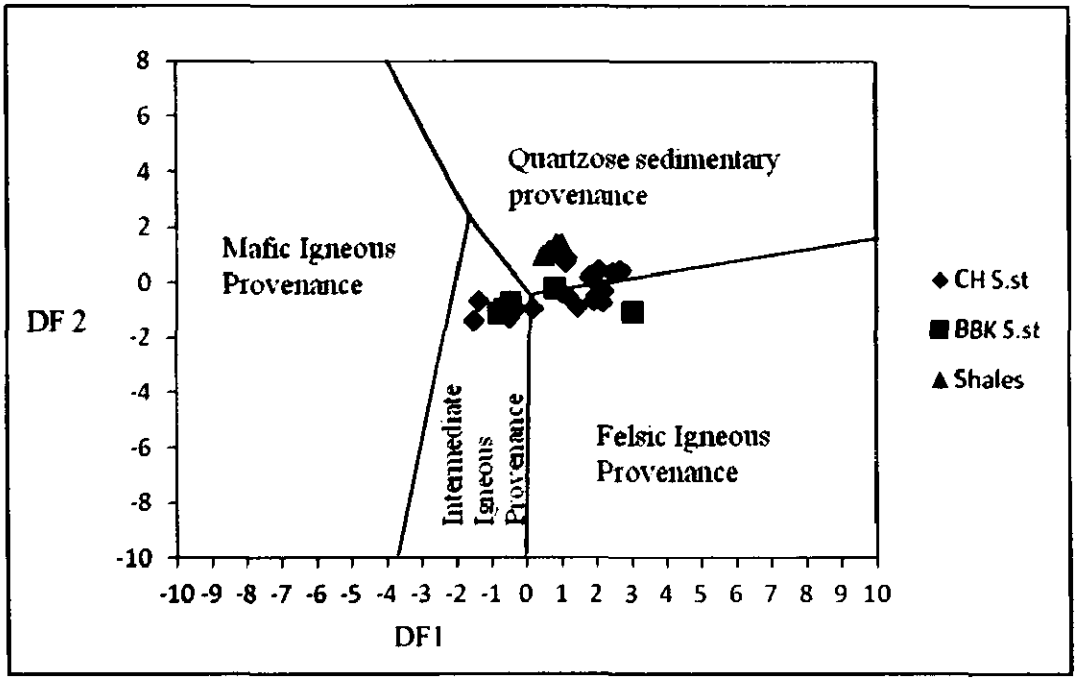

Figure 4.2.3: Discriminant function diagram for provenance signatures of Talchir sandstones and shales, Chirimiri, district Koriya, Chhattisgarh, India, using major oxide ratios (after Roser and Korsch, 1988), where DF1 = $30.638TiO_2/Al_2O_3$ – $12.541Fe_2O_3^t/Al_2O_3$ + $7.329MgO/Al_2O_3$ +$12.031Na_2O/Al_2O_3$ + $35.402K_2O/Al_2O_3$ – 6.382, DF2 = $56.500TiO_2/Al_2O_3$ – $10.879Fe_2O_3$ (t)/Al_2O_3 + $30.875MgO/Al_2O_3$ – $5.404Na_2O/Al_2O_3$ + $11.112K_2O/Al_2O_3$ – 3.89

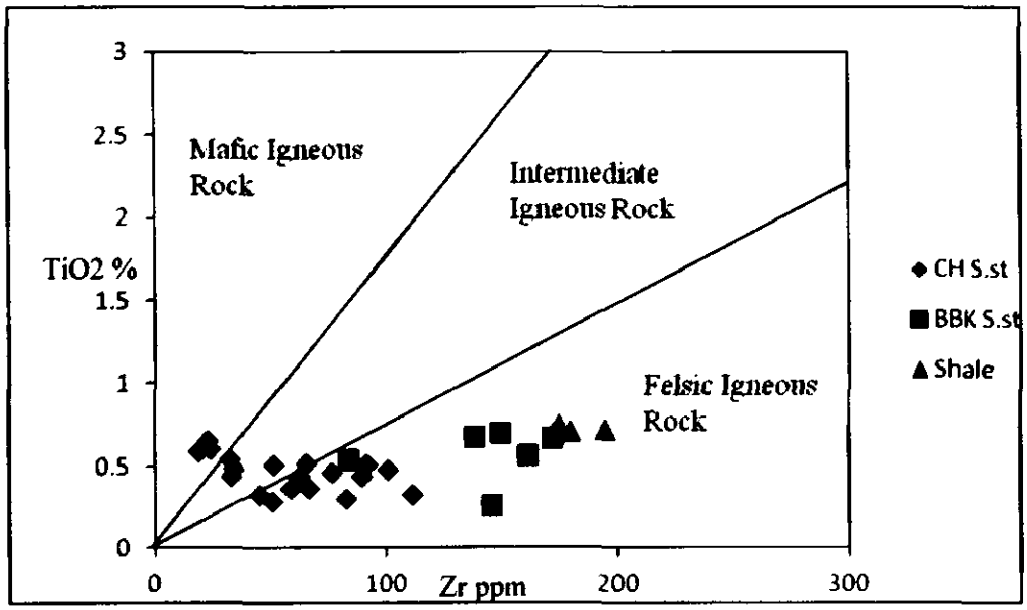

Figure 4.2.4: TiO_2 versus Zr plot for sandstones and shales of Talchir Formation Chirimiri, district Koriya, Chhattisgarh, India (Hayashi et. al., 1997).

Apart from major elements, concentrations of trace elements like Zr, Th, Hf, Y, Co, Cr, Sc, Ni and REE and their elemental ratios are most suited for elucidating provenance and tectonic setting because of their relatively low mobility during sedimentary processes and low residence time in sea water (Holland, 1978; Cullers et al, 1979; Bhatia ad Crook, 1986; Wronkiewicz and Condie, 1987; and Cox et al., 1995). Furthermore, HFSE such as Zr, Hf, Nb and Y, are partitioned into melt during crystallization (Feng and Kerrich, 1990) and are more enriched in felsic material than mafic source, and therefore, believed to reflect the composition of the provenance (Taylor and McLennan, 1985).

The La and Th are immobile elements and are found in higher proportion in felsic source whereas, concentration of trace elements like Co and Sc are higher in mafic igneous source (Taylor and McLennan, 1985; Wronkiewicz and Condie, 1987). Therefore, higher values of Th/Sc, Th/Co and La/Sc display crustal derivation and lower values indicate a mantel source. The La/Sc ratio in Chirimiri sandstones ranges from 2.04 to 5.04 (average 3.63), in Baikunthpur sandstone it ranges from 3.44 to 4.25 (average 3.85) and 4.36-4.75 in associated shales (average 4.48), Th/Sc in Chirimiri sandstones ranges from 0.79 to 1.48 (average 1.16), in Baikunthpur sandstones from 1.24 to 1.80 (average 1.50) and 1.57 to 1.84 in associated shales (average 1.67). The average ratios of La/Sc and Th/Sc of sandstones and shales of Talchir Formation are higher than Upper Continental Crust and Post Archean Australian Shale (UCC La/Sc = 2.21,Th/Sc= 0.79 and PAAS La/Sc = 2.38, Th/Sc 0.91 McLennan, 2001), indicating evolved sedimentary input. Same results are obtained when the geochemical data of Talchir clastics is plotted in La/Sc versus Th/Co diagram (Figure 4.2.5).

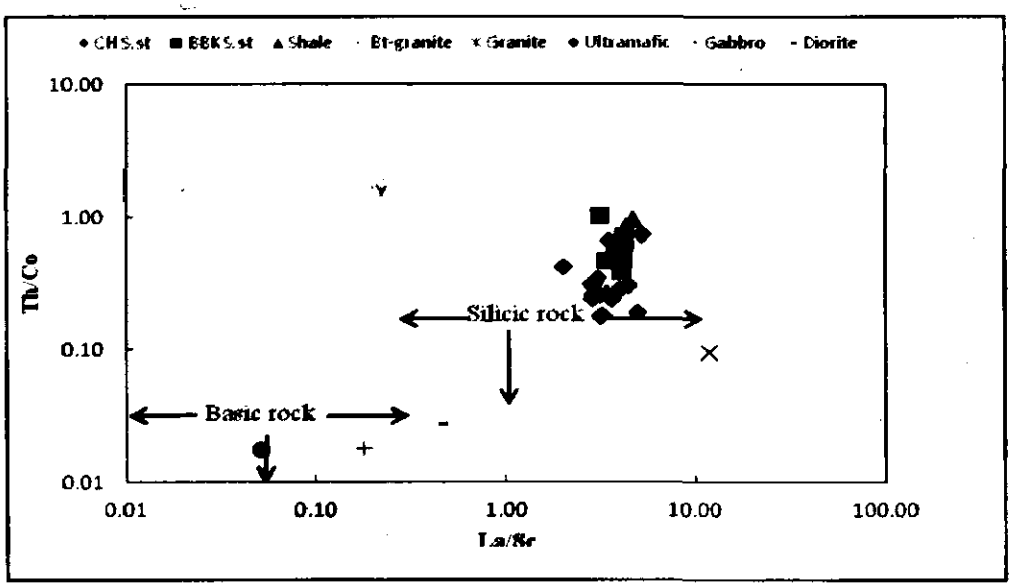

Figure 4.2.5: Th/Co versus La/Sc plot (Cullers, 2002) showing silicic composition of sandstones and shales of Talchir Formation in Chirimiri, district Koriya, Chhattisgarh, India. Biotite Granite, Granite, Ultramafic, Gabbro, Diorite rocks after (Chakraborty and Roy, 2013)

In addition, REE patterns and Eu anomalies are also used as good tool for the interpretation of provenance because felsic and mafic rocks contain significantly different REE pattern and Eu/Eu* anomaly values. Felsic rocks are characterized by sharp negative Eu anomalies with higher concentration of LREE's, whereas mafic rocks show small or positive anomalies (Taylor and McLennan, 1985; Wronkiewicz and Condie, 1987; 1989, Cullers. 1995; 2000). Results similar to felsic rocks are observed in the REE chondrite normalized patterns of analysed sandstones and shale samples of Talchir Formation (Figure 3.5.1) in which samples show enrichment in LREEs (average La/Sm_N in Chirimiri sandstone 4.93, in Baikunthpur sandstone 4.78 and in shales 4.58; La/Yb_N in Chirimiri sandstone 9.56, Baikunthpur sandstone 11.36 and in shales 11.76) with slightly negative Eu anomaly which depicts the felsic composition of provenance for the studied rock samples.

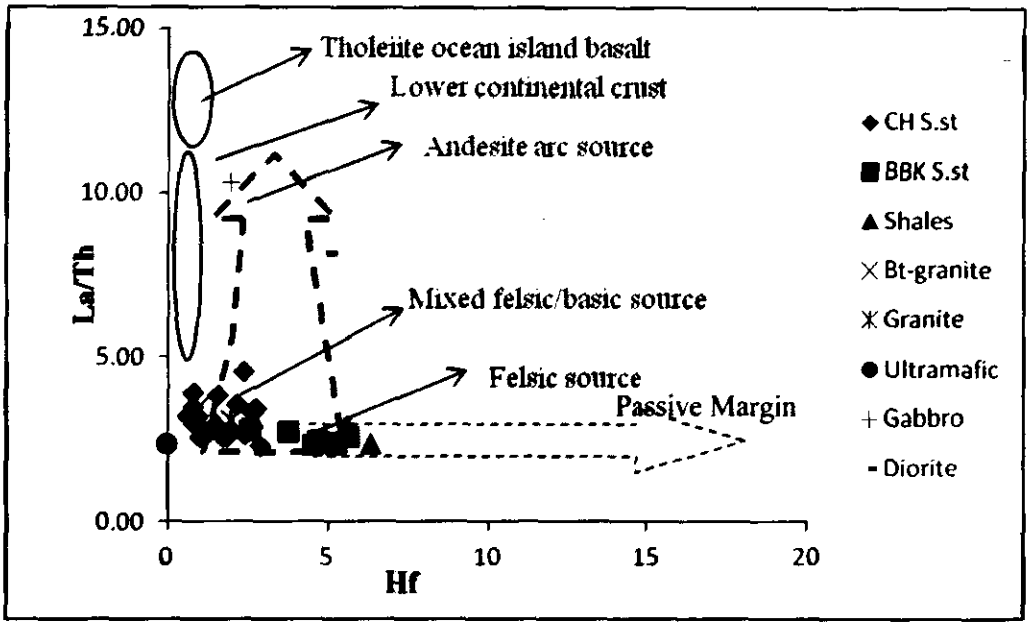

igure 4.2.6: Bivariate plot La/Th versus Hf (Floyd and Leveridge, 1987) for bulk iscrimination of different arc composition and sources for sandstones and shales of Talchir ormation, Chirimiri, district Koriya, Chhattisgarh, India. Biotite Granite, Granite, Jltramafic, Gabbro, Diorite rocks after (Chakraborty and Roy, 2013)

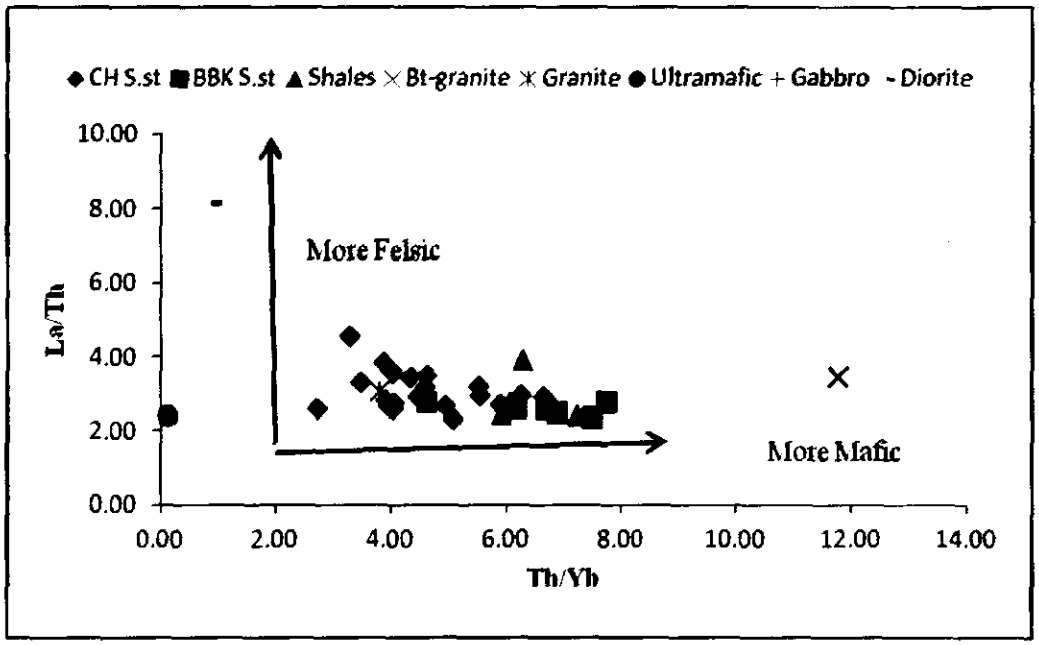

;ure 4.2.7: La/Th versus Th/Yb bivariate plot (McLennan et al., 1980) for sandstones and shales Talchir Formation, Chirimiri, district Koriya, Chhattisgarh, India. Biotite Granite, Granite, ramafic, Gabbro, Diorite rocks after (Chakraborty and Roy, 2013)

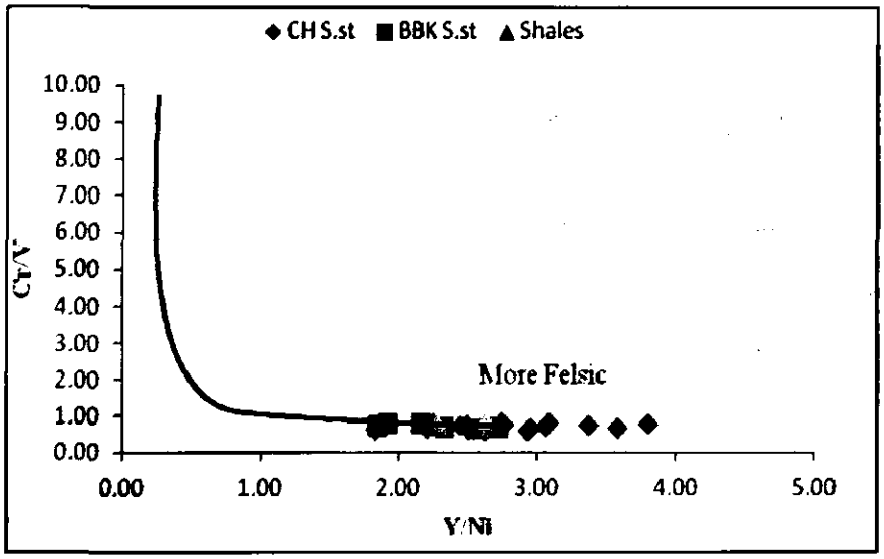

Figure 4.2.8. Bivariate plot of Cr/V versus Y/Ni (Floyd and Leveridge, 1987) for the Talchir sandstones and shales, Chirimiri, district Koriya, Chhattisgarh, India

The ΣLREE/ΣHREE ratio in Chirimiri sandstones ranges from 4.87 to 8.74 (average 7.43) in Baikunthpur sandstones its range is 6.72 to 10.19 (avg.8.56), whereas in associated shale samples this ratio ranges between 8.30 to 9.82 (average 8.90) suggesting that the components of the rocks under discussion were derived from predominantly felsic rocks. The Gd/Yb_N ratio also helps to understand the nature of source rocks and the composition of the continental crust (Taylor and McLennan, 1985). The Gd/Yb_N ratio in Chirimiri sandstones ranges from 1.00 to 2.94 (average 1.80) in Baikunthpur 1.57 to 2.30 (average 2.11) and in shales it is 2.15 to 2.37 (average 2.25). The average value of Gd/Yb_N ratio greater than 2 in Baikunthpur sandstones and associated shales, suggest that the parent area was composed of moderately depleted HREE rocks. Furthermore, the Eu/Eu* ratio in all the clastic rocks are either close to or more (Table 4.2.1). When the data of Talchir clastics is plotted in binary plot involving Eu/Eu* and Gd/Yb_N (Figure 4.2.9) majority of samples lie in Archean field either due to their high Eu/Eu greater than 1 values or high Gd/Yb_N is greater than 2. High Eu/Eu* ratio is attributed to the abundance of plagioclase resulted either due to its supply from basic, ultrabasic rock or accumulation through sorting (McLennan et al., 1993). Geochemical signatures like

relatively high content of TiO_2, positive Eu anomaly and $(Gd/Yb)_N$ ratio greater than 2 in few samples speak for the presence of basic material in the provenance.

To explore this possibility, data of Talchir clastics is plotted in La/Th versus Hf (Figure 4.2.6) and La/Th versus Th/Yb_N diagrams (Figure 4.2.7). La/Th ratio differentiates between mafic and felsic composition, whereas, Hf indicates degree of recycling of sediments. From both diagram slight basic affinity of sediments is indicated. But it is more appropriate to effectively constrain the presence of mafic and ultramafic rocks using ratios and diagrams which involve TTEs. Geochemical ratios involving TTEs are quite helpful to constrain contribution from mafic source. According to Condie (1993) and duely supported by McLennan (2000), the Cr, Ni, Co and V concentrations in the upper crust are 83ppm, 44ppm, 107ppm, and 17 ppm respectively. The elevated Cr and Ni abundances (Cr >150ppm and Ni >100) and low Cr/Ni ratios (between 1.3 and 1.5) are indicative of presence of ultramafic rocks in the source area (Garver et al., 1996). The Ni in Chirimiri sandstones ranges from 2.41 to 9.24 (average 6ppm), in Baikunthpur sandstone 7.39 to 16.84 (average 13ppm) and 13.07 to 14.18 (average 14ppm) in associated shale, Cr content ranges from 14 to 38 (average 29ppm) in Chirimiri sandstone, in Baikunthpur sandstone 33 to 81 (average 62 ppm) and 69.22 to 77.97 (average, 74 ppm) in associated shales. The average value of Cr/Ni ratio is 5.19 in Chirimiri sandstones, 5.04 in Baikunthpur sandstones and 5.39 in shales, which is significantly higher than the presented Cr/Ni values for mafic and ultramafic rocks (Garver et al., 1996). Binary diagram Cr/V versus Y/Ni (Hiscott, 1984; McLennan et al., 1993) is based on the index of enrichment of Cr over ferruginous trace elements, while Y/Ni monitors the general level of ferromagnesian trace elements (Ni). The mafic and ultramafic rocks tend to have higher Cr/V and lower Y/Ni ratios.

It is evident from this diagram that samples plots are inclined towards felsic source rather than mafics. To further refute the possibility of the contribution from mafic and ultramafic rocks, source indicators such as La/Sc, Th/Sc, La/Co, Th/Cr of the Talchir clastics are compared with respective rock types acquiring debris from mafic or felsic rocks (Table 4.2.1). The ratio comparison firmly refutes any contribution from typical mafic and ultramafic rocks. And therefore geochemical signatures indicating mafic affinity of the detritus (example, high TiO_2, Gd/Yb_N and Eu/Eu* values) are source characteristics. To specify the rock type (s) which took

part in the genesis of sediments for the clastic rocks, composition of probable source rock (s) presently exposed in the south east to north west direction are plotted in La-Th-Sc, Th-Sc-Zr/10 and Th-Co-Zr/10 diagram (Figure 4.4.4 (a) and (b)). The identification of provenance is based upon paleocurrent direction which is ESE to NWN. In this direction granite, granodiorite and anorthosite constituting Chotanagpur Craton is exposed (Ghosh, 1983; Ghose, 1992; Ghose and Mukherjee, 2000, Ghose et al., 2005). In these figures sample plots cluster in and around compositional range of Granite and Biotite Granite. This confirms that the forgone interpretation that the parent rock for Talchir clastics are felsic granitoids.

The positive Eu anomaly resulted due to derivation of some plagioclase from anorthosite exposed in this Craton. It has been observed that granitoids rocks of Aravalli craton contain relatively high content of HREE (Ahmad et al., 1991). The biotite granite also posses' relatively higher concentration of HREE compared to granite (Table 3.1.1) which probably contributed to high Gd/Yb_N values in these sediments. Furthermore, the higher concentrations of LILE, HFSE and REE in Baikunthpur sandstones and shales have also been acquired from Biotite granite in the later course of deposition when this suit of rock got exposed to weathering and erosion.

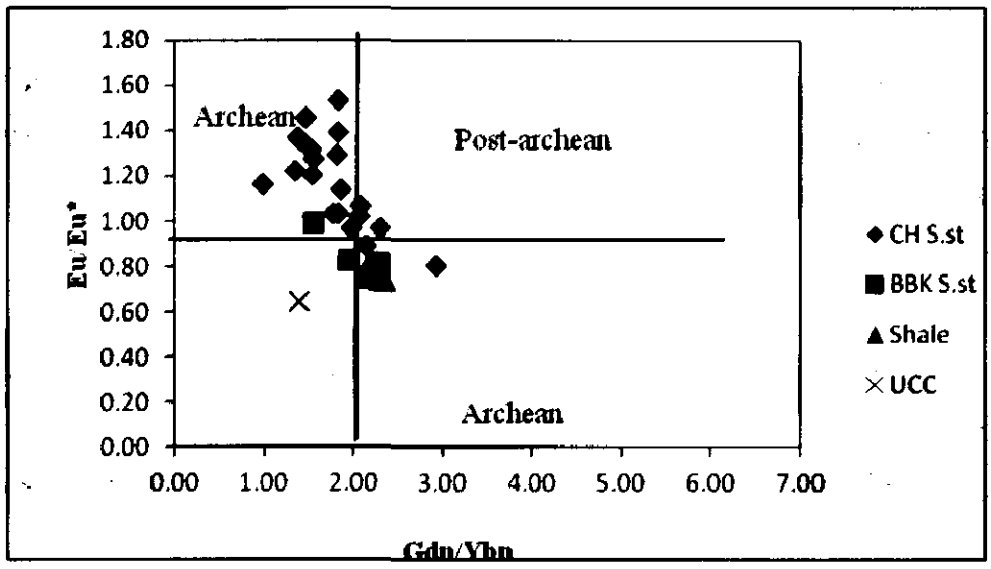

Figure 4.2.9: Plot of Eu/Eu* versus (Gd/Yb) n (McLennan and Taylor, 1991) for sandstone and shales of the studied samples of Talchir Chirimiri, district Koriya, Chhattisgarh, India

4.3 Evaluation of Sorting Effect

The higher concentration of heavy minerals in sedimentary rock is ascribed to hydraulic sorting or recycling of sediments. The heavy minerals noted in petrographic study of these Talchir sandstones include zircon, rutile, epidote, and garnet. Among all these heavy minerals zircon is important for evaluation of sorting and recycling aspects. Zircon is resistant to weathering and therefore can be transported for long distances. Presence of large number of zircon grains in sediments has been attributed to more than one recycling of the sediments. It is evident from petrographic modes that zircon abundance in Talchir coarse clastics as well as in shales is not normally high. ICV (index of compositional maturity) gives primary idea about the effect of recycling or sediment sorting in clastic rocks. If the value of ICV<1 it depicts that the sediments are either recycled or intensely weathered first cycle sediments (Barshad, 1966 and Johnsson, 1988, 1993, 2000). The values of ICV in the sandstones and shale samples are relatively less than 1 which suggests that either the Talchir clastics are intensely weathered or the product of multi recycling phases.

The geochemical abundance of Zr, Th and Sc is a better tool to infer the sorting or recycling history of the sediments. Non-recycled sediments show simple positive correlation between Th/Sc and Zr/Sc ratios, whereas rapid increase in Zr/Sc ratio indicates addition of zircon through recycling or sorting (McLennan et al., 1993). The average Zr/Sc ratio of Upper continental crust is 13.57 (McLennan, 2001). The Zr/Sc ratios of the Chirimiri sandstones ranges from 2.32-15.82, (average; 9.29), in Baikunthpur sandstones it ranges from 8.11-13.64 (average 10.81) and in associated shales from 11.63-13.64 (average; 12.26). On the otherhand Th/Sc ratio value in Chirimiri sandstones ranges from 0.79 to 1.48 (average, 1.16), in Baikunthpur sandstones from 1.15 to 1.80 (average, 1.51), and in Shales from 1.57 to 1.84 (average, 1.66). There is not significant disproportionate increase in Zr/Sc ratio compared to Th/Sc ratio (Figure 5.3.1) which negates the possibility of accumulation of zircon through sorting or recycling.

Relative to crustal abundance, Zr abundances are similar in sediments in glacial and arid climates but increase in the humid, temperate and tropical climate due to zircon concentration following removal of other minerals in solution (Van de Kamp, 2010). And therefore, Zr/Th serves as a good measure for the evaluation of recycling (Zimmermann and Bahlburg, 2003). The average value of Zr/Th ratio in

Chirimiri sandstones is 7.50, in Baikunthpur sandstone it is 6.94 and in associated shales 7.32. The Zr/Th ratio is not higher than UCC (17.76) which further attests the effect of sediment sorting or recycling was least. This suggests that the clastic rocks of Talchir Formation have been produced by the deposition of predominantly first cycle sediments. The samples of Talchir Formation were deposited in cold climate, which indicates that the sandstones and associated shales of Talchir Formation are first cycle sediments they are not recycle sediments.

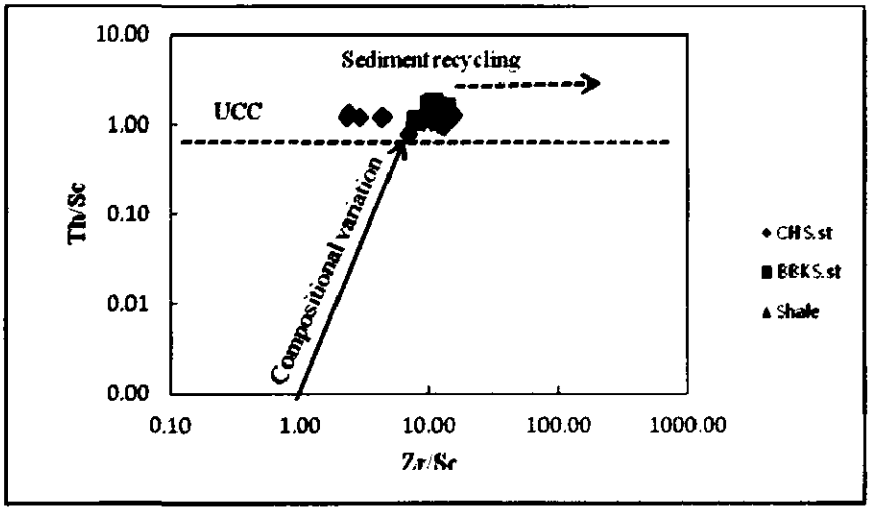

Figure 4.3.1: Th/Sc versus Zr/Sc (after McLennan et al., 1993) provenance and recycling discrimination diagram for sandstones and shales of Talchir Formation Chirimiri, district Koriya, Chhattisgarh, India

4.4 Tectonic Setting

The chemical composition of the source rock is a function of the tectonic setting and exerts major control on the sedimentary rocks chemistry. Therefore geochemistry of sedimentary rocks can be used to evaluate tectonic settings (Taylor and McLennan, 1985, Roser and Korsch 1986, McLennan and Taylor 1991). However specific tectonic environment do not necessarily produce rocks with distinct chemical composition (McLennan et al., 1990; Bahlburg, 1998). Concentrations of major oxides and Trace elements has been utilised in this study to ascertain the tectonic setting of the depositional basin of the studied rocks. Roser and Korsch (1986) used K_2O/Na_2O against SiO_2 to discriminate tectonic setting of the clastic sedimentary rocks. In this plot (Figure 4.4.1) the sandstones and shales fall in passive

margin but close to active continental margin setting. Whereas, in the discrimination diagram proposed by Bhatia (1983), Baikunthpur sandstones, associated shales and majority of the Chirimiri sandstone samples fall in active continental margin except few (Figure 4.4.2).

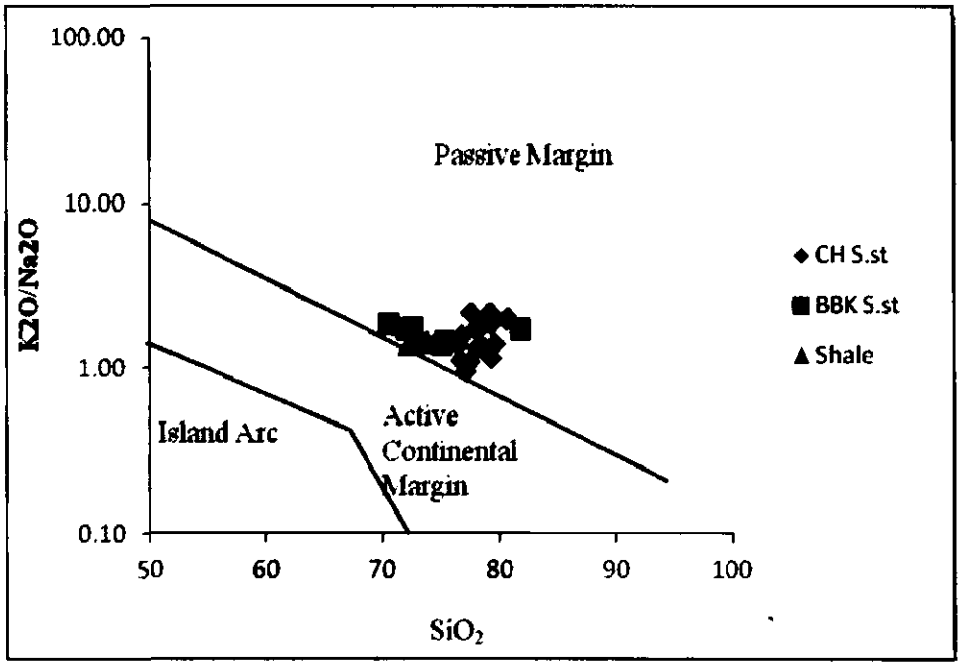

Figure 4.4.1: The (K_2O/Na_2O) versus SiO_2 (Roser and Korsch, 1986) discrimination diagram to decipher tectonic setting of sandstones and shales of Talchir Formation, Chirimiri, district Koriya, Chhattisgarh, India.

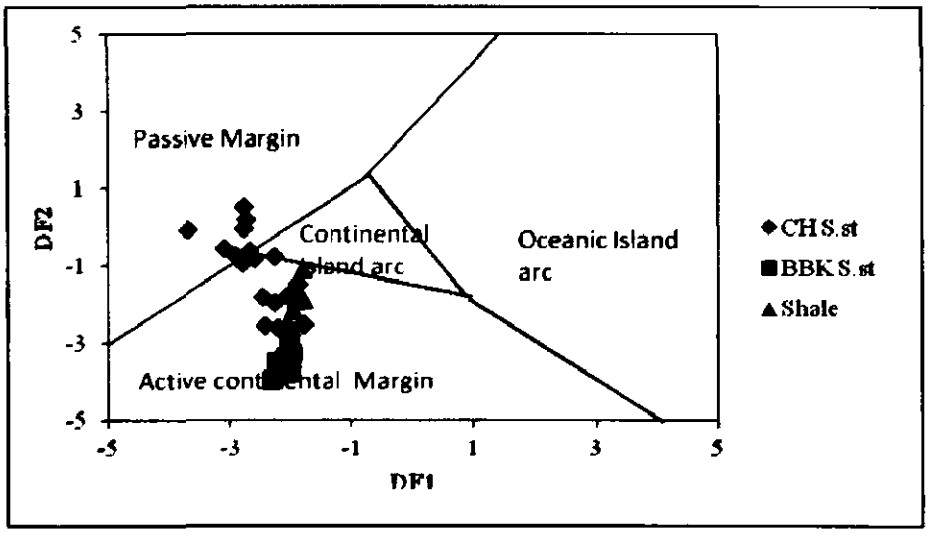

Figure 4.4.2: Discriminant function diagram for tectonics settings of Talchir sandstones and shales, Chirimiri, district Koriya, Chhattisgarh India, using major oxide ratios (Bhatia, 1983), where DF1 = $-0.0447SiO_2-0.972TiO_2+0.008Al_2O_3-0.267Fe_2O_3{}^t+0.208FeO-3.082MnO+0.140MgO+0.195CaO+0.719Na_2O-0.032K_2O+7.510P_2O_5+0.303$, DF2=$-0.421SiO_2+1.988TiO_2-0.526Al_2O_3-0.551Fe_2O_3-1.610FeO+2.720MnO+0.881MgO-0.907CaO-0.177Na_2O-1.840K_2O+7.244P_2O_5+43.57$.

Futhermore, the discrimination of tectonic setting of the clastic rocks of Talchir Formation has been evaluated on the basis of major oxides using (Bhatia, 1983). $Fe_2O_3^t$ % + MgO% as the discriminating parameters against which abundances or the ratios of the oxides are plotted (Figure 4.4.3). It is clear from this diagram that most of the data of Talchir Formation clastics plot in active continental margin field with minor spread into Continental island arc.

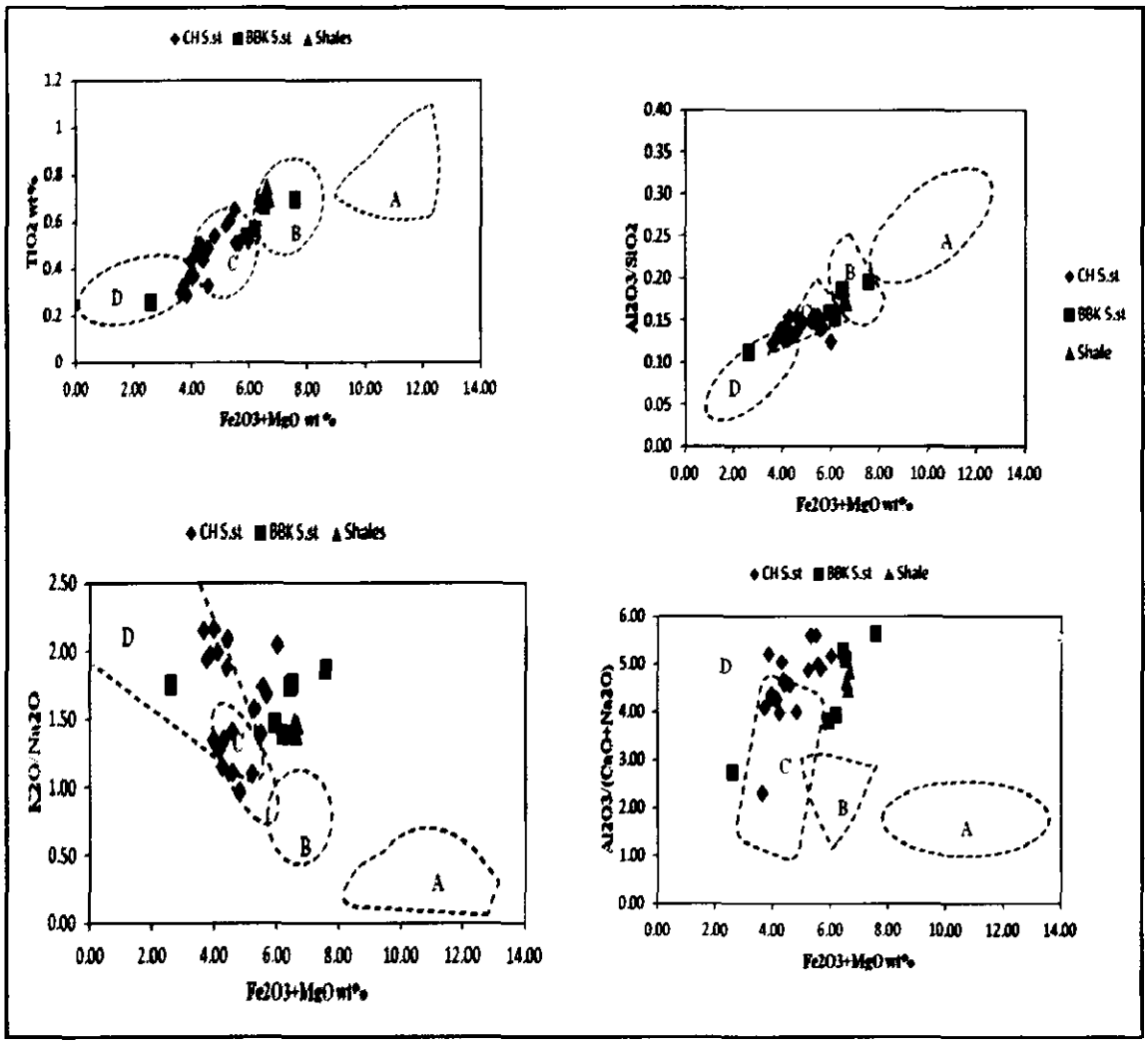

Figure 4.4.3: Major Element composition of Talchir sandstones and shales, Chirimiri district Koriya, Chhattisgarh India for discrimination of tectonic setting plotted against $Fe_2O_3^{(t)}$ +MgO wt % (where Fe_2O_3 represents total iron). Dotted lines represent major fields of tectonic setting. Fields are A – Oceanic island arc; B – Continental Island arc; C – Active continental margin; D – Passive margin (Bhatia, 1983).

Immobile trace elements that have low residence time in sea water like La, Th, Sc, Nd, Zr, Hf, Nb, Ti are considered better discriminator of tectonic setting due to their primary abundance (Holland, 1978, McLennan, 1980; McLennan et al., 1990). In La-Th-Sc diagram (Figure 4.4.4), sandstones and associated shales samples fall in active and passive continental margin, whereas in Th-Sc-Zr/10 (Bhatia and Crook, 1986) sandstones and associated samples fall in active continental margin and continental island arc fields (Figure 4.4.5 (a)) and outside but close to active continental margin in Th-Co-Zr/10 (Figure 4.4.5 (b)). To further authenticate the tectonic setting of Chirimiri basins selected trace elements ratios of Talchir clastic are compared with the sedimentary rocks evolved in different settings (Table 4.4.1). It is amply clear from this table (4.4.1) that majority of trace element ratios closely match with their rocks deposited in active margin setting. The results regarding the tectonic setting inferred from trace element abundances, to a larger extent are major elements based diagrams and petrographic modes of Talchir Formation. All the petro-chemical parameters indicate that Talchir sedimentary rocks were evolved in an active margin tectonic setting. Some of the trace element ratios such as Zr/Hf, Th/Sc, La/Sc, La/Th and Th/U are sensitive indicators of tectonic setting (Bhatia and Crook 1986; Floyd and Leveridge1987) but these ratios show large deviation in the analysed samples of Talchir Formation (Table 4.4.1) when compared with different tectonic settings of the depositional basin. This variation in tectonic setting can be attributed to variation in the source.

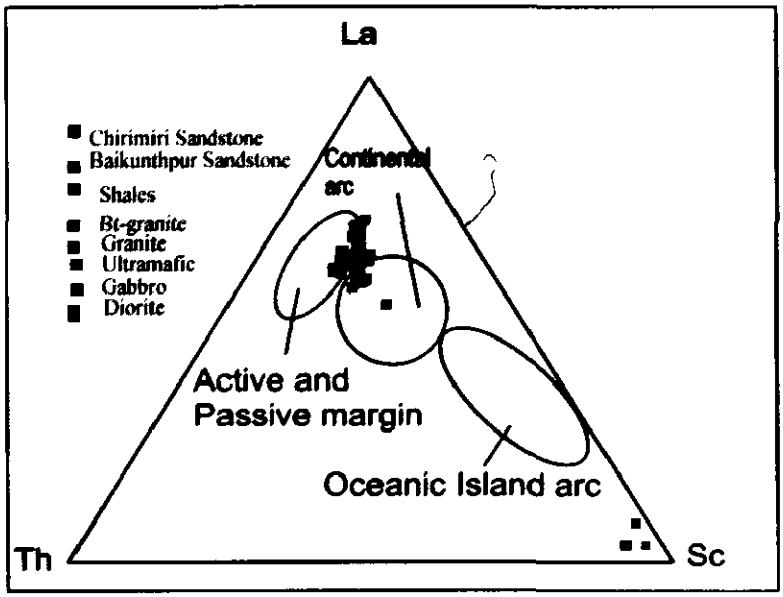

Figure 4.4.4: La-Th-Sc ternary diagram (Bhatia and Crook, 1986) for sandstones and shales of Talchir Formation with associated rocks biotite granite, granite, ultramafic, gabbro, and diorite (Chakraborty and Roy 2013) Chirimiri, district Koriya, Chhattisgarh, India.

Table 4.4.1: Comparison of average ratios of trace elements of sandstones of Talchir Formation, Chirimiri area, Son-Mahanadi basin district Koriya, Chhattisgarh India with greywacke from various tectonic settings (Bhatia and Crook, 1986)

Elements ratio	Passive margins	Continental Island arc	Active Continental margin	Ocean Island arc	Chirimiri sandstone	Baikunthpur sandstone	Shale
Rb/Sr	0.05	0.65	0.89	1.19	0.63	0.77	0.81
Th/Sc	3.06	0.85	2.56	0.15	1.17	0.22	1.67
Zr/Hf	29.5	36.3	26.3	45.7	34.05	32.49	31.45
La/Th	2.2	2.36	1.77	4.26	3.11	2.57	2.7
La/Sc	6.25	1.82	4.55	0.55	3.63	3.85	4.48
Th/U	5.6	4.6	4.8	2.1	8.69	9	7.32
(Eu/Eu*)	9.8	7.18	-	-	1.18	0.84	8.49
*Gd/Yb_N	3.67	3.19	-	-	1.80	2.11	3.43
*La/Sm_N	1.4	1.3	-	-	4.93	4.78	1.35
*La/Yb_N	0.74	0.76	-	-	9.56	11.36	0.75

*Average data from McLennan et al., 1990

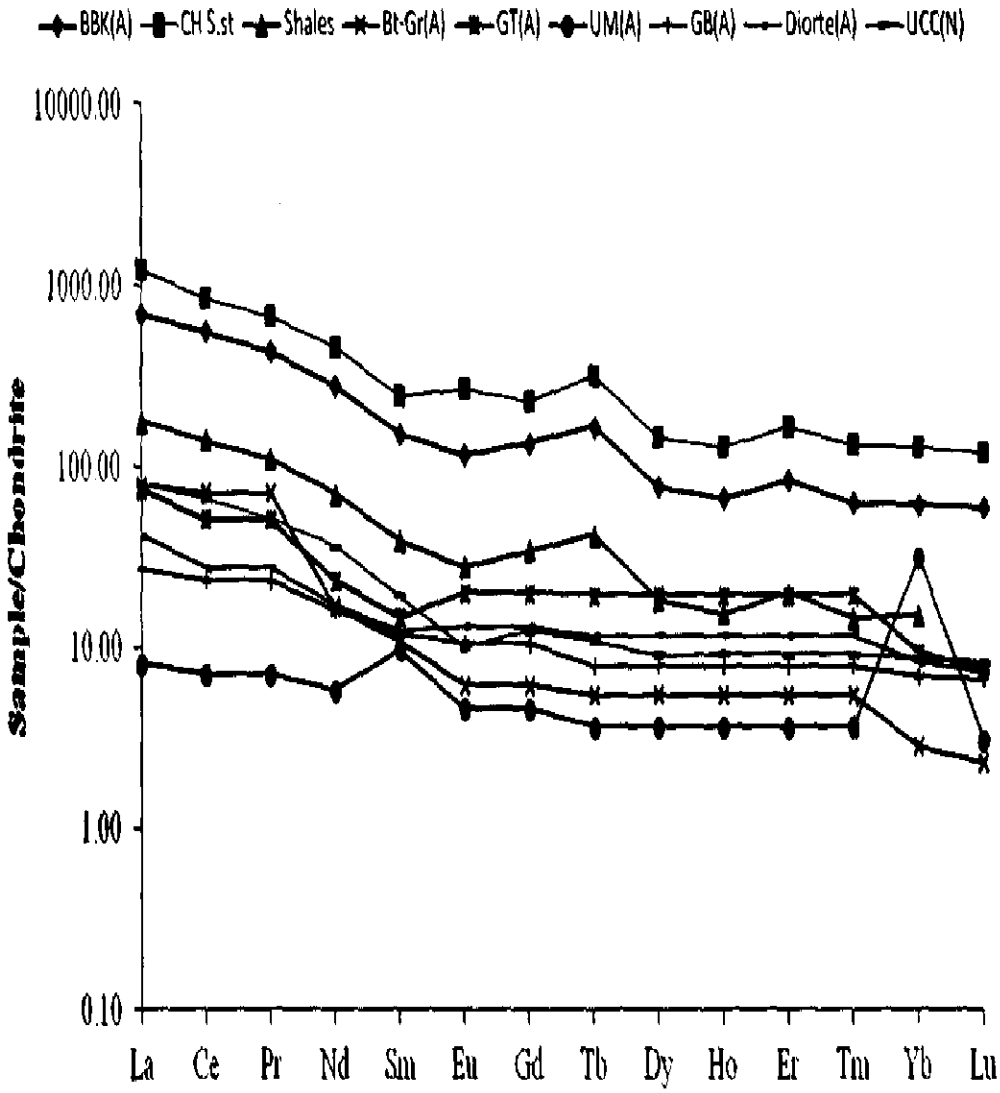

Figure 4.4.6: Rare earth element chondrite normalised plot for sandstones and associated shales of Talchir Formation and associated rocks Biotite, granite, Granite, Ultramafic, Gabbro and Dlorite (Chakraborty and Roy, 2013) exposed in the Son-Mahanadi basin Chhattisgarh, India.

The Gondwana basins of peninsular India are traditionally considered as extensional rift basins due to the overwhelming evidence of fault controlled synsedimentary subsidence. However, disposition of the Gondwana basin of peninsular India and their structural architecture indicate that the kinematics of all these basins is not purely extensional. To maintain Kinematic compatibility with other basins as well as the bulk lateral extension, some basins have been proved to be of strike slip origin. The Satpura basin of central India has been suggested to be pull apart basin that developed above a releasing jog of a left stepping strike-slip fault system defined by Son-Narmada and Tapti faults (Chakraborty and Ghosh, 2005; Tewari and Maejima, 2010). The tectonic setting of Talchir clastics inferred from their modal mineralogy and geochemical abundance indicate the presence of Chirimiri basin in active continental margin setting. The active continental margin setting comprises continental margin of Andean type marked by plate convergence and orogenic volcanic rocks and strike-slip continental margin. Consequently, sedimentary basins associated with active continental margin have diverse geomorphic setting. And all these basins are associated with thick and elevated continental crust (Bhatia and Crook, 1986).

In this context the Chirimiri basin can also be considered as a local pull-apart basin, which received sediments from fault bounded basement uplift. The sediments deposited in pull-apart basins show mineralogical and chemical signatures resembling to the basins of active continental margin setting (Dickinson et al., 1985; Bhatia and Crook, 1986; Bock, 2000). The Intracratonic basins are generally the consequence of extensional tectonics. In some cases, these extensional basins are asymmetric with an overall increase in thickness towards one of the bounding faults (Dunbar and Sawyer, 1988), indicating that the basin-bounded faults are active during sedimentation inducing subsidence and creating space for preservation of sediments.

The basin-fill strata are also affected by intra-basinal gravity faults reflecting synsedimentary downward displacement that generate accommodation space for sediment deposition throughout the history of basin evolution (Bally, 1980). The Son-Mahanadi basin is tectonically, divided into three blocks i.e., Son, Hasdo-Arand and Mahanadi separated from each other by ENE-WSW trending prominent basement ridge (Dotiwala and Pangtey, 1997). The CITZ consists of two parallel structural belts of unequal width. The narrow northern belt represents the collapsed early Proterozoic

Mahakoshal rift zone, which developed into a fold belt and is presently confined to the Son-Narmada Belt (SONA) lineament. The Mesoproterozoic Sausar Mobile Belt (SMB) comprising tectonically imbricated Sausar metasediments and pre-Sausar gneiss, granulites, and the Chhotanagpur Granite Gneiss Complex (CGGC) belt represents the southern belt.

The Central Indian Shear Zone (CIS) marks the southern boundary of the Sausar Mobile belt (SMB) and also of the CITZ in its central sector (Acharyya, 2003). Integrated modelling of residual gravity and magnetic anomalies reveals large up warps and down warps in the basement which are fault controlled. It has brought out transverse ridges separating the Son-Mahanadi basin into number of sub basins (Singh et al., 2013). Spatial distribution of rock units, variation in the thickness of sediments, different disposition of structural elements and contrasting lineament-trends of these three blocks suggest that each underwent a different sedimentation and tectonic history (Dotiwala and Pangtey, 1997). The Chirimiri basin lies in between Son-Narmada south fault and CIS and is an example of local pull a part basin generated due to tectonic movement of the bounding faults (i.e. Son-Narmada south fault and Central Indian shear).

CHAPTER – 5

PALEOWEATHERING & PALEOCLIMATE

PALEOWEATHERING AND PALEOCLIMATE

5.1 General Statement

Weathering is the combination of processes by which physical disintegration and chemical decomposition of pre-existing rocks takes place. Weathering occurs as a result of exposures of rocks to sub-aerial environment on the surface of the earth. Beside water other climatic conditions play significant role. Since temperature promotes chemical reaction and therefore, chemical weathering is more vigorous at higher temperature while in cold frigid glacial climate the chemical weathering activity is weak (Brady and Carroll, 1994; Blum et al., 1998) Chemical weathering becomes more pronounced and extensive under warm humid climatic conditions. In favourable conditions leaching of alkalis particularly K^+, Na^+ and Ca^{2+}, from feldspar take place which has pronounced effect on the composition of detritus generated from silicate rocks, whereas large cations Al, Si, Rb and Sr remain fixed in the weathered residue. Early stages of weathering marks the depletion of $CaO+Na_2O$ and later stages include removal of K_2O resulting in the formation of kaolinite and gibbsite (Nesbitt et al., 1980).

Clay minerals are hydrous aluminium phyllosilicates, with variable amounts of iron, magnesium, alkali metals, alkaline earths and are formed when primary minerals decompose to form minerals like illite, smectite, chlorite, and kaolinite under the influence of precipitation and temperature. Being ultrafine in nature, their identification requires special analytical techniques like XRD and SEM. The occurrence of clay minerals in surficial and sub-surficial environments of the earth and their response to physical and chemical changes has become a common basic need worldwide.

The global distribution of clay minerals reveals a latitudinal zonation that strongly reflects the pedogenic and climatic zonation (Biscaye, 1965; Griffin et al., 1968; Chamley, 1989). In tropical to subtropical environments, both lacustrine and marine clay-mineral assemblages have often been a useful guide to paleoclimatic settings because hydrolysis of rock-forming silicates in tropical conditions can change rapidly in response to climatic phenomena (Stoffers and Hecky, 1978; Kalindekafe et al., 1996; Gingele, 1996). There are evidences that climate controls the occurrence and abundance of secondary clay minerals in soil (Birkeland, 1984). Clay mineral

formation models suggest that clay mineral species are formed by and subsequently equilibrate with the intensity of weathering of the soil. Moreover, the species are predicted to form within distinct ranges of climate (Folkoff and Meentemeyert, 1987).

Several models have been developed for clay minerals formation based on observations, thermo-chemical theory, and experimental studies (Garrels and Christ, 1965; Rai and Lindsay, 1975; Kittrick, 1977; Folkoff, 1983). These models indicate that individual clay minerals are found in equilibrium with the chemical potential or ionic activities of the soil system. This also indicates that individual minerals exist along a sequence of weathering according to their stability and weatheribility. The field observations has also established that a general relationship between regional climate and individual clay mineral occurrence (Alexander et al., 1939). Clay mineral composition indicates the intensity of weathering, especially the degree of hydrolysis at source area which is used as paleoclimatic indicators (Chamley, 1989; Thiry, 2000; Thamban et al., 2002; Dou et al., 2010).

5.2 Weathering

The intensity and duration of weathering can be quantitatively evaluated by examining the relationship between alkali and alkaline elements (Nesbitt and Young, 1982, 1996) with Chemical Index of Alteration; (CIA) which is defined as

$$CIA = [Al_2O_3/ Al_2O_3+CaO^*+Na_2O+K_2O] *100$$

Where CaO* is the amount of carbonate incorporated in the silicate fraction of the rocks. The large amount of aluminous clay minerals (kaolinite) formed during intensive chemical weathering reflects high CIA values 80–100 for mud formed under tropical conditions. Conversely in glacial environments, where abrasion is dominant over chemical weathering, common CIA values range from 50 to 70 (Nesbitt and Young, 1982) and the CIA values of Talchir clastics indicates low to moderate degree of chemical weathering in the catchment area. The CIA values calculated for Chirimiri sandstones 47.37 to 70.59 (average, 61.58), in Baikunthpur sandstone 50 to 65 (average, 61.02) and 62.17 – 62.78 (average, 63) in shales. These values are greater than average UCC = 47 (Taylor and McLennan, 1985) but less than PAAS (Post Archean average shale) = 70. CIA values in the range of 50-60 show intermediate weathering in the region (Fedo et al., 1995). The samples of sandstones and shales of Talchir Formation are replotted on Al_2O_3-(CaO+Na_2O)-K_2O (A-CN-K diagram) ternary diagram (Figure 5.2.1) to quantify CIA values and to evaluate

sediment deviation from their original source rock composition (Nesbitt and Young, 1984; 1989). In this diagram average values of Precambrian rocks, (biotite-granite, granite, ultramafic, gabbro and diorite) exposed in the vicinity of study area near Pathalgaon (Charaborty and Roy, 2013) suspected to be the source rocks and UCC (Taylor and McLennan, 1985). The sample plotting pattern in the diagram suggests relatively intermediate weathering (Figure 5.2.1). The analysed samples follow ideal weathering trend towards illite – muscovite composition. Harnois (1988), proposed a new measure for chemical weathering i.e., Chemical Index of Weathering (CIW). CIW is identical to CIA but eliminates the use of K_2O from equation and does not account for the aluminium associated with K-feldspar.

The values of CIW are sometimes very high for K-feldspar rich rock, whether the rock is chemically altered or not (Fedo et al., 1995). The Chemical index of weathering is calculated as

CIW = {[Al2O3/Al2O3+CaO*+Na2O]*100}

Like CIA, CIW is also a measure of the extent of conversion of feldspars to clays (Nesbitt and Young, 1984, 1989; Fedo et al., 1995; Maynard et al., 1995). The calculated value of CIW in Chirimiri sandstones are 32.18 to 76.68 (average 70.37), in Baikunthpur sandstones 61.13 to 76.23 (average 71.04) and 72-74 (average, 73) in shales which confirms moderate chemical weathering. Plagioclase Index of Alteration (PIA) which is an alternative to CIW (Fedo et al., 1995) is used to evaluate weathering of plagioclase because silicate rocks contains abundant amount of plagioclase. This is calculated as

$$PIA = [(Al_2O_3-K_2O)/ (Al_2O_3+CaO+ Na_2O-K_2O)]*100$$

The PIA value of upper continental crust is 45 (Taylor and McLennan, 1985) and values upto 100 demarcate the complete conversion of plagioclase mineral into secondary minerals. The calculated values of PIA for Chirimiri sandstones ranges from 48.34 to 72.97 (average 61.58), in Baikunthpur sandstones 52.97 to 70.77 (average 65.11) and in shales 67 to 69 (average, 68), PIA values do not show large variation and are consistent with the values of CIA interpretation.

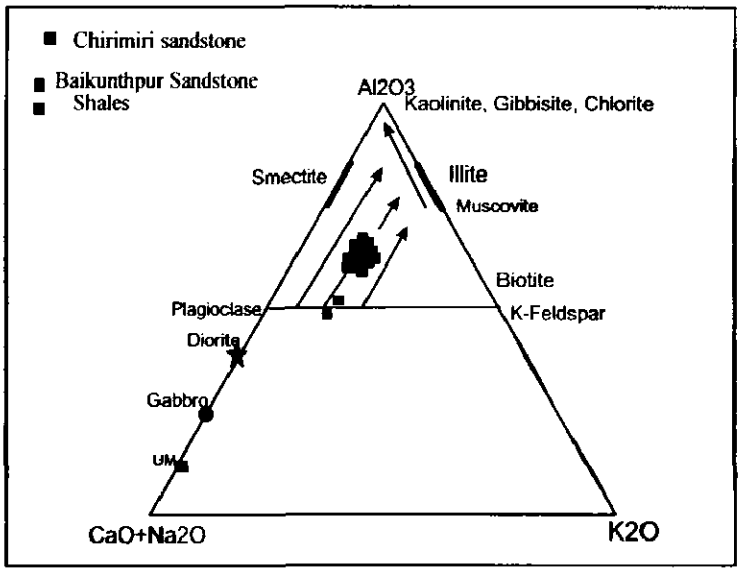

Figure 5.2.1 A-CN-K ternary diagram showing weathering trend of sediments of Talchir Formation, Chirimiri, district Koriya, Chhattisgarh, India (Nesbitt and Young 1984).

The K_2O/Al_2O_3 ratio of Talchir clastics (0.16 to 0.22 in Chirimiri sandstones, 0.19 to 0.22 in Baikunthpur sandstones and 0.21 in all shales samples), indicating presence of illite in appreciable quantity amongst the clay minerals present in these rocks. Similarly the K_2O versus Al_2O_3 diagram (Figure 5.2.2), Talchir sandstone and shale samples cluster close to illite line. These lines of evidence endorse low to moderate degree of chemical weathering.

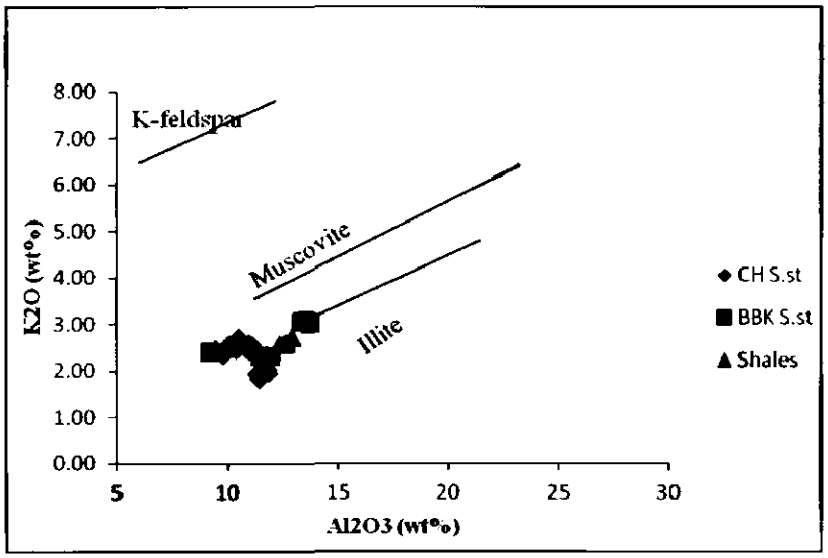

Figure 5.2.2 K_2O versus Al_2O_3 bivariate diagram showing distribution of sandstones and shales of Talchir Formation, Chirimiri, district Koriya (Cox et al., 1995).

Th/U ratio is also a very good indicator of intensity of weathering of sedimentary rocks. In oxidizing conditions U^{4+} gets oxidised to U^{6+} and gets readily dissolved in solution and transported to the basin, while Th^{4+} remains insoluble and intact within the system. Highly reducing sedimentary environment leads to uranium enrichment resulting in low Th/U ratios and vice-versa (McLennan and Taylor 1980, 1991; McLennan, et al., 1990). The Th/U ratio in Chirimiri sandstones ranges from 6.37-10.81 (average, 8.69), in Baikunthpur sandstones 8.17 to 9.61 (average 9) and in shales 6.87-7.91 (average, 7.32). These values are greater than Th/U ratio of UCC = 3.8 (Taylor and McLennan, 1985), as well as the probable source rocks (Figure 5.2.3). This signifies that low U values and high Th/U ratios are not primary. However, it is difficult to infer that high values of Th/U are exclusively due to oxidizing environment because Th abundances in the rocks under study are also higher than the probable source rocks. Moreover, sample points also do not clearly define a weathering trend. Nevertheless, loss of U due to oxidation cannot be ruled out.

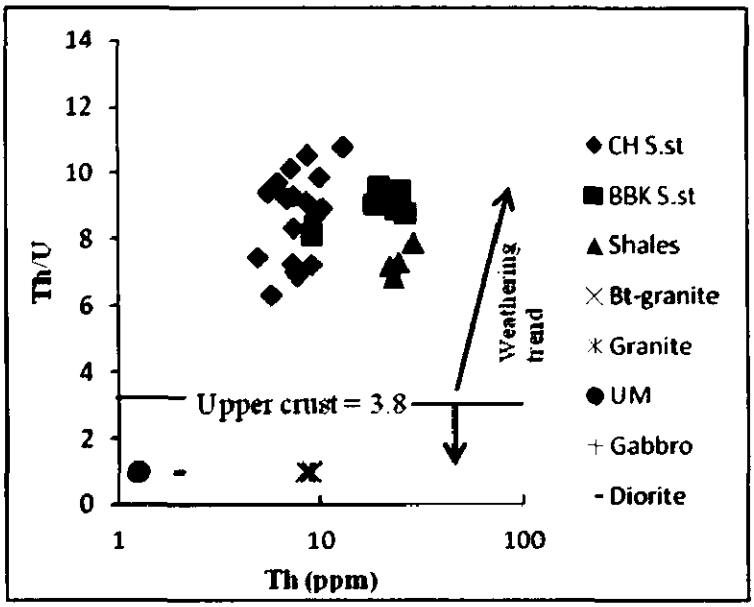

Figure 5.2.3 Th/U versus Th bivariate plot for the sandstones and shales of Talchir Formation Chirimiri, district Koriya, Chhattisgarh, India. Bt-granite, granite, ultramafic, gabbro, diorite (Chakrabortv and Rov. 2013)

All these results suggest the detritus for the studied Talchir sandstones and shales of Chirimiri area were supplied from a provenance that suffered low to moderate degree of weathering under oxidising conditions.

5.3 Paleo Redox Conditions

The U/Th ratio is generally used as redox indicator of the depository basin. The ratio counts values below 1.25 for oxic conditions (Nath et al., 1997). Shales of Talchir Formation have U/Th values ranging between 0.13-0.15 (average, 0.14), in Chirimiri sandstones from 0.10 to 0.12 (average, 0.12) and in Baikunthpur sandstone 0.11 to 0.12 (average, 0.11). Other indicators used to infer the chemical environment of the deposition of the basin are V/Cr, Ni/Co and Cu/Zn. Values less than 2 for V/Cr (Shaw et al., 1990; Jones and Manning, 1994), less than 5 for Ni/Co (Dypvik, 1984; Dill, 1986; Jones and Manning, 1994) and low values of Cu/Zn (Halberg, 1976) are suggestive of oxidizing environment. V/Cr in Chirimiri sandstone range from 1.19 to 1.69 (average, 1.39) in Baikunthpur sandstone 1.22 to 1.51 (average, 1.34) and in shales 1.07 to 1.41 (average, 1.26), Ni/Co in Chirimiri sandstones 0.15 to 0.39 (average, 0.25), in Baikunthpur sandstones 0.27 to 0.46 (average, 0.37) and 0.43 to 0.51 (average, 0.47) in shales and Cu/Zn in Chirimiri sandstones 0.13 to 0.26 (average, 0.18), in Baikunthpur sandstone 0.16 to 0.26 (average, 0.22) shales possess 0.19-0.26 (average, 0.22). The isotopic study of nodular carbonates of basal Talchir Formation from Damodar and Mahanadi basin of Peninsular India, show that they have highly negative values of stable isotopes δ^{18} O and δ^{13} C (mean -19.5‰ and -9.7‰ w.r.t PDB) suggesting a fresh water environment for deposition (Ghosh et al., 2002a; Bhattacharya et al., 2001). The isotopic analysis supports the elemental ratios for oxidising conditions during the deposition of sediments of Talchir Formation under shallow lacustrine environment in Chirimiri basin.

5.4 Paleoclimatic Conditions

Paleoclimatology is the study of ancient climates. Since direct observations of climate were not available before the onset of 19th century, but now it can be inferred from proxy variables that include non-biotic evidence such as lake beds sediments and ice cores, and biotic evidence including tree rings and coral. Continental blocks of Permo-Carboniferous Gondwana sediments (India, Australia, Antarctica, South Africa and South America) record evidence of the Late Paleozoic Ice Age (LPIA), and global climatic fluctuation from Icehouse to Greenhouse (Frakes et al., 1992; Isbell et al., 2003, 2011; Fielding et al., 2008a). These changes are recorded in the form of sedimentological and stratigraphic features such as (remnants of preserved vegetation, animals, plankton, Stable Isotopes, sediments cores, Pollens, tree rings etc.) (Fielding

et al., 2008a, 2008b; Isbell et al., 2008a, 2008b; Rocha-Campos et al., 2008), paleosol characteristics (Tabor et al., 2008), paleobotanical records (Pfefferkorn et al., 2008). Petrochemistry (Suttner and Dutta, 1986; Visser and Young, 1990; Skilbeck and Cawood, 1994; Diekmann and Wopfner, 1996; Scheffler et al., 2003; Islam et al., 2004; Ghosh and Sarkar, 2010; Ghosh et al., 2012) and isotope geochemistry of sedimentary rocks provide clues regarding ancient climate (Montanez et al., 2007; Zeng et al., 2012). The parameters that largely influence the formation of clay minerals are the nature of parent material, precipitation, temperature, and time.

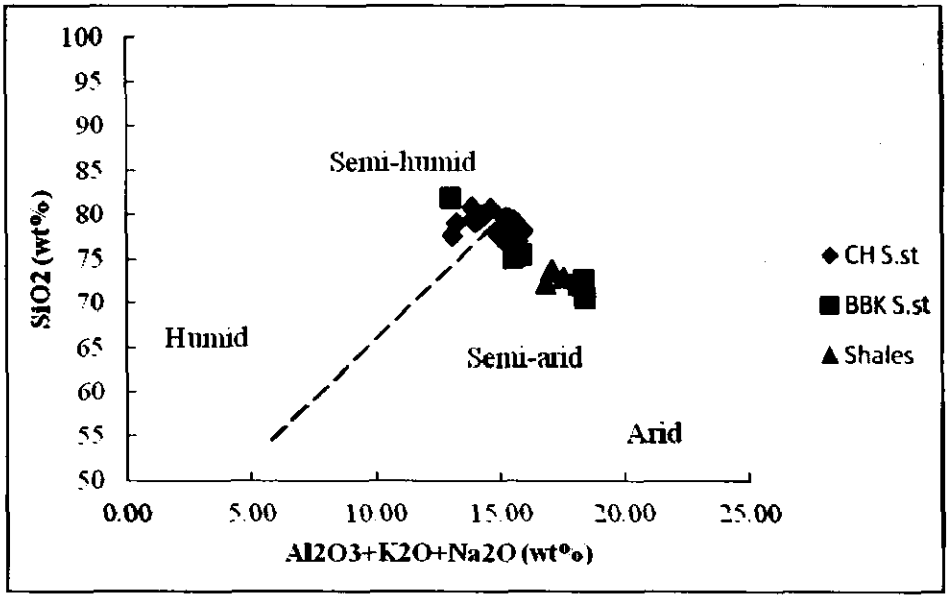

Figure 5.4.1: Bivariate plots between SiO_2 versus $Al_2O_3+K_2O+Na_2O$ for sandstones and shales of Talchir Formation, Chirimiri, district Koriya, Chhattisgarh, India. (Suttner and Dutta, 1986)

The glacial sediments are considered to contain abundant amount of quartz and feldspars in clay size fraction (Menking, 1997; Moore and Reynolds, 1997) because chemical weathering in cold glacial climatic condition is not very active, therefore, feldspars and quartz do not decompose and get preserved. Primary clay minerals e.g. illite and chlorite are typically found as the product of intense physical weathering of micas by glaciers in the absence of chemical weathering (Biscaye, 1965; Chamley, 1989). On the otherhand smectite and kaolinite are more likely to be produced from the weathering of silicate minerals during soil formation which are the indicators of the climates conducive to chemical weathering (Chamley, 1989).

The XRD analysis has been undertaken to determine species and proportion of clay minerals in the shales and matrix of sandstones. Four samples of shale and five matrix rich samples of sandstone (3 Chirimiri and 2 Baikunthpur sandstones) have been subjected for this purpose. The prepared samples were run on the X-ray machine operated at 40 kV to 20 mA using Cu-Kα radiations of wavelength 1.5418 Å. The scanning speed was maintained at 0.02^0 2θ per sec. The data is generated at 2θ range of 3^0 to 60^0. The XRD results of sandstones and shales are summarised in Tables (5.4.2 to 5.4.10) and shown in Figures (5.4.2 to 5.4.10). Clay minerals like smectite, illite, chlorite, and kaolinite are found, whereas quartz is the most abundant non clay mineral followed by K-feldspar and plagioclase. Carbonate (calcite) in very small amount has also been identified in these samples. Chlorite and Illite generally does not survive in more intense chemical weathering regimes, therefore its presence in these sediments as detrital clay is a reliable indicator of cold, frigid and/or dry climates (Chamley, 1989) (Plate 5.4.1 (A) and (B)). Smectite group of minerals may indicate monsoonal climates, with alternating wet and dry season that promote the formation of kaolinite (Chamley, 1989; Millot, 1970). Smectite may also indicate the presence of volcano-clastic input such as ash (Nadeau and Reynolds, 1981; Chamley, 1989) or a basaltic terrain subjected to temperate weathering conditions. Analyses of numerous ancient sediments in many parts of the world indicate very less abundance of smectite in sediments formed prior to the Mesozoic era with the exception of those of the Permian period (from 299 million to 251 million years ago) and the Carboniferous Period (359.2 million to 299 million years ago), in which it is relatively abundant (Grim, R. E., 1953). Abundance of smectite has been reported in Siwalik group of rocks in Himalayas despite of felsic source rocks (Huyghe et al., 2011), increase in seasonal variability and aridity can be linked to the formation of authigenic smectite (Plate 5.4.2 (D)).

Presence of carbonates in some of the samples is also a good indicator of cold climate. Kaolinite indicates moist and temperate to tropical conditions of weathering and is a characteristic mineral of humid climate. Its presence in cold climate suggests that the kaolinite is recycled from the source rock (Plate 5.4.2 (C)). Yang et al., (2014) correlation study of paleolatitudes, temporal variations of chemical index of alteration of Permocarboniferous sediments from different Gondwana basins in India and the world, advocates for low to high latitude land surface temperature of 20^0C higher than

the calculated for contemporaneous sea surface temperature gradient, which might have led to deglaciation of ice-sheets that provided conducive conditions for small scaled chemical weathering indicated by clastics rocks of Talchir Formation.

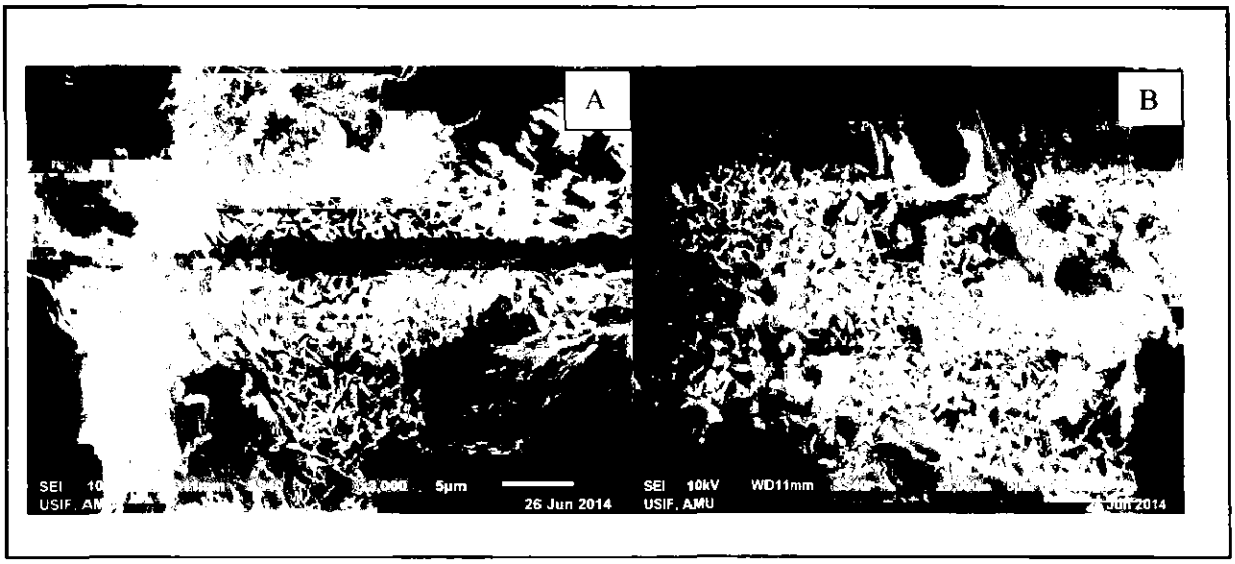

Plate 5.4.1: Scanning electron microphotograph showing (A) Chlorite and (B) Illite clay minerals in samples of Talchir Formation

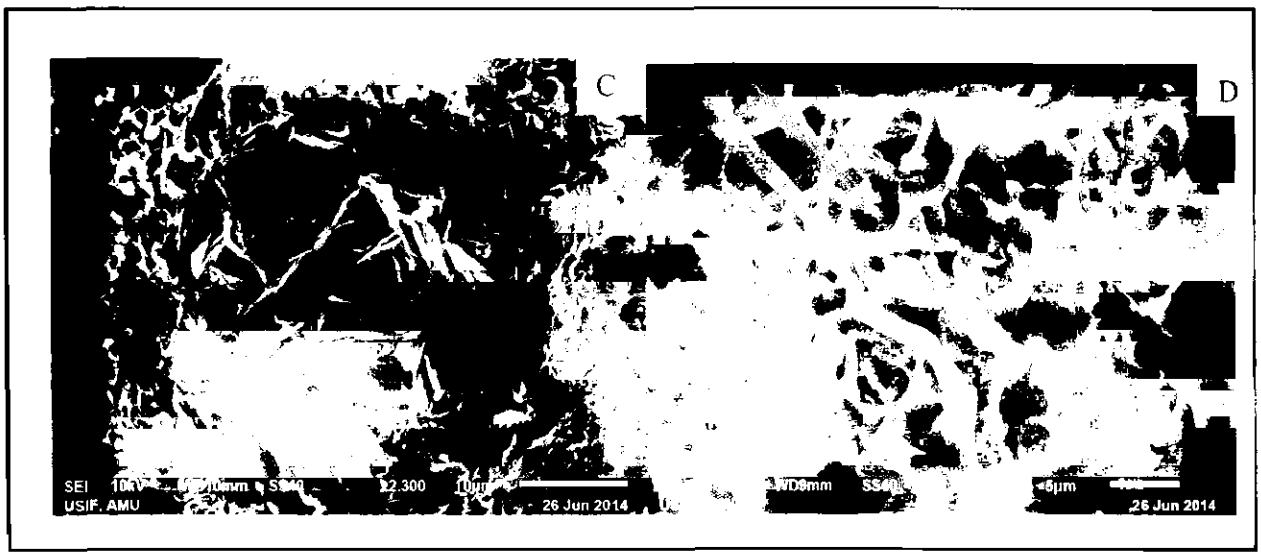

Plate 5.4.2: Scanning electron microphotograph showing (C) Kaolinite and (D) Smectite clay minerals in samples of Talchir Formation

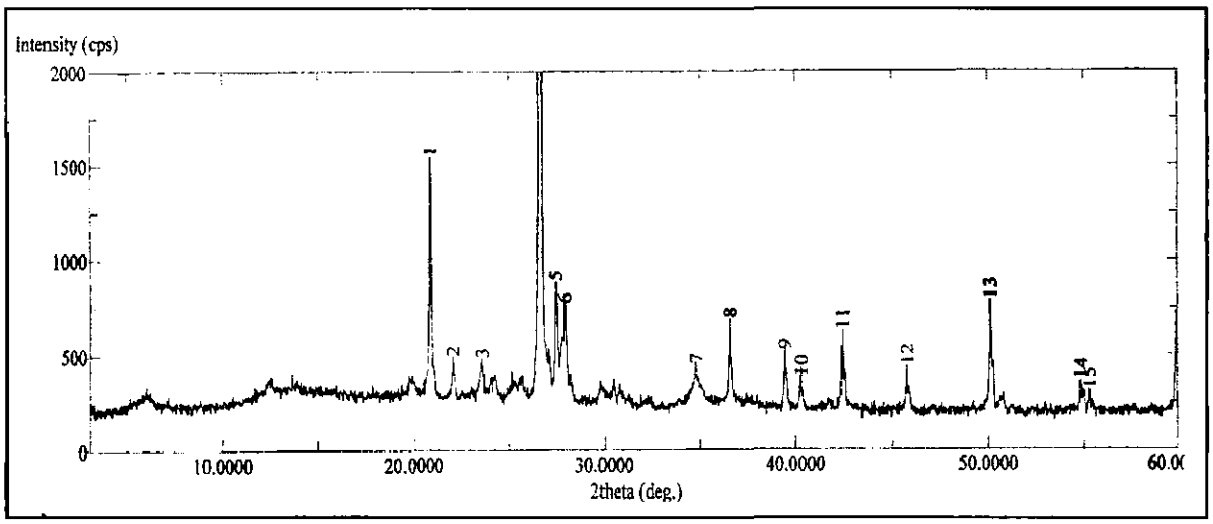

Figure 5.4.2: Showing clay mineral peak for Baikunthpur sandstone, Chirimiri, district Koriya, Chhattisgarh, India.

Table 5.4.2: Showing XRD data of (BBK1) Baikunthpur sandstone sample.

Peak	2θ	d-value	Intensity	Mineral	Reference
1	20.84	4.25	1550	Quartz/Kaolinite	*3896/1169
2	22	4.036	496	Feldspar	Moore and Reynolds, 1997
3	23.56	3.773	487	Smectite	Moore and Reynolds, 1997
4	26.62	3.345	6366	Quartz	*3895
5	27.44	3.247	889	Feldspar	Moore and Reynolds
6	27.92	3.192	773	Smectite/Illite	Moore and Reynolds
7	34.78	2.577	452	Chlorite	*878
8	36.54	2.457	693	Quartz	^PDF-33-1161
9	39.44	2.282	527	Kaolinite	*3036
10	40.3	2.236	384	Quartz	*3895
11	42.44	2.128	627	Quartz	*3895
12	45.78	1.98	442	Quartz/Carbonate	*3895/^PDF-41-1475
13	50.12	1.816	788	Kaolinite/Quartz	*3035
14	54.86	1.672	366	Kaolinite/Quartz	*2292
15	55.34	1.658	315	Smectite	*7496

Note ^The standards used for comparison of the data of XRD are taken from JCPDS, *Taken from Godovikov classifications 1997 Institute of experimental mineralogy, Russian Academy of sciences.
[1] X-ray Diffraction and the Identification and Analysis of Clay Minerals (Moore and Reynolds, 1997)

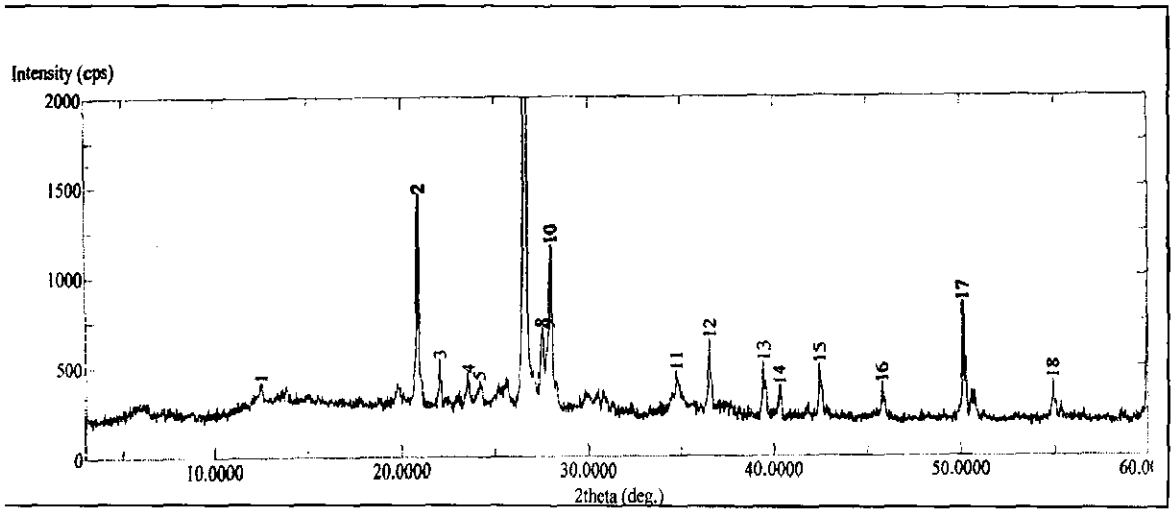

Figure 5.4.3: Showing clay mineral peak for Baikunthpur sandstone, Chirimiri, district Koriya, Chhattisgarh, India.

Table 5.4.3: Showing XRD data of (BBK5) Baikunthpur sandstone sample.

Peak	2θ	d-value	Intensity	Mineral	Reference
1	12.5	7.075	415	Kaolinite	Moore and Reynolds
2	20.86	4.25	1460	Quartz/Kaolinite	*3895/1169
3	22.04	4.02	540	Feldspar	Moore and Reynolds
4	23.58	3.769	462	Smectite	Moore and Reynolds, 1997
5	24.18	3.677	420	Carbonate	^PDF-5-378
6	26.62	3.345	6203	Quartz/Illite	*3895
7	26.7	3.336	3380	Quartz/Illite	*3895
8	27.48	3.243	712	Feldspar	Moore and Reynolds
9	27.82	3.2042	708	Feldspar	Moore and Reynolds
10	27.96	3.188	1175	Smectite/Feldspar	Moore and Reynolds
11	34.76	2.578	472	Kaolinite	*5859
12	36.54	2.457	642	Quartz	^PDF-33-1161
13	39.46	2.281	520	Kaolinite	*3036
14	40.3	2.236	386	Quartz	*3895
15	42.44	2.128	506	Quartz	*3895
16	45.78	1.98	396	Quartz/Carbonate	*3895/^PDF-41-1475
17	50.12	1.818	850	Kaolinite/Quartz	*3035
18	54.88	1.671	416	Kaolinite/Quartz	*2292

Note ^The standards used for comparison of the data of XRD are taken from JCPDS, *Taken from Godovikov classifications 1997 Institute of experimental mineralogy, Russian Academy of sciences. ! X-ray Diffraction and the Identification and Analysis of Clay Minerals (Moore and Reynolds, 1997)

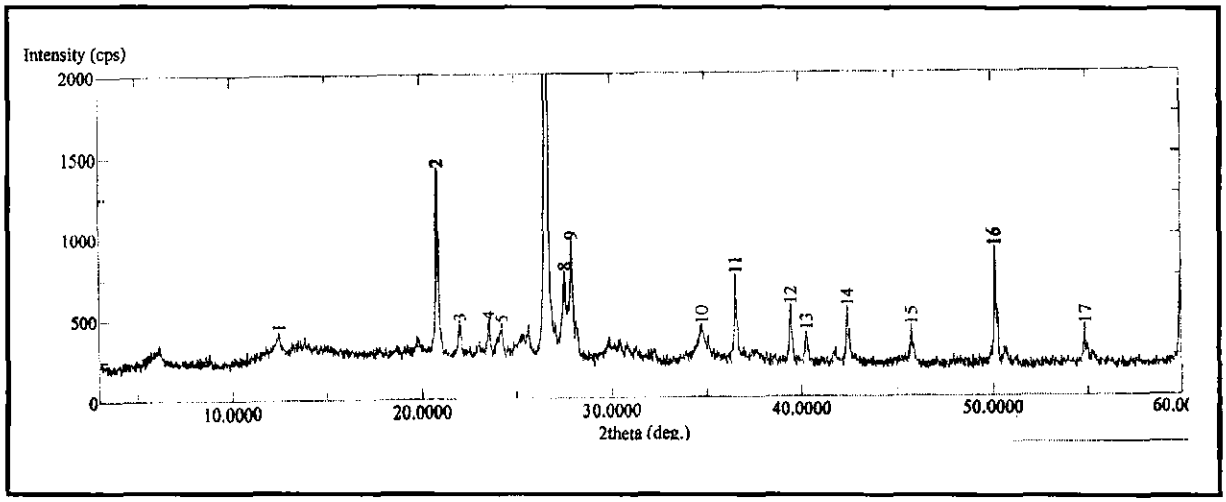

Figure 5.4.4: Showing clay mineral peak for Shale (BK1), Chirimiri, district Koriya, Chhattisgarh, India.

Table 5.4.4: Showing XRD data of (BK1) shale sample.

Peak	2θ	d-spacing	Intensity	Mineral	Reference
1	12.48	7.086	427	Kaolinite	*1169
2	20.84	4.258	1428	Quartz/Kaolinite	*3895/1169
3	22.02	4.033	482	Feldspar	Moore and Reynolds, 1997
4	23.54	3.776	498	Smectite	Moore and Reynolds, 1997
5	24.24	3.668	471	Illite	Moore and Reynolds, 1997
6	26.62	3.345	6432	Quartz	*3895
7	26.7	3.336	3519	Quartz/Illite	*3895
8	27.56	3.233	788	Feldspar	Moore and Reynolds, 1997
9	27.92	3.192	975	Feldspar	Moore and Reynolds, 1997
10	34.76	2.578	450	Kaolinite	*5859
11	36.54	2.457	760	Quartz	^PDF-33-1161
12	39.46	2.281	567	Kaolinite	*3036
13	40.28	2.237	407	Quartz	*3895
14	42.44	2.128	551	Quartz	*3895
15	45.78	1.98	438	Quartz/Carbonate	*3895/^PDF-41-1475
16	50.12	1.818	919	Kaolinite/Quartz	*3035
17	54.88	1.671	438	Kaolinite/Quartz	*2292

Note ^ The standards used for comparison of the data of XRD are taken from JCPDS, *Taken from Godovikov classifications 1997 Institute of experimental mineralogy, Russian Academy of sciences. ! X-ray Diffraction and the Identification and Analysis of Clay Minerals (Moore and Reynolds, 1997)

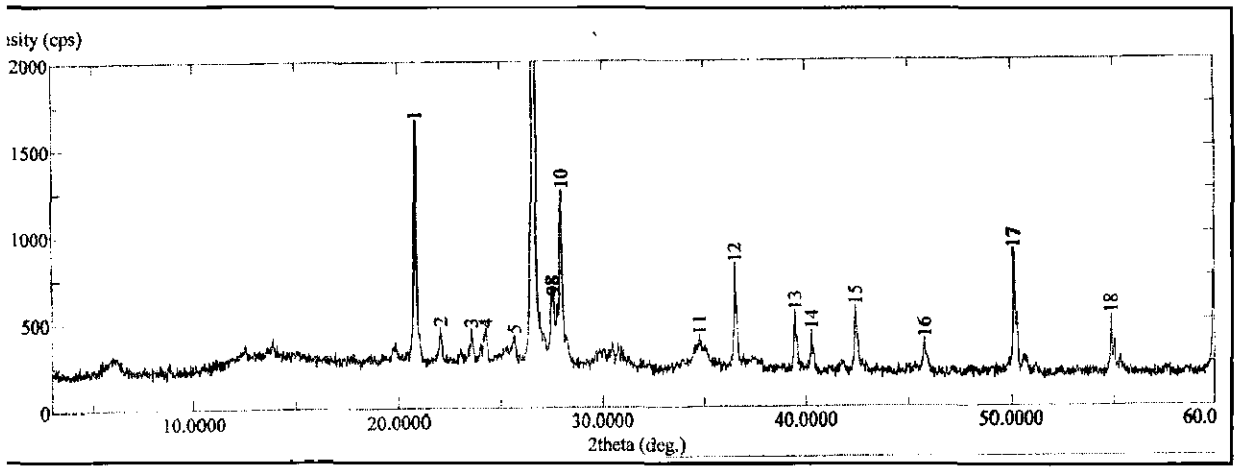

Figure 5.4.5: Showing clay mineral peak for Shale sample (BK2), Chirimiri, district Koriya, Chhattisgarh, India.

Table 5.4.5: Showing XRD data of (BK2) shale sample.

Peak	2θ	d-spacing	Intensity	Mineral	Reference
1	20.84	4.25	1663	Quartz/Kaolinite	*3895/1169
2	22.02	4.033	472	Feldspar	Moore and Reynolds, 1997
3	23.54	3.776	464	Smectite	Moore and Reynolds, 1997
4	24.26	3.665	465	Illite	Moore and Reynolds, 1997
5	25.66	3.468	428	Illite	Moore and Reynolds, 1997
6	26.64	3.343	6535	Quartz/Illite	*3895
7	26.68	3.338	4204	Quartz/Illite	*3895
8	27.5	3.24	702	Feldspar	Moore and Reynolds, 1997
9	27.56	3.233	642	Feldspar	Moore and Reynolds, 1997
10	27.92	3.192	1257	Smectite/Illite	Moore and Reynolds, 1997
11	34.76	2.578	417	Kaolinite	*5859
12	36.54	2.457	829	Quartz	^PDF-33-1161
13	39.46	2.281	554	Kaolinite	*3036
14	40.28	2.237	443	Quartz	*3895
15	42.44	2.128	581	Quartz	*3895
16	45.78	1.98	395	Quartz/Carbonate	*3895/^PDF-41-1475
17	50.12	1.818	905	Kaolinite/Quartz	*3035
18	54.88	1.671	524	Kaolinite/Quartz	*2292

Note ^The standards used for comparison of the data of XRD are taken from JCPDS, *Taken from Godovikov classifications 1997 Institute of experimental mineralogy, Russian Academy of sciences.
[1] X-ray Diffraction and the Identification and Analysis of Clay Minerals (Moore and Reynolds, 1997)

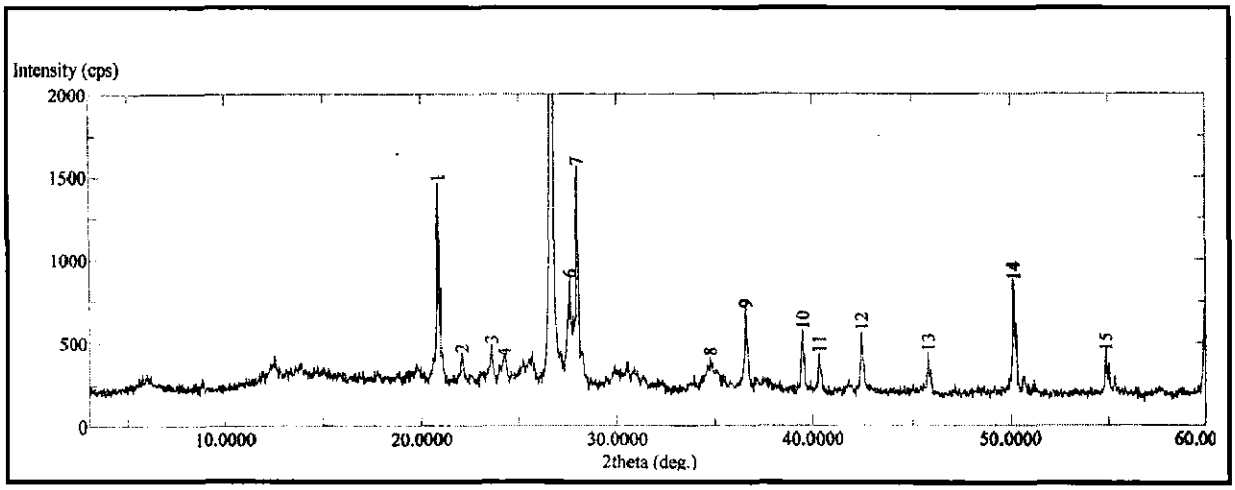

Figure 5.4.6: Showing clay mineral peak for Shale samples (BK3), Chirimiri, district Koriya, Chhattisgarh. India.

Table 5.4.6: Showing XRD data of (BK3) shale sample.

Peak	2θ	d-spacing	Intensity	Mineral	Reference
1	20.86	4.254	1469	Quartz/Kaolinite	*3895/1169
2	22.02	4.033	440	Feldspar	Moore and Reynolds
3	23.56	3.773	494	Smectite	Moore and Reynolds, 1997
4	24.22	3.6717	418	Carbonate	^PDF-5-378
5	26.64	3.343	6748	Quartz/Illite	*3895
6	27.56	3.233	886	Feldspar	Moore and Reynolds
7	27.94	3.19	1564	Smectite/Feldspar	Moore and Reynolds
8	34.76	2.578	419	Kaolinite	*5859
9	36.54	2.457	709	Quartz	^PDF-41-586
10	39.48	2.28	575	Kaolinite	*3036
11	40.28	2.237	435	Quartz	*3895
12	42.44	2.128	566	Quartz	*3895
13	45.78	1.98	447	Quartz/Carbonate	*3895/^PDF-41-1475
14	50.14	1.817	873	Kaolinite/Quartz	*3035
15	54.84	1.672	447	Kaolinite/Quartz	*2292

Note ^The standards used for comparison of the data of XRD are taken from JCPDS, *Taken from Godovikov classifications 1997 Institute of experimental mineralogy, Russian Academy of sciences. ! X-ray Diffraction and the Identification and Analysis of Clay Minerals (Moore and Reynolds, 1997)

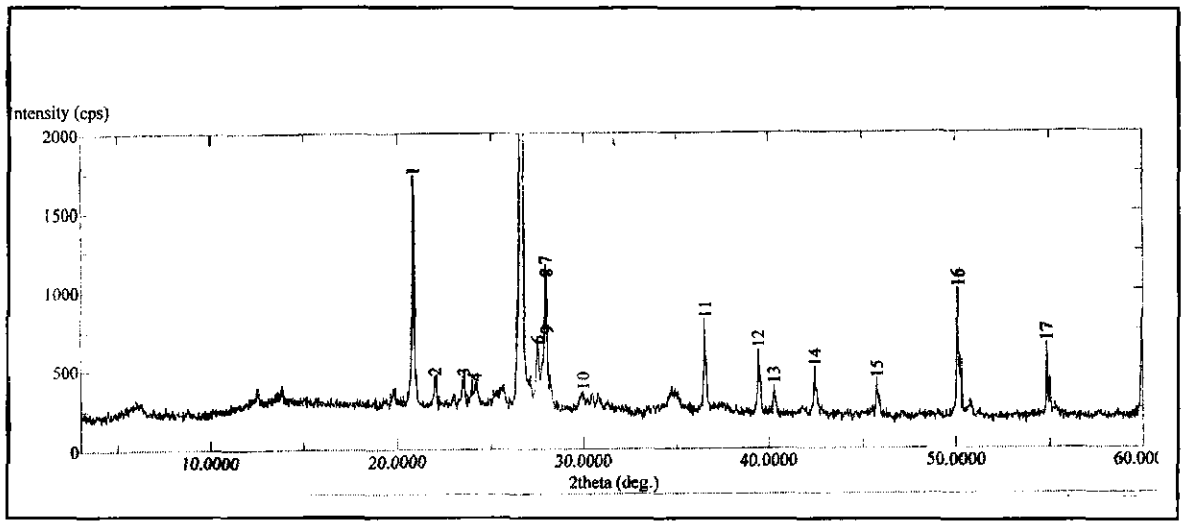

Figure 5.4.7: Showing clay mineral peak for shale samples (BK4), Chirimiri, district Koriya, Chhattisgarh, India.

Table 5.4.7: Showing XRD data of (BK4) shale sample.

Peak	2θ	d-spacing	Intensity	Mineral	Reference
1	20.84	4.25	1736	Quartz/Kaolinite	*3895/1169
2	22	4.03	461	Feldspar	Moore and Reynolds, 1997
3	23.56	3.77	459	Smectite	Moore and Reynolds, 1997
4	24.2	3.67	426	Carbonate	^PDF-5-378
5	26.62	3.34	7216	Quartz	*3895
6	27.52	3.23	665	Feldspar	Moore and Reynolds, 1997
7	27.92	3.19	1162	Smectite/Illite	Moore and Reynolds, 1997
8	27.96	3.188	1088	Smectite/Feldspar	Moore and Reynolds, 1997
9	28.02	3.181	729	Smectite/Feldspar	Moore and Reynolds, 1997
10	29.96	2.98	370	Quartz	Moore and Reynolds, 1997
11	36.54	2.457	818	Quartz	^PDF-33-1161
12	39.46	2.281	634	Kaolinite	*3096
13	40.28	2.237	402	Quartz	*3895
14	42.44	2.128	514	Quartz	*3895
15	45.78	1.98	437	Quartz/Carbonate	*3895/^PDF-41-1475
16	50.12	1.818	1014	Kaolinite/Quartz	*3035
17	54.86	1.672	669	Kaolinite/Quartz	*2292

ote ^ The standards used for comparison of the data of XRD are taken from JCPDS, *Taken from odovikov classifications 1997 Institute of experimental mineralogy, Russian Academy of sciences. ! -ray Diffraction and the Identification and Analysis of Clay Minerals (Moore and Reynolds, 1997)

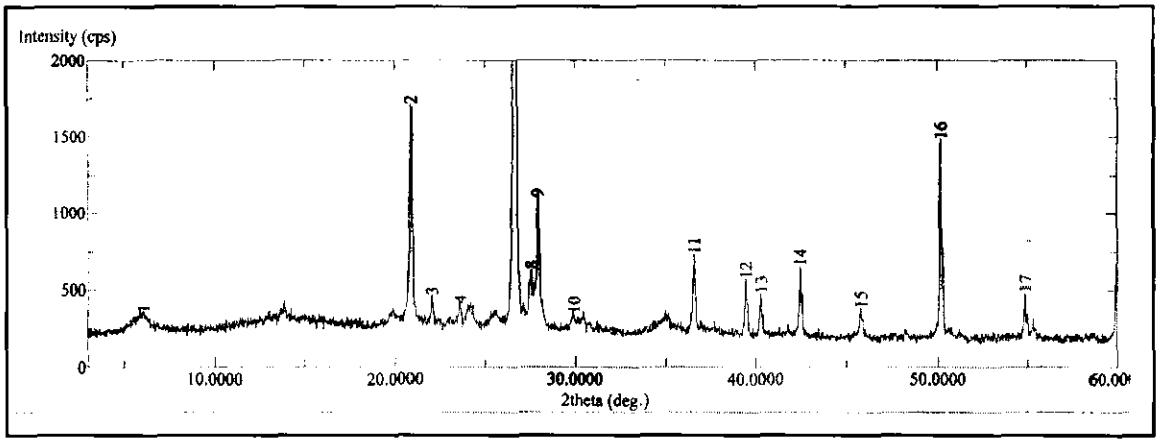

Figure 5.4.8: Showing clay mineral peak for Chirimiri sandstones (NT5), Chirimiri, district Koriya, Chhattisgarh, India.

Table 5.4.8: Showing XRD data of (NT5) Chirimiri sandstone sample.

Peak	2θ	d-spacing	Intensity	Mineral	Reference
1	6.12	14.42	356	Chlorite	Moore and Reynolds, 1997
2	20.88	4.25	1707	Quartz/Kaolinite	*3895/1169
3	22	4.036	465	Feldspar	Moore and Reynolds, 1997
4	23.6	3.766	415	Smectite	Moore and Reynolds, 1997
5	26.62	3.345	6843	Quartz/Illite	*3895
6	26.64	3.343	8059	Quartz/Illite	*3895
7	26.68	3.338	6171	Quartz/Illite	*3895
8	27.54	3.236	632	Feldspar	Moore and Reynolds, 1997
9	27.92	3.192	1102	Smectite/Illite	Moore and Reynolds, 1997
10	29.94	2.982	348	Quartz	Moore and Reynolds, 1997
11	36.56	2.455	734	Quartz	^PDF-33-1161
12	39.46	2.281	574	Kaolinite	*3036
13	40.3	2.236	481	Quartz	*3895
14	42.44	2.128	655	Quartz	*3895
15	45.78	1.98	388	Quartz/Kaolinite	*3895/^PDF-41-1475
16	50.16	1.817	1483	Kaolinite/Quartz	*3035
17	54.88	1.671	486	Kaolinite/Quartz	*2292

Note ^ The standards used for comparison of the data of XRD are taken from JCPDS, *Taken from Godovikov classifications 1997 Institute of experimental mineralogy, Russian Academy of sciences. ! X-ray Diffraction and the Identification and Analysis of Clay Minerals (Moore and Reynolds, 1997)

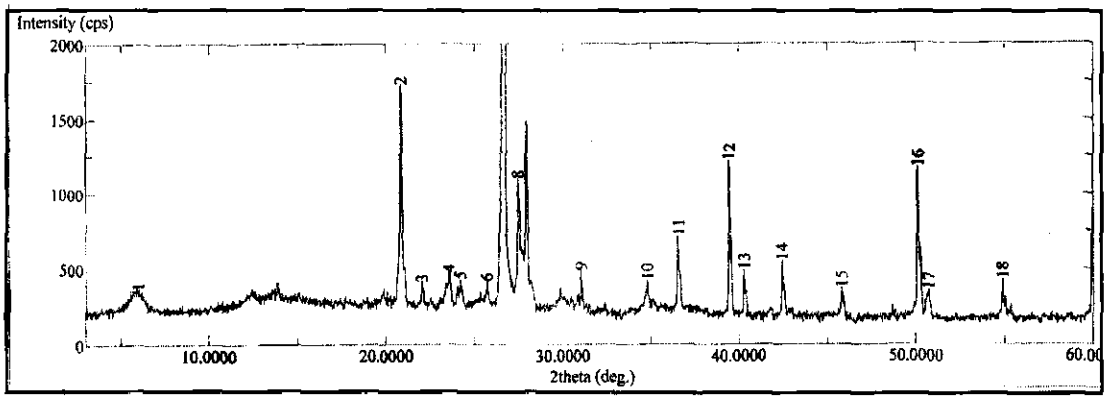

Figure 5.4.9: Showing clay mineral peak for Chirimiri sandstones (GN5), Chirimiri, district Koriya, Chhattisgarh, India.

Table 5.4.9: Showing XRD data of (GN5) Chirimiri sandstone sample.

Peak	2θ	d-spacing	Intensity	Mineral	Reference
1	5.98	14.76	360	Smectite	*6100
2	20.86	4.25	1722	Quartz/Kaolinite	*3895/1169
3	22	4.03	407	Feldspar	Moore and Reynolds, 1997
4	23.54	3.77	473	Smectite	Moore and Reynolds, 1997
5	24.2	3.67	430	Carbonate	^PDF-5-378
6	25.68	3.46	416	Illite	Moore and Reynolds, 1997
7	26.64	3.346	10240	Quartz/Illite	*3895
8	27.46	3.24	1096	Feldspar	Moore and Reynolds, 1997
9	31.04	2.878	491	Smectite	*6100
10	34.78	2.57	421	Chlorite	*878
11	36.54	2.45	710	Quartz	^PDF-33-1161
12	39.46	2.28	1271	Kaolinite	*3096
13	40.3	2.23	491	Quartz	*3895
14	42.44	2.12	553	Quartz/Carbonate	*3895
15	45.78	1.98	368	Kaolinite/Quartz	*3895/^PDF-41-1475
16	50.14	1.817	1167	Kaolinite/Quartz	*3035
17	50.72	1.798	354	Carbonate	^PDF-41-586
18	54.88	1.67	424	Kaolinite/Quartz	*2292

Note ^The standards used for comparison of the data of XRD are taken from JCPDS, *Taken from Godovikov classifications 1997 Institute of experimental mineralogy, Russian Academy of sciences. ! X-ray Diffraction and the Identification and Analysis of Clay Minerals (Moore and Reynolds, 1997)

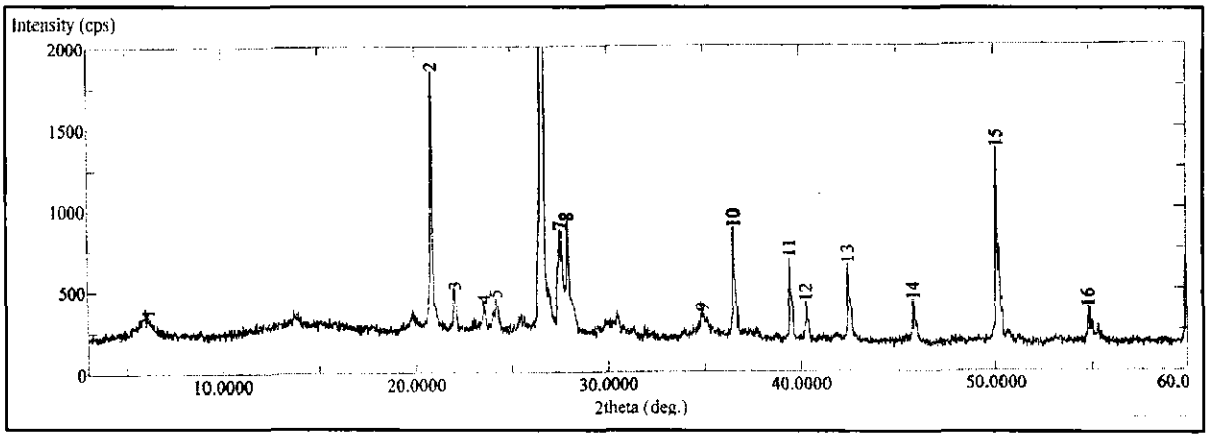

Figure 5.4.10: Showing clay mineral peak for Chirimiri sandstone (NT1), Chirimiri, district Koriya, Chhattisgarh, India.

Table 5.4.10: Showing XRD data of (NT1) sandstone sample.

Peak	2θ	d-spacing	Intensity	Mineral	Reference
1	6.12	14.429	350	Illite/Smectite	*1169
2	20.86	4.25	1844	Quartz/Kaolinite	*3895/1169
3	22.06	4.026	504	Feldspar	Moore and Reynolds, 1997
4	23.56	3.77	423	Smectite	Moore and Reynolds, 1997
5	24.18	3.677	453	Carbonate	^PDF-5-378
6	26.64	3.343	8711	Quartz/Illite	*3895
7	27.56	3.233	870	Feldspar	Moore and Reynolds, 1997
8	27.9	3.195	928	Smectite/Illite	Moore and Reynolds, 1997
9	34.9	2.568	365	Kaolinite	*878
10	36.56	2.455	880	Quartz	^PDF-33-1161
11	39.46	2.281	395	Kaolinite	*3036
12	40.3	2.236	422	Quartz	*3895
13	42.44	2.128	659	Quartz	*3895
14	45.78	1.98	432	Quartz/Carbonate	*3895/PDF-41-1475
15	50.12	1.818	1359	Kaolinite/Quartz	*3035
16	54.86	1.672	381	Kaolinite/Quartz	*2292

Note. ^ The standards used for comparison of the data of XRD are taken from JCPDS, *Taken from Godovikov classifications 1997 Institute of experimental mineralogy, Russian Academy of sciences. ! X-ray Diffraction and the Identification and Analysis of Clay Minerals (Moore and Reynolds, 1997)

CONCLUSION

CONCLUSION

The purpose of the present study is to investigate the petrological and geochemical characters of the Talchir Formation exposed around Chirimiri town, district Koriya, Chhattisgarh. The study area forms a part of Son-Mahanadi master Gondwana basin. The sandstone and shale belonging to Talchir Formation the lowermost unit of Gondwana Supergroup are exposed in streams as isolated bodies. Complete succession of Talchir Formation, from top to bottom, is not found exposed in the investigated area, but on the basis of lithology exposed in other parts of Son-Mahanadi basin a generalised stratigraphic order of deposition is established. Fining upward sequence has been observed in the basin which advocates for glacio-fluvial conditions. On the basis of detailed petrography and geochemical analysis following important conclusions are drawn:-

1. The sandstones of Talchir Formation are classified as arkose, sub-arkose, and lithic-arkose types. These sandstones are comprised of mono crystalline quartz ranging from angular to subrounded grains. In some of these grains strain lamellae has been also observed.

2. In QtFL and QmFLt ternary plots indicates continental block provenance. Continental block is further classified into three regions i.e., craton interior, transitional continental region, and basement uplift. The majority of these sediments show their source lie in transitional region followed by basement uplift and recycled orogen provenance. The rock fragment based Qp-Lv-Ls diagram suggests that some of these sediments have also been derived from collision suture and fold thrust belt regions.

3. The K_2O concentration in sandstones and shales of Talchir Formation Chirimiri area is higher than Na_2O. This interpretation is in concurrence with the modal composition of sandstone, where K-feldspar significantly dominates over plagioclase.

4. In Qm-P-K ternary diagram Chirimiri sandstones contain Qm = 70, K = 26.37 and Baikunthpur sandstones Qm = 54.31, K = 41.24, the average SiO_2/Al_2O_3 ratio in Chirimiri sandstones is 7.24 while in Baikunthpur sandstones 6.28,

which suggest that the Baikunthpur sandstones of Talchir Formation are compositionally more immature than Chirimiri sandstones.

5. Relatively high values of Rb in Talchir Formation sandstones (particularly in Baikunthpur sandstones) indicate dominance of K-feldspar bearing rocks in the source terrain. The concentration of HFSE, LILE and TTE in Baikunthpur sandstones is relatively higher than Chirimiri sandstones.

6. The distinctive modal mineralogy and geochemical characteristics of Chirimiri and Baikunthpur sandstones illustrate that their detritus were supplied by two different types of rock. The average value of Gd/Yb_N ratio is greater than 2 in Baikunthpur sandstones and associated shales, suggest that their source area was composed of moderately depleted HREE rocks.

7. The first indication about the nature of provenance composition is obtained from major element mobility assessment diagrams wherein a magmatic relationship between Al_2O_3 and Zr except K, Ca and Cs exists. These relationships in these sandstones and shales indicate that their primary abundances have not been affected by post depositional processes. Binary diagrams of mobile elements, K_2O versus Rb, Sr and Ba and Rb versus Sr and Ba also display positive linear relationship observed as in primary igneous rocks. These relationships suggest that the detritus of Talchir rocks was predominantly derived from an igneous terrain.

8. The average K_2O/Na_2O ratio in Chirimiri sandstones is 1.62, Baikunthpur sandstones 1.67 and in shales 1.49. The automorphic inclusion of heavy minerals in sandstones like zircon and tourmaline found in monocrystalline quartz, and grains of perthite in conjunction with K_2O/Na_2O ratio indicate predominance of granitic rocks in the source terrain.

9. The CIA values of Chirimiri sandstones (average 61.58), Baikunthpur sandstones (average 61.02) and shales (average 66.66). These values are closer to composition of Upper Continental Crust (50.47). Suggesting Upper Continental Crust like source for these rocks of Talchir Formation.

10. In CaO-Na_2O-K_2O ternary diagram samples of Talchir clastics cluster in the field of granite and granodiorite. This interpretation is also supported by Al_2O_3/TiO_2 ratio in Talchir clastics which suggests that the source terrain was composed of intermediate to felsic igneous rocks.

11. The major element discriminant function diagram suggests predominantly a source having siliceous composition, possessing intermediate to felsic components for the studied clastics of Talchir Formation of Chirimiri area (Figure 4.2.3). Immobile elements based binary diagram (TiO_2 versus Zr) firmly endorses the inferences of major element data.

12. High content of TiO_2, positive Eu anomaly and $(Gd/Yb)_N$ ratio greater than 2 in few samples articulate for the presence of basic material in the provenance. But trace elements ratio e.g. La/Sc, Th/Sc, La/Co, Th/Co, Th/Cr, Cr/Ni and binary diagrams like Th/Co-La/Sc, La/Th-Hf, La/Th-Th/Yb and Cr/V-Y/Ni confirm the felsic composition of the source terrain and refute the presence of mafic component.

13. The majority of the constituent sandstone grains of Talchir Formation are angular in shape signifying that these sediments belong to first cycle of erosion and have been transported for short distance, whereas presence of few subrounded to rounded grains indicate second cycle of erosion. The ICV, Zr/Th ratio (<17.76 UCC), and the binary plot of Zr/Sc-Th/Sc also support this inference that these clastics are first cycle sediments.

14. The tectonic setting of Talchir clastics inferred from their modal mineralogy and geochemical abundance indicates the location of Chirimiri basin in an active continental margin setting. The active continental margin setting comprises of continental margin of Andean type marked by plate convergence and orogenic volcanic rocks and strike-slip continental margin. Subsequently, sedimentary basins associated with active continental margins have diverse geomorphic setting (Bhatia and Crook, 1986). In this context the Chirimiri basin can also be considered as a local pull-apart basin, which received sediments from fault bounded basement uplift. The sediments deposited in pull-apart basins show mineralogical and chemical signatures resembling to

the basins of active continental margin setting (Dickinson et al., 1985; Bhatia and Crook, 1986; Bock, 2000).

15. The CIA, PIA, CIW suggest low to moderate weathering conditions of the source terrain. The reported stable isotopic analysis also supports the elemental ratios for oxidising conditions during the deposition of sediments of Talchir Formation under shallow lacustrine environment in Chirimiri basin.

16. The presence of characteristic clay minerals like illite, chlorite, new smectite, detrital kaolinite and non-clay minerals, feldspar and carbonate depicts shift from semi arid to semi- humid conditions in cold climate at the time of deposition of Talchir clastics during Permo-carboniferous period. The correlation of paleolatitudes, temporal variations of chemical index of alteration of Permocarboniferous sediments from different Gondwana basins of India and the world, also advocates for climate change as a global phenomenon from glacial to post glacial transitions (Yang et al., 2014).

REFERENCES

Acharyya, S.K., 2003. The Nature of Mesoproterozoic Central Indian Tectonic zone with exhumed and reworked older Granulites. Gondwana Research, v. 6, No. 2, p. 197-214.

Ahmad, N., 1975a. Upper Carboniferous Glaciation in India. Proc. 8th International Congress on Carboniferous Stratigraphy Paleogeography. Moscow, v. 6, p. 1-8.

Ahmad, N., 1975b. Son valley Talchir glacial deposits. Bulletin Geological Society of India, v. 16, p. 475-484.

Ahmad, T. and Rajamani, V., 1991. Geochemistry and petrogenesis of the basal Aravalli Volcanics near Nathdwara, Rajasthan, India. Precambrian Res. v. 49, p. 185-204.

Alexander, L. T., Hendrik, S. B and Nelson, R. A. 1939. Minerals present in soil colloids: II. Estimation in some representative soils. Soil Science, v. 48, p. 273-79.

Armstrong Altrin, J. S., Lee, Y. I and Verma, S. P., 2004. Geochemistry of sandstones from the Upper Miocene Kudankulam Formation, Southern India: implications for provenance, weathering and tectonic setting. Journal of Sedimentary Research, v.74, p. 285-297.

Bahlburg, H., 1998. The geochemistry and provenance of Ordovician turbidites in the Argentine Puna. In: Pankhurst, R.J and Rapela, C.W. (eds) The Proto-Andean Margin of Gondwana, Geological Society of London, Special Publications, v. 142, p. 127-142

Bally, A.W. 1980. Basins and Subsidence: A Summary. In: Bally, A.W. et al. (eds.), Dynamics of Plate Interiors, Geodynamics Series 1, v. 1, p. 5–20 AGU-GSA, Washington D.C.

Bangert, B., Stollhofen, H., Lorenz, V. and Armstrong, R., 1999. The geochronology and significance of ash-fall tuffs in the glacio-genic Carboniferous-Permian Dwyka Group of Namibia and South Africa. Journal of African Earth Science, v. 29, p. 33-49.

Barshad, I., 1966. The effect of a variation in precipitation on the nature of clay *mineral formation in soils from acid and basic igneous rocks*, Proceedings International Clay Conference, p. 167-173.

Basu, A., 1976. Petrology of Holocene Fluvial sand Derived from Plutonic Source Rocks: Implications to Paleoclimatic Interpretation," Journal of Sedimentary Petrology, v. 46, No. 3, p. 696-709.

Bhatia, M.R and Crook, K.A.W., 1986. Trace elements characteristics of greywacke and tectonic setting discrimination of sedimentary basins. Contribution to Mineralogy and Petrology, v. 92, p. 181-193.

Bhatia, M.R., 1983. Plate tectonics and geochemical composition of sandstones. Journal of Geology, v. 91, p. 115-125.

Bhattacharya H. N and Bhattacharya, B., 2006. A Permo- Carboniferous Tide-Storm Interactive System: Talchir Formation, Raniganj Basin, India, Journal of Asian Earth Sciences, v. 27, No. 3, p. 303-311.

Bhattacharya H. N and Bhattacharya, B., 2010. Soft Sediment Deformation Structures from an Ice-Marginal Storm-Tide Interactive System, Permo-Carboniferous Talchir Formation, Talchir Coal basin, India, Sedimentary Geology, v. 223, No. 3-4, p. 380-389.

Bhattacharya, B. and Bhattacharya, H. N., 2012. Implications of Mud-Clast Conglomerates within Late Palaeozoic Talchir Glacio-Marine Succession, Talchir Basin, India, Indian Journal of Geosciences, v. 66, No. 1, p. 69-78.

Bhattacharya, H. N Chakraborty, A and Bhattacharya, B. 2005. Significance of Transition between Talchir Formation and Karharbari Formation in Lower Gondwana Basin Evolution—A Study in West Bokaro Coal Basin, Jharkhand, India, Journal of Earth System Science, v. 114, No. 3, p. 275-286.

Bhattacharya, H. N., Bhattacharya, B., Chakraborty, I and Chakraborty, A., 2004. Sole Marks in Storm Event Beds in the Permo-Carboniferous Talchir Formation, Raniganj Basin, India, Sedimentary Geology, v. 166, No. 3-4, p. 209-222.

Bhattacharya, S.K., Ghosh, P and Chakrabarti, A., 2002b. Carbon and Oxygen Isotopic composition of Carbonate Concretions of the Talchir Formation and their Paleoenvironmental implications, Journal Geological Society of India, v. 60, p. 677-686.

Birkeland, P. W. 1984. Soils and geomorphology. New York: Oxford University Press.

Biscaye, P., 1965, Mineralogy and sedimentation of recent deep-sea clay in the Atlantic Ocean and adjacent seas and oceans: Geological Society of America Bulletin, v. 76, p. 803-832.

Blakey, R.C., 2008. Gondwana paleogeography from assembly to breakup—a 500m.y. odyssey. In: Fielding, C.R., Frank, T.D., Isbell, J.L. (Eds.), Resolving the Late Paleozoic Ice Age in Time and Space: Geological Society of America Special Paper v. 441, p. 1–28.

Blandford, W.T., Blandford, H.F and Theobald, W., 1856. On the geological structure and relations of the Talcheer Coalfield in the district of Cuttack. Memoire Geological Survey of India, v. 1, pt. 1, p. 33-89.

Blum, J. D., Gazis, C. A., Jacobson, A. D, 1998. Carbonate verse silicate weathering in the Raikhot watershed within the High Himalayan Crystalline Series, Geology, v. 26, p. 411- 414.

Bock, B., Bahliburg, H., Worner, G and Zimmermann, U., 2000. Tracing Crustal Evolution in the Southern Central Andes from Late Precambrian to Permian with Geochemical and Nd and Pb Isotope Data. The Journal of Geology, v. 108, p. 515–535.

Brady, P. V., and Carroll, S. A., 1994. Direct effects of CO2 and temperature on silicate weathering: possible implications for climate control, Geochimica Cosmochimica Acta, v. 58, p. 1853 -1856.

Buggisch, W., Wang, X., Alekseev, A.S., Joachimski, M.M., 2011. Carboniferous–Permian carbon isotope stratigraphy of successions from China (Yangtze platform), USA (Kansas) and Russia (Moscow Basin and Urals). Palaeogeography, Palaeoclimatology, Palaeoecology v. 301, p. 18–38.

C. S. Rao Raja, 1983. Chirimiri Coalfield, In: Coal Resources of Madhya Pradesh and Jammu & Kashmir, Bulletins of Geological Survey of India, Series A, v. 3, No. 45, p. 44-55.

Caputo, M.V, and Crowell, J.C., 1985. Migration of glacial centres across Gondwana during Paleozoic Era. Geological Society of America Bulletin, v. 96, p. 1020–1036.

Casshyap, S. M and Qidwai, H.A., 1978a. Grain size characters of ancient fluviatile deposits an example from Lower Gondwana rocks of Pench valley coalfield, central India, Journal Geological Society of India, v. 19, p. 240-250.

Casshyap, S. M and Qidwai, H.A., 1978b. Sediment transports direction in fluviatile Karharbari sandstone, Giridih basin, Bihar, Journal Earth Science, v. 5, p. 95-101.

Casshyap, S. M. and Qidwai, H. A. 1974. Glacial Sedimentation of Late Palaeozoic Talchir diamictite, Pench Valley Coalfields, Central India, Geological Society of America Bulletin, v. 85, No. 5, p.749-760.

Casshyap, S. M., 1970b. Sedimentary cycles and environment of deposition of the coal measures of lower Gondwana, India, Journal of Sedimentary Petrology, v. 40, p. 1302-1317.

Casshyap, S. M., 1973. Paleocurrents and paleogeographic reconstruction in the Barakar (Lower Gondwana) sandstones of Peninsular India, Sedimentary Geology, v. 9, p. 283-303.

Casshyap, S. M., 1980. Lithofacies analysis of the Later Permian Raniganj Coal Measures (Mahuda Basin) and their paleogeographic implications. In Gondwana Five, M. M Cresswell and P. Vella (Eds.), Balkemna, Rotterdam, p. 125-132, v. 24, p. 134-147.

Casshyap, S. M., and Qidwai, H.A., 1971. Paleocurrent analysis of Lower Gondwana sedimentary rocks, Pench valley coalfield, M.P, Sedimentary Geology, v. 5, p. 135-145.

Casshyap, S.M and Srivastava, V.K., 1987. Glacial and Proglacial Talchir sedimentation in Son-Mahanadi Gondwana basin, Paleogeographic

reconstruction: in Gondwana VI, American Geophysical union, Washington, Monograph, v. 41, p. 167-182.

Casshyap, S.M. and Srivastava, V.K., 1983c. Sedimentary evolution of marine and continental facies in a pre-Siwalik Tertiary basin of southern Himachal Pradesh. Journal Geological Society of India.

Casshyap, S.M., 1970a. Barakar paleocurrent patterns in some Lower Gondwana coalfields of M.P and Bihar, International Symposium Stratigraphy Mineral Resource of Gondwana System, A.M.U., Aligarh (Abs.), p. 18.

Casshyap, S.M., 1979. Patterns of sedimentation in Gondwana basins. In: Laskar, B., Raja Rao, C.S (Eds.), Fourth International Gondwana Symposium, Calcutta, India, Hindustan Publishing Corporation, Delhi 2, p. 525-551.

Casshyap, S.M., Tewari, R.C. and Khan, Z.A., 1983a. Quantitative lithofacies study of late Paleozoic coal measures of eastern India Gondwana basins and sedimentologic implications. International Symposium of Recent Advances Quantitative Stratigraphic Correlation, I.I.T., Kharagpur, p. 17-18.

Casshyap, S.M., Dev., P. and Raghuvanshi, A.K.S., 1983b. Ichnofossils from Bhuj Formation (Cretaceous) as Paleo environmental parameter. Current Science, v. 52, p. 73-74.

Casshyap, S.M., Tewari, R.C. and Khan, Z.A., 1983d. Quantitative lithofacies study of late Paleozoic coal measures of eastern India Gondwana basins and Sedimentological implications. International Symposium Recent Advances Quantitative Stratigraphic Correlation, I.I.T., Kharagpur, p. 17-18.

Chakraborty, C and Ghosh, S. K., 2005. Pull-apart origin of the Satpura Gondwana basin central India, Journal of Earth System Science, v. 114, No. 3, p. 259-273.

Chakraborty, C and Ghosh, S.K., 2008. Pattern of sedimentation during the Late Paleozoic, Gondwanaland glaciation: An example from the Talchir Formation, Satpura Gondwana basin, central India, Journal Earth System Science, v. 117, No. 4, p. 499–519.

Chakraborty, K and Roy, A., 2013. Petrogenesis of Ultramafic-Mafic to Felsic plutonic rock associations from Southern portion of Chhotanagpur Gneissic

Complex in Central India, Journal Geological Society of India, v. 81, p. 309-329.

Chamley, H., 1989. Clay sedimentology, New York, Springer-Verlag, Berlin.

Condie, K. C, 1993. Chemical composition and evolution of the upper continental crust: Contrasting results from surface samples and shales. Chemical Geology, v. 104, p. 1 – 37.

Cox, R., Lowe, D.R., Cullers, R.L., 1995. The influence of sediment recycling and basement composition on evolution of mudrock chemistry in the south-western United States: Geochimica et Cosmochimica Acta, v. 59, No. 14, p. 2919-2940.

Crowell, J.C., Frakes, L.A., 1970. Phanerozoic glaciation and the causes of ice ages. American Journal of Science, v. 268, p. 193–224.

Cullers, R. L, and Podkovyrov V. N., 2002. The source and origin of terrigenous sedimentary rocks in the Mesoproterozoic Ui group, south-eastern Russia. Precambrian Research, v. 117, p. 157–183.

Cullers, R.L., 1994a. The chemical signature of source rocks in size fractions of Holocene stream sediment derived from metamorphic rocks in the Wet Mountains region, USA. Chemical Geology, v. 113, p. 327–343.

Cullers, R.L., 1994b. The controls on the major and trace element variation of shales, siltstones and sandstones of Pennsylvanian-Permian age from uplifted continental blocks in Colorado to platform sediment in Kansas, U.S.A., Geochimica et Cosmochimica Acta, v. 58, p. 4955-4972.

Cullers, R.L., 1995. The control on the major and trace elements evolution of shales, siltstones and sandstones of Ordovician to tertiary age in the wet mountains region, Colorado, U.S.A., Chemical Geology, v. 123, p. 107-131.

Cullers, R.L., Basu, A and Suttner, L., 1988. Geochemical signature of provenance in sand-size material in soils and stream sediments near the Tobacco Root batholiths, Montana, U.S.A., Chemical Geology, v. 70, p. 335-348.

Cullers, R.L., Chaudhuri, S., Kilbane, N. and Koch, R., 1979. Rare earths in size fractions and sedimentary rocks of Pennsylvanian- Permian age from the

mid-continent of the U.S.A. Geochimica Cosmochimica Acta, v. 43, p. 1285-1302.

Cullers, R.L., Barrett, T., Carlson, R., Robinson, B., 1987. Rare earth element and mineralogic changes in Holocene soil and stream sediment: a case study in the Wet Mountains, Colorado, USA. Chemical Geology, v. 63, p. 275–297.

Cullers, R.L., Stone, J., 1991. Chemical and mineralogical comparison of the Pennsylvanian Fountain Formation, Colorado, USA (an uplifted continental block) to sedimentary rocks from other tectonic environments. Lithos, v. 27, p. 115–131.

Das, S. N. and Sen, D. P., 1980. Depositional History of Permo- Carboniferous Tillites and Associated Sediments in West Bokaro Gondwana Basin, Bihar, Journal of the Geological Society of India, v. 21, No. 1, p. 30-38.

Dasch EJ., 1969. Strontium isotopes in weathering profiles, deep-sea sediments and sedimentary rocks. Geochimica Cosmochimica Acta, v. 33, p. 1521–1552.

Dasgupta, P and Sahoo, R., 2007. Facies characteristics of the basal part of Talchir Formation, Talchir basin, India- depositional history revisited. Journal of Earth System Science, v. 116, No. 1, p. 15-20.

Dickinson W. R and Suczek, C. A., 1979. Plate Tectonics and Sandstone Compositions, American Association of Petroleum, Geological Bulletin, v. 63, No. 12, p. 2164-2182.

Dickinson, W. R. 1985. Interpreting Provenance Relations from Detrital Modes of Sandstones, In: G. G. Zuffa, Ed., Provenance of Arenites, D. Reidel Publications Corporation, New York, p. 333-361.

Dickinson, W. R., Beard, L. S., Brakenridge, G. R., Erjavee, J. R., Ferguson R. C and Inman, K. F., 1983. Provenance of North American Phanerozoic Sandstones in Relation to Plate Tectonic Setting. Geological Society of American Bulletin, v. 94, No. 2, p. 222-235.

Diekmann, B., Wopfner, H., 1996. Petrographic and diagenetic signatures of climatic changes in peri and postglacial Karoo sediments of SW Tanzania. Palaeogeography, Palaeoclimatology, Palaeoecology, v. 125, p. 5–25.

Dill, H., 1986. Metallogenesis of early Paleozoic graptolite shales from the Graefenthal Horst (northern Bavaria-Federal Republic of Germany), Economic Geology, v. 81, p. 889-903.

Dotiwala, S. and Pangtey, K. K. S., 1997. KDMIPE, AAPG, Search and Discovery Article, American Association of Petroleum Geologist, International Conference and Exhibition, Vienna.

Dunbar, J.A. and Sawyer, D.S., 1988. Continental rifting at pre-existing lithospheric weaknesses, Nature, v. 333, p. 450–452.

Dypvik, H., 1984. Geochemical compositions and depositional conditions of Upper Jurassic and Lower Cretaceous Yorkshire clays, England: Geological Magazine, v. 121, No. 5, p. 489-504.

Fedo C. M., Nesbitt, H. W. and Young, G. M., 1995. Unravelling the effects of K-metasomatism in sedimentary rocks and paleosols: Implications for Paleoweathering conditions and provenance, Geology, v. 23 p. 921-924.

Feistmantel, O., 1882. The flora of the Damuda and Panchet divisions, Pal. Indica, Geological Survey of India, Series, v. 12, p. 1-149.

Feng, R and Kerrich, R., 1990. Geochemistry of fine-grained clastic sediments in the Archean Abitibi greenstone belt, Canada: implications for provenance and tectonic setting. Geochimica et Cosmochimica Acta, v. 54, p. 1061-1081.

Fielding, C.R., Frank, T.D., Birgenheier, L.P., Rygel, M.C., Jones, A.T., Roberts, J., 2008a. Stratigraphic imprint of the Late Paleozoic Ice Age in eastern Australia: a record of alternating glacial and non-glacial climate regime. Journal of the Geological Society of London v. 165, p. 129–140.

Fielding, C.R., Frank, T.D., Birgenheier, L.P., Rygel, M.C., Jones, A.T., Roberts, J., 2008d. Stratigraphic record and facies associations of the late Paleozoic ice age in Eastern Australia (New South Wales and Queensland). In: Fielding, C.R., Frank, T.D., Isbell, J.L. (Eds.), Resolving the Late Paleozoic Ice Age in Time and Space: Geological Society of America Special Paper, v. 441, p. 41–57.

Fielding, C.R., Frank, T.D., Isbell, J.L., 2008b. The late Paleozoic ice age — a review of current understanding and synthesis of global climate patterns. In: Fielding, C.R., Frank, T.D., Isbell, J.L. (Eds.), Resolving the Late Paleozoic Ice Age in Time and Space: Geological Society of America Special Paper, v. 441, p. 343–354. Resolving the Late Paleozoic Ice Age in Time and Space. In: Fielding, C.R., Frank, T.D., Isbell, J.L. (Eds.), Geological Society of America Special Publication, 441. Boulder, CO.

Floyd, P.A. and Leveridge, B.E. 1987. Tectonic environment of Devonian Gramscatho basin, south Cornwall: framework mode and geochemical evidence from turbiditic sandstones. Journal of the Geological Society London, v.144, p. 531–542.

Folk, R. L. 1968. Bimodal Supermature Sandstones: Product of Desert Floor, Proceedings 23rd International Gondwana Congress, v. 8, p. 9-32.

Folk, R. L. 1980. Petrology of Sedimentary Rocks, Austin, Texas, Hemphill, p. 182.

Folkoff, M. E. 1983. Environmental control of the geography of secondary clay minerals in the A-horizon of United States soils. Ph.D. dissertation University of Georgia, Athens.

Folkoff, M.E and Meentemeyer, V, 1987. Climatic control of the Geography of clay minerals genesis, Annals of the Association of American Geographers, v. 77, No. 4, p. 635-650.

Fox, C. S., 1931. Coal in India-II. The Gondwana system and related Formations. Memoire of Geological Survey of India, v. 58, p. 1-241.

Fox, C. S., 1934. The Lower Gondwana coalfields of India, Memoire Geological Survey of India, v. 59, p. 1-386.

Frakes, L.A., Francis, J.E., 1998. A guide to Phanerozoic cold polar climates from high latitude ice-rafting in the Cretaceous. Nature, v. 333, p. 547–549.

Frakes, L.A., Francis, J.E., Syktus, J.I., 1992. Climate Modes for the Phanerozoic. Cambridge University Press, Cambridge. 274 p.

Garver, J.I., Royce, P.R. & Smick, T.A. 1996. Chromium and nickel in shale of the Taconic foreland: a case study for the provenance of fine-grained sediments

with an ultramafic source. Journal of Sedimentary Research, v. 66, p.100–106.

Ganju, P.N and Srivastava, V.K., 1959. Pebble fabric analysis of the Talchir boulder bed in the Jharia Coalfield, Bihar. Journal Geological Survey of India, v. 1, p. 105-115.

Ghose, N.C and Mukherjee, D., 2000. Chhotanagpur Gneissic Complex, Eastern India a kaleidoscope of global events. In: A.N. Trivedi, B.C. Sarkar, N.C. Ghose and Y.R.Dhar (Eds.), Geology and Mineral Resources of Bihar and Jharkhand, Platinum Jubilee Commemorative Volume, Indian School of Mines, Dhanbad, Institute of Geoexploration Environment Monographs 2, Patna, p. 33-58.

Ghose, N.C., 1983. Geology, tectonics and evolution of the Chhotanagpur Gneissic Complex, Eastern India. Recent Researches in Geology, v. 10, p. 211-247.

Ghose, N.C., 1992. Chhotanagpur Gneissic Complex, Eastern India, Present status and future prospect. Indian Journal of Geology, v. 64, No. 1, p.100-121.

Ghose, N.C., Mukherjee, D., and Chatterjee, N., 2005. Plume generated Mesoproterozoic mafic-ultramafic magmatism in the Chhotanagpur Mobile belt of Eastern Indian Shield Margin, Journal Geological Society of India, v. 66, No. 6, p. 725-740.

Ghosh, P., Bhattacharya, S.K., Dayal., A.M., Ebihara, M., Sarin, M.M and Chakrabarti, A., 2002a. Trace elements and isotopic studies of Permo-carboniferous carbonate nodules from Talchir sediments of peninsular India: Environmental and provenance implications. Proceedings Indian Academy of Science (Earth Planet Science), v. 111, No. 2, p. 87-101.

Ghosh, P.K and Basu, A., 1969. A note on the classification of the Lower Gondwanas of India Record. Geological Survey of India, v. 97, pt. 2, p. 168-171.

Ghosh, P.K and Mitra, N.D., 1975. History of Talchir sedimentation in Damodar valley Basins, Memoir Geological Survey of India, v. 105, 117 p.

Ghosh, S and Sarkar, S., 2010. Geochemistry of Permo-Triassic mudstone of the Satpura Gondwana basin, central India: Clues for provenance, Chemical Geology. v. 277, No. 1-2, p. 78 – 100.

Ghosh, S., 1954. Discovery of new locality of marine Gondwana formation near Manendragarh in Madhya Pradesh, Science cult, v. 19, 620 p.

Ghosh, S., Sarkar, S and Ghosh, P., 2012. Petrography and major element geochemistry of the Permo-Triassic sandstones, central India: Implications for provenance in an intracratonic pull-apart basin. Journal of Asian Earth Sciences, v. 43, No. 1, p. 207-240.

Gingele, F. X., 1996. Holocene climatic optimum in southwest Africa: Evidence from the marine clay mineral record, Palaeogeography, Palaeoclimatology, Palaeoecology, v. 122, p. 77–87.

Griffin, J., Windom, H and Goldberg, E .D., 1968. The distribution of clay minerals in the world ocean: Deep Sea Resources, v. 15, p. 433–459.

Grim, R.E., 1953. Clay Mineralogy, New York, Toronto London, McGraw Hill Book company INC.

Gulbranson, E.L., Montanez, I.P., Schmitz, M.D., Limarino, C.O., Isbell, J.L., Marenssi, S.A., Crowley, J.L., 2010. High-precision U–Pb calibration of Carboniferous glaciation and climate history, Paganzo Group, NW Argentina. Geological Society of America Bulletin, v. 122, p. 1480–1498.

Hallberg, R.O., 1976, A geochemical method for investigation of palaeoredox in southern Africa. Palaeogeography, Palaeoclimatology, Palaeoecology, v. 81, p. 49–57.

Harnois, L., 1988. The CIW index: a new Chemical Index of Weathering. Sedimentary Geology, v. 55, p. 319-322.

Harris, R.C and Adams, J.A.S., 1966. Geochemical and mineralogical studies on the weathering of granites rocks, American Journal of Science, v. 264, p. 146-173.

Hayashi, K., Fujisawa, H., Holland, H and Ohmoto, H., 1997. Geochemistry of ~ 1.9 Ga Sedimentary rocks from north eastern Labrador, Canada. Geochimica et Cosmochimica Acta, v. 61, p. 4115-4137.

Hiscott, C.N., 1984. Ophiolitic source rock for Tarconic age flysch: Trace element evidence, Geological Society of America Bulletin, v. 95, p. 1261-1267.

Holland, H.D, 1978. The Chemistry of the Atmosphere and Oceans, Wiley, New York, p. 351.

Holland, T. D, 1926. Indian geological terminology Gondwanaland and Gondwana system, Memoire Geological Survey of India, v. 32, p. 77-80.

Hughes, T.W.H., 1885. The southern coalfields of the Rewah Gondwana Basin: Umaria, Korar, Johila, Sohapur, Kurasia, Koreagarh, Jhilimili. Memoire of Geological Survey of India, v. 21, p.136-251.

Huyghe, P., Guilbaud, R., Bernet, M., Galy, A and Gajurel, A.P., 2011. Significance of the clay mineral distribution in fluvial sediments of Neogene to Recent Himalayan Foreland Basin (west-central Nepal), Basin Research, v. 23, No. 3, p. 332-345.

Hyde, W.T., Crowley, T.J., Tarasov, L., Paltier, W.R., 1999. The Pangean ice age: studies with a coupled climate ice sheet model. Climate Dynamics, v. 15, p. 619–62

Ingersoll, R. V., Bullard, T. F., Ford, R. L., Grimm, J. P., Pickle J. D and Sares, S. W. 1984. The Effect of Grain Size on Detrital Modes: A Test of the Gazzi-Dickinson Point Counting Method, Journal of Sedimentary Research, v. 54, No. 1, p. 103-106.

Isbell, J.L., Miller, M.F., Wolfe, K.L., Lenaker, P.A., 2003. Timing of late Paleozoic glaciation in Gondwana: was glaciation responsible for the development of northern hemisphere cyclothems? In: Chan, M.A., Archer, A.W. (Eds.), Extreme depositional environments: mega end members in geologic time: Geological Society of America Special Paper, v. 370, p. 5–24.

Islam, M.S.U., Chowdhury, K.R., Ishiga, H., 2004. Geochemistry of the Gondwana sedimentary rocks from the Barapukuria Basin, Bangladesh, Geosciences Journal, v. 10, p. 83–102.

Jha, N., 2006. Permian Palynology from India and Africa - A Phytogeographic Paradigm, Journal of Palaeontological Society of India, v. 51, No.1, p. 43 - 55.

Johnsson, M.J, 1993. The system controlling the composition of clastic sediments. In: Processes Controlling the Composition of Clastic Sediments (Eds M.J. Johnsson and A. Basu), Geological Society of America. Special Paper, v. 284, p. 1–19.

Johnsson, M.J., 1993. The system controlling the composition of clastic sediments. In: Johnsson, M.J., Basu, A. (Eds.), Processes Controlling the Composition of Clastic Sediments, Special Paper Geological Society of America, v. 284, p. 1 –19.

Johnsson, M.J., Stallard, R.F., and Meade, R.H., 1988. First cycle quartz arenites in the Orinoco River Basin, Venezuela and Colombia, Journal of Geology, v. 96, p. 263-277.

Jones, B., Manning, D.C., 1994. Comparison of geochemical indices used for the interpretation of paleo-redox conditions in Ancient mudstones: Chemical Geology, v. 111, No. 1-4, p. 111-129.

Kalisdekafle, L .S. N., Dolozim, M.B and Yureticrh, R., 1996. Distribution and origin of clay minerals in the sediments of Lake Malawi, HI Johnson, T.C., and Odada. E.O., eds. The Limnology. Climatology and Paleoclimatology of the East African Lakes: Amsterdam, Gordon & Breach, p. 443-460

Kalsbeek, F., 1971. The composition of sands from the Fiskeneasset region, South West Greenland, and its bearing on the bedrock geology of the area. Gronlands Geologiske Undersogelser. Rapport, v. 40, p. 12.

Kalsbeek, F., 1974. Sand analysis as a method of estimating bedrock compositions in Greenland. Gronlands Geologiske Undersogelser, Bulletin, v. 111, p. 32.

Khan, Z.A., 1978. Lithofacies, Sedimentation trends and Paleoflow characters of Karharbari and Barakar strata in East Bokaro Coalfield, Bihar. Unpublished Ph.D. thesis, A.M.U., Aligarh, 297 p.

Kittrick, J. A. 1977. Mineral equilibria. In Dixon and Weed, p. 1-25.

Krishnan, M. S., 1949. Geology of India and Burma. Higginbothoms (P) Ltd., Madras, 536 p.

Krishnan, M. S., 1982. Geology of India and Burma, CBS Publishers and Distributors, India, p. 536 eds. VI.

Kumar, A., 1984. Raniganj sedimentation in Damodar valley coalfield of Eastern India. Unpublished Ph.D. thesis, A.M.U., Aligarh.

Kutty, T.S., 1969. Some contributions to the stratigraphy of the Upper Gondwana Formations of the Pranhita-Godavari valley, Central India, Journal Geological Society of India, v. 10, p. 33-48.

Le maitre, R. W., 1976. The chemical variability of some common igneous rocks: Journal of Petrology, v. 17, p. 589-637.

Lindsey, D.A., 1999. An evaluation of alternative chemical classifications of sandstones. U.S.G.S. Open File Report 99-34, 23p.

Lopez-Gamundi, O.R., 1997. Glacial–postglacial transition in the late Paleozoic basins of Southern South America. In: Martini, I.P. (Ed.), Late Glacial and Postglacial Environmental Changes: Quaternary Carboniferous–Permian, and Proterozoic. Oxford University Press, Oxford U.K., p. 147–168.

Madhavaraju, J., and Ramasamy, S., 2002, Petrography and geochemistry of Late Maastrichtian - Early Paleocene sediments of Tiruchirapalli Cretaceous, Tamil Nadu - Paleoweathering and provenance implications: Journal of the Geological Society of India, v. 59, p. 133-142.

Maynard, J.B., Sutton, S.J., Robb, L.J., Ferraz, M.F., and Meyer, F.M., 1995. A paleosol developed on hydrothermally altered granite from the hinterland of the Witwatersrand basin: characteristics of a source basin fill. Journal of Geology, v.103, p. 357-377.

McLennan, S. M., 2001. Relationships between the trace element composition of sedimentary rocks and upper continental crust. Geochemistry Geophysics Geosystems, v. 2, p. 1525-2027.

McLennan, S. M., Hemming, S., McDaniel, D. K., and Hanson, G. N., 1993. Geochemical approaches to sedimentation, provenance, and tectonics, in Johnsson, M. J., and Basu, A., eds., Processes Controlling the composition

of clastics of sediments: Boulder, Colorado, Geological Society of America, special paper v. 284

McLennan, S.M., and Taylor, S.R., 1980, Rare earth element-thorium correlations in sedimentary rocks and the composition of the continental crust: Geochimica et Cosmochimica Acta, v. 44, p. 1833-1839

McLennan, S.M., and Taylor, S.R., 1991, Sedimentary rocks and crustal evolution: tectonic setting and secular trends: Journal of Geology, v. 99, p. 1-21.

McLennan, S.M., Fryer, B.J. and Young, G.M., 1979. The geochemistry of the carbonate rich Espanola Formation (Huronian) with emphasis on the rate earth elements. Canadian Journal of Earth Science, v.16, p. 230-239.

McLennan, S.M., Taylor, S.R., McCulloch, M.T., and Maynard, J.B., 1990, Geochemical and Nd-Sr isotopic composition of deep-sea turbidites: Crustal evolution and plate tectonic associations: Geochimica et Cosmochimica Acta, v. 54, p. 2015-2050.

Medlicott, H.B and Blandford, W.T., 1879. A manual of the geology of India, Chiefly complied from the observation of the Geological Survey of India, v. 1 and 2, p. 1-144, 445-817.

Meert, J.G. & Van der Voo, R., 1997. The assembly of Gondwana 800–550 Ma, Journal of Geodynamics, v. 23, p. 223–235,

Menking K, M., 1997. Climatic signals in clay mineralogy and grain size-variations in Owens lake core O L-92, southeast California, Geological Society of America, 317.

Mial, A.D., 1984. Principles of sedimentary basin analysis. Berlin, Sringer – Verlag, 490p.

Middleburg, J.J., Van der weijden, H and Woittiez, J.R.W, 1988. Chemical process affecting the mobility of major, minor and trace elements during weathering of granitic rocks, Chemical Geology, v. 68, p. 253-273.

Millot, G. 1970. Geology of Clays, (Farrand, W.R., and Paquet, H., trans.).Springer-Verlag New York.

Milodowski, A. E and Zalasiewicz, J. A., 1991. Redistribution of rare earth elements during diagenesis of turbidite/ hemipelagite mudrock sequences of Llandovery age from central Wales, in Mortan, A. C., Todd, S. P., and Haughton, P. W. D., eds., Development in Sedimentary Provenance studies, Geological society of London, special Publication, v. 57, p. 101 – 124.

Mitra, N.D., 1972. Depositional conditions of the Panchet sediments of the Damodar valley area and their bearing on the classification of the Gondwana, Record Geological Survey of India, v. 99, p. 165-170.

Montanez, I.P., Tabor, N.J., Niemeier, D., DiMiichele, W.A., Frank, T.D., Fielding, C.R., Isbell, J.L., Birgenheier, L.P., Rygel, M.C., 2007. CO_2 forced climate and vegetation instability during late Paleozoic deglaciation. Science, v. 315, p. 87–91.

Moore, D. M., and Reynolds, R. C., Jr., 1997. X-ray diffraction and the identification and analysis of clay minerals: second edition, New York, Oxford University Press, 332 p.

Mukhopadhyay, G. and Bhattacharya, H. N., 1994. Facies Analysis of Talchir Sediments (Permo-Carboniferous), Dudhi Nala, Bihar, India—A Glaciomarine Model, IXth Inter- national Gondwana Symposium, Oxford and IBH Publication, New Delhi, v. 2, p. 737-753.

Mukhopadhyay, G., Mukhopadhyay, S. K., Roychowdhury, M. and Parui, P. K., 2010. Stratigraphic Correlation between Different Gondwana Basins of India, Journal of Geological Society of India, v. 76, p. 251-266.

Nadeau, P. H., and Reynolds, R. C., Jr. 1981. Volcanic components in pelitic sediments, Nature, v. 294, p. 72-74.

Nath, B.N., Bau, M., Ramalingeswara Rao, B., Rao, Ch. M., 1997. Trace and rare earth elemental variation in Arabian Sea sediments through a transect across the oxygen minimum zone: Geochimica et Cosmochimica Acta, v. 61, No. 12, p. 2375-2388.

Nesbitt, H. W., 1979. Mobility and fractionation of rare earth elements during weathering of granodiorites, Nature, v. 279, p. 206 – 210.

Nesbitt, H. W., MacRae, N. D and Kronberg, B. I., 1990. Amazon deep sea fan muds: light REE enriched products of extreme chemical weathering, Earth Planets Science Letters, v. 100, p. 118 -123.

Nesbitt, H.W., Young, G.M., 1982. Early Proterozoic climates and plate motions inferred from major element chemistry of lutites, Nature, v. 299, p.715–717.

Nesbitt, H.W., Young, G.M., 1984. Prediction of some weathering trends of plutonic and volcanic rocks based on thermodynamic and kinetic considerations. Geochimica et Cosmochimica Acta, v. 48, p. 1523–1534.

Pandey, J and Dave, A., 1998. Stratigraphy of Indian Petroliferous basins. XVI Indian Colloq. Micropaleontology Stratigraphy, National Institute of Oceanography, Dona Paula, Goa, 248 p.

Pascoe, E.H., 1968. A manual of Geology of India and Burma. Govt of India press, Calcutta, v. 2, p. 485-1343.

Pettijohn, F. J., Potter, P. E. and Siever, R. 1972. Sand and Sandstone, Springer-Verlag, Berlin, p. 241.

Pettijohn, F.J., 1975. Sedimentary Rocks, Third edition, Harper and Row, New York, p. 628.

Pfefferkorn, H.W., Gastaldo, R.A., Dimichele, W.A., Philips, T.L., 2008. Pennsylvanian tropical floras from the United States as a record of changing climate. In: Fielding, C.R., Frank, T.D., Isbell, J.L. (Eds.), Resolving the late Paleozoic ice age in time and space: Geological Society of America Special Paper, 441, pp. 305–316.

Qidwai, H.A., 1972. Lower Gondwana Sedimentation in the Pench valley Coalfield, M.P. Ph.D. thesis, A.M.U., Aligarh, 311 p.

Radhakrishna, B.P., 1991. Indian Gondwana, Geological Society of India, Bangalore.

Rai, D. and Lindsay, W. L. 1975. A thermodynamic model for predicting the formation, stability and weathering of common soil minerals. Soil Science Society of America Proceedings 32:443-44.

Rais, S., 1985. Stratigraphy and sedimentation of the Talchir Group, south of Ambikapur, district Sarguja (Madhya Pradesh). Unpublished Ph.D thesis, A.M.U

Rais, S., 1997. Talchir glacigenic sedimentation (Late Carboniferous) in Gungatta river section of the Son-Mahanadi Gondwana Basin, sarguja district, Madhya Pradesh, India. Bulletin Indian Geological Association, v. 30, No. 1-2, p. 21-29.

Ramakrishnan, M., and Vaidyanadhan, R., 2008. Geology of India, Geological Society of India, v. 2, p. 959, Bangalore.

Ramanamurthy, B.V., 1985. Gondwana sedimentation in Ramagundam-Mantheni area, Godavari valley Basin, Journal of Geological Society of India, v. 26, p. 43-55.

Ranjan, R., Banerjee, R., Shrivastava, V.K., Majumdar, A., Roy, M.K. and Maithani, P.B, June, 2012. Sedimentological and Geochemical Studies of Lower Gondwana Sediments in parts of Pench-Kanhan Sub-basin, Satpura Gondwana Basin, Chhindwara District, Madhya Pradesh: Implication for Uranium Mineralisation Gondwana Geological Magazine v. 27, No.1,

Rao, D.V., Rao, S.M.V and Balaram, V., 1994. Trace and Rare earth element abundances in Athgarh and Talchir sediments: Implications for provenance and processes. 9th international Gondwana symposium, Hyderabad, India, p. 10-14.

Rizvi, S.R.A., 1972. Geology and Sedimentation trends in Palamau coalfields, Bihar, India. Memoir Geological Survey of India, v. 104, 108 p.

Robinson, P.L., 1967. The Indian Gondwana formations-A review. International Union of Geological sciences, Bueons Aires, UNESCO, p. 201-268.

Rollinson, H.R., 1993. Using Geochemical Data: Evaluation, Presentation Interpretation. Longman Scientific and Technical, New York.

Roser, B.P and Korsch, R.J., 1986. Determination of tectonic setting of sandstone suites using SiO_2 content and K_2O/Na_2O ratio. Journal of Geology, v. 67, p. 119-139.

Roser, B.P and Korsch, R.J., 1988. Provenance signatures of sandstone-mudstone suites determined using discrimination function analysis of major-element data. Chemical Geology, v. 37, p. 119-139.

Roy, A., Ramchandra, H. M. and Bandyopadhyay, B. K. 2000. Supracrustal Belts and their Significance in the Crustal Evolution of Central India. Proceedings Dr. M.S Krishnan Birth Century, Seminar, Geological Survey of India, Special. Publication, No. 55, p. 361-380.

Roychowdhury, M.K., Sastry, M.U.A., Shah, S.C., Singh, G and Ghosh, S.C., 1973. Triassic floras in India. In K.S.W. Campbell (Ed.), Gondwana Geology, 3rd International Gondwana Symposium, Australia National University Press, Canberra, p. 149-159.

Rudnick, R. L and Gao, S. 2003. Composition of the Continental Crust, Treatise on Geochemistry, v. 3, p. 1-64, Elsevier.

Sageman, B. B and Lyons, T. W., 2005. Geochemistry of fine-grained sediments and sedimentary rocks, 'Sediments, Diagenesis, and Sedimentary Rocks' Treatise on Geochemistry, Second Edition, v. 7, p. 115-158, Elsevier, New York.

Scheffler, K., Hoernes, S., Schwark, L., 2003. Global changes during Carboniferous– Permian glaciations of Gondwana: linking polar and equatorial climate evolution by geochemical proxies. Geology, v. 31, p. 605–608.

Scotese, C.R., 1997. The paleomap Project: paleogeographic atlas and plate tectonic software, Department of Geology, university of Texas, TX.

Sengupta, S., 1970. Gondwana sedimentation around Bheemaram, Pranhita-Godavari valley, India Journal of Sedimentary Petrology, v. 40, p. 140-170.

Shaw, T.J., Geiskes, J.M., Jahnke, R.A., 1990. Early diagenesis in differing depositional environments: the response of transition metals in pore water: Geochimica et Cosmochimica Acta, v. 54, No. 5, p. 1233-1246.

Singh, B., Swarnapriya, C and Rao, B. N., 2013. Structures and tectonics of Son-Mahanadi rift basin, India derived from joint interpretation of gravity and magnetic data incorporating constraints from borehole and seismic

information. 10th Biennial International Conference & Exploration, CSIR-NGRI, Uppal Road, Hyderabad. P. 409

Skilbeck, C.G., Cawood, P.A., 1994. Provenance history of a Carboniferous Gondwana margin forearc basin, New England Fold Belt, eastern Australia: modal and geochemical constraints. Sedimentary Geology, v. 93, p. 107–133.

Srivastava, V.K and Israili, S. H., 1968. Bearing of heavy mineral studies on the position of the Karharbari beds in the Daltonganj coalfield, Bihar, coalfield of Paleontology society of India, v. 11, p. 20-25.

Stopperps, P. and Heckyr, .E., 1978. Late Pleistocene-Holocene evolution of the Kin-Tanganyika Basin, in Matter, A. and Tucker, M.E., eds., Modern and Ancient Lake Sediments: International Association of Sedimentologists, Special Publication 2, p. 43-55.

Suess, E., 1885. Das Antlitz der Erde, Band I, p. 768 (The Face of the Earth)

Suttner, L.J and Dutta, P.K., 1986. Alluvial sandstone composition and Paleoclimate, I Framework Mineralogy Journal of sedimentary petrology, v. 56, No.3 p 329-345.

Tabor, N.J., Montanez, I.P., Scotese, C.R., Poulsen, C.J., Mack, G.H., 2008. Paleosol archives of environmental and climatic history in paleotropical western Pangea during the latest Pennsylvanian through Early Permian. In: Fielding, C.R., Frank, T.D., Isbell, J.L. (Eds.), Resolving the Late Paleozoic Ice Age in Time and Space: Geological Society of America Special Paper, 441, p. 291–303.

Taylor S. R. and McLennan S. M., 1985. The Continental Crust: Its Composition and Evolution. Blackwell, Oxford. 321p.

Tewari, R. C. and Casshayap, S. M., 1982. Palaeoflow Analysis of Late Paleozoic Gondwana Deposits of Giridih and Adjoining Basins and Paleogeographic Implications, Geological Society of India, v. 23, No. 2, p 67- 79.

Tewari, R.C. and Veevers, J.J., 1993. Gondwana basins of India occupy the middle of a 7500km sector of radial valleys and lobes in central-eastern Gondwana. Gondwana Eight, Balkema, Rotterdam, p. 507-512.

Tewari, R. C., 1998. Channel sandstone bodies in fluvial Permian–Triassic Gondwana succession of peninsular India; Journal of Geological Society of India, v. 51, p. 747–754

Tewari, R. C., 1999. Sedimentary-Tectonic Status of Permian- Triassic Boundary (250Ma) in Gondwana Stratigraphy of Peninsular India. Gondwana Research, v. 2, No. 2, p. 185-189.

Tewari, R.C and Maejima, W., 2010a. Origin of Gondwana basins of Peninsular India. Journal of Geosciences, v. 53, Art. 3, p. 43- 49. Osaka City University.

Tewari, R.C., 1980. Lithofacies, Sedimentary petrology and Paleogeography of Gondwana lithicfill of Giridhi and adjoining coalfields, Bihar, Unpublished, Ph.D. thesis, A.M.U., Aligarh.

Thamban. M., Rao, V.P and Schneider, R.R., 2002. Reconstruction of late Quaternary monsoon oscillations based on clay mineral proxies using sediment cores from the western margin of India. Marine Geology, v. 186, p. 527-539.

Thiry, M., 2000. Palaeoclimatic interpretation of clay minerals in marine deposits: an outlook from the continental origin. Earth Science Review, v. 49, p. 201-221.

Van De Kamp, P., 2010. Arkose, Subarkose, Quartz sand, and associated muds derived from felsic plutonic rocks in glacial to tropical humid climate. Journal of sedimentary Research, v. 80, p. 895-918.

Veevers, J. J. and Tewari, R.C. 1995. Gondwana Master Basin of Peninsular India between Tethys and the Interior of the Gondwanaland Province of Pangea, Memoire of the Geological Society of America, No. 187, p. 1-73.

Veevers, J.J., Powell, M., 1987. Late Paleozoic glacial episodes in Gondwanaland reflected in transgressive–regressive depositional sequences in Euro-America Geological Society of America Bulletin, v. 98, p. 475–487.

Visser, J.N.J., Young, G.M., 1990. Major element geochemistry and paleoclimatology of the Permo-Carboniferous glacigene Dwyka Formation

and postglacial mudrocks in southern Africa. Palaeogeography, Palaeoclimatology, Palaeoecology, v. 81, p. 49–57.

Von Eynatten H, barcelo-vidal, C, and Pawlowsky-glahn, V., 2003. Composition and discrimination of sandstones: a statistical evaluation of different analytical methods. Journal of sedimentary research, v. 73, No. 1, p. 47–57.

Vredenburg, E., 1914. The Classification of the Gondwana System, Proceeding Ist session, Indian Science Congress, pt 3.

Wadia, D.N., 1926. Geology of India, Macmillan Publishers., London, p. 536.

Walker, R. G., 1967. Colour of Recent Sediments in Tropical Mexico: A Contribution to the Origin of Red Beds, Geological Society of America Bulletin, v. 78, No. 7, p. 917-920.

Weltje, G.J and Von Eynatten, H 2004. Quantitative provenance analysis of sediments review and outlook, Sedimentary Geology, v. 171, p. 1-11.

White, W. M., 2013. Geochemistry, Wiley-Blackwell; edition (1).

Wronkiewicz, D.J and Condie, K.C., 1987. Geochemistry of Archean shales from Witwatersrand supergroup, South Africa: source area weathering and provenance. Geochimica et Cosmochimica Acta, v. 51, p. 67-78.

Wronkiewicz, D.J. and Condie, K.C., 1989. Geochemistry and provenance of sediments from the Pongola Supergroup, South Africa: evidence for a 3.0 Ga-old continental craton. Geochimica Cosmochimica Acta, v. 53, p. 1537-1549.

Yang, J., Cawood, P.A., Du, Y., Feng, B., and Yan, J., 2014. Global continental weathering trends across the early Permian glacial to Post glacial transition, correlating high and low paleolatitudes sedimentary recordes, Geology, The Geological Society of America, v. 42, No. 10, p. 835-838.

Zeng, J., Cao, C.Q., Davydov, V.I., Shen, S.Z., 2012. Carbon isotope chemostratigraphy and implications of palaeoclimatic changes during the Cisuralian (early Permian) in the southern Urals, Russia. Gondwana Research, v. 21, p. 601–610.

Ziegler, A.M., Hulver, M.L., Rowley, D.B., 1997. Permian World topography and climate. In: Martini, I.P. (Ed.), Late Glacial and Postglacial Environmental Changes: Quaternary Carboniferous–Permian, and Proterozoic. Oxford University Press, Oxford, U.K., p. 111–146.

Zimmermann, U and Bahlburg, H., 2003. Provenance analysis and tectonic setting of the Ordovician clastic deposits in the southern Puna Basin, NW Argentina. Sedimentology, v. 50, p. 1079–1104.

PUBLICATIONS

International Journal of Geosciences, 2014, 5, 122-130
Published Online January 2014 (http://www.scirp.org/journal/ijg)
http://dx.doi.org/10.4236/ijg.2014.51013

Scientific Research

Provenance, Tectonics and Paleoclimate of Permo-Carboniferous Talchir Formation in Son-Mahanadi Basin, Central India with Special Reference to Chirimiri: Using Petrographical Interpretation

Khansa Zaidi[1*], Sarwar Rais[1], Abdullah Khan[1], Mohd Masroor Alam[2]
[1]Department of Geology, Aligarh Muslim University, Aligarh, India
[2]Department of Civil Engineering, Aligarh Muslim University, Aligarh, India
Email: *khansa.scholar@gmail.com, raissarwar56@gmail.com

Received October 28, 2013; revised November 29, 2013; accepted December 24, 2013

ABSTRACT

The present study deals with the petrographic interpretation of Talchir Formation sandstone, in and around Chirimiri area, Koriya district, Chhattisgarh state India located in Son-Mahanadi basin. This basin is an elongate graben showing northwest-southeast trend and considered to be one of the largest intra-cratonic rift basins of Indian peninsula. Talchir Formation is the lowermost unit of thick classical Gondwana sedimentary succession and rests unconformably on Precambrian basement. The petrographic studies consisting of point count show the presence of quartz as a dominant framework mineral with subordinate amounts of feldspars and rock fragments. The data plot in the fields of cratonic interior and transitional margin of continental block provenance. In the Qt (quartz)-F (feldspar)-L (lithic fragments) triangular diagram, indicating the source of these sediments was located in transitional margin and continental block provenance. The petrographic classification suggests that this formation in the study area dominantly contains compositionally immature to submature arkosic, sub-arkosic and lithic-arkosic sandstones. The bivariate plot between Qp/(F+R) vs. Qt/(F+R) indicates changes in climatic conditions from semi-arid to semi-humid during Permo-Carboniferous period.

KEYWORDS

Son-Mahanadi; Talchir Formation; Chirimiri; Provenance; Tectonics; Petrography; Paleoclimate

1. Introduction

The compositions of sandstone have been widely used by sedimentologists during past several decades to decipher the provenance, paleoclimate and tectonic setting of the source areas [1-9]. The characters of detrital framework grains are substantially affected by the nature of processes that act in the depositional basin and also by the type of transporting medium and distance of transport [8,10]. Determination of different aspects of provenance viz its location with respect to depositional basin, lithology, climate and tectonic setting is some of the important parameters of basin analysis [11].

The Gondwana sediments of Peninsular India mark the resumption of sedimentation during Permo-Carboniferous after a long hiatus since Proterozoic. The sedimentation in Gondwana basins of India evolved through a complex interplay of faulting, changes in sea level and climate [12]. The basinal geometry was modified by tectonic movement during different periods. Indian plate is an assembly of several micro continents, sutured along early/middle Proterozoic Mobile belts [13-15]. These mobile belts became the locales of rift nucleation and played a fundamental role in the mechanism of rift propagation along reactivated ancient shear zones [15-18]. These intra-cratonic rifts are referred to as Gondwana basins.

*Corresponding author.

The Gondwana basins are linearly arranged along the present day river valleys viz. Koel-Damodar, Son-Mahanadi and Pranhita-Godavari (Figure 1(b)). The sediments are mostly made up of clastics of glacial and glacigene rocks at the base followed by coal measures and red beds at the top [19]. The Talchir Formation, the lowermost member of Gondwana sequence of India, is suggested to be of glacial, glacio-fluvial, glacio-lacustrine and/or glacio-marine depositional environment [20-32]. The Talchir Formation is marked by uniformly deposited olive green sandstone, conglomerate, thinly laminated shales, siltstone, and varves with typical glacigene facies tillite mostly at the base.

The present study is based on modal analysis of

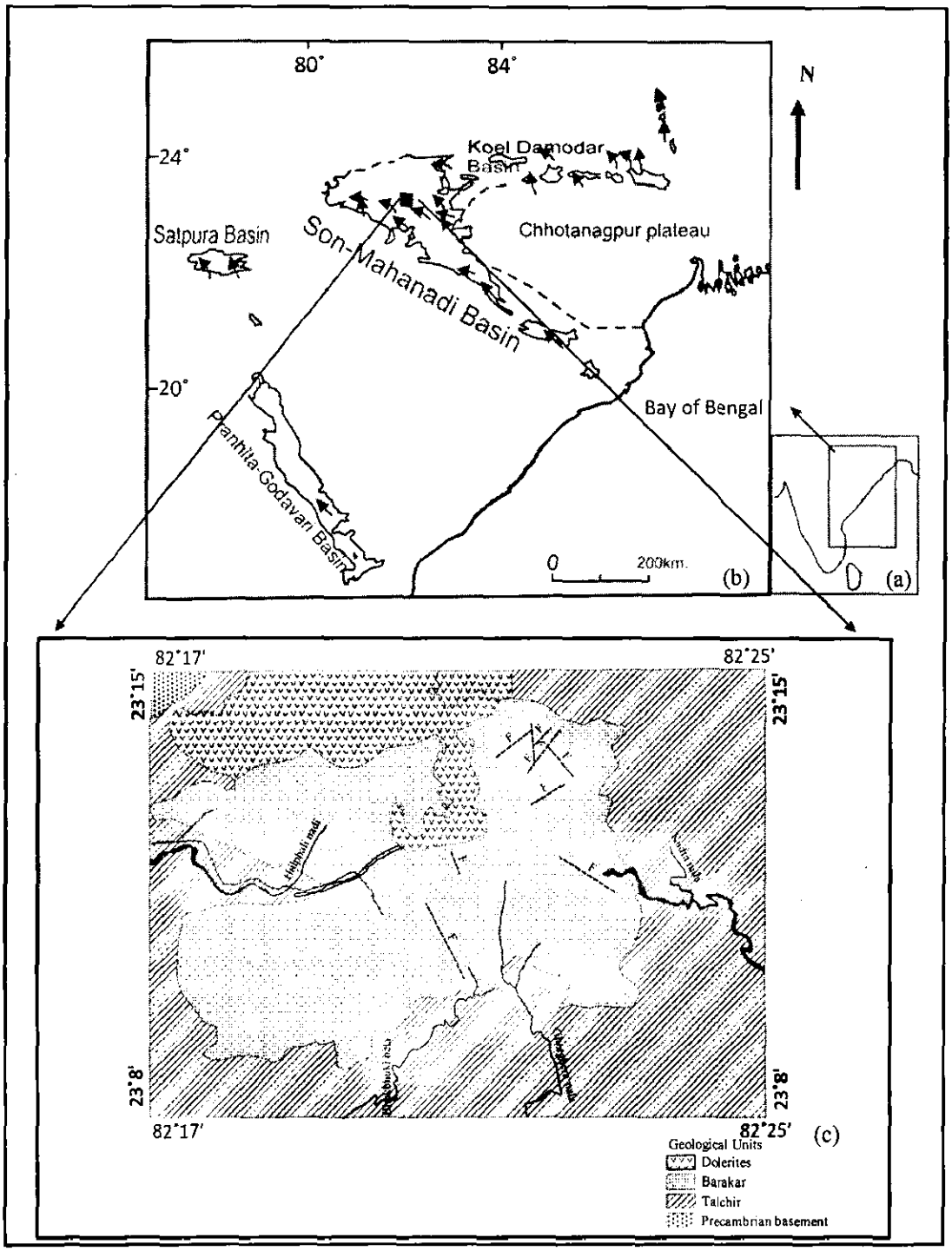

Figure 1. (a) Map of India shown inset; (b) The outline map of Peninsular India showing Gondwana basins and paleohighlands. Arrows indicate direction of Permian-Triassic paleoslope modified by Tewari and Veevers, 1993; (c) Map showing study area modified after Raja Rao 1983.

sandstones of Talchir Formation of Chirimiri, Koriya district, Chhattisgarh state, located in Son-Mahanadi basin (**Figure 1(c)**). The aim of the study is to interpret the possible provenance, tectonic setting and paleoclimate variability that led to the deposition of these sandstones during Permo-Carboniferous period.

2. Geological Setting

The Chirimiri coalfield, the study area, is a part of Son-Mahanadi basin falls between latitudes 23°8'N to 23°15'N and longitudes 82°17'E to 82°25'E. Talchir Formation is exposed along streams flowing in the vicinity of Chirimiri town. Olive green, thinly laminated shales and medium grained sandstone succeeded by lemon yellow alternate beds of shale and sandstones are found exposed in this area. The Chirimiri area was surveyed by C.S Raja Rao and stratigraphic succession was proposed (**Table 1**) [33].

The Son-Mahanadi graben is one of the largest intracratonic rift basins of peninsular India. The Mahakoshal supracrustal lie in the north of Son-Mahanadi Gondwana basin. The rocks of Sausar mobile belt and Betul supracrustals are exposed in the south, whereas the eastern and south eastern fringes of the Son-Mahanadi basin are constituted by granite-gneissic complex of Chotanagpur terrain and Precambrian rocks of Singhbhum and Bastar craton respectively [34]. To the west of the basin unclassified Precambrian migmatites and geneisses are exposed. Tectonically, the basin has been divided into three blocks *i.e.*, Son, Hasdo-Arand and Mahanadi separated from each other by ENE-WSW trending prominent basement ridge [35]. Spatial distribution of rock units, variation in the thickness of sediments, different disposition of structural elements and contrasting lineament-trends of these three blocks suggest that each underwent a different sedimentation and tectonic history [35].

3. Material and Methods

The current study deals with petrographic interpretations of Talchir sandstones in Chirimiri area. 50 Talchir sandstone samples have been collected along the stream cuttings in and around Chirimiri, where they are found exposed. The streams from where these samples have been collected are Halphali, Kudra, Bhukbhuki, and Ghorghera (**Figure 1(c)**). Out of these 50, only 29 representative samples of sandstone were selected for petrographic studies. Thin sections of the selected samples were prepared by standard technique. Modal analysis of samples was carried out using point counting method to determine the quantitative mineralogical aspects of these sandstones. About 350 points per thin section were counted (**Table 2**) using Gazzi-Dickenson's method [36]. The counted grains were recalculated into percentage as summarised in (**Table 3**).

Table 1. Stratigraphic succession of Chirimiri, coalfield Koriya district, Chhattisgarh (Raja Rao, 1983).

Age	Formation	Lithology
Upper Cretaceous to lower Eocene (?)	Deccan Traps	Basic flows, dykes and sills.
Lower Permian	Barakar	Essentially sandstone with subordinate Shales and coal seams (230 m to 435 m).
Upper Carboniferous to Early Permian	Talchir	Predominantly olive green shales and Medium to fine grained sandstone.
	UNCONFORMITY	
Precambrian basement		Granite, Gniesses and Quartzite

Table 2. Key for petrographic and other parameters used in this study (modified after Dickinson 1985).

	QFR
Q	Total Quartz grains (Qm + Qp)
Qm	monocrystalline quartz
Qp	polycrystalline quartz
F	Total Feldspar (P + K)
P	Plagioclase
K	alkali feldspar
R	Total rock fragments including chert
	QtFL
Qt	Total quartz grains (Qm + Qp)
Qm	monocrystalline quartz
Qp	polycrystalline quartz
F	Total Feldspar (P + K)
P	Plagioclase
K	alkali feldspar
L	Total lithic fragments
	QmFLt
Qm	monocrystalline quartz
F	Total Feldspar (P + K)
P	Plagioclase
K	alkali feldspar
Lt	Total rock fragments including polycrystalline quartz
	QpLvLs
Qp	polycrystalline quartz
Lv	Total volcanic and Meta-volcanic rock fragments
Ls	Total sedimentary rock fragments
	LmLvLs
Lm	Total metamorphic rock fragments
Lv	Total volcanic rock fragments
Ls	Total sedimentary rock fragments
	Qp/F + RF vs. Qt/F + RF
Qt	Total quartz grains (Qm + Qp)
Qm	monocrystalline quartz
Qp	polycrystalline quartz
F	Total Feldspar (P + K)
RF	Total rock fragments

Table 3. Recalculated detrital composition of Talchir sandstones of Chirimiri area, Koriya district.

S.No	QFR			QtFL			QmFLt			QpLvLs			Qp/(F + R)	Qt/(F + R)	QmPK		
	Q	F	R	Qt	F	L	Qm	F	Lt	Qp	Lv	Ls			Qm	P	K
NT1	71.23	16.44	12.33	60.46	38.37	1.17	71.23	16.44	12.33	0	0	100	0.11	1.52	60.47	0	39.55
NT2	70.42	15.49	14.08	57.89	40.35	1.76	70.42	15.49	14.08	0	0	100	0.21	1.37	56.90	0	43.1
NT3	69.62	18.99	11.39	52.40	43.26	4.34	69.62	18.99	11.39	0	0	100	0.25	1.1	55	15	30
NT5	61.54	19.23	19.23	55.26	39.48	5.26	61.54	19.23	19.23	0	0	100	0.21	1.23	58.33	5.55	36.12
NT7	67.57	18.92	13.51	54.17	29.17	16.7	67.57	18.92	13.51	0	0	100	0.13	1.18	65	0	35
NT8	91.67	4.86	3.47	68.94	28.43	2.63	91.67	4.86	3.47	66.66	0	33.34	0.03	1.38	70.49	4.26	25.25
NT9	80.13	16.03	3.85	68.57	24.58	6.85	80.13	16.03	3.85	0	0	100	0.17	1.55	73.61	2.47	23.92
NT10	73.53	13.24	13.24	76.36	23.64	0	73.53	13.24	13.24	0	0	0	0.12	1.55	76.36	1.81	21.83
NT12	71.11	22.22	6.67	58.1	37.4	4.5	71.11	22.22	6.67	0	0	0	0.06	1.56	60	7.5	32.5
NT13	70.71	20.20	9.09	83.54	16.46	0	70.71	20.20	9.09	0	0	0	0.11	1.56	85.71	1.3	12.99
NT14	71.43	23.81	4.76	62.92	35.96	1.12	71.43	23.81	4.76	33.33	0	66.67	0.26	1.64	63.64	0	36.36
GN1	73.36	18.22	8.41	77.38	17.86	4.76	54.55	27.27	18.18	70	0	30	0.28	2.05	66.66	4.44	28.9
GN2	64.10	25.00	10.90	72.12	21.15	6.73	67.31	21.15	11.54	45.5	0	54.5	0.16	1.54	76	3	21
GN3	67.57	21.62	10.81	69.70	24.24	6.06	69.70	24.24	6.06	0	0	100	0.23	1.68	74.2	3.22	22.58
GN4	61.74	26.85	11.41	61.90	29.25	8.84	60.54	29.25	10.20	13.33	0	86.67	0.03	1.62	67.42	3.02	29.56
GN5	84.52	11.90	3.57	77.65	20.00	2.35	77.65	20.00	2.35	0	0	100	0.2	0.91	79.53	8.43	12.04
GN6	74.65	14.08	11.27	74.20	17.35	8.45	67.74	17.74	14.52	33.33	0	66.67	0.17	2	79.24	0	20.76
GN7	76.11	19.44	4.44	68.75	27.60	3.65	62.50	27.60	9.90	66.67	16.7	16.67	0.21	1.05	69.38	9.82	20.8
GN8	79.40	16.08	4.52	78.61	18.41	2.99	64.68	18.41	16.92	80.02	11.4	8.57	0.7	1.95	77.84	1.2	20.96
GN9	79.14	10.07	10.79	63.16	29.47	7.37	56.00	32.00	12.00	44.44	0	55.56	0.16	1.69	65.85	3.04	31.11
GN10	71.64	22.39	5.97	70.78	26.23	2.99	68.81	26.24	4.95	40	10	50	0.06	1..46	72.39	2.6	25.01
GN11	82.05	11.11	6.84	87.27	10.91	1.82	82.50	10.00	7.50	80	0	20	0.15	1.92	87.27	2	10.73
BK1	71.43	14.29	14.29	49.25	42.25	8.50	45.54	43.56	10.90	0	14.29	85.71	0.11	0.83	51	0	49
BK3	59.70	22.39	17.91	53.00	44.00	3.00	52.11	45.07	2.82	100	0	0	0.05	1.14	53.62	0	46.38
BK4	63.37	28.71	7.92	70.00	24.00	6.00	53.33	26.67	20.00	100	0	0	0.05	1.43	42.3	3.84	53.86
BK5	51.28	25.64	23.08	41.00	53.00	6.00	39.64	54.05	6.31	0	33.33	66.67	0.17	1.17	45.5	0	54.5
BK6	73.96	20.71	5.33	38.89	55.56	5.56	38.89	55.56	5.55	100	0	0	0.35	0.63	63.69	10.71	25.6
BK7	77.92	10.39	11.69	63.32	33.67	3.02	60.80	38.07	1.13	90	0	10	0.26	1.72	66.66	16.66	16.68
KN3	74.11	14.29	11.61	56.62	40.44	2.94	56.92	42.31	0.77	75	0	25	0.03	1.3	57.37	0	42.63

. Petrography

hese sandstones are predominantly coarse to medium rained. Quartz is the chief component of these thin sections. It occurs in three varieties, monocrystalline, polycrystalline, and stretched (**Plates 1(a) and (b)**), the percentage of quartz ranges from 38.89 to 83.54 percent. he mono-crystalline quartz has both straight to slightly undulatory extinction with angular to subrounded grains. etrital feldspar comes next to quartz, followed by rock agments. Feldspar form 10.9 to 55.56 percent in these ndstones followed by rock fragments which range from 3.47 to 23.08 percent. Three varieties of feldspar, that is, orthoclase, plagioclase and microcline have been recorded in these sandstones (**Plates 1(c)-(e)**). Feldspar grains are fresh, coarse to medium in size and sub rounded in shape. Some feldspar grains also exhibits slight alteration (**Plate 1(d)**). Orthoclase is more abundant than rest of the feldspar varieties. Heavy minerals observed in these thin sections include zircon, rutile, garnet and epidote, along with rock fragments of granite/gneiss, schist (**Plate 1(g)**), chert, shale and siltstone. Clay matrix is the common binding material present, along

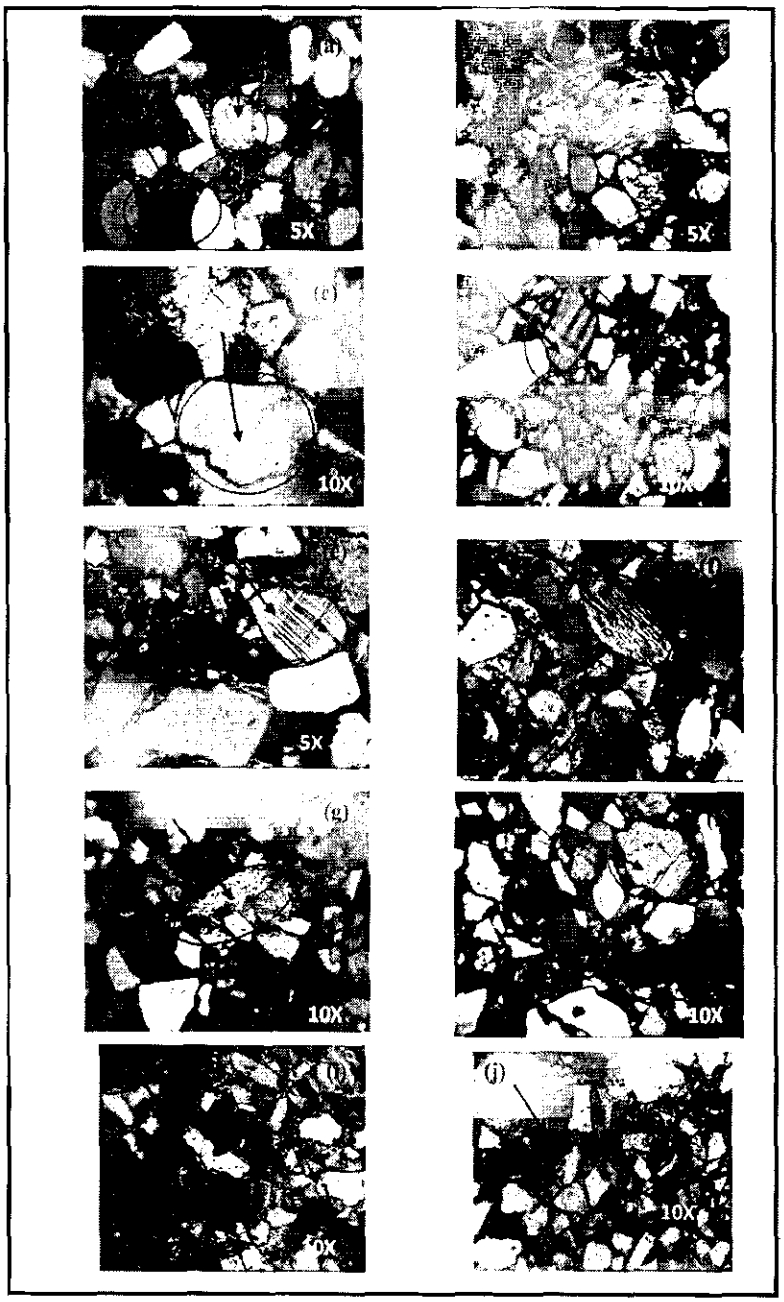

Plate 1. (a) Photomicrographs of Talchir Formation of Chirimiri area, Koriya district, Chhattisgarh, arrows showing monocrystalline quartz grains and polycrystalline quartz; (b) Stretched quartz; (c) Orthoclase grain showing iron staining; (d) Plagioclase grain slightly altered; (e) Microcline grain; (f) Perthite grain; (g) Schist fragment; (h) Plagioclase grain with inclusion of quartz; (i) Pore filling clay matrix; (j) Undifferentiated matrix (black in colour) and Iron cement (black arrow).

with ferruginous cement occurring at the edges of the grain or in small patches. Pore filling matrix is also common in these sandstones of Talchir Formation (**Plate 1(i)**) Undifferentiated matrix (**Plate 1(j)**) and few patches of calcite cement have also been encountered in framework of some of these studied samples.

The studied Talchir sandstone specimens of Chirimiri area have been classified according to Folk's classification [37] into three categories viz arkose, subarkose, and lithic arkose (**Figure 2**).

5. Provenance, Tectonic Setting and Paleoclimate

The studied sandstones of Talchir Formation, Chirimiri area have been plotted in QtFL diagram (**Figure 3(a)**), where most of the samples concentrate on continental block provenance and recycled orogen. QmFLt ternary plot also shows the same result (**Figure 3(b)**). The QmPK plot (**Figure 4(a)**) of the studied samples shows that these Talchir sandstones have been derived from continental block provenance. The QpLvLs (**Figure 4(b)**)

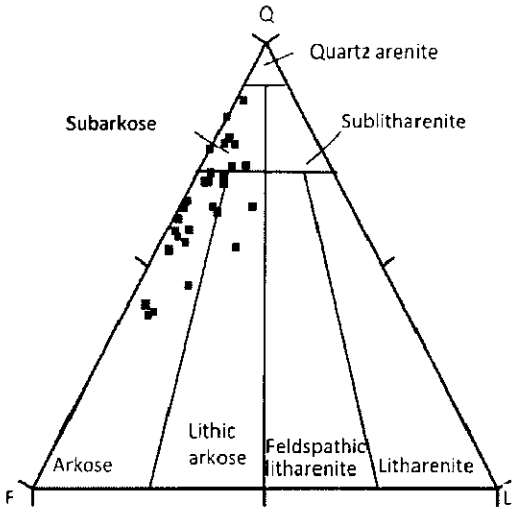

igure 2. **Classification of Talchir sandstone, Chirimiri area, oriya district, Chhattisgarh (after Folk, 1980).**

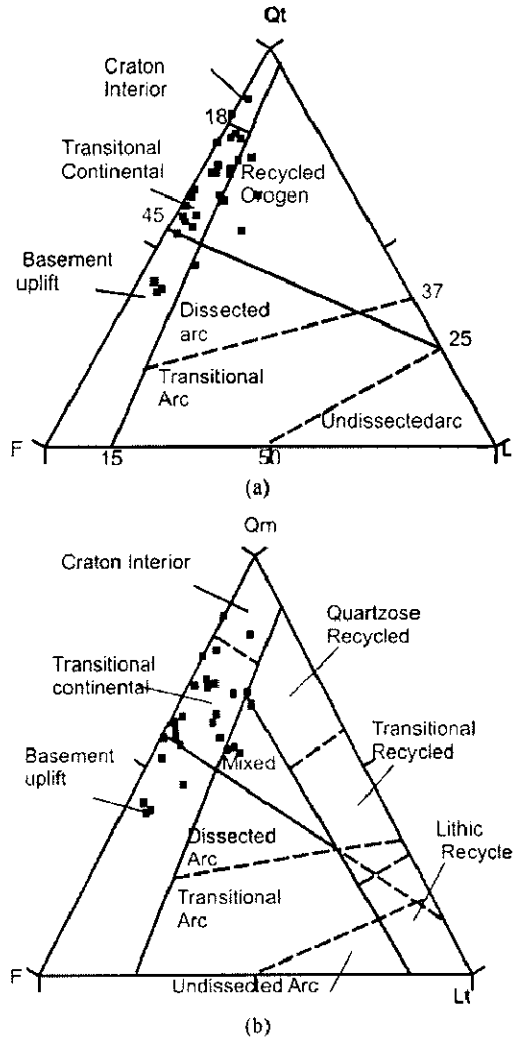

igure 3. **(a) Triangular diagram QtFL of Talchir sand-ones, Chirimiri, Koriya for Provenance (after Dickinson *et l.*, 1985). (b) Triangular diagram QmFLt of Talchir sand-ones, Chirimiri. Koriya for Provenance (after Dickinson *et l.*, 1985).**

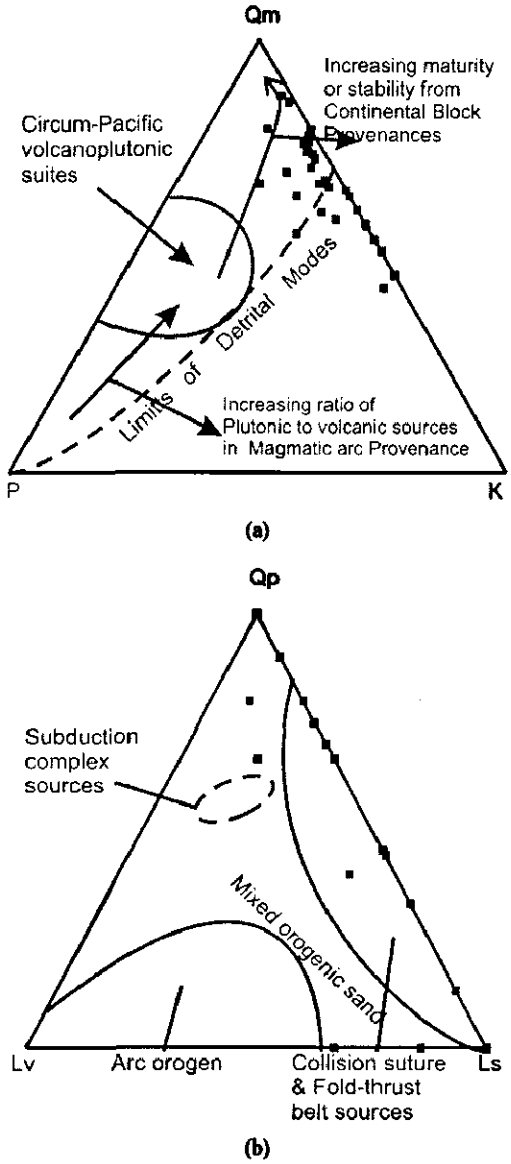

Figure 4. (a) Triangular diagram QmPK of Talchir sandstones, Chirimiri, Koriya district, for Provenance (after Dickinson *et al.*, 1985). (b) Triangular diagram QpLvLs of Talchir sandstones, Chirimiri, Koriya district for Provenance (after Dickinson *et al.*, 1985).

diagram based on lithic fragments population, suggests collision suture and fold thrust belt as source of these sandstones. The study of past climate of Permo-Carboniferous period is based on mineral composition of sandstone using bivariate plot between Qt/(F + R) vs. Qp/(F + R) as shown in (**Figure 5**). The samples show variation in climate, changing gradually from semi-arid to semi-humid.

6. Results and Discussion

The modal analysis of studied Talchir sandstones (**Table 3**), plotted on ternary diagram indicates that the sediments of Talchir Formation of Chirimiri, Koriya district,

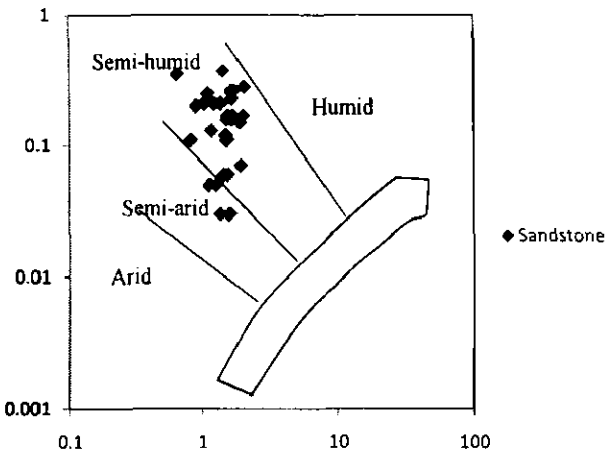

Figure 5. Bivariate log-log plot of Qt/(F + R) and Qp/(F + R) ratios of Talchir sandstones, Chirimiri, Koriya district, in climate discrimination diagram (after Suttner and Dutta, 1986).

Chhattisgarh were derived from continental block provenances and recycled orogen (**Figure 3(a)**). Within these major provenances sediments were derived from transitional continental block, basement uplift and small inputs also came from mixed field as shown in (**Figure 3(b)**). Continental block comprises variety of rocks, ranging from felsic-intermediate-mafic igneous, metamorphic and sedimentary to volcano-sedimentary assemblages. Recycled orogen sediments are sedimentary and subordinate volcanic rocks, which are metamorphosed and exposed to the surface by erosion and uplift of fold belts and thrusts. Some of these sediments were derived from recycled orogeny as shown in (**Figure 4(b)**). It can be interpreted from the present study that these sediments were derived from transitional continental region of continental block, which are generally of intermediate composition and provided compositionally immature to sub-mature sediments to the basin as shown in (**Figure 4(a)**). The palaeoflow data indicates that, in this part of peninsular India depositing streams were flowing from East-South- East to West-North-West during late Paleozoic [22]. On the basis of type of detrital framework components and available paleocurrent data it may be suggested that the provenance of the studied sandstone samples was probably Chotanagpur/Singhbhum craton and some other metasediments exposed in the vicinity of the basin. The studied samples show (**Figure 5**) that during late Palaeozoic era the climate changed gradually due to drifting of Indian sub continent towards the equator [8].

The quartz grains in shape ranges from angular to subrounded with strain lamellae in some of these grains. Angularity of some quartz grains indicate that these are first cycle of erosion sediments or have suffered some short distance of transportation whereas subrounded to rounded grains are either of second cycle or have been transported for longer distance. The preponderance of non-undulatory monocrystalline quartz over undulatory quartz suggests plutonic source. Automorphic inclusion of heavy mineral like zircon and tourmaline in monocrystalline quartz and grains of perthite (**Plate 1(f)**) are direct evidences of granitic source. Some mono crystalline quartz, are free from inclusions of heavy mineral and shows slight undulose extinction signifying that older gneiss or schist rocks might be the source [38]. The presence of iron oxide cement on feldspar grains also depict humid climate [10,39,40].

7. Conclusions

On the basis of the petrological data of the sandstone specimens of Talchir Formation (Permo-Carboniferous) collected from Chirimiri, Koriya district, Chhattisgarh, the following conclusions can be drawn:

1) These sandstones samples are compositionally immature to submature and have been classified as arkosic, subarkosic and lithic arkosic type.

2) Constituent grains of these sediments suggest their derivation continental block provenance.

3) Paleocurrent data indicate that the source area of these sandstones was somewhere in the East-South-East of the basin, which may be Chhotanagpur/Singhbhum complex with some contribution from Bastar craton also.

4) During the deposition of these Talchir sandstones, climate changed from semiarid to semi humid.

Acknowledgements

The authors are thankful to Dr. L.A.K Rao, Chairman and Dr. A.H.M. Ahmad, Incharge of sedimentology laboratory Department of Geology, A.M.U. Aligarh for providing the necessary facilities to carry out the research work. The financial assistance to Khansa Zaidi in the form of UGC (Maulana Azad National Senior Research Fellowship) is also gratefully acknowledged. The authors are also thankful to anonymous reviewer for suggesting necessary corrections in the manuscript.

REFERENCES

[1] F. J. Pettijohn, P. E. Potter, and R. Siever, "Sand and Sandstone," Springer-Verlag, Berlin, 1972, p. 241.

[2] W. R. Dickinson and C. A. Suczek, "Plate Tectonics and Sandstone Compositions," *American Association of Petroleum, Geological Bulletin*, Vol. 63, No. 12, 1979, pp. 2164-2182.

[3] W. R. Dickinson, "Compositions of Sandstones in Circum-Pacific Subduction Complexes and Fore-Arc Basins," *American Association of Petroleum Geologists Bulletin* Vol. 66, No. 2, 1982, pp. 121-137

[4] W. R. Dickinson, "Interpreting Provenance Relations from Detrital Modes of Sandstones," In: G. G. Zuffa, Ed.,

Provenance of Arenites, D. Reidel Publ. Co., New York, 1985, pp. 333-361. http://dx.doi.org/10.1007/978-94-017-2809-6_15

5] W. R. Dickinson, "Provenance and Sediment Dispersal in Relation to Paleotectonics and Paleogeography of Sedimentary Basins," In: K. L Kleinspehn and C. Paola, Eds., *New Perspectives in Basin Analysis*, Springer, New York, 1988, pp. 3-25. http://dx.doi.org/10.1007/978-1-4612-3788-4_1

6] W. R. Dickinson, L. S. Beard, G. R. Brakenridge, J. R. Erjavee, R. C. Ferguson and K. F. Inman, "Provenance of North American Phanerozoic Sandstones in Relation to Plate Tectonic Setting," *Geological Society of American Bulletin*, Vol. 94, No. 2, 1983, pp. 222-235. http://dx.doi.org/10.1130/0016-7606(1983)94<222:PONAPS>2.0.CO;2

7] P. E. Potter, "South America and a Few Grains of Sand, Pt. I. Beach Sands," *Journal of Geology*, Vol. 94, No. 3, 1986, pp. 301-319. http://dx.doi.org/10.1086/629031

8] L. J. Suttner and P. K Dutta.., "Alluvial Sandstone Composition and Paleoclimate, I. Framework Mineralogy," *Journal of Sedimentary Petrology*, Vol. 56, No. 3, 1986, pp. 329-345.

9] R. Cox and R. D. Lowe, "Quantifications of the Effects of Secondary Matrix on the Analysis of Sandstone Composition, and a Petro-Chemical Technique for Retrieving Original Framework Grain Modes of Altered Sandstones," *Journal of Sedimentary Research*, Vol. 66, No. 3, 1996, pp. 548-558.

10] A. Basu, "Petrology of Holocene Fluvial sand Derived from Plutonic Source Rocks: Implications to Paleoclimatic Interpretation," *Journal of Sedimentary Petrology*, Vol. 46, No. 3, 1976, pp. 696-709.

11] Hota, *et al.*, "Provenance Variability during Damuda Sedimentation in the Talchir Gondwana Basin, India—A Statistical Assessment," *International. Journal of Geosciences*, Vol. 2, No. 2, 2011, pp. 120-137.

12] Mukhopadhyay, *et al.*, "Stratigraphic Correlation between Different Gondwana Basins of India," *Journal of Geological Society of India*, Vol. 76, No. 3, 2010, pp. 251-266. http://dx.doi.org/10.1007/s12594-010-0097-6

13] S. M. Naqvi and J. J. W. Rogers, "Precambrian Geology of India," Clarendon Press, Oxford, 1987, p. 223.

14] B. P. Radhakrishna and S. M. Naqvi, "Precambrian Continental Crust of India and Its Evolution," *Journal of Geology*, Vol. 94, No. 2, 1986, pp. 145-166. http://dx.doi.org/10.1086/629020

15] N. D. Mitra, "Tensile Resurgence along Fossil Sutures: A Hypothesis on the Evolution of Gondwana Basins of Peninsular India," *Abstracts of Proceedings 2nd Symposium on Petroliferous Basins of India*, Vol. 3, Dehradun, 1994, pp. 55-62

16] G. C. Chatterjee and P. K. Ghosh, "Tectonic Framework of Peninsular Gondwana of India," *Records Geological Survey of India*, Vol. 98, No. 2, 1970, pp. 1-15.

17] S. K. Biswas, "A Review on the Evolution of Rift Basins in India during Gondwana with Special Reference to Western Indian Basins and Their Hydrocarbon Prospects," *Proceedings of Indian National Science Academy Special Issue*, Vol. 65, No. 3, 1999, pp. 261-283.

[18] S. K. Acharyya and A. Roy, "Tectono-Thermal History of the Central Indian Tectonic Zone and Reactivation of Major Fault/Shear Zones," *Journal of Geological Society of India*, Vol. 55, No. 3, 2000, pp. 239-256.

[19] R. C. Tewari, "Sedimentary-Tectonic Status of Permian-Triassic Boundary (250Ma) in Gondwana Stratigraphy of Peninsular India," *Gondwana Research*, Vol. 2, No. 2, 1999, pp. 185-189. http://dx.doi.org/10.1016/S1342-937X(05)70142-8

[20] S. M. Casshyap and H. A. Qidwai, "Glacial Sedimentation of Late Palaeozoic Talchir diamictite, Pench Valley Coalfields, Central India," *Geological Society of America Bulletin*, Vol. 85, No. 5, 1974, pp.749-760. http://dx.doi.org/10.1130/0016-7606(1974)85<749:GSOLPT>2.0.CO;2

[21] S. N. Das and D. P. Sen, "Depositional History of Permo-Carboniferous Tillites and Associated Sediments in West Bokaro Gondwana Basin, Bihar," Journal of the *Geological Society of India*, Vol. 21, No. 1, 1980, pp. 30-38.

[22] R. C. Tewari and S. M. Casshayap, "Palaeoflow Analysis of Late Paleozoic Gondwana Deposits of Giridih and Adjoining Basins and Paleogeographic Implications," *Geological Society of India*, Vol. 23, No. 2, 1982, pp 67-79.

[23] N. Eyles and A. M. McCabe, "The Late Devensian (<22000YBP) Irish Sea Basin: The Sedimentary Record of a Collapsed Ice Sheet Margin," *Quaternary Science Review*, Vol. 8, No. 4, 1989, pp. 307-351. http://dx.doi.org/10.1016/0277-3791(89)90034-6

[24] P. K. Bose, G. Mukhopadhyay and H. N. Bhattacharya, "Glaciogenic Coarse Clastics in a Permo-Carboniferous Bedrock trough in India: A Sedimentary Model," *Sedimentary Geology*, Vol. 76, No. 1-2, 1992, pp. 79-97. http://dx.doi.org/10.1016/0037-0738(92)90140-M

[25] G. Mukhopadhyay and H. N. Bhattacharya, "Facies Analysis of Talchir Sediments (Permo-Carboniferous), Dudhi Nala, Bihar, India—A Glaciomarine Model," *IXth International Gondwana Symposium*, Oxford and IBH Publication, New Delhi, Vol. 2, 1994, pp. 737-753.

[26] J. J. Veevers and R.C. Tewari, "Gondwana Master Basin of Peninsular India between Tethys and the Interior of the Gondwanaland Province of Pangea," *Memoire of the Geological Society of America*, No. 187, 1995, pp. 1-73.

[27] W. Maejima, R. Das, K. L. Pandya and M. Hayashi, "Deglacial Control on Sedimentation and Basin Evolution of Permo-Carboniferous Talchir Formation, Talchir Gondwana Basin, Orissa, India," *Gondwana Research*, Vol. 72, No. 2, 2004, pp. 339-352. http://dx.doi.org/10.1016/S1342-937X(05)70788-7

[28] H. N. Bhattacharya, B. Bhattacharya, I. Chakraborty and A. Chakraborty, "Sole Marks in Storm Event Beds in the Permo-Carboniferous Talchir Formation, Raniganj Basin, India," *Sedimentary Geology*, Vol. 166, No. 3-4, 2004, pp. 209-222. http://dx.doi.org/10.1016/j.sedgeo.2003.12.003

[29] H. N. Bhattacharya, A. Chakraborty and B. Bhattacharya, "Significance of Transition between Talchir Formation

and Karharbari Formation in Lower Gondwana Basin Evolution—A Study in West Bokaro Coal Basin, Jharkhand, India," *Journal of Earth System Science*, Vol. 114, No. 3, 2005, pp. 275-286. http://dx.doi.org/10.1007/BF02702950

[30] H. N. Bhattacharya and B. Bhattacharya, "A Permo-Carboniferous Tide-Storm Interactive System: Talchir Formation, Raniganj Basin, India," *Journal of Asian Earth Sciences*, Vol. 27, No. 3, 2006, pp. 303-311. http://dx.doi.org/10.1016/j.jseaes.2005.04.006

[31] H. N. Bhattacharya and B. Bhattacharya, "Soft Sediment Deformation Structures from an Ice-Marginal Storm-Tide Interactive System, Permo-Carboniferous Talchir Formation, Talchir Coalbasin, India," *Sedimentary Geology*, Vol. 223, No. 3-4, 2010, pp. 380-389. http://dx.doi.org/10.1016/j.sedgeo.2009.12.002

[32] B. Bhattacharya and H. N. Bhattacharya, "Implications of Mud-Clast Conglomerates within Late Palaeozoic Talchir Glacio-Marine Succession, Talchir Basin, India," *Indian Journal of Geosciences*, Vol. 66, No. 1, 2012, pp. 69-78.

[33] C. S. Rao Raja, "Chirimiri Coalfield," In: *Coal Resources of Madhya Pradesh and Jammu & Kashmir, Bulletins of Geological Survey of India*, Series A, Vol. 3, No. 45, 1983, pp. 44-55.

[34] A. Roy, H. M. Ramchandra and B. K. Bandyopadhyay, "Supracrustal Belts and Their Significance in the Crustal Evolution of Central India," *Proceedings Dr. M.S Krishnan Birth Cent, Sem.*, Geological Survey of India, Special Publication, No. 55, 2000, pp. 361-380.

[35] S. Dotiwala and K. K. S. Pangtey, KDMIPE, AAPG, Search and Discovery Article, American Association of Petroleum Geologist, International Conference and Exhibition, Vienna, 1997.

[36] R. V. Ingersoll, T. F. Bullard, R. L. Ford, J. P. Grimm, J. D. Pickle and S. W. Sares, "The Effect of Grain Size on Detrital Modes: A Test of the Gazzi-Dickinson Point Counting Method," *Journal of Sedimentary Research*, Vol. 54, No. 1, 1984, pp. 103-106.

[37] R. L. Folk, "Petrology of Sedimentary Rocks," Hemphill, Austin, 1980.

[38] F. J. Pettijohn, "Sedimentary Rocks," 3rd Edition, Harper and Row, New York, 1975, 628pp.

[39] R. G. Walker, "Colour of Recent Sediments in Tropical Mexico: A Contribution to the Origin of Red Beds," *Geological Society of America Bulletin*, Vol. 78, No. 7, 1967, pp. 917-920. http://dx.doi.org/10.1130/0016-7606(1967)78[917:CORSIT]2.0.CO;2

[40] R. L. Folk, "Bimodal Supermature Sandstones: Product of Desert Floor," *Proceedings 23rd International Gondwana Congress*, Vol. 8, 1968, pp. 9-32.

Volume : 3 | Issue : 7 | July 2014 • ISSN No 2277 - 8179

Research Paper

Geology

KEYWORDS : Talchir, Son valley, Provenance, Weathering, Tectonics, Palaeozoic

Provenance, Weathering and Tectonic Setting of Talchir Formation in Parts of Son Valley Sub Basin Chhattisgarh, India During Late Paleozoic Era: Petrological and Geochemical Evidences

Khansa Zaidi Research Scholar, Department of Geology, Aligarh Muslim University, Aligarh India.

Dr. Sarwar Rais Associate Professor, Department of Geology, Aligarh Muslim University Aligarh India.

ABSTRACT

*The Talchir Formation (Permo-carboniferous) is the lowermost unit of Gondwana Supergroup which rests unconformably over the Precambrian basement of Indian peninsula. Modal analysis and geochemistry of Talchir sandstones and shales of Chirimiri area, Son valley sub basin, Chhattisgarh, is carried out to know nature of provenance and its composition, weathering condition and tectonic setting of both source area and depositional basin. These characters are determined with the help of QtFL parameter, and bivariate plot between TiO2 vs Zr, geochemical proxies [A/ACNK)*100] and ratio of major oxide K2O/Na2O vs SiO2 have been utilised to achieve this aim. The petrochemical attributes of the clastic rocks of Talchir Formation suggest that these sediments have been derived from continental block having rocks of mixed composition which was subjected to moderate weathering during late Palaeozoic time. These sediments were deposited in basin situated at passive margin.*

Introduction

Synthesis of compositional and textural properties of sediments and information from other lines of evidence help in interpreting the characters of source area (Pettijohn, F. J., Potter, P. E., and Siever, R., 1987). The provenance of sandstones has traditionally been elucidated by modal composition using classical petrographic techniques. But sandstones with a significant amount of finer fraction may not be suitable for such study. In such kind of sandstones geochemical abundances, especially ratios of trace elements, which are present in finer grade material, may provide crucial information about the provenance (Cullers, R.L. and Stone, J., 1991; Cullers, R.L. and Berendsen, P., 1998).

Weathering involves the conversion of unstable minerals, mainly feldspars and micas into clay. The bulk chemical changes that take place during weathering processes provide an insight to understand past climatic conditions (Nesbitt, H. W., Markovics, G., and Price, R.C., 1980; Nesbitt, H. W., and Young, G. M., 1982; Nesbitt, H. W., and Young, G. M., 1982; Nesbitt, H. W., and Young, G. M., 1984). Chemical index of alteration (CIA) is a good measure to assess the degree of chemical weathering of the source terrain (Nesbitt, H. W., and Young, G. M., 1984, 1989). Plate tectonics controls the characteristics of the detrital grains and chemistry of sandstones (Dickinson, W.R., and Suczek, C.A., 1979; Dickinson, W. R., Beard, L. S., Brakenridge, G. R., Erjavee, J. R., Ferguson, R. C., and Inman, K. F., 1983; Bhatia, M.R., 1983; Roser and Korsch, 1986). Bivariate plot of K_2O/Na_2O ratio versus SiO_2 demonstrates three tectonic setting of sedimentary basins (Roser and Korsch, 1986). In the present study of sandstones and shales of Talchir Formation of Chirimiri area, petrographic and geochemical proxies have been employed to identify the provenance, weathering and tectonic setting of the depositional basin of these sediments.

Geology of the study area

Study area is situated in the vicinity of Chirimiri coalfield (23°8'-23°15'N: 82°17'-82°25'E) Koriya district, Chhattisgarh. Chirimiri coalfield is located in the Son-Mahanadi graben which is one of the largest intracratonic rift basins of peninsular India. It is surrounded by unclassified Precambrian rocks. The basin is a failed rift which diagonally cuts three major cratons namely Bastar, Singhbhum and Chotanagpur terrain (Figure1). Tectonically, the Son-Mahanadi basin has been divided into three blocks, each separated from the other by ENE-WSW trending prominent ridges. The blocks are Son Graben, Hasdo-Arand High and Mahanadi Graben. Contrasting nature of sediments and structural characters of the rocks suggest that each of these blocks has different sedimentation and tectonic history (Dotiwala, Sucheta, Pangtey, 1997).

In Chirimiri area (Hasdo-Arand sub basin), Talchir Formation is exposed along stream channels (Figure 2). The basal units of the formation are olive green sandstones with thinly laminated shales and unstratified medium grained sandstone succeeded by lemon yellow alternate beds of shale and sandstone. Table 1 presents the stratigraphic succession of Talchir Formation in Chirimiri area.

Table.1 Stratigraphic succession of Talchir Formation in Chirimiri, Koriya district, Chhattisgarh (simplified after C.S. Raja Rao, 1983).

Age	Formation	Lithology
Upper Cretaceous to lower Eocene (?)	Deccan Traps	Basic flows, dykes and sills.
Lower Permian	Barakar	Essentially sandstone with subordinate Shales and coal seams (230m to 435m).
Upper Carboniferous to Early Permian	Talchir	Predominantly olive green shales and Medium to fine grained sandstone.
	UNCONFORMITY	
Precambrian basement		Granite, Gniesses and Quartzite

Figure 1: Map showing geology of the study area Chirimiri in parts of Son-Mahanadi basin, Chhattisgarh India (C. S. Rao Raja, 1983)

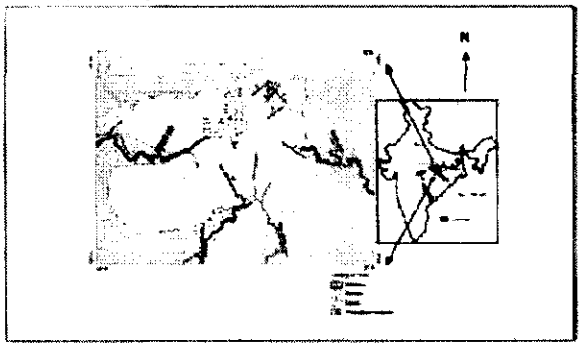

Material and Methods

Representative samples sandstone and shale belonging to Talchir Formation have been collected at an interval of 1m along the stream sections in and around Chirimiri town. Out of total 50 only 29 fresh sandstones samples were selected for petrographic study. Thin sections were prepared and studied for modal composition under petrologic microscope. About 350 points per thin sections were counted using Gazzi-Dickenson's method (R. V. Ingersoll, T. F. Bullard, R. L. Ford, J. P. Grimm, J. D. Pickle and S. W. Sares, 1984). Because of their fine grain nature samples of shales were not examined under microscope. The counted grains of sandstone were recalculated into percentage and summarised in Table 2. Small chips of only 26 out of

Volume : 3 | Issue : 7 | July 2014 • ISSN No 2277 - 8179

29 sandstones and 3 shale samples were powdered in a grinder upto -200 meshes. Fused disc shape pellets were prepared and XRF analysis carried in the laboratories of National Institute of Oceanography, Goa. The trace elements and rare earth elements (REE) concentration of these studied Talchir samples were determined using open Acid-digestion method at National Centre of Antarctic and Ocean Research, Goa.

Table 2 average values for Petrographic data of QtFL for sandstones and geochemical data analysed for Sandstones and shales of Talchir Formation in study area. Samples of Bhukbhuki nala designated as (BK) are the shales

S.No	Qt	F	L	S.No	CIA	TiO_2	Zr	K_2O/Na_2O	SiO_2
NT1	60	38	1	NT1	64	0	35	1	77
NT2	58	40	2	NT2	62	1	33	1	77
NT3	52	43	4	NT3	65	1	92	1	78
NT5	55	39	5	NT5	66	1	20	1	78
NT7	54	29	17	NT6	67	1	23	1	77
NT8	69	28	3	NT7	66	1	24	2	77
NT9	69	25	7	NT8	61	0	34	1	79
NT10	76	24	0	NT9	62	0	112	1	80
NT12	58	37	5	NT10	61	0	77	1	79
NT13	84	16	0	NT12	60	0	101	1	79
NT14	63	36	1	KN1	60	1	162	1	75
KN3	57	40	3	KN3	60	1	84	1	75
GN1	77	18	7	GN1	59	1	46	2	80
GN2	72	21	6	GN2	63	1	66	2	79
GN3	70	24	9	GN3	63	1	52	2	78
GN4	62	29	2	GN4	62	1	52	2	81
GN5	78	20	8	GN5	63	0	92	2	78
GN6	74	17	4	GN6	61	1	63	2	79
GN7	69	28	3	GN8	61	1	90	2	79
GN8	79	13	7	GN9	60	0	59	2	79
GN9	63	29	3	GN10	60	1	67	2	81
GN10	71	26	2	GN11	49	0	83	2	78
GN11	87	11	9	BBK1	64	1	146	2	72
BBK1	49	42	3	BBK2	63	1	150	2	73
BBK3	53	44	6	BBK4	64	1	172	2	71
BBK4	70	24	6	BBK5	52	0	139	2	82
BBK5	41	53	6	BK1	63	0	175	1	73
BBK6	39	56	3	BK2	63	0	180	1	74
BBK7	63	34	3	BK3	62	0	195	1	72

Results and Discussion

Provenance and Weathering

The QtFL ternary diagram (Dickinson, et al., 1983) of sandstones of Talchir Formation of Chirimiri area (Figure 2) suggests that the majority of these sediments were derived from transitional continental region of continental block. However, a few samples indicate recycled orogen and basement uplift as their source.

Figure 2: Triangular diagram QtFL of Talchir sandstone for Provenance (after Dickinson et. al., 1983) where Qt = total quartz, F = feldspar, L = lithic fragments.

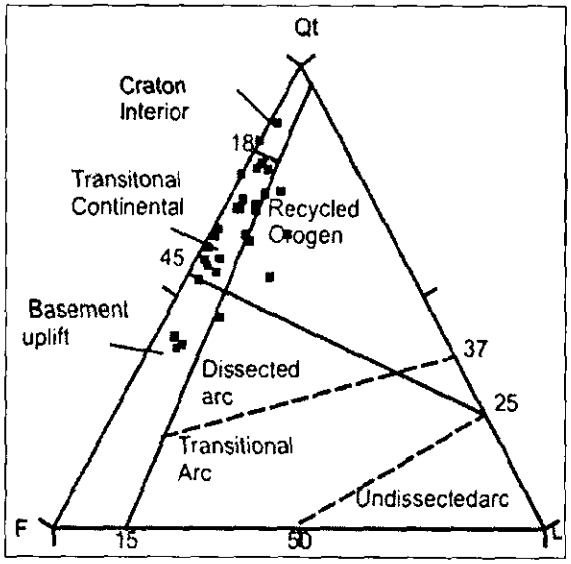

Relationship among alkali and alkaline earth elements are indicators of the intensity and duration of weathering in sedimentary rocks (Nesbitt, H. W., and Young, G. M., 1982). The Chemical Index of Alteration (CIA) has a range which defines intensity of weathering. The equation of CIA is $[Al_2O_3/ (CaO+Na_2O+K_2O)]$ *100 (Nesbitt, H. W., and Young, G. M., 1982) .The equation is used to calculate the weathering intensity of sandstones and shales of the study area. Where the oxides are expressed as molar proportions and CaO represents the Ca in silicate fractions only. These values range from 49 to 67 in sandstones and from 62 to 63 in shales. These values are greater than the CIA values of upper continental crust (UCC). This indicates that the under discussion Talchir sandstones and shales were derived from rocks whose chemical compositions are similar to UCC under moderate weathering conditions. The TiO_2 vs. Zr plot (Figure 3) of Hayashi et al., (1997) suggests that most of the studied Talchir sandstones and shales have a source in felsic and intermediate igneous rocks, whereas only three of these analysed samples show their derivation from mafic igneous rocks.

Figure 3: Bivariate plot between TiO_2 wt % vs. Zr ppm (after Hayashi et al., 1997) for Talchir sandstones and shales of Chirimiri, Koriya district, Chhattisgarh.

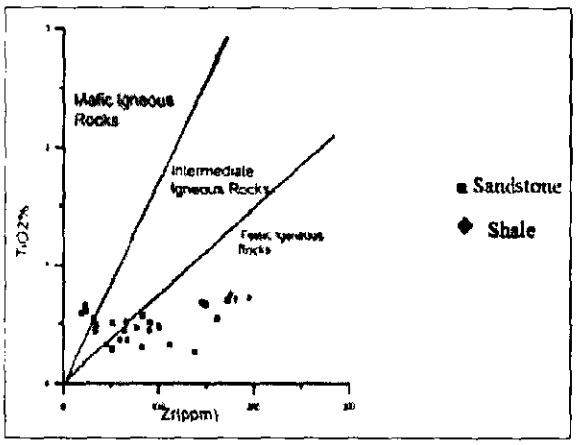

Tectonic setting

The bivariate plot K_2O/Na_2O vs. SiO_2 (Roser and Korsch, 1986) shows (Figure 4) that Talchir sandstones and shale samples, collected from Chirimiri area were deposited at the edge of passive continental margin. This observation supports the earlier inference that these clastics have been derived from transitional continental region of continental block (Figure 2).

Figure 4: Bivariate plot between K2o/Na2O vs SiO_2 (after Roser and Korsch, 1986) for Talchir sandstone and shale of Chirimiri, Koriya district, Chhattisgarh.

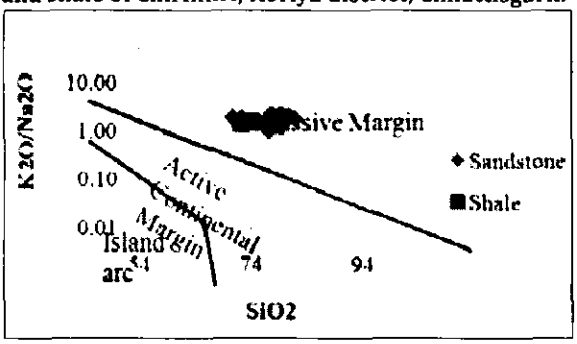

Conclusion

Modal composition and geochemical characters of Talchir sandstone and shale samples collected from Chirimiri area, Koriya district, Chhattisgarh, India, show that they were derived from transitional continental block provenance and deposited in a passive margin basin. The Chemical Index of Alteration (CIA) values ranging from 49 to 67 in sandstones and 62 to 63 in shales; are greater than CIA value of UCC (i.e. 50). This shows that the detritus for these Talchir sediments were subjected to moderate weathering conditions and the source rocks have similar chemical composition to UCC. The provenance of these clastics was predominantly felsic with minor intermediate and mafic components.

Acknowledgement

The authors are thankful to the Prof. Mahshar Raza, Chairman, Department of Geology, A.M.U, Aligarh. We are also grateful to Dr. Abhay Mudholkar, National Institute of Oceanography and Dr. Thamban Meloth, National Centre of Antarctic Ocean Research, Goa for help and providing necessary facilities to carry out the geochemical analysis. We are also thankful to Dr. M. S. Khan, Associate Prof. D/O Geology A.M.U, for going through the manuscript and giving fruitful suggestions. The financial assistance to Miss Khansa Zaidi in the form of Maulana Azad National Senior Research Fellowship is duly acknowledged.

REFERENCE

1. Pettijohn, F. J., Potter, P. E., and Siever, R., 1987: "Sand and Sandstone" (Berlin: Springer-Verlag), 1972, 241. | 2. Cullers, R.L. and Stone, J., 1991: Chemical and mineralogical composition of the Pennsylvanian mountain, Colorado, U.S.A. (an uplifted continental block) to sedimentary rocks from other tectonics environments. Lithos, Vol. 27. pp. 115-131. | 3. Cullers, R.L. and Berendsen, P., 1998: The provenance and chemical variation of sandstones associated with the mid-continent rift system, U.S.A. European Journal of Mineralogy, Vo. 10. pp. 987-1002. | 4. Nesbitt, H. W., Markovics, G., and Price, R.C., 1980: Chemical process affecting alkalis and alkaline earths during continental weathering: Geochemica et Cosmochimica Acta, Vol. 44, pp. 1659-1666. | 5. Nesbitt, H. W., and Young, G. M., 1982: Early Proterozoic climate and plate motions inferred from major element chemistry of lutites, Nature, Vol. 299, pp 715-717. | 6. Nesbitt, H. W., and Young, G. M., 1984: Prediction of some weathering trends of plutonic and volcanic rocks based on thermodynamic and kinetic consideration: Geochimica et cosmochimica acta, Vol. 48, pp 1523-1534. | 7. Nesbitt, H. W., and Young, G. M., 1989: Formation and diagenesis of weathering profiles: Journal of Geology, Vol. 97, pp 129-147. | 8. Dickinson, W.R., and Suczek, C.A., 1979 "Plate tectonics and sandstone compositions" American Association of Petroleum, Geological Bulletin, Vol. 63, pp.2164-2182. | 9. Dickinson, W. R., Beard, L. S., Brakenridge, G. R., Erjavee, J. R., Ferguson, R. C., and Inman, K. F., 1983, "Provenance of North American Phanerozoic sandstones in relation to plate tectonic setting," Geological Society of American Bulletin, Vol. 94, pp. 222-235. | 10. Bhatia, M.R., 1983: Plate tectonic and geochemical composition of sandstones: Journal of geology. Vol. 91. pp. 611-627. | 11. Roser and Korsch, 1986; Determination of tectonic setting of sandstone-mudstone suites using sio2 content and K2O/Na2o ratio, Journal of Geology. Vol. 94. No. 5. | 12. Dotiwala, Sucheta, Pangtey, 1997, K.K.S., K.D.M.I.P.E, A.A.P.G, Search and Discovery Article: American Association of Petroleum Geologist, International Conference and Exhibition Vienna, Austria | 13. C. S. Rao Raja, "Chirimiri Coalfield," In: Coal Resources of Madhya Pradesh and Jammu & Kashmir, Bulletins of Geological Survey of India, Series A, Vol. 3, No. 45, 1983, pp. 44-55. | 14. R. V. Ingersoll, T. F. Bullard, R. L. Ford, J. P. Grimm, J. D. Pickle and S. W. Sares, "The Effect of Grain Size on Detrital Modes: A Test of the Gazzi-Dickinson Point Counting Method," Journal of Sedimentary Research, Vol. 54, No. 1, 1984, pp. 103-106. | 15. Hayashi, K.; Fujisawa, H.; Holland, H.D. and Ohmoto, H. 1997: Geochemistry of ~1.9 Ga sedimentary rocks from northeastern Labrador, Canada. Geochimica Cosmochimica Acta vol.61, pp.4115-4137. | |